Environmental Dynamics and Megaherbivore Adaptations in a Middle Pleistocene Glacial Microrefugium: Isotopic Evidence from the Megalopolis Basin (Southern Greece)

Dissertation

der Mathematisch-Naturwissenschaftlichen Fakultät

der Eberhard Karls Universität Tübingen

zur Erlangung des Grades eines

Doktors der Naturwissenschaften

(Dr. rer. nat.)

vorgelegt von

M.Sc. Effrosyni Roditi

aus Athen, Griechenland

Tübingen

2024

Gedruckt mit Genehmigung der Mathematisch-Naturwissenschaftlichen Fakultät der Eberhard Karls Universität Tübingen.

Tag der mündlichen Qualifikation:	16.12.2024
Dekan:	Prof. Dr. Thilo Stehle
1. Berichterstatter/-in:	Prof. Dr. Katerina Harvati
2. Berichterstatter/-in:	Prof. Dr. Hervé Bocherens
3. Berichterstatter/-in:	PD. Dr. Britt M. Starkovich

Table of Contents

Acknowledgments

This dissertation would not have been possible without the support and encouragement of many people, to whom I am deeply grateful.

First and foremost, I would like to express my deepest gratitude to my supervisors, Prof. Katerina Harvati (Paleoanthropology, University of Tübingen) and Prof. Hervé Bocherens (Biogeology, University of Tübingen), for their exceptional guidance in my academic endeavours, for their unconditional support during difficult times, and for giving me the opportunity to pursue this research and expand my interests, skills and knowledge. Your belief in my potential and your invaluable advice have been fundamental in shaping both this work and my academic growth.

I would also like to extend a special mention and a big thanks to Dr. George Konidaris, who dedicated significant effort and time to the progress of this project, as well as to my own academic development. Thank you for your immense scientific contribution, your belief in my abilities and continuous encouragement to approach my work with confidence.

I am deeply grateful to co-authors and collaborators Dr. Athanassios Athanassiou (Ephorate of Paleoanthropology-Speleology), Prof. Vangelis Tourloukis (University of Ioannina), Dr. Panagiotis Karkanas (Malcolm H. Wiener Laboratory, ASCSA), and Dr. Eleni Panagopoulou (Ephorate of Paleoanthropology-Speleology). Thank you for the enriching discussions, your expertise and your contributions, all of which have been vital in shaping the quality and depth of this work. I have learned a lot while working with you and hope to continue our collaboration for many years to come. Furthermore, I would like to thank PD Dr. Britt Starkovich (Zooarchaeology, University of Tübingen) for agreeing to act as the third reviewer of this thesis and Prof. Vangelis Tourloukis for dedicating valuable time to be part of my doctoral committee.

A heartfelt thank you goes to the members of the Paleobiology group (University of Tübingen), especially Dr. Dorothee Drucker, Peter Tung, Ruth Rey, Valentina García-Huidobro, and Dr. Chris Baumann. Your scientific input and invaluable assistance at the lab were crucial to the success of this research, and I am deeply appreciative of your time and effort. In addition, I would like to thank all members of the CROSSROADS project for the collaboration and for making fieldwork a truly enjoyable, fun and memorable experience. My appreciation also goes to my friends, colleagues and ex-

colleagues of the Palaeoanthropology group for their unwavering support and companionship throughout the years. Special thanks go to my office mates Jana Kunze, Melania Ioannidou, and Carolin Röding for their friendship, encouragement, and reassuring words during challenging times.

Moreover, I am grateful to the following institutions: The Ephorate of Palaeoanthropology and Speleology (Hellenic Ministry of Culture) for granting access to the materials and permission to undertake the study and to the Curt-Engelhorn-Zentrum Archäometrie gGmbH for performing the strontium isotope analysis. Finally, this project would not have been possible without the financial support of ERC StG. PaGE and ECR CoG. CROSSROADS (awarded to Katerina Harvati).

To my family, especially my parents, Petros and Katerina—words cannot express how grateful I am for your unconditional love, endless support and encouragement in every aspect of my life. Thank you for giving me strength and inspiration, and for empowering my perseverance. Last but not least, to my partner, Sven — I consider myself extremely lucky to have someone so supportive, caring and understanding by my side. Thank you for being my shining light in my dark days.

Abstract

After the Mid-Pleistocene Climate Transition, Eurasian ecosystems were governed by longer (~100 ky) but higher amplitude climatic periodicity (glacial-interglacial cycles). The increased intensity of the glacial cycles impacted floral, faunal, and hominin biogeography. Glacial refugial areas in peninsular southern European regions had a prominent role in the survival and persistence of several temperate taxa during adverse periods; however, little is known about the environmental conditions that governed these areas. This cumulative dissertation explores landscape dynamics, climate, and hydrology of a putative micro-refugium in the Megalopolis Basin (Peloponnese, Greece) at the southernmost part of the Balkan Peninsula through the ecological characterization of two extinct megaherbivore species, the European straight-tusked elephant (*Palaeoloxodon antiquus*) and the European hippopotamus (*Hippopotamus antiquus*).

Individual megaherbivore ecologies were reconstructed through isotopic biogeochemistry to infer millennial, decadal, and annual scale climatic and environmental conditions in the area between ca. 700 and 430 ka. The studied specimens originated from five Middle Pleistocene fossiliferous sites in the Megalopolis Basin, namely Marathousa 1 (ca. 430 ka), Marathousa 2 (ca. 450 ka), Kyparissia 3 (ca. 650 ka), Kyparissia 4 (ca. 700 ka), and Kyparissia-T (early Middle Pleistocene). The contextual association of faunal specimens with hominin activity, either directly in the form of butchering marks or indirectly through their stratigraphic and spatial association with stone tools, extended interpretations to the hominin paleoenvironmental niche in the basin.

Three studies present carbon, oxygen, and strontium isotope analyses on enamel carbonates of a straight-tusked elephant (*P. antiquus)* and five hippopotamus (*H. antiquus)* specimens to reconstruct their foraging patterns, habitat and mobility, as well as the climatic conditions in the basin during different chrono-stratigraphic intervals. A sequential sampling strategy on herbivore teeth that grow over multiple years, such as the continuously growing hippopotamus tusks and the elephant molars, provides sub-annual and decadal-scale stable isotope data for the selected individuals.

Carbon isotopes of both *P. antiquus* and *H. antiquus* enamel carbonates revealed the persistence of C_3-dominated ecosystems and a mosaic of habitats in the basin,

including forested patches and mesic open woodlands/grasslands. Oxygen isotopes indicated mild climatic conditions, even during severe glacial periods. The intra-tooth isotopic profiles revealed moderate seasonality in the basin. Individual palaeoecological inferences suggest dynamic environments and taxon-specific adaptations to shifting resource availability. Multi-annual fluctuations in the carbon isotopic composition of *Palaeoloxodon antiquus,* in conjunction with strontium isotopic data, suggested limited mobility within the basin for the exploitation of diverse micro-habitats during the MIS 12 glacial period. Carbon isotope profiles of *Hippopotamus antiquus* demonstrated seasonal dietary adaptations and multi-annual fluctuations in available resources, while oxygen isotopes revealed variable hydrological or climatic conditions.

Despite climatic oscillations, the Megalopolis Basin provided a diverse array of subsistence sources, thus facilitating the survival of these megaherbivores through Middle Pleistocene glacial or stadial periods. These results offer further substantiation to the basin's role as a micro-refugium, an area in which organisms survived through adverse conditions and from which they were able to re-establish viable populations in northern settings during climatic amelioration, but also highlighted the resilience and adaptability of both megafauna and hominin populations to changing environments.

Zusammenfassung

Nach dem mittelpleistozänen Klimaumbruch unterlagen die eurasischen Ökosysteme einer längeren (~100 ky) und stärkeren klimatischen Periodizität (Glazial-Interglazial-Zyklen) als zuvor. Diese zunehmende Intensität der Gletscherzyklen wirkte sich auf die Flora, die Fauna und die Biogeographie der Homininen aus. Während ungünstiger Perioden spielten glaziale Refugialgebiete auf den südeuropäischen Halbinseln, z.B. dem Balkan, eine herausragende Rolle für das Überleben und Fortbestehen verschiedener Taxa der gemäßigten Breiten. Über die Umweltbedingungen, die in diesen Refugialgebieten herrschten, ist jedoch wenig bekannt. Im Fokus dieser kumulative Dissertation steht das vermeintliche Mikrorefugium im Megalopolis-Becken (Peloponnes, Griechenland) im südlichsten Teil der Balkanhalbinsel. Anhand der ökologischen Charakterisierung von zwei ausgestorbenen Megaherbivoren-Arten, dem Europäischen Elefanten mit geradem Stoßzahn (*Palaeoloxodon antiquus*) und dem Flusspferd (*Hippopotamus antiquus*), wurden die Landschaftsdynamik, das Klima und die Hydrologie des Megalopolis-Beckens untersucht.

Isotopenanalysen ermöglichen die Rekonstruktion der Ökologie einzelner Megaherbivoren. Abhängig vom beprobten Material können diese Analysen Rückschlüsse auf die Klima- und Umweltbedingungen einer Region mit einer Auflösung von Jahrtausenden, Jahrzehnten oder Jahren liefern. Das hier untersuchte Material stammt aus fünf mittelpleistozänen Fossilfundstellen im Megalopolis-Becken: Marathousa 1 (ca. 430 ka), Marathousa 2 (ca. 450 ka), Kyparissia 3 (ca. 650 ka), Kyparissia 4 (ca. 700 ka) und Kyparissia-T (frühes Mittelpleistozän). Die kontextuelle Verbindung der analysierten Fauna mit homininen Aktivitäten, entweder direkt in Form von Schlachtspuren oder indirekt durch ihre stratigraphische und räumliche Verbindung mit Steinwerkzeugen, erweiterte die Interpretationen der paläoökologischen Nische der Homininen im Becken.

In drei Studien wurden Kohlenstoff-, Sauerstoff- und Strontium-Isotopenanalysen an Zahnschmelzkarbonaten eines Europäischen Waldelefanten (*P. antiquus*) und von fünf Flusspferden (*H. antiquus*) durchgeführt, um deren Nahrungsverhalten, Lebensraum und Mobilität sowie die klimatischen Bedingungen im Becken während verschiedener chronostratigraphischer Intervalle zu rekonstruieren. Eine Strategie zur sequenzielle Probenahme an Pflanzenfresserzähnen, die über

mehrere Jahre hinweg wachsen, wie z. B. kontinuierlich wachsende Nilpferdstoßzähne und Elefantenmolaren, liefert für die ausgewählten Individuen stabile Isotopendaten auf subjährlicher und dekadischer Ebene.

Die Kohlenstoffisotope der Zahnschmelzkarbonate von *P. antiquus* und *H. antiquus* zeigten, dass im Megalopolis-Becken C_3-dominierte Ökosysteme und ein Mosaik von Lebensräumen, einschließlich bewaldeter Flächen und mesischer offener Wälder/Grünland, fortbestehen. Die Sauerstoffisotope weisen auf milde klimatische Bedingungen hin, selbst während der schweren Eiszeiten. Die Isotopenprofile zwischen den Zähnen zeigten eine mäßige Saisonalität im Becken. Einzelne paläoökologische Schlussfolgerungen deuten auf dynamische Umgebungen und Taxon-spezifische Anpassungen an die wechselnde Verfügbarkeit von Ressourcen hin. Mehrjährige Schwankungen in der Kohlenstoff-Isotopenzusammensetzung von *Palaeoloxodon antiquus* in Verbindung mit Strontium-Isotopendaten deuten auf eine begrenzte Mobilität innerhalb des Beckens hin, um verschiedene Mikrolebensräume während der MIS 12-Eiszeit zu nutzen. Die Kohlenstoff-Isotopenprofile von *Hippopotamus antiquus* zeigten saisonale Anpassungen der Ernährung und mehrjährige Schwankungen der verfügbaren Ressourcen, während die Sauerstoff-Isotopen variable hydrologische oder klimatische Bedingungen erkennen ließen.

Trotz klimatischer Schwankungen bot das Megalopolis-Becken eine Vielzahl von Nahrungsquellen und erleichterte so das Überleben von Megaherbivoren während der glazialen oder stadialen Perioden des Mittelpleistozäns. Diese Ergebnisse untermauern die Rolle des Beckens als Mikrorefugium, ein Gebiet in dem Organismen bei vergleichsweise günstigen Bedingungen überlebten und von dem aus sie bei einer Klimaverbesserung nördlichere Gefilde neubesiedeln konnten. Darüber hinaus spiegeln die Ergebnisse die Widerstandsfähigkeit und Anpassungsfähigkeit sowohl der Megafauna als auch der Homininenpopulationen an sich verändernde Umgebungen wieder.

List of Publications

This cumulative dissertation includes two accepted manuscripts and one manuscript ready for submission in fulfillment of the requirements. Percentages of own contribution to manuscripts are listed in parentheses (scientific idea/data generation/analysis and interpretation/paper writing).

Accepted manuscripts

- Study I (50/80/80/80):
  Roditi, E., Bocherens, H., Konidaris, G. E., Athanassiou, A., Tourloukis, V., Panagopoulou, E., & Harvati, K. (2025). First stable isotope results on the ecology of the straight-tusked elephant (*Palaeoloxodon antiquus*) from the Middle Pleistocene Marathousa 1 (Peloponnese, Greece). In K. Harvati & M. Ioannidou (Eds.), *Human Evolution at the CROSSROADS: Research in Greece and beyond*. Tübingen University Press.

- Study II (70/80/90/60):
  Roditi, E., Bocherens, H., Konidaris, G. E., Athanassiou, A., Tourloukis, V., Karkanas, P., Panagopoulou, E., & Harvati, K. (2024). Life-history of *Palaeoloxodon antiquus* reveals Middle Pleistocene glacial refugium in the Megalopolis basin, Greece. *Scientific Reports*, *14*(1), 1390.

Manuscript ready for submission

- Study III (80/80/90/80):
  Roditi, E., Bocherens, H., Konidaris, G.E., Athanassiou, A., Tourloukis, V., Panagopoulou, E., Karkanas, P., & Harvati, K. (in prep.). Ecological variability of *Hippopotamus antiquus* from the Middle Pleistocene of Megalopolis Basin (Greece): Evidence for dynamic habitats in a glacial microrefugium.

List of Abbreviations

ca.	*circa*
CHO-7	Choremi 7
CO_2	Carbon dioxide
DEH	Dental Enamel Hypoplasia
e.g.	*exempli gratia*
EMPT	Early-Middle Pleistocene Transition
i.e.	*id est*
IRMS	Isotope Ratio Mass Spectrometry
ka	*kilo annum*
KYP-3	Kyparissia 3
KYP-4	Kyparissia 4
KYP-T	Kyparissia T
LGM	Last Glacial Maximum
LI	Lignite seam I
LII	Lignite seam II
LIII	Lignite seam III
Ma	*mega annum*
MAR-1	Marathousa 1
MAR-2	Marathousa 2
m.a.s. l	meters above sea level
Mb	Member
MIS	Marine Isotope Stage
M3	Permanent upper third molar
I1	Upper first incisor
TRP-4	Tripotamos 4
spp.	species (plural)
VPDB	Vienna Peedee Belemnite
VSMOW	Vienna Standard Mean Ocean Water
‰	per mille

List of Figures

–This page is left intentionally blank –

1 Introduction

1.1. Theoretical background

The Middle Pleistocene (0.78–0.12 Ma) is a period of great importance for hominin evolution and dispersal across Africa and Eurasia. The presence of hominins in the latter dates back to the Early Pleistocene (~1.8 Ma) (Gabunia et al., 2000; Garcia et al., 2010); however, early hominin occurrences in the Eurasian fossil record remain scarce. On the contrary, compelling evidence for the establishment of persistent populations in the Eurasian continent exists from the early Middle Pleistocene (ca. 700 ka) onwards (Gamble, 2017; Moncel et al., 2021; Rodríguez et al., 2022). Emerging research also highlights a contemporaneous shift in lithic technology and the spread of bifacial stone tool production in Southwest Europe (Moncel & Ashton, 2018; Moncel et al., 2020), among other innovations and adaptations (Galway-Witham et al., 2019; Mondanaro et al., 2020; Roebroeks, 2001).

The pattern of hominin dispersal and the associated biological, behavioural, and cultural shifts are often correlated to environmental and climatic forces (Blain et al., 2021; Moncel et al., 2018; Timmermann et al., 2022). The dawn of this gradual transformation can be traced to the Early–Middle Pleistocene transition (EMPT), otherwise known as the “Middle Pleistocene Revolution”, a global climatic transition in glacial-interglacial periodicity from ~40 thousand years (ka) cycles to ~100 ka cycles, that took place between 1.4 and 0.4 My (Berends et al., 2021; Head & Gibbard, 2015; Herbert, 2023). The EMPT was also characterized by higher amplitude variability in global climate and greater intensity of glacials and interglacials, which intensified after 900 ka and persisted until ~420 ka (MIS 12–11 transition). The event was further accompanied by increased expansion of ice sheets, significant sea level changes (Herbert, 2023), as well as progressively increasing seasonality and aridity (Fidalgo, Rosas, Bartolini-Lucenti, et al., 2023; Joannin et al., 2007; Palombo, 2014; Strani et al., 2019).

The climatic shifts of the EMPT subsequently encouraged a biotic turnover. A major gradual restructuring in vegetation communities occurred from ~900 ka onwards. A number of studies have demonstrated the disappearance of sub-

tropical ecosystems and the subsequent expansion of open landscapes, as a response to aridification. Alternations between wooded steppe/steppe vegetation and thermophilous arboreal taxa in the Mediterranean region paralleled glacial/interglacial cyclicity (Bertini et al., 2015; Magri et al., 2017; Panagiotopoulos et al., 2020 and references therein). The extensive pollen record of the Tenaghi Philippon (Greece) sequence indicates that the Balkan peninsula experienced a notable decrease in floristic diversity after MIS 16 (676–621 ka) (Tzedakis et al., 2006). An increase in the abundance of *Quercus* (oak) around the same time marked the establishment of a more Mediterranean-type climate with drier conditions (Margari et al., 2018; Tzedakis et al., 2006). The spread of more open landscapes during the EMPT enabled the migration and dispersal of African and Palearctic faunal elements —some of which were well-adapted to grasslands and open habitats— into Eurasia. Major consecutive biotic events resulted in the "late Villafranchian–Epivillafranchian/Galerian large mammal turnover", which saw the disappearance of several late Villafranchian taxa, such as the mammoth *Mammuthus meridionalis* and the hyena *Pachycrocuta*, and the appearance of migrant carnivoran taxa, e.g., *Crocuta crocuta* and *Panthera pardus*, as well as large herbivores, e.g., *Cervus elaphus, Sus scrofa, Mammuthus trogontherii,* and *Palaeoloxodon,* in the continent (Konidaris & Kostopoulos, 2024; Palombo, 2014; Strani et al., 2021).

Among them, the genus *Palaeoloxodon*, commonly referred to as straight-tusked elephants, originated in Africa and migrated towards Eurasia through the Levantine corridor at the end of the Early Pleistocene (Saegusa et al., 2009). Since then, palaeoloxodonts dispersed rapidly to Europe and Asia, where they comprised a common component in the Middle–Late Pleistocene faunal assemblages of the continent. The oldest occurrences of the genus are recorded in SW Europe close to the Early/Middle Pleistocene boundary (0.9–0.8 My) with the European straight-tusked elephant *Palaeoloxodon antiquus* (Davies, 2002; Palombo et al., 2010; Palombo, 2017). The species derived from the Pliocene–Pleistocene East African *Palaeoloxodon recki,* which migrated to Eurasia at ~1.0 Ma (Athanassiou, 2022a). In the northern latitudes of Europe (i.e., central Europe, which represents the northern-most limit of the *P. antiquus* known expansion; Palombo et al. 2010: fig. 6), *P. antiquus* was widely distributed during interglacial or interstadial phases,

whereas during the intervening glacial stages, when open habitats with cold- and drought-tolerant taxa prevailed, the range of the taxon was mostly restricted to southern European regions, which acted as refuge areas for temperate biomes (Lister, 2004; Tsoukala & Lister, 1998). The climatic cooling and the associated vegetational shifts, i.e., a trend to more open, steppic landscapes, at the end of the Eemian (MIS 5e), resulted in the reduction of its population in northern and central Europe. Since then, the species is assumed to have persisted mostly in southern Mediterranean regions (but see Mol et al., 2007 for the Netherlands) until the last glacial period of the Late Pleistocene (Athanassiou, 2022a; Braun & Palombo, 2012; Palombo, 2017; Stuart, 2005). *Palaeoloxodon antiquus* occupied a broad spectrum of habitats, including mild humid, warm to warm-temperate environments, with moderately wooded to wooded landscapes, as well as wooded or even arid grasslands (Davies, 2002; Palombo et al., 2010). Dental micro- and mesowear analyses indicate that *P. antiquus* demonstrated high dietary flexibility, exhibiting foraging behaviour that ranged from exclusively browsing to grazing depending on the available resources (Rivals et al., 2019; Saarinen & Lister, 2016). Despite its ecological adaptability, the environmental tolerances of the species are generally associated with temperate climatic conditions.

Another megaherbivore of African origin that became widely dispersed in Eurasia at the onset of the EMPT is *Hippopotamus* spp. The earliest occurrence of the genus *Hippopotamus* in Eurasia is thought to date to the Early Pleistocene (~2.0 Ma). The early fossil record of the taxon in Europe is sparse and includes specimens from Elis (Greece), Fontana Acetosa and Chiusi Basin (Italy), as well as Mencal-9 (Spain) (Athanassiou, 2022b; Fidalgo, Rosas, Madurell-Malapeira, et al., 2023; Iannucci et al., 2023; Mecozzi, 2023 and references therein). After ca. 1.5 My, the European *Hippopotamus antiquus* was widely diffused in the northern circum-Mediterranean regions, whereas even northern and central European latitudinal expansions beyond the Mediterranean were discontinuous and mostly associated with interglacial periods (Athanassiou, 2022b; Konidaris & Kostopoulos, 2024; Martínez-Navarro et al., 2015). During the Epivillafranchian, the species reached its apparent maximum geographic range, expanding to the United Kingdom, Germany, the North Sea, and the Netherlands (Adams et al., 2022; Fidalgo, Rosas, Madurell-Malapeira, et al., 2023 and references therein; Kahlke, 2001). The distribution patterns of *Hippopotamus antiquus* in the fossil record reveal a

preference for humid, temperate environments (Fidalgo, Rosas, Madurell-Malapeira, et al., 2023 and references therein), while a higher affinity to aquatic habits in comparison to extant hippopotamus has been implied for this species, based on isotopic and anatomical indices (Palmqvist et al., 2003; Palmqvist et al., 2022). Nonetheless, the ecological tolerances and the niche of the species remain uncertain until now (Fidalgo, Rosas, Madurell-Malapeira, et al., 2023). Despite the debate surrounding its last occurrence, the species' extinction could tentatively be correlated to MIS 11 (Marra et al., 2018). In the second half of the Middle Pleistocene, *H. antiquus* was gradually replaced by the smaller in size *Hippopotamus amphibius* (Athanassiou et al., 2018; G. Konidaris et al., 2023; Martino & Pandolfi, 2022).

Previous studies have established that climatic instability and the intensity of glacial episodes during the Middle Pleistocene had a significant influence on the phylogeny, demography, and biogeography of several vertebrate and plant taxa (Dennell et al., 2011; Koutsodendris et al., 2019; Macaluso et al., 2023; Magri & Palombo, 2013; Scotti-Saintagne et al., 2021; Stewart et al., 2010; Tzedakis et al., 2006), among which *P. antiquus* and *H. antiquus*. Both taxa demonstrated wide biogeographic ranges during warmer, interglacial periods but their populations contracted to Southern European refugial areas during glacial periods (see Fidalgo et al., 2024; Fidalgo, Rosas, Madurell-Malapeira, et al., 2023; G. Konidaris et al., 2023 for *H. antiquus* and Athanassiou, 2022a; Davies, 2002; Palombo et al., 2010 for *P. antiquus*). The same has been hypothesized also for Pleistocene hominins, including the Middle Pleistocene *Homo heidelbergensis* (*sensu lato*) (Dennell et al., 2011; Harvati & Reyes-Centeno, 2022; Roksandic et al., 2018; Stewart & Stringer, 2012), which is considered to have shared a similar ecological niche as the two megaherbivores and a preference for temperate environments (G. E. Konidaris & V. Tourloukis, 2021; Trájer, 2024).

The concept of glacial refugia in Europe was originally applied to temperate and boreal plant and animal taxa, whose geographical distribution was restricted to South European peninsulas, i.e. the Iberian, Italian, and Balkan peninsulas, during the Last Glacial Maximum (LGM) (Bennett et al., 1991; Hewitt, 1999, 2000; Svenning et al., 2008). Since then, the concept has expanded to include various scenarios of shifting species biogeography and biodiversity. In general, it defines

an area in which organisms persist through unfavourable conditions (or through glacial/interglacial cycles) and from which they can potentially expand but, depending on the parameters considered, the definition may differ (e.g., macro- and micro-refugia, *in-situ* or *ex-situ*; see Tzedakis et al., 2013 and Jones, 2022 for an overview). Nonetheless, the "traditional" refugia —the South European peninsulas— continue to be pertinent in Paleolithic archaeology.

In the Balkan Peninsula, a plethora of studies investigating the status of Pleistocene refugia have focused on the Greek record (Jones, 2022). The more or less continuous presence of temperate biomes, including thermophilous and mesophilous taxa, relict sub-tropical species, and several warm-adapted faunal elements, many of which persisted locally, evolved or adapted, and re-colonized northern latitudes despite the climatic fluctuations and the glacial intensity of the Pleistocene, shows that the region featured important refugial areas. Here, the concept of the "refugium within refugium" (Gómez & Lunt, 2007) is preferred, since this scale of analysis takes into account the variable topography and microclimatic conditions of the region under study, as well as the fragmentary nature of suitable habitats for temperate biota. The term, which is hereafter treated as synonymous with "microrefugium" (Jones, 2022), defines a single, smaller area within the major, traditional refuge region (e.g., Greece or the Balkan Peninsula), in which a population persisted through the adverse glacial or stadial conditions. Within this interpretative context, ample archaeological and paleoenvironmental evidence has been provided for the Late Pleistocene refugial nature of the Peloponnese and Epirus in Greece (e.g., Karaiskou et al., 2014; Roditi & Starkovich, 2022; Tourloukis & Harvati, 2018; Tzedakis et al., 2003; Tzedakis et al., 2004); however, the Middle Pleistocene archaeological record remains limited and knowledge of the dominant climatic and vegetative dynamics during that time in the region is still scanty (Tourloukis & Harvati, 2018; Tourloukis & Karkanas, 2012).

1.2 The Megalopolis Basin: A putative micro-refugium in central Peloponnese

In the Megalopolis Basin (Central Peloponnese, Greece), recent research efforts have given prominence to its potential role as a microrefugium (e.g., Field et al., 2018; G. Konidaris et al., 2023; Konidaris et al., 2022; Konidaris et al., 2024;

Konidaris et al., 2018; Michailidis et al., 2018; Vlachos & Delfino, 2016). The locale is an intramontane tectonic half-graben extending to an area of 250 km², with its main axis running in a northwest-southeast direction. It is flanked by the Mainalo, Lykaion, and Taygetos mountain ranges to the east, west, and south, respectively. The basin, situated at an altitude of ~330–450 meters above sea level, developed on the Mesozoic to Paleogene bedrock of the Peloponnese during the Late Miocene to Pliocene epoch. During the Early to Middle Pleistocene, lacustrine and fluvio-lacustrine deposits testify to the periodic presence of a large lake (Van Vugt et al., 2000; Vinken, 1965).

The Megalopolis Basin has yielded rich Pleistocene faunal assemblages through a long-spanning stratigraphic sequence, including temperate species such as the Barbary macaque *Macaca sylvanus*, the European pond turtle *Emys orbicularis,* and several temperate-adapted birds (Athanassiou et al., in press; Athanassiou et al., 2018; Konidaris et al., 2022; Konidaris et al., 2018; Michailidis et al., 2018; Vlachos & Delfino, 2016; Vlachos et al., in press). The abundance of *Palaeoloxodon antiquus* and *Hippopotamus antiquus* remains through multiple chrono-stratigraphic periods is noteworthy and known from past decades of fieldwork, although many specimens lacked precise stratigraphic context (Athanassiou, 2022a, 2022b; Melentis, 1965; Melentis, 1961, 1963). Recent fieldwork by a collaborative team from the Ephorate of Palaeoanthropology-Speleology of the Hellenic Ministry of Culture (Greece) and the University of Tübingen (Germany) targeting the Middle Pleistocene Marathousa Member (Mb) of the Choremi Formation (Vinken, 1965) within the Megalopolis lignite mines has identified several new fossil-bearing sites and recovered hippopotamuses and elephants, among other vertebrate fossils, from well-defined stratigraphic contexts (Athanassiou, 2018; Athanassiou et al., in press; Athanassiou et al., 2018; Karkanas et al., in press; Konidaris et al., 2024; Konidaris et al., 2018; Thompson et al., 2018). The deposits of the Choremi Formation capture the transition of the basin's environment from a lacustrine (Marathousa Mb) to a fluvial (Megalopolis Mb) one (Van Vugt et al., 2000). The Marathousa Mb, representing the period between ca. 900–300 ka, comprises a series of three main lignite seams —abbreviated as LI, LII, and LIII and further subdivided into smaller lignitic units (LIa–c, LIIa–b, LIIIa–c)— alternating with clastic sediments (Tourloukis, Muttoni, et al., 2018; Van Vugt et al., 2000). The recurring deposition of lignite and detrital units reflects

the cyclicity of limnic to limnotelmatic conditions during interglacial/glacial oscillations, respectively (Karkanas et al., 2018; Okuda et al., 2002; Vinken, 1965). The fossil-bearing deposits are found within the clastic units and are thus considered to be associated with glacial (or stadial) periods. The excellent preservation of organic remains and the abundance of faunal materials recovered from the extensive, successive deposits of the Megalopolis Basin provide the opportunity for a multi-disciplinary diachronic paleoenvironmental investigation, encompassing a climatically and environmentally turbulent phase for European ecosystems.

In addition to faunal and palaeobotanical remains, traces of hominin presence, namely lithic artifacts and human-induced taphonomic alterations on bones, were unearthed at the sites of Marathousa 1 (MAR-1; ca. 430 ka) (Panagopoulou et al., 2018; Tourloukis, Thompson, et al., 2018), Marathousa 2 (MAR-2, ca. 450 ka)(Karkanas et al., in press; G. Konidaris et al., 2023), Kyparissia 3 (KYP-3; ca. 650 ka), Kyparissia 4 (KYP-4; ca. 700 ka), Tripotamos 4 (TRP-4; ca. 400 ka), and Choremi 7 (CHO-7; ca. 280 ka) (Karkanas et al., in press; Konidaris et al., 2024). The first discovery of archaeological evidence attributed to the Lower Paleolithic in the Megalopolis Basin came from Marathousa 1, stratigraphically placed between LIIb and LIIIa (Panagopoulou et al., 2018; Tourloukis, Muttoni, et al., 2018; Tourloukis, Thompson, et al., 2018). The site yielded associated cultural, faunal, and botanical remains dated to ca. 430 ka (glacial MIS 12), among which the partial skeleton of a butchered straight-tusked elephant (Field et al., 2018; Konidaris et al., 2018; Panagopoulou et al., 2018; Tourloukis, Thompson, et al., 2018). Until recently, Marathousa 1 was considered the oldest open-air archaeological site in Greece and Southeast Europe (Tourloukis & Harvati, 2018). However, the latest discovery of lithic artifacts at Kyparissia 4, situated close to the top of LI shortly after the Matuyama/Bruhnes reversal (LIb, 780 ka) and dated between 780 ka and ca. 670 ka based on biochronological data, has now pushed back the earliest evidence of hominins in Greece (Karkanas et al., in press; Konidaris et al., 2024; van Kolfschoten et al., in press).

1.3 Methodological Background: Stable and radiogenic isotopes in paleoecology

Stable and radiogenic isotope analyses provide a rigorous approach to exploring the paleoecology of extinct species. Applications of isotopic analyses on fossil mammalian skeletal tissues provide valuable insights into a taxon's diet, habitat preference, trophic position, physiology, and mobility patterns, while they can further derive environmental and climatic conditions (e.g., Bocherens & Drucker, 2013; Bocherens et al., 1996; Britton, 2020; Kohn & Cerling, 2002; Schwarcz et al., 2010). Widespread and well-established stable and radiogenic isotopic approaches comprise carbon, oxygen, and strontium analyses of mammalian tooth enamel. Enamel, dentine, and bone consist of an inorganic fraction, a calcium-phosphate-based mineral called bioapatite, and an organic fraction, i.e., proteins and collagen. The inorganic component of enamel is notably higher (~95% by weight) in comparison to dentine and bone (70% and 65% by weight, respectively), making it more resistant to post-depositional, diagenetic alterations (Koch et al., 1997; LeGeros, 1991; Wang & Cerling, 1994). In conjunction with the highly mineralized nature of the tissue, the denser and less porous crystalline structure of enamel bioapatite justifies the advantage of dental enamel proxies over bone and dentine in extracting information from deep-time assemblages and regions with unfavourable conditions for collagen preservation, such as Greece (Iliopoulos & Stathopoulou, 2023). Enamel forms in an accretionary manner and, unlike bone, does not remodel after its formation and mineralization, thereby recording isotopic information within finite time intervals in each increment (Lee–Thorp, 2002). Within a single tooth, the temporal resolution of isotopic variability largely depends on the time of tooth formation and the processes surrounding enamel apposition and mineralization (Norwood et al., 2023; Passey & Cerling, 2002; Passey, Cerling, et al., 2005; Zazzo et al., 2005; Zazzo et al., 2012). When incremental sampling is employed, intra-tooth variation in stable and radiogenic isotopic ratios could therefore represent short-term, infra-annual or multi-annual changes.

Carbon isotopes (^{13}C /^{12}C)

Carbon isotope ratios ($^{13}C/^{12}C$) —expressed as $\delta^{13}C$* — in herbivore enamel serve as a critical method for inferring the diet of primary producers and reconstructing their preferred foraging habitats. The carbon isotopic values in herbivore enamel bioapatite trace the carbon isotopic composition of the bulk vegetation comprising the animal's diet at the time of tooth mineralization (Bocherens & Drucker, 2013; Bocherens et al., 1996; DeNiro & Epstein, 1978), with a quantifiable isotopic fractionation due to metabolic and physiological processes (Cerling et al., 2021; Cerling & Harris, 1999; Passey, Robinson, et al., 2005). Naturally occurring variation in the carbon isotopic composition of terrestrial plants is primarily influenced by carbon fixation and the photosynthetic pathway they utilize (C_3, CAM, C_4) (Bender, 1971; Farquhar et al., 1989). In modern terrestrial ecosystems, plants using the C_3 photosynthetic pathway (or Calvin cycle), comprising trees, shrubs, and cool-season grasses, typically exhibit $\delta^{13}C$ values between −36‰ and −22‰, with an average $\delta^{13}C$ of −27‰ (Farquhar et al., 1989; Kohn, 2010; Metcalfe, 2021; O'Leary, 1988). In contrast, C_4 plants, predominantly warm-season tropical grasses and sedges, demonstrate substantially higher $\delta^{13}C$ values ranging between −17‰ and −9‰ with an average $\delta^{13}C$ of −13‰. Plants using the Crassulacean acid metabolism (CAM) for photosynthesis exhibit intermediate values between the C_3 and C_4 vegetation; however, CAM plants, mostly cacti and succulents, usually don't contribute significantly to the diet of herbivores.

The wide range (~14‰) of $\delta^{13}C$ values in C_3 vegetation is a result of additional intrinsic and extrinsic, environmentally controlled variation. Environmental controls of $\delta^{13}C_{C3}$ include CO_2 respiration, irradiance, soil salinity, temperature, and precipitation. Under conditions of water stress and/or reduced atmospheric CO_2 pressure (pCO_2), C_3 plants demonstrate an enrichment in the heavier isotope (^{13}C), resulting in higher $\delta^{13}C$ values. On the other hand, lower light intensity, higher humidity, and the contribution of ^{13}C-depleted carbon dioxide produced by decomposing leaf litter influence the isotopic signatures of plants growing under closed canopy conditions towards lower $\delta^{13}C$ value (Kohn, 2010; van der Merwe & Medina, 1991; Vogel, 1978). This range of environmental variation in C_3 vegetation

*Carbon isotopic abundances are expressed as δ (delta) values, wherein $\delta^{13}C = [(^{13}C/^{12}C)_{sample}/(^{13}C/^{12}C)_{standard} - 1] \times 1000$ (‰, VPDB).

communities can be used to deduce the habitat composition and foraging conditions of primary producers, distinguishing between more open landscapes and/or xeric conditions, which will be reflected in higher $\delta^{13}C_{enamel,}$ and more densely forested and/or humid environments, expected to manifest as lower $\delta^{13}C_{enamel}$ values (Drucker et al., 2008) (Figure 1).

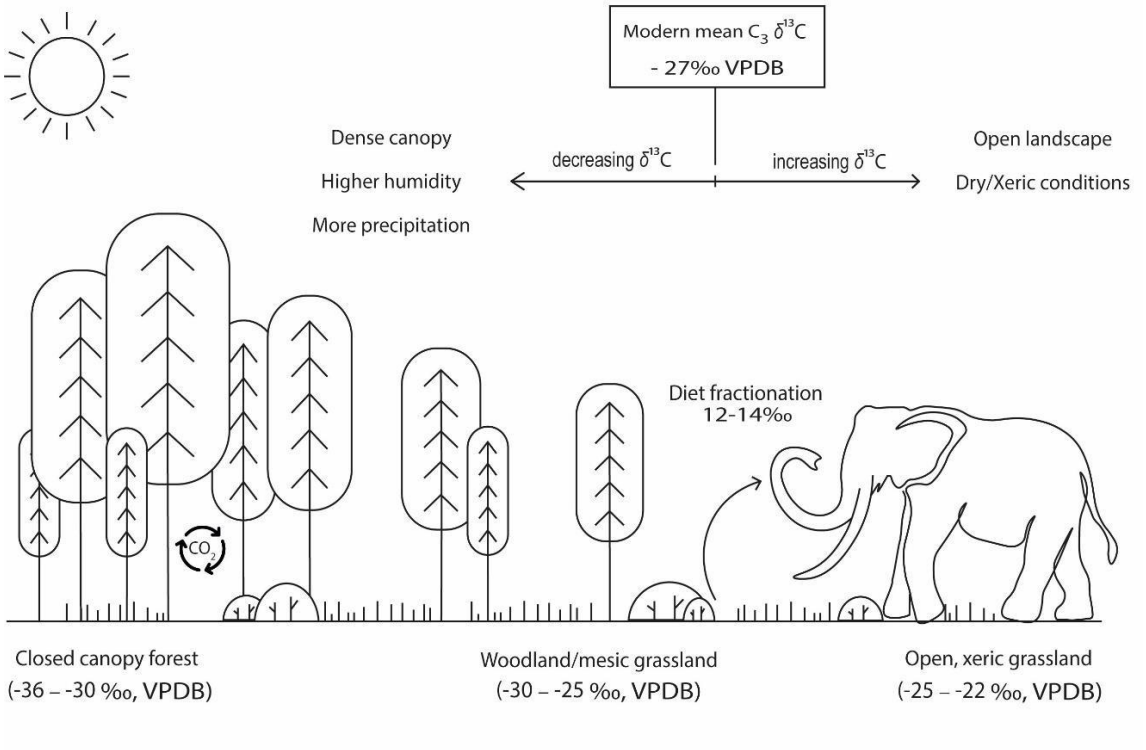

Figure 1: *Simplified schematic illustration of carbon isotope (^{13}C /^{12}C) variation in modern C_3 ecosystems and herbivore tooth enamel. Cut-off values for different habitats are based on Metcalfe, 2021 and Kohn, 2010.*

Oxygen Isotopes ($^{18}O/^{16}O$)

Oxygen isotope ratios ($^{18}O/^{16}O$)—reported using the delta notation as $\delta^{18}O$[†]— in mammalian skeletal tissues derive from the oxygen isotopic composition of body water (Bryant & Froelich, 1995; Longinelli, 1984; Sponheimer & Lee-Thorp, 1999). The $\delta^{18}O$ signature of the latter is accordingly determined by oxygen fluxes related to the animal's physiology and metabolism, for instance, respiration and water loss through urination, as well as drinking behaviour and the isotopic composition of ingested water (Britton, 2020; Kohn, 1996; Pederzani & Britton, 2019). Evaporation-insensitive (or obligate-drinking) taxa, such as elephants, that obtain

[†] $\delta^{18}O = [(^{18}O/^{16}O)_{sample}/(^{18}O/^{16}O)_{standard} - 1] \times 1000$ (‰, VSMOW)

water primarily through drinking from meteoric water sources, are expected to reflect more faithfully the isotopic composition of local water bodies, in comparison to evaporation-sensitive (non-obligate drinking) herbivores, which reflect the oxygen isotopic composition of food sources (i.e., leaf water), subjected to additional fractionation (Levin et al., 2006).

Oxygen isotopes in the global water cycle and, by extension, mammalian skeletal tissues bespeak geospatial and climatic influences (Britton, 2020; Dansgaard, 1964; Pederzani & Britton, 2019; Sponheimer & Lee-Thorp, 1999). Broader geographical variability in the oxygen isotopic composition of meteoric water is partly a function of decreasing $\delta^{18}O$ values of precipitation with increasing distance from the coast due to progressive rainout. An altitudinal effect is also created by progressive rainout, leading to elevated $\delta^{18}O$ values with decreasing elevation (Britton et al., 2009; Dansgaard, 1964; Pederzani & Britton, 2019; Rozanski et al., 1993). On a local, site-specific scale, the $\delta^{18}O$ of meteoric water in middle and high-latitude regions, such as Greece, is most prominently governed by the oxygen isotopic composition of precipitation and the effects of temperature upon it (Argiriou & Lykoudis, 2006; Britton, 2020; Dotsika et al., 2010; Pederzani & Britton, 2019; Rozanski et al., 1993). In this context, lower $\delta^{18}O_{\text{enamel bioapatite}}$ values are usually characteristic of cooler and more humid climatic conditions, and higher enamel oxygen isotopic ratios are indicative of warmer conditions and/or higher aridity (Bocherens & Drucker, 2013; Britton, 2020; Dansgaard, 1964; Pederzani & Britton, 2019; Rozanski et al., 1993). When incremental sampling of tooth enamel is applied at an appropriate resolution, variability in oxygen stable isotope ratios within a single tooth is expected to reflect the temperature and precipitation effect on a sub-annual scale, thus permitting investigations of seasonality, wherein the cooler and wetter winter months demonstrate lower $\delta^{18}O$ values, while elevated $\delta^{18}O$ values characterise warm and dry summers. The aforementioned geographical and environmental controls upon the oxygen isotopic composition of water bodies and, subsequently, enamel bioapatite, permit the use of stable oxygen isotopes for paleoclimatic reconstructions and studies of past mobility (Bocherens & Drucker, 2013; Britton, 2020; Pederzani & Britton, 2019).

Hydrological processes can complicate the relationship between $\delta^{18}O_{\text{source water}}$ and $\delta^{18}O_{\text{precipitation}}$ (Bocherens & Drucker, 2013; Pederzani & Britton, 2019). Long-

resident water bodies, such as lakes, are subjected to isotopic mixing of distinct seasonal rainfall signatures, resulting in isotopic averaging and dampening of the infra-annual oxygen isotopic variability. In such cases, the incremental variability of enamel bioapatite will also appear attenuated (Pederzani & Britton, 2019; Steinman & Abbott, 2013; Stuart-Williams & Schwarcz, 1997; Vystavna et al., 2021). Additionally, the influx of non-local water, for instance, water originating from higher altitudes or glacial meltwater, could further alter the isotopic composition of the source water, leading to lower $\delta^{18}O$ values than precipitation and obscured seasonal signals (Pederzani & Britton, 2019; Rank et al., 2018; Rodhe, 1998). Despite the good correspondence between $\delta^{18}O_{water}$ and $\delta^{18}O_{precipitation}$ obtained from several stable isotopic studies of obligate-drinking terrestrial taxa, close consideration must be given to the influence of such processes when interpreting $\delta^{18}O_{enamel}$ (Figure 2).

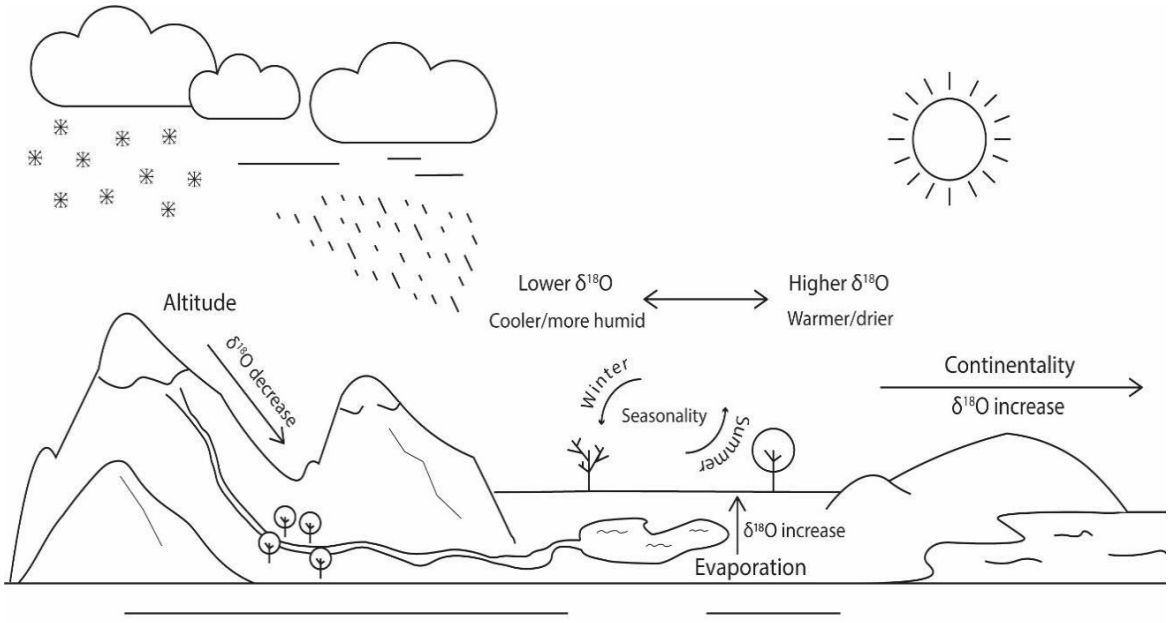

***Figure 2**: Schematic illustration of various sources influencing variation in oxygen isotopic ratios ($^{18}O/^{16}O$) of water bodies and, subsequently, tooth enamel (based on Pederzani & Britton, 2019).*

Strontium isotopes ($^{87}Sr/^{86}Sr$)

In terrestrial ecosystems, strontium is sourced from the erosion of local geological substrates, upon which it is released into soils, groundwater, or surface water sources and is subsequently absorbed by plants (Bentley, 2006; Capo et al., 1998; Price et al., 2002). The dominant control of $^{87}Sr/^{86}Sr$ ratios in soils and water

bodies is the local geological substrate. The strontium isotope composition of the parent bedrock material varies according to the geochemical composition of the bedrock and its age (Bataille et al., 2020; Bentley, 2006; Britton, 2020; Capo et al., 1998; Price et al., 2002). Following the principle of radioactive decay, ^{87}Rb (Rubidium) decays to ^{87}Sr, with a half-life of 4.96 × 1010 (Rotenberg et al., 2012). Over the course of geological time, rocks are progressively enriched in ^{87}Sr while the amount of ^{86}Sr remains constant. This results in isotopically distinct signatures, wherein older geological units will have higher $^{87}Sr/^{86}Sr$ ratios than younger ones. Nonetheless, deviations from the local bedrock strontium signature can be introduced due to atmospheric deposition (e.g., sea spray, exogenous dust), necessitating prior establishment of a multi-proxy strontium reference baseline and investigations on the contribution of non-local strontium sources (Bataille et al., 2020; Capo et al., 1998; Crowley et al., 2017; Frank et al., 2021; Wallace, 2018).

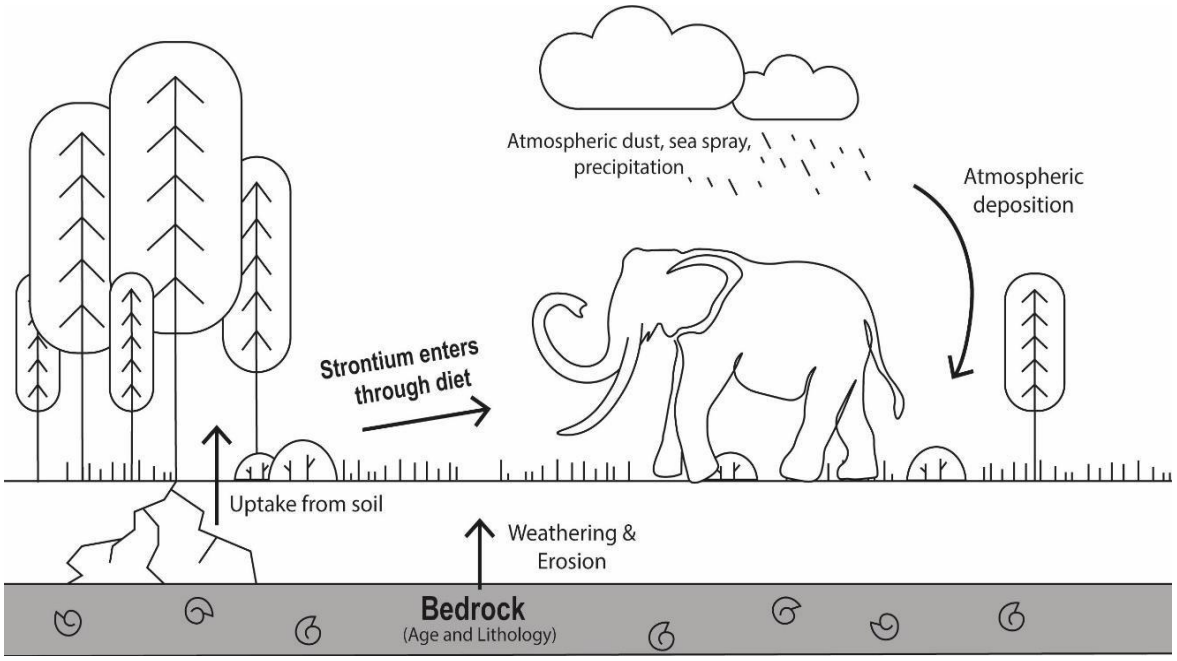

***Figure 3**: Simplified visualization of strontium isotope cycling in terrestrial ecosystems (adapted from Bataille et al. 2020).*

The strontium isotopic composition of herbivore enamel reflects that of ingested vegetation, which is primarily influenced by the local soil $^{87}Sr/^{86}Sr$ ratios, and to a lesser extent that of ingested water (Bataille et al., 2020; Bentley, 2006; Britton, 2020; Price et al., 2002; Slovak & Paytan, 2012). Within the food chain, primary consumers assimilate strontium through their diet and, unlike with carbon and oxygen stable isotopes, $^{87}Sr/^{86}Sr$ ratios are not modified by biological processes

between the source and the target tissue (i.e., fractionation) (Flockhart et al., 2015). Thus, incremental enamel $^{87}Sr/^{86}Sr$ ratios reflect the average strontium dietary intake at the time of enamel formation and maturation, and can be directly compared to biogenic (floral and faunal), soil, and bedrock strontium isotopic signatures from the area of interest, to determine the provenance and investigate movement patterns in animals and humans. When strontium isotope ratios are combined with oxygen and carbon isotope analyses, they can provide inferences for landscape use (Figure 3).

2 Objectives and research design

Considering the significance of the Mid-Pleistocene Transition for the evolution of both modern terrestrial ecosystems and hominin lineages in Eurasia, the paucity of paleoclimatic and paleoenvironmental data from the Middle Pleistocene in comparison to the preceding (Pliocene–Early Pleistocene) and succeeding (Late Pleistocene) periods is problematic. Recent efforts to elucidate the environmental context that facilitated hominin adaptations and shaped behavioural, cultural, and social dynamics during this timeframe have brought forth the remarkable regional variability in ecosystem and environmental conditions, governed by altitudinal, latitudinal, and topographic differences across and within the regions (e.g., Magri et al., 2017; Palombo, 2016). This raises the necessity to construct local-scale datasets before a broader synthesis of the evidence can be achieved.

Ensuing this concept, the principle aim of this doctoral research was to evaluate the status of the Megalopolis Basin as a potential glacial microrefugium for both fauna and hominin populations during the Middle Pleistocene. The absence of fossil hominin specimens from the region omitted a direct application of biogeochemical methods from investigations of the hominin paleoenvironmental niche in the basin. To address the situation, an approach exploring individual megaherbivore ecologies with a clear connection to anthropogenic activity was implemented. The European straight-tusked elephant *Palaeoloxodon antiquus* constituted an important food resource for hominins in Eurasia since the late Early/early Middle Pleistocene (Agam & Barkai, 2018; Gaudzinski-Windheuser et al., 2023; G. Konidaris & V. Tourloukis, 2021; Palombo & Cerilli, 2021; Starkovich, 2023). On the other hand, the exploitation of *Hippopotamus antiquus* was seemingly not practised as frequently, based on the scarce occurrence of anthropogenic marks on specimens belonging to this taxon, despite its abundance in the Eurasian fossil record (Fidalgo, Rosas, Madurell-Malapeira, et al., 2023; G. Konidaris et al., 2023 and references therein); nonetheless, the Megalopolis Basin has provided one of the few cases where hippopotamus remains exhibit anthropogenic modifications, indicative of carcass exploitation (Konidaris et al., 2023). The direct (e.g., cutmarks, percussion marks) or contextual association of the faunal remains to hominin occupancy in the area (Athanassiou et al., in press;

Karkanas et al., in press; G. Konidaris et al., 2023; Konidaris et al., 2024; Konidaris et al., 2018; Tourloukis, Thompson, et al., 2018) provided the opportunity to extend environmental and climatic inferences from the faunal remains to the reconstruction of the hominin paleoecological niche (Figure 4).

The main objectives of this work were:

1) to reconstruct the ecological characteristics of two extinct Middle Pleistocene megaherbivores, *Palaeoloxodon antiquus* and *Hippopotamus antiquus*.
2) to identify potential temporal differences in the ecological attributes of the aforementioned taxa between ~700 ka to 430 ka, and, by extension, in climatic or environmental conditions.
3) to provide a high-resolution landscape, climate, and hydrological reconstruction of the prevailing conditions in the Megalopolis Basin during the Middle Pleistocene hominin occupation.

To meet the aforementioned research objectives, three case studies employed stable (carbon and oxygen) and radiogenic (strontium) isotopic techniques on *Palaeoloxodon antiquus* and *Hippopotamus antiquus* specimens. **Study I** (Appendix A) provides an inter-regional comparison of *P. antiquus* stable isotopic data from the Megalopolis Basin to specimens from other Pleistocene European contexts, aiming to examine the range of variation in habitat and climatic preferences and/or tolerances of the species. In addition, this study was directed towards evaluating potential disparity in the environmental conditions between inter-glacial sites and Marathousa-1 in the Megalopolis Basin. **Study II** (Appendix B) expanded on the ecological investigation of the extinct proboscidean to provide temporally high-resolute, infra-annual inferences on its habitat and mobility patterns, as well as the climatic conditions surrounding its habitation within the region of interest. Here, a multi-isotope approach was implemented with the inclusion of strontium isotopes next to carbon and oxygen isotopic analyses. Finally, **Study III** (Appendix C) focuses on the exploration of the *Hippopotamus antiquus* ecology in the Megalopolis Basin through different chrono-stratigraphic phases, spanning from ca. 700 to 430 ka. The application of incrementally sampled carbon and oxygen isotopes on *Hippopotamus* teeth enabled the examination of seasonal and multi-annual dietary and hydrological changes, offering insights into

the species' adaptability and resilience to climatic and environmental fluctuations over time. Each of these studies provided a window into the ecological tolerances and adaptations of the two megaherbivores, but also into the conditions surrounding the presence of Middle Pleistocene hominins in the area.

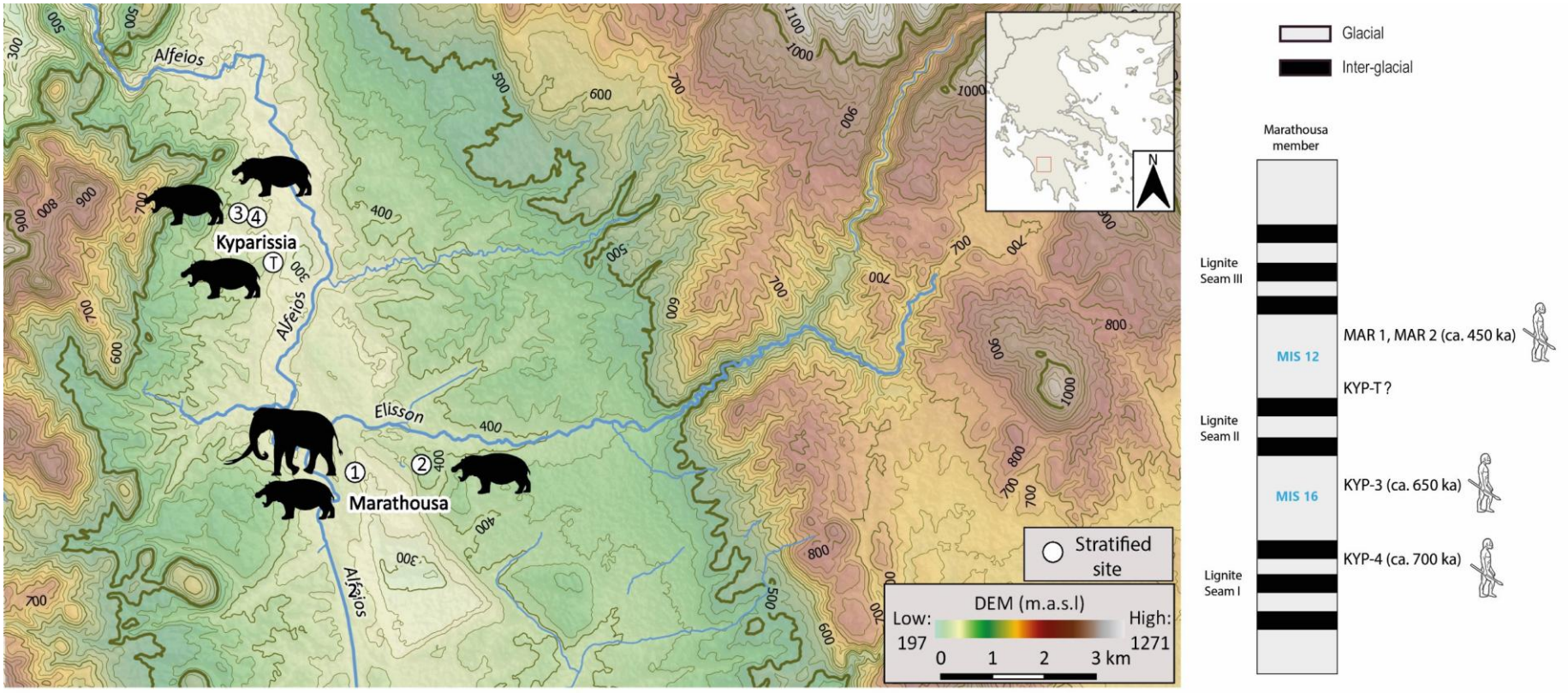

Figure 4: Left: Map of the Megalopolis Basin showing the geographical location of the studied specimens. Right: Simplified illustration of the stratigraphic position of the specimens. The straight-tusked elephant from MAR-1 (ca. 430 ka) and the hippopotamus from MAR-2 (ca 450 ka) are directly associated with hominins through the presence of cutmarks on a few skeletal elements. The hippos from KYP-3 (ca. 650 ka) and KYP-4 (ca.700 ka) are spatially and stratigraphically associated with lithic artefacts. The hippo from MAR-1 post-dates the archaeological horizon (ca. 430 ka). Finally, there is no anthropogenic evidence linking the hippo from KYP-T to hominin activity at the site.

3 Results and discussion

This chapter provides an overview of the methodological approaches and key findings from the articles comprising this dissertation, as listed in the List of Publications and detailed in the APPENDIX. In-depth methodological discussions for each case study are provided within the respective manuscripts.

3.1 Study I (Appendix A)

To explore the paleoenvironmental context of hominin occupation in the Megalopolis Basin and its potential significance as a glacial refugium in the Middle Pleistocene epoch, the first study investigated the broader foraging habitat and climatic context of a *Palaeoloxodon antiquus* individual from the open-air site of Marathousa 1 (MAR-1). The partial skeleton of the straight-tusked elephant was excavated *in situ* from unit UA3c in Area A (Giusti et al., 2018; Karkanas et al., 2018; Konidaris et al., 2018; Panagopoulou et al., 2018). The stratigraphic sequence of MAR-1, which was systematically excavated between 2014 and 2019, has been dated to ca. 430 ka and correlated to the glacial MIS 12 on the basis of radiometric, biochronological, and magnetostratigraphic evidence (Blackwell et al., 2018; Butiseacă et al., 2024; Doukas et al., 2018; Jacobs et al., 2018; Tourloukis, Muttoni, et al., 2018). The proboscidean remains included the cranium, still preserving both upper third molars (M3s), as well as several postcranial elements belonging to a male individual in late adulthood (Konidaris et al., 2018). In addition to indirect indications of hominin presence through the stratigraphic and contextual association of the skeleton with lithic artifacts (Giusti et al., 2018; Panagopoulou et al., 2018; Tourloukis, Thompson, et al., 2018), which had been used for butchering activities (Guibert-Cardin et al., 2022), the individual also exhibited traces of direct association with hominin activity through the presence of cutmarks on few skeletal elements, suggesting anthropogenic carcass exploitation (Konidaris et al., 2018).

A series of sequential enamel samples was obtained with a handheld rotary tool from the fragmented third upper right molar (M3) of the MAR-1 *Palaeoloxodon antiquus,* extending perpendicularly along the height of the tooth crown (Figure 5). The samples were chemically prepared following well-established pretreatment

protocols (Bocherens et al., 1996; Koch et al., 1997), to remove organic components, exogenous carbonates, and contaminants. Stable isotope ratios were, subsequently, obtained from enamel carbonates through isotope ratio mass spectrometry (IRMS) at the Biogeology laboratory of the University of Tübingen. Stable carbon and oxygen isotope ratios were analyzed for each sample separately and the average $\delta^{13}C$ and $\delta^{18}O$ solutions were calculated from the serial isotopic series. This approach was preferred to bulk enamel sampling, wherein a single sample is collected superficially and parallel to the direction of tooth growth, as it reduces potential bias introduced due to the uneven distribution of seasonal signals along both the enamel thickness and the tooth growth axis, following the observations of Liu et al. (2022) for elephantine specimens.

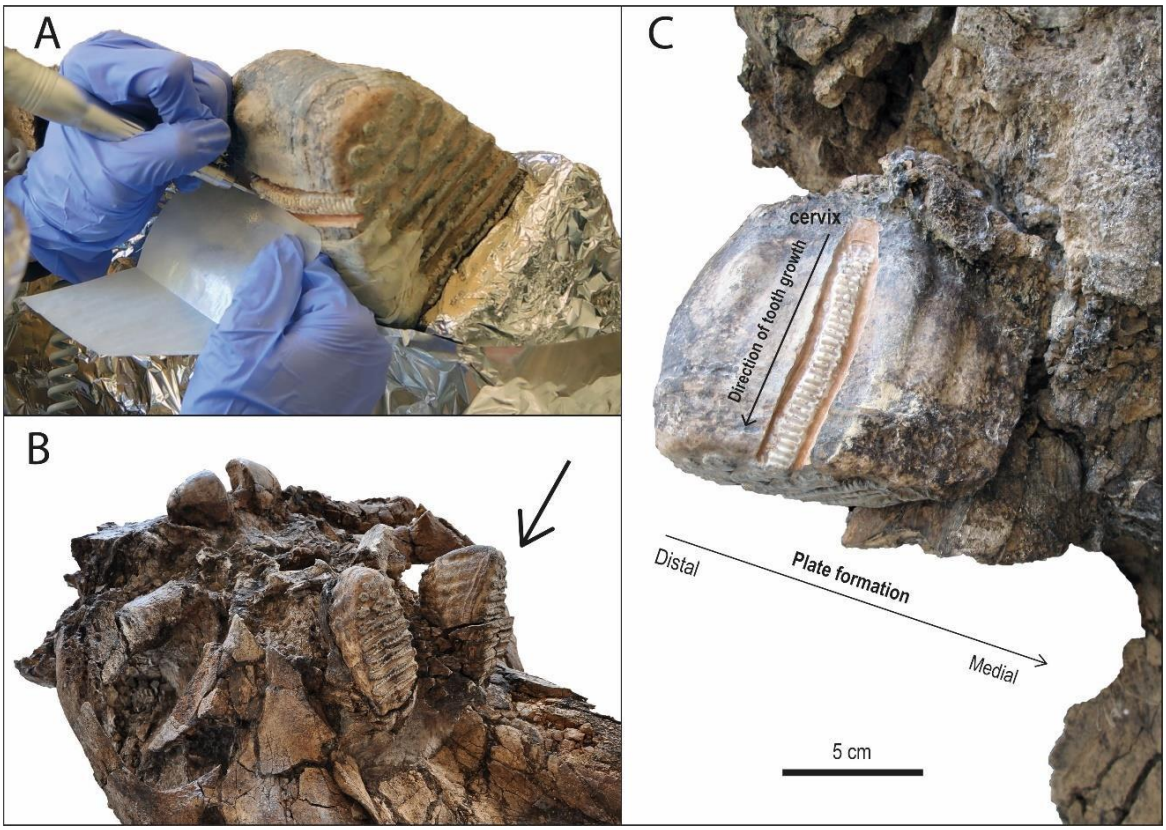

***Figure 5**: A) Sequential sampling of the MAR-1 elephant molar using a handheld rotary tool; B) Ventral view of the P. antiquus skull. The arrow points to the sampled upper molar; C) Schematic illustration of elephantine tooth formation on the sampled M3 specimen.*

The average carbon and oxygen isotope values of the MAR-1 *P. antiquus* individual were examined against published isotopic data of straight-tusked elephant specimens from Middle Pleistocene interglacial sites in Italy and Germany. The comparative dataset included bulk enamel carbon and oxygen isotope ratios from

Mauer (Pushkina et al., 2014), Steinheim an der Murr (Pushkina et al., 2014), and Neumark-Nord 1 (Grube et al., 2010) in Germany, as well as from specimens found at the sites of La Polledrara (Palombo et al., 2005), Casal de' Pazzi (Briatico & Bocherens, 2023; Palombo et al., 2005), and Poggetti Vecchi (Capalbo, 2018) in Italy.

The carbon isotope ratios of the MAR-1 straight-tusked elephant revealed a diet comprising predominantly C_3 vegetation. The mean carbon isotope ratio of the studied individual suggested a mesic foraging habitat with C_3 woodland/open grassland vegetation. The inter-regional comparison revealed similar vegetative conditions to Italian specimens attributed to the interglacial MIS 7. More specifically, the elephant from MAR-1 demonstrated a similar $\delta^{13}C$ value to the *P. antiquus* individual from Poggetti Vecchi (MIS 7, Italy), which likely inhabited an analogous C_3 mesic woodland environment (Capalbo, 2018), while straight-tusked elephants from Casal de' Pazzi (MIS 7, Italy) occupied a wider range of habitats, including mesic woodlands —similarly to the MAR-1 elephant—, as well as more forested biomes (Briatico & Bocherens, 2023; Palombo et al., 2005). On the other hand, relatively higher $\delta^{13}C$ values were observed in the La Polledrara elephant population (Palombo et al., 2005), suggesting an environment with higher aridity and/or more open landscapes in Italy during MIS 9 compared to Greece during MIS 12. Lastly, the comparison of $\delta^{13}C$ values between the straight-tusked elephant from MAR-1 in Greece and those from Mauer (MIS 15) (Pushkina et al., 2014), Steinheim an der Murr (MIS 11) (Pushkina et al., 2014), and Neumark-Nord 1 (MIS 5) (Grube et al., 2010) in Germany indicated more densely forested and humid habitats in the latter.

The oxygen isotopic data provided the basis for broader climatic inferences. The studied elephant molar from MAR-1 yielded lower average oxygen isotopic ratios in comparison to the specimens from the three Italian interglacial localities. This result suggested that climatic conditions in the Megalopolis Basin were cooler and/or more humid compared to conditions at Casal de' Pazzi, Poggetti Vecchi, and La Polledrara in Italy. Contrariwise, the higher mean $\delta^{18}O$ value of the MAR-1 elephant in comparison to specimens from Mauer and Steinheim an der Murr indicated that at MAR-1 the climate was likely warmer and drier than at the two German localities. The incongruous elevated oxygen isotope ratios of the Neumark-

Nord 1 population were attributed to evaporative enrichment of the source water from which the elephants were drinking, as suggested by (Grube et al., 2010).

This study presented the first isotopic results for *Palaeoxodon antiquus* in Greece, complementing the relatively scant biogeochemical record of the species in Europe. The broader ecological characteristics of the species were used to investigate climatic and vegetative conditions in the Megalopolis Basin within a European Middle Pleistocene context. The isotopic results supported the attribution of MAR-1 to a glacial stage, revealing colder climatic conditions in the eastern peri-Mediterranean area during MIS 12. The study further revealed that despite glacial conditions, the Megalopolis Basin maintained a moderately humid environment with open woodlands and grasslands, similar to the interglacial landscapes of Italy, and supported sufficient C_3 plant resources to facilitate the survival of faunal populations, thereby indicating that the impact of the MIS 12 glacial in the area was milder.

3.2 Study II (Appendix B)

Expanding upon the findings of Study I, this study furthered the ecological investigation of the MAR-1 straight-tusked elephant, aiming to provide highly resolute, sub-annual and multi-annual scale information on the foraging and movement patterns of the studied individual, as well as on potential climatic oscillations in the Megalopolis Basin during the MIS 12 glacial period. An incremental sampling approach perpendicularly to the tooth growth axis allowed the generation of intra-tooth isotopic profiles, thus providing a long and continuous record of carbon ($\delta^{13}C$), oxygen ($\delta^{18}O$), and strontium ($^{87}S/^{86}Sr$) isotopic data. The analysed isotopic sequences enabled the assessment of short-term changes in the elephant's diet and habitat, climate, and movement patterns, respectively. Given an estimated ontogenetic age of 64–71 years (Konidaris et al., 2018) and the pattern of elephantine molar formation (Metcalfe & Longstaffe, 2012; Uno et al., 2020), the timespan reflected in the isotopic series obtained from the second distalmost lamella of the upper third molar represents the final decade of the elephant's life.

The specific geometry of enamel formation, which involves the secretion of enamel increments at an oblique angle in relation to the tooth's growth axis, and a

secondary stage of mineral deposition known as enamel maturation, combined with the geometry of conventional sampling can effectuate dampening of the primary isotopic input signal (Green et al., under review; Passey & Cerling, 2002; Passey, Cerling, et al., 2005; Uno et al., 2020). This obscures an accurate manifestation of the amplitude of short-term fluctuations in the isotopic data series. To overcome this limitation, a mathematical correction (inverse modelling) was employed, which considers the specific parameters of enamel formation and sampling geometry in conjunction with the measured isotopic ratios, to provide a better estimation of the primary carbon and oxygen isotopic input signal (Passey, Cerling, et al., 2005; Uno et al., 2020; Yang et al., 2020).

Intra-tooth variation in carbon stable isotopes was used to investigate changes in diet, vegetation composition, and plant resource availability. Throughout the examined timeframe, the MAR-1 elephant subsisted on C_3 vegetation. The range of $\delta^{13}C$ values suggested the persistence of mesic conditions and a habitat composed of woodland with open grassland areas. Periodic variation in the $\delta^{13}C$ series was consistent with seasonal changes in the vegetation ingested by the individual. In addition to seasonal fluctuations, a quasi-sinusoidal pattern consonant with multi-annual variation in the $\delta^{13}C$ values was conspicuous and more prominent than the intra-annual pattern in both measured and modelled data, suggesting shifting habitats or dietary habits over the course of several years.

The oxygen isotopic series also demonstrated fluctuating $\delta^{18}O$ values at regular intervals, which likely corresponded to climatic seasonality of low to moderate amplitude based on the range of variation. However, the multi-annual fluctuations discerned in the carbon isotopic series were not observed here, suggesting that significant climate changes, which in turn impacted the availability of plant resources, were unlikely to have been the main control behind the shifts observed in habitat utilisation and/or the diet of the elephant. This raised a hypothesis of the potential movement of the individual between areas with different microhabitats.

Strontium isotope ratios of tooth enamel bioapatite were used to investigate the movement or ranging patterns of the elephant. In this study, the interpretation of strontium isotope ratios, typically conducted against a regional strontium isotopic baseline, was facilitated by a published dataset of bioavailable strontium developed

specifically for the Peloponnese (Frank et al., 2021). The published data were further supplemented by strontium isotope ratios measured from *Hippopotamus antiquus* dental specimens, which had been recovered within the Megalopolis Basin, in order to refine the local baseline. The measured $^{87}Sr/^{86}Sr$ ratios from the three hippopotami showed good correspondence to the strontium isotopic composition of the local geology. The intra-tooth $^{87}Sr/^{86}Sr$ ratios from the MAR-1 elephant appeared relatively consistent and ranged within the expected values of the local predominant geological outcrops, thereby suggesting a limited-ranging behaviour within the Megalopolis Basin. No evidence for long-distance mobility — a response to severe environmental stress and resource decline observed in both extant and extinct proboscideans (Bai et al., 2022; Bonhof & Pryor, 2022; Wang et al., 2021)— was identified in our study.

When considered altogether, the results from the intra-tooth carbon, oxygen and strontium isotopic investigation of the straight-tusked elephant from MAR-1 suggested a scenario of nomadic, irregular mobility between diverse microhabitats or environmental zones within the Megalopolis Basin. Overall, the decadal-scale isotopic data indicated that the area experienced moderate but consistent seasonal fluctuations in climate and plant productivity, which allowed, nonetheless, the persistence of a diverse ecosystem with heterogeneous foraging resources. The relative consistency in climatic parameters and the diversity of available foraging habitats, the latter of which is in agreement with other paleoenvironmental indices from the site (Butiseacă et al., 2024; Field et al., 2018; Konidaris et al., 2024; Konidaris et al., 2018; Kyrikou et al., in press; Michailidis et al., 2018), permitted the continuous inhabitation of the basin by the straight-tusked elephant for the examined decade and aided the survival of the individual, as well as of other temperate faunal species and potentially also hominins, during the particularly severe MIS 12 glacial.

3.3 Study III (Appendix C)

The final contribution to this cumulative dissertation presents the first enamel intra-tooth isotopic biogeochemical study of the extinct European hippopotamus (*Hippopotamus antiquus)*. In Study III, carbon and oxygen stable isotope analyses were conducted on five *Hippopotamus* dental specimens from the Megalopolis Basin to investigate their dietary regime, as well as the vegetative, climatic, and

hydrological conditions facilitating the presence of the taxon in the area. The sampled dental elements originated from five archaeo-paleontological localities discovered within the Marathousa Mb. More specifically, the study included a third molar from KYP-4 (ca. 700 ka), a lower canine from KYP-3 (ca. 650 ka, MIS 16), an upper first incisor from KYP-T (early Middle Pleistocene), a third molar from MAR-1 (ca. 430 ka, MIS 12) and an upper canine from MAR-2 (ca. 450 ka, MIS 12) (Athanassiou et al., in press; Athanassiou et al., 2018; G. Konidaris et al., 2023; Konidaris et al., 2024) (Figure 6). The different chronostratigraphic origins of each specimen permitted a diachronic view of the prevailing conditions during the early– mid-Middle Pleistocene.

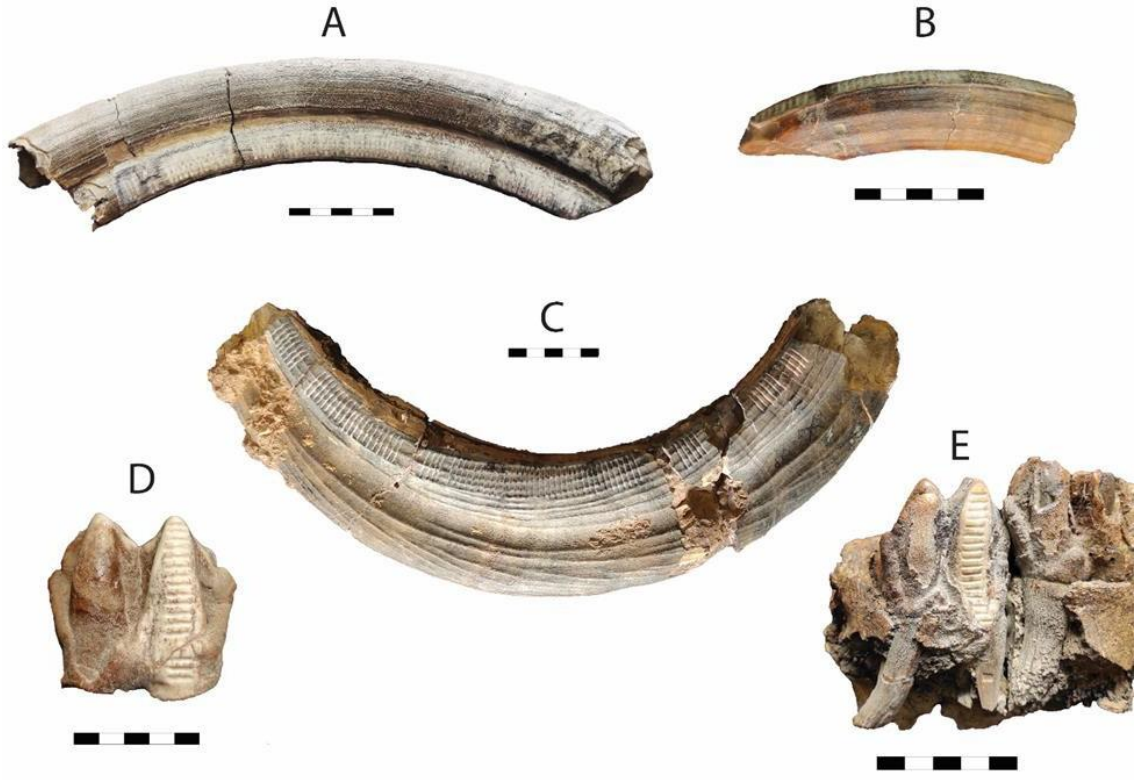

Figure 6*: Sequentially sampled Hippopotamus antiquus dental specimens from the Middle Pleistocene stratigraphic sequence of the Megalopolis Basin. A) Upper canine from MAR-2; B) upper first incisor from KYP-T; C) lower canine from KYP-3; D) upper third molar from MAR-1; E) upper third molar from KYP-4.*

All specimens were sampled sequentially along the tooth growth axis, thus providing infra-annual and multi-annual isotopic records. The recorded timespan depends on tooth-specific parameters of growth, enamel formation, and maturation. Hippopotamus canines and incisors are continuously growing,

thereby providing longer isotopic records. On the other hand, the formation of third molars is completed within ~2.5 years (Green et al., 2023), hence capturing a shorter time interval of the individual's life history.

The five hippopotami from the Middle Pleistocene sequence of the Megalopolis Basin demonstrated diets relying purely on C_3 vegetation. The range of values indicated habitats comprising mesic woodland with open grassland areas. The inter-site comparison of the carbon isotopic composition suggested more dense canopy cover and/or humid environments for individuals recovered from the early Middle Pleistocene sequence of the Kyparissia mine (KYP-4, KYP-3, and KYP-T) compared to those found within the mid-Middle Pleistocene sequence of the Marathousa mine (MAR-1, MAR-2). This pattern was consistent with broader environmental trends in the northern peri-Mediterranean regions, wherein moister conditions supported the persistence of more forested habitats from ca. 800 ka until ~600 ka (Sánchez Goñi et al., 2023; Strani et al., 2019). Thereafter, the increased intensity of glacial maxima and progressively drier conditions resulted in more open landscapes and a turnover in vegetation communities, especially during the MIS 12 glacial period (Strani, 2021; Strani et al., 2019; Tzedakis et al., 2006; Vera-Polo et al., 2024; Zanazzi et al., 2022).

Individual life history reconstructions of the five specimens revealed variability in climatic and hydrological conditions in the Megalopolis Basin, as well as dietary and environmental fluctuations. The carbon and oxygen isotopic series of three individuals (KYP4-1004, KYP3-46, and MAR-2B-2) correlated significantly, indicating dietary or habitat shifts in response to changing climatic conditions. Additionally, a visual examination of the carbon isotope profiles confirmed fluctuating $\delta^{13}C$ values in all five individuals, which likely signify seasonally adaptive diets.

The isotopic record of the MAR-1 hippopotamus molar demonstrated a drier and more open habitat during the deposition of layer UB2, which post-dates the archaeological horizon at the site. The habitat reconstruction is in agreement with the results from the study of plant remains, wood charcoal and phytoliths (Field et al., 2018), as well as of stable isotopes on leaf waxes (Butiseacă et al., 2024), and pollen (Kyrikou et al., in press), recording a transition to warmer conditions with more open vegetation at the upper part of the MAR-1 sequence. However,

compared to the other studied hippopotami, the $\delta^{18}O$ values of MAR-1B-8 were not indicative of warmer/drier conditions. This discrepancy was attributed to the potential mixing of meltwater in the hippo pool, as suggested by the analysis of diatoms and ostracods at MAR-1 (Bludau et al., 2021), thus resulting in more negative oxygen isotope ratios and an attenuated seasonal signal.

Aside from sub-annual variation in feeding habits, the isotopic profiles of the Marathousa 2 upper canine (MAR-2B-2) recorded a gradual shift in both carbon and oxygen isotopic series, which was attributed to multi-annual environmental or ecological change. The $\delta^{13}C$ and $\delta^{18}O$ series were inversely correlated, hinting towards either a broad-scale shift in climatic conditions, which in turn impacted the hydrological regime and the surrounding plant communities, or the relocation of the individual to a different water pool. More specifically, the distal half of the canine yielded higher $\delta^{18}O$ values and lower amplitude variation in oxygen isotopic ratios, which could be the result of evaporative enrichment and isotopic mixing of seasonal signals in a stagnant water body (Pederzani & Britton, 2019). The proximal half of the profile demonstrated lower $\delta^{18}O$ values and higher amplitude variation, which could be consistent with the transition to a smaller water body.

The carbon and oxygen intra-tooth isotope ratios of the KYP3-46 lower canine recorded a larger amplitude of variation (3‰ and 4.6‰, respectively), indicating some degree of instability in preferred food sources or a variable climatic/hydrological setting during the recorded timespan. The specimen also exhibited linear dental enamel hypoplasia (DEH) (Figure 7), a dental pathology associated with physiological or nutritional stress during the time of tooth formation in large mammals (Barrón-Ortiz et al., 2019; Franz-Odendaal et al., 2003; Goodman, 1991; Guatelli-Steinberg et al., 2012; Kierdorf et al., 2016; Mead, 1999). The serial isotopic profiles demonstrated at least two major ecological shifts, one of which coincided with an enamel defect. The observed DEH seemingly overlaps with more negative $\delta^{18}O$ values and was, therefore, tentatively correlated to cooler conditions. In addition, it is noteworthy that the KYP-3 individual exhibited the lowest carbon isotopic ratios in the sample, suggesting it may have occupied a habitat with more dense canopy cover than the rest of the hippos.

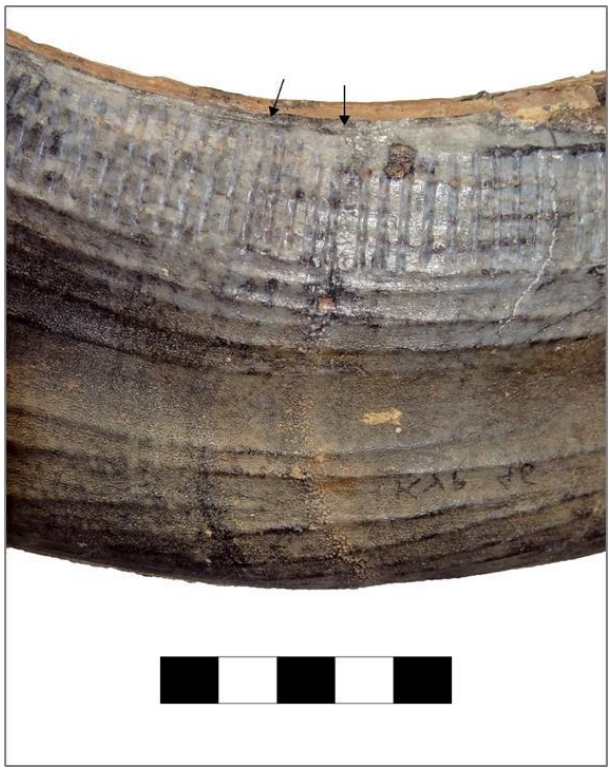

Figure 7: *Enamel defects (linear DEH, black arrows) on the H. antiquus lower canine from KYP-3.*

Finally, mild DEH in the form of linear grooves was also recorded on the KYPT-842 incisor, extending through the sampling area in regular intervals. The $\delta^{18}O$ series from this specimen demonstrated consistent and continuous low amplitude variation, characteristic of seasonal fluctuations. Variability in $\delta^{13}C$ values was, however, more pronounced and of higher amplitude. The periodicity in carbon and oxygen isotopic ratios, in combination with the frequency of DEH, suggested seasonal stress events, which likely coincided with cooler temperatures.

Overall, the intra-tooth stable isotopic analysis of *H. antiquus* from the Middle Pleistocene sequence of the Megalopolis Basin provided new insights into the ecology of the species. The research revealed that climatic shifts conditioned the feeding strategies and, by extension, habitat utilization of the studied individuals. In addition, preliminary observations suggest a low tolerance to colder temperatures for the species. Taken together, these results have broader implications for the environmental reconstruction of the area, implying complex environmental dynamics and relatively frequent changes in resource availability, as well as in hydrological conditions. Nevertheless, no major climatic changes were identified in the long term, and fluctuations in preferred subsistence resources were likely compensated by habitat diversity, supporting the species' survival in the area even during harsher glacial periods.

4 Concluding remarks

The three case studies presented in this cumulative dissertation investigated the ecological attributes of two extinct Middle Pleistocene megaherbivore species from the Megalopolis Basin, Southern Greece, through isotopic biogeochemistry. The reconstruction of individual life histories served as a proxy for temporally resolute inferences on environmental and climatic conditions in the area during glacial (or stadial) periods, extending through different timescales, from infra-annual to millennial-scale observations.

The paleoecological reconstruction of the straight-tusked elephant (*Palaeoloxodon antiquus*) and the European hippopotamus (*Hippopotamus antiquus*) from the Megalopolis Basin demonstrated a higher adaptive capacity for the former taxon and an increased sensitivity for the latter, in accordance with previous observations for the species (Fidalgo, Rosas, Bartolini-Lucenti, et al., 2023). The isotopic data proposed individualistic adaptive responses to shifting environmental conditions for both species. In the case of the straight-tusked elephant from Marathousa-1, a seasonally adaptive diet and a pattern of nomadic, multi-year mobility to facilitate the exploitation of different microhabitats were inferred (Study II). Nomadic mobility has been commonly attributed to resource limitations and unpredictability of resource availability in extant animal taxa and is often associated with patchy, dynamic landscapes (Teitelbaum & Mueller, 2019). On the other hand, the narrow-ranging *Hippopotamus antiquus* demonstrated ecological and physiological responses (Study III). Seasonal and multi-year dietary or habitat changes were inferred for the five hippopotami individuals too; however, hydrological variation, such as water level or water temperature fluctuations, likely played an equally important role in the taxon's distribution and fitness. The incidence of mild DEH in two early Middle Pleistocene individuals suggested periodically stressful conditions for the species in the area. The availability of preferred terrestrial and aquatic habitats has been identified as a crucial control for population abundance and structure of the extant common hippopotamus (*H. amphibius*) and further influences hippo movement and distribution patterns (Fritsch et al., 2022; Lewison, 2007; Stears et al., 2019; Stommel et al., 2016), despite restricted home ranges. The limited strontium isotope data from three *H.*

antiquus specimens, that were presented in Study II, corresponded to local values of the dominant geological units in the Megalopolis Basin but long-term, spatially resolute mobility patterns of the studied individuals have not yet been extensively investigated and could provide further information on the adaptive responses of this extinct taxon.

The aforementioned inferences highlighted the existence of heterogeneous and dynamic environments in the area, which prompted a high level of adaptability for its inhabitants and necessitated the ability to exploit a diverse array of resources. Although the study focused on faunal remains, the findings may also have a bearing on hominin populations in the area, who likely experienced similar environmental shifts. The discovery of anthropogenic remains within the detrital layers of the Megalopolis Basin and, more importantly, their association with some of the analysed specimens (De Caro et al., 2024; Karkanas et al., in press; Konidaris et al., 2018; G. E. Konidaris et al., 2023; Tourloukis, Thompson, et al., 2018), implies either a relatively high adaptive capacity for the local Middle Pleistocene hominin populations or a broad ecological niche. The investigation of cultural remains from the Megalopolis Basin is currently underway and could provide important insight into Middle Pleistocene hominin subsistence strategies, adaptations, and potential responses to environmental changes.

A mosaic of different microhabitats in the Megalopolis Basin counterweighted the seasonal or multi-annual changes in climate, which seemingly also affected to some extent the composition and distribution of plant communities, as well as of aquatic habitats. Despite glacial conditions, the evidence from the Megalopolis Basin suggests partial ecosystem resilience with the persistence of diverse C_3 plant resources and a lack of severe expressions of environmentally adverse conditions for temperate taxa, e.g., extreme aridity. This allowed the two megaherbivores to inhabit the area even during periods with less optimal environmental parameters. In addition, the broader, millennial-scale comparison of the reconstructed environmental attributes from the five sites does not show any drastic changes in vegetation or moisture levels within the timeframe represented by the analyzed specimens but rather highlights the dominance of mesic conditions and the endurance of woodland habitats with variable degrees of openness. These findings, together with the presence of warm-adapted faunal and floral taxa through

multiple stratigraphic units of the basin (Athanassiou, 2018; Athanassiou et al., in press; Athanassiou et al., 2018; Field et al., 2018; Konidaris et al., 2022; Konidaris et al., 2024; Kyrikou et al., in press; Michailidis et al., 2018; Vlachos et al., in press), have significant implications for better understanding the nature of the area, hinting towards its definition as a long-term climate refugium, in which the effects of glaciations and climatic perturbations were mitigated.

The research undertaken here complements the already available paleoenvironmental data putting forth the Megalopolis Basin as a glacial microrefugium (Athanassiou, 2018; Athanassiou et al., in press; Athanassiou et al., 2018; Butiseacă et al., 2024; Field et al., 2018; G. Konidaris et al., 2023; Konidaris et al., 2022; Konidaris et al., 2024; Kyrikou et al., in press; Michailidis et al., 2018; Vlachos & Delfino, 2016; Vlachos et al., in press) but also serves as the basis for the construction of a high-resolution diachronic paleoenvironmental record for the Middle Pleistocene in Greece. Given the fragmentary nature of such long sequences, the Megalopolis Basin is a rare case providing fertile ground for further investigations, with the incorporation of interdisciplinary approaches through multiple stratigraphic scales. Ultimately, the construction of an isotopic paleoecological dataset for emblematic taxa, such as the straight-tusked elephant *Palaeoloxodon antiquus* and the hippopotamus *Hippopotamus antiquus,* could expand spatially to incorporate specimens from other Greek regions, many of which lack paleoenvironmental records. Such an endeavour would greatly contribute to explorations of habitat variability and niche separation, as well as to the definition of the ecological limits of both resident fauna and hominin populations.

5 References

Adams, N. F., Candy, I., & Schreve, D. C. (2022). An Early Pleistocene hippopotamus from Westbury Cave, Somerset, England: support for a previously unrecognized temperate interval in the British Quaternary record. *Journal of Quaternary Science*, *37*(1), 28–41.

Agam, A., & Barkai, R. (2018). Elephant and Mammoth Hunting during the Paleolithic: A Review of the Relevant Archaeological, Ethnographic and Ethno-Historical Records. *Quaternary*, *1*(1), 3. https://www.mdpi.com/2571-550X/1/1/3

Argiriou, A. A., & Lykoudis, S. (2006). Isotopic composition of precipitation in Greece. *Journal of Hydrology*, *327*(3), 486–495. https://doi.org/https://doi.org/10.1016/j.jhydrol.2005.11.053

Athanassiou, A. (2018). Pleistocene vertebrates from the Kyparíssia lignite mine, Megalopolis Basin, S. Greece: Rodentia, Carnivora, Proboscidea, Perissodactyla, Ruminantia. *Quaternary International*, *497*, 198–221.

Athanassiou, A. (2022a). The Fossil Record of Continental Elephants and Mammoths (Mammalia: Proboscidea: Elephantidae) in Greece. In E. Vlachos (Ed.), *Fossil Vertebrates of Greece Vol. 1: Basal vertebrates, Amphibians, Reptiles, Afrotherians, Glires, and Primates* (pp. 345–391). Springer International Publishing. https://doi.org/10.1007/978-3-030-68398-6_13

Athanassiou, A. (2022b). The fossil record of continental hippopotamids (Mammalia: Artiodactyla: Hippopotamidae) in Greece. *Fossil Vertebrates of Greece Vol. 2: Laurasiatherians, Artiodactyles, Perissodactyles, Carnivorans, and Island Endemics*, 281–299.

Athanassiou, A., Konidaris, G. E., Tourloukis, V., Thompson, N., Giusti, D., Panagopoulou, E., Karkanas, P., & Harvati, K. (in press). The Middle Pleistocene large mammal fauna from Kyparissia (Peloponnese, S. Greece): New collected material. In K. Harvati & M. Ioannidou (Eds.), *Human Evolution at the CROSSROADS: Research in Greece and beyond*. Tübingen University Press.

Athanassiou, A., Michailidis, D., Vlachos, E., Tourloukis, V., Thompson, N., & Harvati, K. (2018). Pleistocene vertebrates from the Kyparíssia lignite mine, Megalopolis Basin, S. Greece: Testudines, Aves, Suiformes. *Quaternary International*, *497*, 178–197. https://doi.org/https://doi.org/10.1016/j.quaint.2018.06.030

Bai, D., Wan, X., Zhang, L., Campos-Arceiz, A., Wei, F., & Zhang, Z. (2022). The recent Asian elephant range expansion in Yunnan, China, is associated with climate change and enforced protection efforts in human-dominated landscapes [Original Research]. *Frontiers in Ecology and Evolution*, *10*. https://doi.org/10.3389/fevo.2022.889077

Barrón-Ortiz, C. I., Jass, C. N., Barrón-Corvera, R., Austen, J., & Theodor, J. M. (2019). Enamel hypoplasia and dental wear of North American late Pleistocene horses and bison: an assessment of nutritionally based extinction models. *Paleobiology*, *45*(3), 484–515. https://doi.org/10.1017/pab.2019.17

Bataille, C. P., Crowley, B. E., Wooller, M. J., & Bowen, G. J. (2020). Advances in global bioavailable strontium isoscapes. *Palaeogeography, Palaeoclimatology, Palaeoecology*, *555*, 109849. https://doi.org/https://doi.org/10.1016/j.palaeo.2020.109849

Bender, M. M. (1971). Variations in the $^{13}C/^{12}C$ ratios of plants in relation to the pathway of photosynthetic carbon dioxide fixation. *Phytochemistry*, *10*(6), 1239–1244. https://doi.org/https://doi.org/10.1016/S0031-9422(00)84324-1

Bennett, K. D., Tzedakis, P. C., & Willis, K. J. (1991). Quaternary Refugia of North European Trees. *Journal of Biogeography*, *18*(1), 103–115. https://doi.org/10.2307/2845248

Bentley, A. R. (2006). Strontium isotopes from the earth to the archaeological skeleton: a review. *Journal of archaeological method and theory*, *13*(3), 135–187.

Berends, C., Köhler, P., Lourens, L., & Van de Wal, R. (2021). On the cause of the Mid-Pleistocene transition. *Reviews of Geophysics*, 59, e2020RG000727. https://doi.org/10.1029/2020RG000727

Bertini, A., Toti, F., Marino, M., & Ciaranfi, N. (2015). Vegetation and climate across the Early–Middle Pleistocene transition at Montalbano Jonico, southern Italy. *Quaternary International*, *383*, 74–88. https://doi.org/https://doi.org/10.1016/j.quaint.2015.01.003

Blackwell, B. A., Sakhrani, N., Singh, I. K., Gopalkrishna, K. K., Tourloukis, V., Panagopoulou, E., Karkanas, P., Blickstein, J. I., Skinner, A. R., & Florentin, J. A. (2018). ESR dating ungulate teeth and molluscs from the Paleolithic site Marathousa 1, Megalopolis Basin, Greece. *Quaternary*, *1*(3), 22.

Blain, H.-A., Fagoaga, A., Ruiz-Sánchez, F. J., García-Medrano, P., Ollé, A., & Jiménez-Arenas, J. M. (2021). Coping with arid environments: A critical threshold for human expansion in Europe at the Marine Isotope Stage 12/11 transition? The case of the Iberian Peninsula. *Journal of Human Evolution*, *153*, 102950. https://doi.org/https://doi.org/10.1016/j.jhevol.2021.102950

Bludau, I. J., Papadopoulou, P., Iliopoulos, G., Weiss, M., Schnabel, E., Thompson, N., Tourloukis, V., Zachow, C., Kyrikou, S., Konidaris, G. E., Karkanas, P., Panagopoulou, E., Harvati, K., & Junginger, A. (2021). Lake-Level Changes and Their Paleo-Climatic Implications at the MIS12 Lower Paleolithic (Middle Pleistocene) Site Marathousa 1, Greece. *Frontiers in Earth Science*, *9*, 441.

Bocherens, H., & Drucker, D. G. (2013). CARBONATE STABLE ISOTOPES | Terrestrial Teeth and Bones. In S. A. Elias & C. J. Mock (Eds.), *Encyclopedia of Quaternary Science (Second Edition)* (pp. 304–314). Elsevier. https://doi.org/https://doi.org/10.1016/B978-0-444-53643-3.00341-1

Bocherens, H., Koch, P. L., Mariotti, A., Geraads, D., & Jaeger, J.-J. (1996). Isotopic biogeochemistry (^{13}C, ^{18}O) of mammalian enamel from African Pleistocene hominid sites. *Palaios*, 306–318.

Bonhof, W. J., & Pryor, A. J. E. (2022). Proboscideans on Parade: A review of the migratory behaviour of elephants, mammoths, and mastodons. *Quaternary Science Reviews*, *277*, 107304. https://doi.org/https://doi.org/10.1016/j.quascirev.2021.107304

Braun, I. M., & Palombo, M. R. (2012). *Mammuthus primigenius* in the cave and portable art: An overview with a short account on the elephant fossil record in Southern Europe during the last glacial. *Quaternary International*, *276-277*, 61–76. https://doi.org/https://doi.org/10.1016/j.quaint.2012.07.010

Briatico, G., & Bocherens, H. (2023). Middle Pleistocene ecology in central Italy. New isotopic insights from fauna tooth enamel of Casal de'Pazzi (Rome, Italy). *Journal of Mediterranean Earth Sciences*, *15*.

Britton, K. (2020). Isotope Analysis for Mobility and Climate Studies. In K. Britton & M. P. Richards (Eds.), *Archaeological Science: An Introduction* (pp. 99–124). Cambridge University Press. https://doi.org/DOI: 10.1017/9781139013826.005

Britton, K., Grimes, V., Dau, J., & Richards, M. P. (2009). Reconstructing faunal migrations using intra-tooth sampling and strontium and oxygen isotope analyses: a case study of modern caribou (*Rangifer tarandus granti*). *Journal of Archaeological Science*, *36*(5), 1163–1172.

Bryant, J. D., & Froelich, P. N. (1995). A model of oxygen isotope fractionation in body water of large mammals. *Geochimica et Cosmochimica Acta*, *59*(21), 4523–4537.

Butiseacă, G. A., Vasiliev, I., van der Meer, M. T. J., Bludau, I. J. E., Karkanas, P., Tourloukis, V., Junginger, A., Mulch, A., Panagopoulou, E., & Harvati, K. (2024). The expression of the MIS 12 glacial stage in Southeastern Europe and its impact over the Middle Pleistocene hominins in Megalopolis Basin (Greece). *Global and Planetary Change*, *242*, 104585. https://doi.org/https://doi.org/10.1016/j.gloplacha.2024.104585

Capalbo, C. (2018). Multiproxy-Based reconstruction of the feeding habits from the late Middle Pleistocene straight-tusked elephant population of Poggetti Vecchi (Southern Tuscany, Italy). *Alpine and Mediterranean Quaternary*, *31*, 113–119.

Capo, R. C., Stewart, B. W., & Chadwick, O. A. (1998). Strontium isotopes as tracers of ecosystem processes: theory and methods. *Geoderma*, *82*(1), 197–225. https://doi.org/https://doi.org/10.1016/S0016-7061(97)00102-X

Cerling, T. E., Bernasconi, S. M., Hofstetter, L. S., Jaggi, M., Wyss, F., Rudolf von Rohr, C., & Clauss, M. (2021). CH_4/CO_2 ratios and carbon isotope enrichment between diet and breath in herbivorous mammals. *Frontiers in Ecology and Evolution*, *9*, 638568.

Cerling, T. E., & Harris, J. M. (1999). Carbon isotope fractionation between diet and bioapatite in ungulate mammals and implications for ecological and paleoecological studies. *Oecologia*, *120*(3), 347–363. https://doi.org/10.1007/s004420050868

Crowley, B. E., Miller, J. H., & Bataille, C. P. (2017). Strontium isotopes ($^{87}Sr/^{86}Sr$) in terrestrial ecological and palaeoecological research: empirical efforts and recent advances in continental-scale models. *Biological Reviews*, *92*(1), 43–59. https://doi.org/https://doi.org/10.1111/brv.12217

Dansgaard, W. (1964). Stable isotopes in precipitation. *Tellus*, *16*(4), 436–468. https://doi.org/https://doi.org/10.1111/j.2153-3490.1964.tb00181.x

Davies, P. (2002). *The straight-tusked elephant (Palaeoloxodon antiquus) in Pleistocene Europe*. University of London, University College London (United Kingdom).

De Caro, D., Tourloukis, V., Thomson, N., Varis, A., Panagopoulou, E., & Harvati, K. (2024). The lithic assemblages from the Palaeolithic survey research in the Megalopolis Basin, Greece. *Journal of lithic studies*, *11*(1), 29

DeNiro, M. J., & Epstein, S. (1978). Influence of diet on the distribution of carbon isotopes in animals. *Geochimica et cosmochimica acta*, *42*(5), 495–506.

Dennell, R. W., Martinón-Torres, M., & Bermúdez de Castro, J. M. (2011). Hominin variability, climatic instability and population demography in Middle Pleistocene Europe. *Quaternary Science Reviews*, *30*(11), 1511–1524. https://doi.org/https://doi.org/10.1016/j.quascirev.2009.11.027

Dotsika, E., Lykoudis, S., & Poutoukis, D. (2010). Spatial distribution of the isotopic composition of precipitation and spring water in Greece. *Global and Planetary Change*, *71*(3), 141-149. https://doi.org/https://doi.org/10.1016/j.gloplacha.2009.10.007

Doukas, C., van Kolfschoten, T., Papayianni, K., Panagopoulou, E., & Harvati, K. (2018). The small mammal fauna from the Palaeolithic site Marathousa 1 (Greece). *Quaternary International*, *497*, 95–107.

Drucker, D. G., Bridault, A., Hobson, K. A., Szuma, E., & Bocherens, H. (2008). Can carbon-13 in large herbivores reflect the canopy effect in temperate and boreal ecosystems? Evidence from modern and ancient ungulates. *Palaeogeography, Palaeoclimatology, Palaeoecology*, *266*(1), 69–82. https://doi.org/https://doi.org/10.1016/j.palaeo.2008.03.020

Farquhar, G. D., Ehleringer, J. R., & Hubick, K. T. (1989). Carbon isotope discrimination and photosynthesis. *Annual review of plant biology*, *40*(1), 503–537.

Fidalgo, D., Madurell-Malapeira, J., Martino, R., Pandolfi, L., & Rosas, A. (2024). An Updated Review of The Quaternary Hippopotamus Fossil Records from the Iberian Peninsula. *Quaternary*, *7*(1), 4. https://www.mdpi.com/2571-550X/7/1/4

Fidalgo, D., Rosas, A., Bartolini-Lucenti, S., Boisserie, J.-R., Pandolfi, L., Martínez-Navarro, B., Palmqvist, P., Rook, L., & Madurell-Malapeira, J. (2023). Increase on environmental seasonality through the European Early Pleistocene inferred from dental enamel hypoplasia. *Scientific Reports*, *13*(1), 16941.

Fidalgo, D., Rosas, A., Madurell-Malapeira, J., Pineda, A., Huguet, R., García-Tabernero, A., Cáceres, I., Ollé, A., Vallverdú, J., & Saladie, P. (2023). A review on the Pleistocene occurrences and palaeobiology of *Hippopotamus antiquus* based on the record from the Barranc de la Boella Section (Francolí Basin, NE Iberia). *Quaternary Science Reviews*, *307*, 108034.

Field, M. H., Ntinou, M., Tsartsidou, G., van Berge Henegouwen, D., Risberg, J., Tourloukis, V., Thompson, N., Karkanas, P., Panagopoulou, E., & Harvati, K. (2018). A palaeoenvironmental reconstruction (based on palaeobotanical data and diatoms) of the Middle Pleistocene elephant (*Palaeoloxodon antiquus*) butchery site at Marathousa, Megalopolis, Greece. *Quaternary International*, *497*, 108–122.

Flockhart, D. T. T., Kyser, T. K., Chipley, D., Miller, N. G., & Norris, D. R. (2015). Experimental evidence shows no fractionation of strontium isotopes ($^{87}Sr/^{86}Sr$) among soil, plants, and herbivores: implications for tracking wildlife and forensic science. *Isotopes in Environmental and Health Studies*, *51*(3), 372–381. https://doi.org/10.1080/10256016.2015.1021345

Frank, A. B., Frei, R., Triantaphyllou, M., Vassilakis, E., Kristiansen, K., & Frei, K. M. (2021). Isotopic range of bioavailable strontium on the Peloponnese peninsula, Greece: A multi-proxy approach. *Science of the Total Environment*, *774*, 145181.

Franz-Odendaal, T. A., Lee-Thorp, J. A., & Chinsamy, A. (2003). Insights from stable light isotopes on enamel defects and weaning in Pliocene herbivores. *Journal of biosciences*, *28*, 765–773.

Fritsch, C. J., Plebani, M., & Downs, C. T. (2022). Inundation area drives hippo group aggregation and dispersal in a seasonal floodplain system. *Mammalian Biology*, *102*(5), 1811–1821.

Gabunia, L., Vekua, A., Lordkipanidze, D., Swisher, C. C., Ferring, R., Justus, A., Nioradze, M., Tvalchrelidze, M., Antón, S. C., Bosinski, G., Jöris, O., Lumley, M.-A.-d., Majsuradze, G., & Mouskhelishvili, A. (2000). Earliest Pleistocene Hominid Cranial Remains from Dmanisi, Republic of Georgia: Taxonomy, Geological Setting, and Age. *Science*, *288*(5468), 1019–1025. https://doi.org/doi:10.1126/science.288.5468.1019

Galway-Witham, J., Cole, J., & Stringer, C. (2019). Aspects of human physical and behavioural evolution during the last 1 million years. *Journal of Quaternary Science*, *34*(6), 355–378. https://doi.org/https://doi.org/10.1002/jqs.3137

Gamble, C. (2017). Thresholds in hominin complexity during the Middle Pleistocene: A persistent places approach. In *Crossing the Human Threshold* (pp. 3-23). Routledge.

Garcia, T., Féraud, G., Falguères, C., de Lumley, H., Perrenoud, C., & Lordkipanidze, D. (2010). Earliest human remains in Eurasia: New 40Ar/39Ar dating of the Dmanisi hominid-bearing levels, Georgia. *Quaternary Geochronology*, *5*(4), 443–451. https://doi.org/https://doi.org/10.1016/j.quageo.2009.09.012

Gaudzinski-Windheuser, S., Kindler, L., MacDonald, K., & Roebroeks, W. (2023). Hunting and processing of straight-tusked elephants 125.000 years ago: Implications for Neanderthal behavior. *Science Advances*, *9*(5), eadd8186.

Giusti, D., Tourloukis, V., Konidaris, G., Thompson, N., Karkanas, P., Panagopoulou, E., & Harvati, K. (2018). Beyond maps: patterns of formation processes at the Middle Pleistocene open-air site of Marathousa 1, Megalopolis Basin, Greece. *Quaternary International*, *497*, 137–153.

Gómez, A., & Lunt, D. H. (2007). Refugia within Refugia: Patterns of Phylogeographic Concordance in the Iberian Peninsula. In S. Weiss & N. Ferrand (Eds.), *Phylogeography of Southern European Refugia: Evolutionary perspectives on the origins and conservation of European biodiversity* (pp. 155-188). Springer Netherlands. https://doi.org/10.1007/1-4020-4904-8_5

Goodman, A. H. (1991). Stress, adaptation, and enamel developmental defects. *Human Paleopathology: Current Synthesis and Future Options*, 280–287.

Green, D. R., Smith, T. M., Olack, G., Williams, I., Colman, A. S., & Uno, K. T. (under review). How Teeth Record and Attenuate Seasonal Signals. *Available at SSRN 4522645*.

Green, D. R., Witzel, C., Colman, A., Kierdorf, H., Smith, T. M., Williams, I. S., Lewis, J. E., Boës, X., Uno, K. T., & Harmand, S. (2023). Hydrological seasonality bracketing

the 3.3 Ma LOM3 archaeological site of Lomekwi, Kenya, via fossil hippopotamid oxygen isotope compositions and Bayesian inverse methods. *AGU23*.

Grube, R., Palombo, M., Iacumin, P., & Di Matteo, A. (2010). What did the fossil elephants from Neumark-Nord eat. In H. Meller (Ed.), *Elefantenreich. Eine Fossilwelt in Europa. Landesamt für Denkmalpflege und Archäologie Sachsen-Anhalt, Halle* (pp. 253–272). Landesamt für Denkmalpflege und Archäologie Sachsen-Anhalt.

Guatelli-Steinberg, D., Ferrell, R. J., & Spence, J. (2012). Linear enamel hypoplasia as an indicator of physiological stress in great apes: Reviewing the evidence in light of enamel growth variation. *American Journal of Physical Anthropology*, *148*(2), 191–204.

Guibert-Cardin, J., Tourloukis, V., Thompson, N., Panagopoulou, E., Harvati, K., Nicoud, E., & Beyries, S. (2022). The function of small tools in Europe during the Middle Pleistocene: The case of Marathousa 1 (Megalopolis, Greece). *Journal of lithic studies*, *9*(1).

Harvati, K., & Reyes-Centeno, H. (2022). Evolution of Homo in the Middle and Late Pleistocene. *Journal of Human Evolution*, *173*, 103279. https://doi.org/https://doi.org/10.1016/j.jhevol.2022.103279

Head, M. J., & Gibbard, P. L. (2015). Early–Middle Pleistocene transitions: linking terrestrial and marine realms. *Quaternary International*, *389*, 7–46.

Herbert, T. D. (2023). The mid-Pleistocene climate transition. *Annual Review of Earth and Planetary Sciences*, *51*(1), 389-418.

Hewitt, G. M. (1999). Post-glacial re-colonization of European biota. *Biological journal of the Linnean Society*, *68*(1-2), 87–112.

Hewitt, G. M. (2000). The genetic legacy of the Quaternary ice ages. *Nature*, *405*(6789), 907–913.

Iannucci, A., Mecozzi, B., & Sardella, R. (2023). Beware of the "Wolf event"–Remarks on large mammal dispersals in Europe and the late Villafranchian faunal turnover. *Alpine and Mediterranean Quaternary*, *36*(1), 75–90.

Iliopoulos, J., & Stathopoulou, E. (2023). Preservation and characterization of collagen in animal skeletal material from Quaternary locations in Greece & Cyprus. *Quaternary International*, *660*, 13–20. https://doi.org/https://doi.org/10.1016/j.quaint.2022.12.008

Jacobs, Z., Li, B., Karkanas, P., Tourloukis, V., Thompson, N., Panagopoulou, E., & Harvati, K. (2018). Optical dating of K-feldspar grains from Middle Pleistocene lacustrine sediment at Marathousa 1 (Greece). *Quaternary International*, *497*, 170–177. https://doi.org/10.1016/j.quaint.2018.06.029

Joannin, S. b., Cornée, J.-J., Moissette, P., Suc, J.-P., Koskeridou, E., Lécuyer, C., Buisine, C. d., Kouli, K., & Ferry, S. (2007). Changes in vegetation and marine environments in the eastern Mediterranean (Rhodes, Greece) during the Early and Middle Pleistocene. *Journal of the Geological Society*, *164*(6), 1119–1131.

Jones, E. L. (2022). What is a refugium? Questions for the Middle–Upper Palaeolithic transition in peninsular southern Europe. *Journal of Quaternary Science*, *37*(2), 136–141. https://doi.org/https://doi.org/10.1002/jqs.3274

Kahlke, R. (2001). Schädelreste von Hippopotamus aus dem Unterpleistozän von Untermaßfeld. *Das Pleistozän von Untermaßfeld bei Meiningen (Thóringen), Teil*, *2*, 483–500.

Karaiskou, N., Tsakogiannis, A., Gkagkavouzis, K., Operator of Parnitha National, P., Papika, S., Latsoudis, P., Kavakiotis, I., Pantis, J., Abatzopoulos, T. J., Triantaphyllidis, C., & Triantafyllidis, A. (2014). Greece: A Balkan Subrefuge for a Remnant Red Deer (*Cervus Elaphus*) Population. *Journal of Heredity*, *105*(3), 334–344. https://doi.org/10.1093/jhered/esu007

Karkanas, P., Tourloukis, V., Thompson, N., Giusti, D., Panagopoulou, E., & Harvati, K. (2018). Sedimentology and micromorphology of the Lower Palaeolithic lakeshore site Marathousa 1, Megalopolis basin, Greece. *Quaternary International*, *497*, 123–136.

Karkanas, P., Tourloukis, V., Thompson, N., Giusti, D., Tsartsidou, G., Athanassiou, A., Konidaris, G., Roditi, E., Panagopoulou, E., & Harvati, K. (in press). The Megalopolis Paleoenvironmental Project (MEGAPAL). In K. Harvati & M. Ioannidou (Eds.), *Human Evolution at the CROSSROADS: Research in Greece and beyond* Tübingen University Press.

Kierdorf, H., Filevych, O., Lutz, W., & Kierdorf, U. (2016). Dental defects as a potential indicator of chronic malnutrition in a population of fallow deer (*Dama dama*) from northwestern Germany. *The Anatomical Record*, *299*(10), 1409–1423.

Koch, P. L., Tuross, N., & Fogel, M. L. (1997). The effects of sample treatment and diagenesis on the isotopic integrity of carbonate in biogenic hydroxylapatite. *Journal of Archaeological Science*, *24*(5), 417–429.

Kohn, M. J. (1996). Predicting animal $\delta^{18}O$: Accounting for diet and physiological adaptation. *Geochimica et Cosmochimica Acta*, *60*(23), 4811–4829. https://doi.org/https://doi.org/10.1016/S0016-7037(96)00240-2

Kohn, M. J. (2010). Carbon isotope compositions of terrestrial C_3 plants as indicators of (paleo)ecology and (paleo)climate. *Proceedings of the National Academy of Sciences*, *107*(46), 19691–19695. https://doi.org/doi:10.1073/pnas.1004933107

Kohn, M. J., & Cerling, T. E. (2002). Stable Isotope Compositions of Biological Apatite. *Reviews in Mineralogy and Geochemistry*, *48*(1), 455–488. https://doi.org/10.2138/rmg.2002.48.12

Konidaris, G.E., & Tourloukis, V. (2021). Proboscidea-*Homo* interactions in open-air localities during the Early and Middle Pleistocene of western Eurasia: a palaeontological and archaeological perspective. In G.E. Konidaris, R. Barkai, V. Tourloukis, K. Harvati (Eds.), Human-elephant interactions: From past to present (pp. 67–104). Tübingen University Press, https://doi.org/10.15496/publikation-55599

Konidaris, G. E., Tourloukis, V., Boni, G., Athanassiou, A., Giusti, D., Thompson, N., Syrides, G., Panagopoulou, E., Karkanas, P., & Harvati, K. (2023). Marathousa 2: A New Middle Pleistocene Locality in the Megalopolis Basin (Greece) with evidence of hominin exploitation of megafauna (Hippopotamus). *PaleoAnthropology*, *2023*(1), 34-55.

Konidaris, G. E., Athanassiou, A., Panagopoulou, E., & Harvati, K. (2022). First record of *Macaca* (Cercopithecidae, Primates) in the Middle Pleistocene of Greece. *Journal of Human Evolution*, *162*, 103104. https://doi.org/https://doi.org/10.1016/j.jhevol.2021.103104

Konidaris, G. E., Athanassiou, A., Tourloukis, V., Chitoglou, K., van Kolfschoten, T., Giusti, D., Thompson, N., Tsartsidou, G., Roditi, E., Panagopoulou, E., Karkanas, P., & Harvati, K. (2024). The late Early-Middle Pleistocene mammal fauna from the Megalopolis Basin (Peloponnese, Greece) and its importance for biostratigraphy and palaeoenvironment. *Quaternary*.

Konidaris, G. E., Athanassiou, A., Tourloukis, V., Thompson, N., Giusti, D., Panagopoulou, E., & Harvati, K. (2018). The skeleton of a straight-tusked elephant (*Palaeoloxodon antiquus)* and other large mammals from the Middle Pleistocene butchering locality Marathousa 1 (Megalopolis Basin, Greece): preliminary results. *Quaternary international*, *497*, 65–84.

Konidaris, G. E., & Kostopoulos, D. S. (2024). The Late Pliocene–Middle Pleistocene Large Mammal Faunal Units of Greece. *Quaternary*, *7*(2), 27.

Konidaris, G. E., Tourloukis, V., Boni, G., Athanassiou, A., Giusti, D., Thompson, N., Syrides, G., Panagopoulou, E., Karkanas, P., & Harvati, K. (2023). Marathousa 2: A New Middle Pleistocene Locality in 1 the Megalopolis Basin (Greece) with Evidence of Hominin Exploitation of Megafauna (*Hippopotamu*s).

Koutsodendris, A., Kousis, I., Peyron, O., Wagner, B., & Pross, J. (2019). The Marine Isotope Stage 12 pollen record from Lake Ohrid (SE Europe): Investigating short-

term climate change under extreme glacial conditions. *Quaternary Science Reviews*, *221*, 105873. https://doi.org/https://doi.org/10.1016/j.quascirev.2019.105873

Kyrikou, S., Marinova, E., Bludau, I., Karkanas, P., Panagopoulou, E., Tourloukis, V., Junginger, A., & Harvati, K. (in press). The Middle Pleistocene MIS 12 palynological record from Marathousa palaeolake in Southern Greece: Highlighting favourable conditions in Marathousa 1 (MAR-1) refugial region during the severe glacial period. In K. Harvati & M. Ioannidou (Eds.), *Human Evolution at the CROSSROADS: Research in Greece and beyond* Tübingen University Press.

Lee–Thorp, J. (2002). Two decades of progress towards understanding fossilization processes and isotopic signals in calcified tissue minerals. *Archaeometry*, *44*(3), 435–446. https://doi.org/https://doi.org/10.1111/1475-4754.t01-1-00076

LeGeros, R. Z. (1991). 6. Calcium Phosphates in Enamel, Dentin and Bone. In *Calcium Phosphates in Oral Biology and Medicine* (Vol. 15, pp. 0). S.Karger AG. https://doi.org/10.1159/000419238

Levin, N. E., Cerling, T. E., Passey, B. H., Harris, J. M., & Ehleringer, J. R. (2006). A stable isotope aridity index for terrestrial environments. *Proceedings of the National Academy of Sciences*, *103*(30), 11201–11205.

Lewison, R. (2007). Population responses to natural and human-mediated disturbances: assessing the vulnerability of the common hippopotamus (*Hippopotamus amphibius*). *African Journal of Ecology*, *45*(3), 407–415.

Lister, A. M. (2004). The impact of Quaternary Ice Ages on mammalian evolution. *Philosophical Transactions of the Royal Society of London. Series B: Biological Sciences*, *359*(1442), 221–241.

Liu, Z., Prendergast, A., Drysdale, R., & May, J.-H. (2022). Comparison of bulk and sequential sampling methodologies on mammoth tooth enamel and their implications in paleoenvironmental reconstructions. *E&G Quaternary Science Journal*, *71*(2), 227–241.

Longinelli, A. (1984). Oxygen isotopes in mammal bone phosphate: a new tool for paleohydrological and paleoclimatological research? *Geochimica et cosmochimica Acta*, *48*(2), 385-390.

Macaluso, L., Bertini, A., Carnevale, G., Eronen, J. T., Martinetto, E., Saarinen, J., Villa, A., Capasso, F., & Delfino, M. (2023). A combined palaeomodelling approach reveals the role as selective refugia of the Mediterranean peninsulas. *Palaeogeography, Palaeoclimatology, Palaeoecology*, *625*, 111699.

Magri, D., Di Rita, F., Aranbarri, J., Fletcher, W., & González-Sampériz, P. (2017). Quaternary disappearance of tree taxa from Southern Europe: Timing and trends. *Quaternary Science Reviews*, *163*, 23–55. https://doi.org/https://doi.org/10.1016/j.quascirev.2017.02.014

Magri, D., & Palombo, M. R. (2013). Early to Middle Pleistocene dynamics of plant and mammal communities in South West Europe. *Quaternary International*, *288*, 63-72.

Margari, V., Roucoux, K., Magri, D., Manzi, G., & Tzedakis, P. (2018). The MIS 13 interglacial at Ceprano, Italy, in the context of Middle Pleistocene vegetation changes in southern Europe. *Quaternary Science Reviews*, *199*, 144–158.

Marra, F., Nomade, S., Pereira, A., Petronio, C., Salari, L., Sottili, G., Bahain, J.-J., Boschian, G., Di Stefano, G., & Falguères, C. (2018). A review of the geologic sections and the faunal assemblages of Aurelian Mammal Age of Latium (Italy) in the light of a new chronostratigraphic framework. *Quaternary Science Reviews*, *181*, 173–199.

Martínez-Navarro, B., Madurell-Malapeira, J., Ros-Montoya, S., Espigares, M.-P., Medin, T., Hortola, P., & Palmqvist, P. (2015). The Epivillafranchian and the arrival of pigs into Europe. *Quaternary International*, *389*, 131–138.

Martino, R., & Pandolfi, L. (2022). The Quaternary *Hippopotamus* records from Italy. *Historical Biology*, *34*(7), 1146–1156.

Mead, A. J. (1999). Enamel hypoplasia in Miocene rhinoceroses (*Teleoceras*) from Nebraska: evidence of severe physiological stress. *Journal of Vertebrate Paleontology*, *19*(2), 391–397.

Mecozzi, B. (2023). The *Hippopotamus* remains from the latest Early Pleistocene site of Cava Redicicoli (Rome, central Italy). *Bollettino della Societa Paleontologica Italiana*, *62*(3), 263–279.

Melentis, J. (1965). Über *Hippopotamus antiquus* DESMAREST aus dem Mittelpleistozän des Beckens von Megalopolis in Peloponnes (Griechenland). *Ann. Géol. Pays Hellén*, *16*, 403-435.

Melentis, J. K. (1961). Die Dentition der pleistozänen Proboscidier des Beckens von Megalopolis im Peloponnes (Griechenland). *Ann. Geol. Pays Helléniques*, *12*, 153–262.

Melentis, J. K. (1963). Die Osteologie der pleistozänen Proboscidier des Beckens von Megalopolis im Peloponnes (Griechenland). *Ann. Geol. Pays Helléniques*, *14*, 1–107.

Metcalfe, J. Z. (2021). C_3 plant isotopic variability in a boreal mixed woodland: implications for bison and other herbivores. *PeerJ*, *9*, e12167–e12167. https://doi.org/10.7717/peerj.12167

Metcalfe, J. Z., & Longstaffe, F. J. (2012). Mammoth tooth enamel growth rates inferred from stable isotope analysis and histology. *Quaternary Research*, *77*(3), 424–432.

Michailidis, D., Konidaris, G. E., Athanassiou, A., Panagopoulou, E., & Harvati, K. (2018). The ornithological remains from Marathousa 1 (middle Pleistocene; Megalopolis basin, Greece). *Quaternary International*, *497*, 85–94.

Mol, D., de Vos, J., & van der Plicht, J. (2007). The presence and extinction of *Elephas antiquus* Falconer and Cautley, 1847, in Europe. *Quaternary International*, *169–170*, 149–153. https://doi.org/https://doi.org/10.1016/j.quaint.2006.06.002

Moncel, M.-H., & Ashton, N. (2018). From 800 to 500 ka in Western Europe. The oldest evidence of Acheuleans in their technological, chronological, and geographical framework. *The emergence of the Acheulean in East Africa and beyond: Contributions in Honor of Jean Chavaillon*, 215–235.

Moncel, M.-H., García-Medrano, P., Despriée, J., Arnaud, J., Voinchet, P., & Bahain, J.-J. (2021). Tracking behavioral persistence and innovations during the Middle Pleistocene in Western Europe. Shift in occupations between 700 and 450 ka at la Noira site (Centre, France). *Journal of Human Evolution*, *156*, 103009. https://doi.org/https://doi.org/10.1016/j.jhevol.2021.103009

Moncel, M.-H., Landais, A., Lebreton, V., Combourieu-Nebout, N., Nomade, S., & Bazin, L. (2018). Linking environmental changes with human occupations between 900 and 400 ka in Western Europe. *Quaternary International*, *480*, 78–94. https://doi.org/10.1016/j.quaint.2016.09.065

Moncel, M.-H., Santagata, C., Pereira, A., Nomade, S., Voinchet, P., Bahain, J.-J., Daujeard, C., Curci, A., Lemorini, C., Hardy, B., Eramo, G., Berto, C., Raynal, J.-P., Arzarello, M., Mecozzi, B., Iannucci, A., Sardella, R., Allegretta, I., Delluniversità, E., . . . Piperno, M. (2020). The origin of early Acheulean expansion in Europe 700 ka ago: new findings at Notarchirico (Italy). *Scientific Reports*, *10*(1), 13802. https://doi.org/10.1038/s41598-020-68617-8

Mondanaro, A., Melchionna, M., Di Febbraro, M., Castiglione, S., Holden, P. B., Edwards, N. R., Carotenuto, F., Maiorano, L., Modafferi, M., Serio, C., Diniz-Filho, J. A. F., Rangel, T., Rook, L., O'Higgins, P., Spikins, P., Profico, A., & Raia, P. (2020). A Major Change in Rate of Climate Niche Envelope Evolution during Hominid History. *iScience*, *23*(11), 101693. https://doi.org/https://doi.org/10.1016/j.isci.2020.101693

Norwood, A. L., Pobiner, B. L., Shedden, K., & Kingston, J. D. (2023). Modeling periodicity in equid serial enamel isotopes as a proxy for precipitation seasonality. *Palaeogeography, Palaeoclimatology, Palaeoecology*, *625*, 111666.

O'Leary, M. H. (1988). Carbon isotopes in photosynthesis. *Bioscience*, *38*(5), 328-336.

Okuda, M., van Vugt, N., Nakagawa, T., Ikeya, M., Hayashida, A., Yasuda, Y., & Setoguchi, T. (2002). Palynological evidence for the astronomical origin of lignite–detritus sequence in the Middle Pleistocene Marathousa Member, Megalopolis, SW Greece. *Earth and Planetary Science Letters*, *201*(1), 143–157. https://doi.org/https://doi.org/10.1016/S0012-821X(02)00706-9

Palmqvist, P., Gröcke, D. R., Arribas, A., & Farina, R. A. (2003). Paleoecological reconstruction of a lower Pleistocene large mammal community using biogeochemical (δ13C, δ15N, δ18O, Sr: Zn) and ecomorphological approaches. *Paleobiology*, *29*(2), 205–229.

Palmqvist, P., Rodriguez-Gomez, G., Figueirido, B., García-Aguilar, J. M., & Pérez-Claros, J. A. (2022). On the ecological scenario of the first hominin dispersal out of Africa. *L'Anthropologie*, *126*(1), 102998.

Palombo, M., Albayrak, E., & Marano, F. (2010). The straight-tusked Elephants from Neumark Nord, a glance to a lost world. *Elefantenreich-Eine Fossilwelt in Europa, Katalog zur Sonderausstellung im Landesmuseum für Vorgeschichte Halle. Halle (Saale)*, 219–247.

Palombo, M. R. (2014). Deconstructing mammal dispersals and faunal dynamics in SW Europe during the Quaternary. *Quaternary Science Reviews*, *96*, 50–71. https://doi.org/10.1016/j.quascirev.2014.05.013

Palombo, M. R. (2016). To what extent could functional diversity be a useful tool in inferring ecosystem responses to past climate changes? *Quaternary International*, *413*, 15-31.

Palombo, M. R. (2017). Discrete dispersal bioevents of large mammals in Southern Europe in the post-Olduvai Early Pleistocene: A critical overview. *Quaternary International*, *431*, 3–19. https://doi.org/https://doi.org/10.1016/j.quaint.2015.08.034

Palombo, M. R., & Cerilli, E. (2021). Human-alephant interactions during the Lower Palaeolithic: scrutinizing the role of environmental factors. In G.E. Konidaris, R. Barkai, V. Tourloukis, K. Harvati (Eds.), Human-elephant interactions: From past to present.

Palombo, M. R., Filippi, M. L., Iacumin, P., Longinelli, A., Barbieri, M., & Maras, A. (2005). Coupling tooth microwear and stable isotope analyses for palaeodiet reconstruction: the case study of Late Middle Pleistocene *Elephas (Palaeoloxodon) antiquus* teeth from Central Italy (Rome area). *Quaternary International*, *126*, 153–170.

Panagiotopoulos, K., Holtvoeth, J., Kouli, K., Marinova, E., Francke, A., Cvetkoska, A., Jovanovska, E., Lacey, J. H., Lyons, E. T., & Buckel, C. (2020). Insights into the evolution of the young Lake Ohrid ecosystem and vegetation succession from a southern European refugium during the Early Pleistocene. *Quaternary Science Reviews*, *227*, 106044.

Panagopoulou, E., Tourloukis, V., Thompson, N., Konidaris, G., Athanassiou, A., Giusti, D., Tsartsidou, G., Karkanas, P., & Harvati, K. (2018). The Lower Palaeolithic site of Marathousa 1, Megalopolis, Greece: overview of the evidence. *Quaternary International*, *497*, 33–46.

Passey, B. H., & Cerling, T. E. (2002). Tooth enamel mineralization in ungulates: implications for recovering a primary isotopic time-series. *Geochimica et Cosmochimica Acta*, *66*(18), 3225–3234.

Passey, B. H., Cerling, T. E., Schuster, G. T., Robinson, T. F., Roeder, B. L., & Krueger, S. K. (2005). Inverse methods for estimating primary input signals from time-averaged isotope profiles. *Geochimica et Cosmochimica Acta*, *69*(16), 4101–4116.

Passey, B. H., Robinson, T. F., Ayliffe, L. K., Cerling, T. E., Sponheimer, M., Dearing, M. D., Roeder, B. L., & Ehleringer, J. R. (2005). Carbon isotope fractionation between diet, breath CO_2, and bioapatite in different mammals. *Journal of Archaeological Science*, *32*(10), 1459–1470.

Pederzani, S., & Britton, K. (2019). Oxygen isotopes in bioarchaeology: Principles and applications, challenges and opportunities. *Earth-Science Reviews*, *188*, 77–107.

Price, T. D., Burton, J. H., & Bentley, R. A. (2002). The Characterization of Biologically Available Strontium Isotope Ratios for the Study of Prehistoric Migration.

Archaeometry, *44*(1), 117–135. https://doi.org/https://doi.org/10.1111/1475-4754.00047

Pushkina, D., Bocherens, H., & Ziegler, R. (2014). Unexpected palaeoecological features of the Middle and Late Pleistocene large herbivores in southwestern Germany revealed by stable isotopic abundances in tooth enamel. *Quaternary International*, *339-340*, 164–178. https://doi.org/https://doi.org/10.1016/j.quaint.2013.12.033

Rank, D., Wyhlidal, S., Schott, K., Weigand, S., & Oblin, A. (2018). Temporal and spatial distribution of isotopes in river water in Central Europe: 50 years experience with the Austrian network of isotopes in rivers. *Isotopes in Environmental and Health Studies*, *54*(2), 115–136.

Rivals, F., Semprebon, G. M., & Lister, A. M. (2019). Feeding traits and dietary variation in Pleistocene proboscideans: A tooth microwear review. *Quaternary Science Reviews*, *219*, 145–153. https://doi.org/https://doi.org/10.1016/j.quascirev.2019.06.027

Rodhe, A. (1998). Snowmelt-dominated systems. In *Isotope tracers in catchment hydrology* (pp. 391–433). Elsevier.

Roditi, E., & Starkovich, B. M. (2022). Investigating Middle Palaeolithic subsistence: zooarchaeological perspectives on the potential character of hominin climate refugia in Greece. *Journal of Quaternary Science*, *37*(2), 181–193.

Rodríguez, J., Willmes, C., Sommer, C., & Mateos, A. (2022). Sustainable human population density in Western Europe between 560.000 and 360.000 years ago. *Scientific Reports*, *12*(1), 6907.

Roebroeks, W. (2001). Hominid behaviour and the earliest occupation of Europe: an exploration. *Journal of Human Evolution*, *41*(5), 437–461.

Roksandic, M., Radović, P., & Lindal, J. (2018). Revising the hypodigm of *Homo heidelbergensis*: A view from the Eastern Mediterranean. *Quaternary International*, *466*, 66–81.

Rotenberg, E., Davis, D. W., Amelin, Y., Ghosh, S., & Bergquist, B. A. (2012). Determination of the decay-constant of ^{87}Rb by laboratory accumulation of ^{87}Sr. *Geochimica et Cosmochimica Acta*, *85*, 41–57. https://doi.org/https://doi.org/10.1016/j.gca.2012.01.016

Rozanski, K., Araguás-Araguás, L., & Gonfiantini, R. (1993). Isotopic patterns in modern global precipitation. *Climate change in continental isotopic records*, *78*, 1–36.

Saarinen, J., & Lister, A. M. (2016). Dental mesowear reflects local vegetation and niche separation in Pleistocene proboscideans from Britain. *Journal of Quaternary Science*, *31*(7), 799-808.

Saegusa, H., Gilbert, W. H., Johnson, P., & Raimon, M. (2009). Elephantidae. In W. H. Gilbert (Ed.), *Homo erectus: Pleistocene Evidence from the Middle Awash, Ethiopia* (pp. 0). University of California Press. https://doi.org/10.1525/california/9780520251205.003.0009

Sánchez Goñi, M. F., Extier, T., Polanco-Martínez, J. M., Zorzi, C., Rodrigues, T., & Bahr, A. (2023). Moist and warm conditions in Eurasia during the last glacial of the Middle Pleistocene Transition. *Nature Communications*, *14*(1), 2700. https://doi.org/10.1038/s41467-023-38337-4

Schwarcz, H. P., White, C. D., & Longstaffe, F. J. (2010). Stable and radiogenic isotopes in biological archaeology: some applications. *Isoscapes: Understanding movement, pattern, and process on Earth through isotope mapping*, 335–356.

Scotti-Saintagne, C., Boivin, T., Suez, M., Musch, B., Scotti, I., & Fady, B. (2021). Signature of mid-Pleistocene lineages in the European silver fir (*Abies alba Mill.*) at its geographic distribution margin. *Ecology and Evolution*, *11*(16), 10984–10999.

Slovak, N. M., & Paytan, A. (2012). Applications of Sr isotopes in archaeology. *Handbook of Environmental Isotope Geochemistry: Vol I*, 743–768.

Sponheimer, M., & Lee-Thorp, J. A. (1999). Oxygen isotopes in enamel carbonate and their ecological significance. *Journal of Archaeological Science*, *26*(6), 723–728.

Starkovich, B. M. (2023). Perception versus reality: Implications of elephant hunting by Neanderthals. *Science Advances*, *9*(5), eadg6072.

Stears, K., Nuñez, T. A., Muse, E. A., Mutayoba, B. M., & McCauley, D. J. (2019). Spatial ecology of male hippopotamus in a changing watershed. *Scientific Reports*, *9*(1), 15392.

Steinman, B. A., & Abbott, M. B. (2013). Isotopic and hydrologic responses of small, closed lakes to climate variability: Hydroclimate reconstructions from lake sediment oxygen isotope records and mass balance models. *Geochimica et Cosmochimica Acta*, *105*, 342–359.

Stewart, J. R., Lister, A. M., Barnes, I., & Dalén, L. (2010). Refugia revisited: individualistic responses of species in space and time. *Proceedings of the Royal Society B: Biological Sciences*, *277*(1682), 661-671. https://doi.org/doi:10.1098/rspb.2009.1272

Stewart, J. R., & Stringer, C. B. (2012). Human evolution out of Africa: the role of refugia and climate change. *Science*, *335*(6074), 1317–1321.

Stommel, C., Hofer, H., & East, M. L. (2016). The effect of reduced water availability in the Great Ruaha River on the vulnerable common hippopotamus in the Ruaha National Park, Tanzania. *PLoS ONE*, *11*(6), e0157145.

Strani, F. (2021). Impact of Early and Middle Pleistocene major climatic events on the palaeoecology of Southern European ungulates. *Historical Biology*, *33*(10), 2260–2275. https://doi.org/10.1080/08912963.2020.1782898

Strani, F., DeMiguel, D., Alba, D. M., Moyà-Solà, S., Bellucci, L., Sardella, R., & Madurell-Malapeira, J. (2019). The effects of the "0.9 Ma event" on the Mediterranean ecosystems during the Early-Middle Pleistocene transition as revealed by dental wear patterns of fossil ungulates. *Quaternary Science Reviews*, *210*, 80–89. https://doi.org/10.1016/j.quascirev.2019.02.027

Strani, F., Sardella, R., & Mecozzi, B. (2021). An overview of the Middle Pleistocene in the north Mediterranean region. *Alpine and Mediterranean Quaternary*, *34*(1), 5-16.

Stuart-Williams, H. L. Q., & Schwarcz, H. P. (1997). Oxygen isotopic determination of climatic variation using phosphate from beaver bone, tooth enamel, and dentine. *Geochimica et Cosmochimica Acta*, *61*(12), 2539–2550. https://doi.org/https://doi.org/10.1016/S0016-7037(97)00112-9

Stuart, A. J. (2005). The extinction of woolly mammoth (*Mammuthus primigenius*) and straight-tusked elephant (*Palaeoloxodon antiquus*) in Europe. *Quaternary International*, *126-128*, 171–177. https://doi.org/https://doi.org/10.1016/j.quaint.2004.04.021

Svenning, J.-C., Normand, S., & Kageyama, M. (2008). Glacial refugia of temperate trees in Europe: insights from species distribution modelling. *Journal of Ecology*, *96*(6), 1117–1127. https://doi.org/https://doi.org/10.1111/j.1365-2745.2008.01422.x

Teitelbaum, C. S., & Mueller, T. (2019). Beyond Migration: Causes and Consequences of Nomadic Animal Movements. *Trends in Ecology & Evolution*, *34*(6), 569–581. https://doi.org/https://doi.org/10.1016/j.tree.2019.02.005

Thompson, N., Tourloukis, V., Panagopoulou, E., & Harvati, K. (2018). In search of Pleistocene remains at the Gates of Europe: Directed surface survey of the Megalopolis Basin (Greece). *Quaternary International*, *497*, 22–32. https://doi.org/10.1016/j.quaint.2018.03.036

Timmermann, A., Yun, K.-S., Raia, P., Ruan, J., Mondanaro, A., Zeller, E., Zollikofer, C., Ponce de León, M., Lemmon, D., Willeit, M., & Ganopolski, A. (2022). Climate effects on archaic human habitats and species successions. *Nature*, *604*(7906), 495–501. https://doi.org/10.1038/s41586-022-04600-9

Tourloukis, V., & Harvati, K. (2018). The Palaeolithic record of Greece: A synthesis of the evidence and a research agenda for the future. *Quaternary International*, *466*, 48–65. https://doi.org/https://doi.org/10.1016/j.quaint.2017.04.020

Tourloukis, V., & Karkanas, P. (2012). The Middle Pleistocene archaeological record of Greece and the role of the Aegean in hominin dispersals: new data and interpretations. *Quaternary Science Reviews*, *43*, 1–15.

Tourloukis, V., Muttoni, G., Karkanas, P., Monesi, E., Scardia, G., Panagopoulou, E., & Harvati, K. (2018). Magnetostratigraphic and chronostratigraphic constraints on the Marathousa 1 Lower Palaeolithic site and the Middle Pleistocene deposits of the Megalopolis basin, Greece. *Quaternary International*, *497*, 154–169. https://doi.org/10.1016/j.quaint.2018.03.043

Tourloukis, V., Thompson, N., Panagopoulou, E., Giusti, D., Konidaris, G. E., Karkanas, P., & Harvati, K. (2018). Lithic artifacts and bone tools from the Lower Palaeolithic site Marathousa 1, Megalopolis, Greece: Preliminary results. *Quaternary International*, *497*, 47–64. https://doi.org/10.1016/j.quaint.2018.05.043

Trájer, A. J. (2024). The habitat utilization and environmental resilience of Homo heidelbergensis in Europe. *Archaeological and Anthropological Sciences*, *16*(5), 1-29.

Tsoukala, E., & Lister, A. (1998). Remains of straight-tusked elephant, *Elephas (Palaeoloxodon) antiquus* Falc. & Caut.(1847) ESR-dated to oxygen isotope Stage 6 from Grevena (W. Macedonia, Greece). *BOLLETTINO-SOCIETA PALEONTOLOGICA ITALIANA*, *37*, 117–140.

Tzedakis, C., Frogley, M., & Heaton, T. (2003). Last Interglacial conditions in southern Europe: evidence from Ioannina, northwest Greece. *Global and Planetary Change - GLOBAL PLANET CHANGE*, *36*, 157-170. https://doi.org/10.1016/S0921-8181(02)00182-0

Tzedakis, P., Emerson, B. C., & Hewitt, G. M. (2013). Cryptic or mystic? Glacial tree refugia in northern Europe. *Trends in ecology & evolution*, *28*(12), 696–704.

Tzedakis, P. C., Frogley, M., Lawson, I., Preece, R., Cacho, I., & Abreu, L. (2004). Ecological thresholds and patterns of millennial-scale climate variability: The response of vegetation in Greece during the last glacial period. *Geology*, *32*, 109–112. https://doi.org/10.1130/G20118.1

Tzedakis, P. C., Hooghiemstra, H., & Pälike, H. (2006). The last 1.35 million years at Tenaghi Philippon: revised chronostratigraphy and long-term vegetation trends. *Quaternary Science Reviews*, *25*(23), 3416–3430. https://doi.org/https://doi.org/10.1016/j.quascirev.2006.09.002

Uno, K. T., Fisher, D. C., Wittemyer, G., Douglas-Hamilton, I., Carpenter, N., Omondi, P., & Cerling, T. E. (2020). Forward and inverse methods for extracting climate and diet information from stable isotope profiles in proboscidean molars. *Quaternary International*, *557*, 92–109.

van der Merwe, N. J., & Medina, E. (1991). The canopy effect, carbon isotope ratios and foodwebs in Amazonia. *Journal of archaeological science*, *18*(3), 249–259.

van Kolfschoten, T., Konidaris, G., Doukas, C., Athanassiou, A., Tourloukis, V., Panagopoulou, E., Karkanas, P., & Harvati, K. (in press). Voles (Rodentia, Mammalia) as a proxy to date the site Kyparissia 4 (Megalopolis Basin, Greece). In K. Harvati & M. Ioannidou (Eds.), *Human Evolution at the CROSSROADS: Research in Greece and Beyond*. Tübingen University Press.

Van Vugt, N., De Bruijn, H., Van Kolfschoten, T., Langereis, C., & Okuda, M. (2000). Magneto-and cyclostratigraphy and mammal-fauna's of the Pleistocene lacustrine Megalopolis Basin, Peloponnesos, Greece. *Geologica Ultrajectina*, *189*, 69–92.

Vera-Polo, P., Sadori, L., Jiménez-Moreno, G., Masi, A., Giaccio, B., Zanchetta, G., Tzedakis, P. C., & Wagner, B. (2024). Climate, vegetation, and environmental change during the MIS 12-MIS 11 glacial-interglacial transition inferred from a high-resolution pollen record from the Fucino Basin of central Italy. *Palaeogeography, Palaeoclimatology, Palaeoecology*, *655*, 112486. https://doi.org/https://doi.org/10.1016/j.palaeo.2024.112486

Vinken, R. (1965). *Stratigraphie und Tektonik des Beckens von Megalopolis (Peloponnes, Griechenland)*

Vlachos, E., & Delfino, M. (2016). Food for thought: Sub-fossil and fossil chelonian remains from Franchthi Cave and Megalopolis confirm a glacial refuge for *Emys orbicularis* in Peloponnesus (S. Greece). *Quaternary Science Reviews*, *150*, 158–171. https://doi.org/https://doi.org/10.1016/j.quascirev.2016.08.027

Vlachos, E., Georgalis, G. L., Konidaris, G. E., Athanassiou, A., Tourloukis, V., Thompson, N., Panagopoulou, E., & Harvati, K. (in press). Preliminary results on the reptiles from the Middle Pleistocene of Marathousa 1, Megalopolis basin (Greece). In K. Harvati & M. Ioannidou (Eds.), *Human Evolution at the CROSSROADS: Research in Greece and beyond*. Tübingen University Press.

Vogel, J. (1978). Recycling of carbon in a forest environment. *Oecologia Plantarum, 13*, 89–94.

Vystavna, Y., Harjung, A., Monteiro, L. R., Matiatos, I., & Wassenaar, L. I. (2021). Stable isotopes in global lakes integrate catchment and climatic controls on evaporation. *Nature Communications*, *12*(1), 7224. https://doi.org/10.1038/s41467-021-27569-x

Wallace, J. (2018). *Reconstructing Equid Mobility in Miocene Florida Using Strontium Isotopes* University of Cincinnati.

Wang, H., Wang, P., Zhao, X., Zhang, W., Li, J., Xu, C., & Xie, P. (2021). What triggered the Asian elephant's northward migration across southwestern Yunnan? *The Innovation*, *2*(3), 100142. https://doi.org/https://doi.org/10.1016/j.xinn.2021.100142

Wang, Y., & Cerling, T. E. (1994). A model of fossil tooth and bone diagenesis: implications for paleodiet reconstruction from stable isotopes. *Palaeogeography, Palaeoclimatology, Palaeoecology*, *107*(3-4), 281–289.

Yang, D., Uno, K. T., Souron, A., McGrath, K., Pubert, É., & Cerling, T. E. (2020). Intra-tooth stable isotope profiles in warthog canines and third molars: Implications for paleoenvironmental reconstructions. *Chemical Geology*, *554*, 119799.

Zanazzi, A., Fletcher, A., Peretto, C., & Hohenstein, U. T. (2022). Middle Pleistocene paleoclimate and paleoenvironment of Central Italy and their relationship with hominin migrations and evolution. *Quaternary International*, *619*, 12-29.

Zazzo, A., Balasse, M., & Patterson, W. P. (2005). High-resolution $\delta^{13}C$ intratooth profiles in bovine enamel: Implications for mineralization pattern and isotopic attenuation. *Geochimica et Cosmochimica Acta*, *69*(14), 3631–3642. https://doi.org/https://doi.org/10.1016/j.gca.2005.02.031

Zazzo, A., Bendrey, R., Vella, D., Moloney, A., Monahan, F., & Schmidt, O. (2012). A refined sampling strategy for intra-tooth stable isotope analysis of mammalian enamel. *Geochimica et Cosmochimica Acta*, *84*, 1–13.

–This page is left intentionally blank –

APPENDIX

–This page is left intentionally blank –

Appendix A

Study I

First stable isotope results on the ecology of the straight-tusked elephant (*Palaeoloxodon antiquus*) from the Middle Pleistocene Marathousa 1 (Peloponnese, Greece)

Authors: Effrosyni Roditi, Hervé Bocherens, George E. Konidaris, Athanassios Athanassiou, Vangelis Tourloukis, Eleni Panagopoulou, Katerina Harvati

Manuscript accepted for publication in: *Human Evolution at the CROSSROADS: Research in Greece and beyond*. Proceedings of the Closing Symposium, February 2022 Tübingen. Paleoanthropology Book Series – Contributions in Paleoanthropology III. Tübingen University Press*.

Accepted: 22.03.2023

* The following version is based on the authors formatting of the manuscript and figures. General layout and position of Tables and Figures may differ in the final published manuscript.

12 FIRST STABLE ISOTOPE RESULTS ON THE ECOLOGY OF THE STRAIGHT-TUSKED ELEPHANT (*PALAEOLOXODON ANTIQUUS*) FROM THE MIDDLE PLEISTOCENE MARATHOUSA 1 (PELOPONNESE, GREECE)

Effrosyni Roditi[1,*], Herve Bocherens[2], George E. Konidaris[1], Athanassios Athanassiou[3], Vangelis Tourloukis[1,4], Eleni Panagopoulou[3], Katerina Harvati[1,5]

[1]Paleoanthropology, Institute for Archaeological Sciences and Senckenberg Centre for Human Evolution and Palaeoenvironment, Department of Geosciences, Eberhard Karls University of Tübingen, Tübingen, Germany
[2]Biogeology, Department of Geosciences and Senckenberg Centre for Human Evolution and Paleoenvironment, Eberhard Karls University of Tübingen, Tübingen, Germany
[3]Hellenic Ministry of Culture, Ephorate of Paleoanthropology–Speleology, Athens, Greece
[4]Department of History and Archaeology, School of Philosophy, University of Ioannina, Ioannina, Greece
[5]DFG Centre for Advanced Studies 'Words, Bones, Genes, Tools', Eberhard Karls University of Tübingen, Tübingen, Germany
**effrosyni.roditi@uni-tuebingen.de*

http://dx.doi.org/10.15496/publikation-97670

Keywords: Stable isotopes; paleoecology; Middle Pleistocene; *Palaeoloxodon*; Megalopolis Basin

12.1 INTRODUCTION

Carbon and oxygen stable isotope analysis of mammalian carbonate bioapatite is, nowadays, a well-established and widely used approach for past ecological investigations and paleoenvironmental reconstructions. Carbon is incorporated into mammalian tissues through their dietary intake. In this regard, the ratios of stable carbon isotopes in the tissues of primary consumers—hereafter expressed using the delta (δ) notation, wherein $\delta^{13}C=[(^{13}C/^{12}C)sample/(^{13}C/^{12}C)standard - 1] \times 1000$— reflect the isotopic composition of the ingested plant matter (DeNiro and Epstein, 1978), enriched by ~14.1 ± 0.5‰ in tooth enamel carbonate of large herbivores (Cerling and Harris, 1999; Passey et al., 2005), due to physiological and metabolic processes. In terrestrial ecosystems, variation in the isotopic signature of plant carbon permits a distinction between the two main photosynthetic pathways, i.e., C_4 and C_3 (Ehleringer and Monson, 1993), with the former group consisting of warm growth season grasses and forbs, which demonstrate higher average $\delta^{13}C$ value (~13‰), and the latter incorporating trees, shrubs, and cool growth season grasses and sedges with a modern average $\delta^{13}C$ value of ~27‰ (Bender, 1971; Kohn, 2010). Within plant communities utilizing the C_3 photosynthetic pathway, additional environmentally controlled fractionation occurs, which is governed by multiple factors, such as degree of canopy closure, water availability, temperature, irradiance,

e. roditi: https://orcid.org/0000-0002-1917-7645
H. Bocherens : https://orcid.org/0000-0002-0494-0126
G. e. Konidaris: https://orcid.org/0000-0002-7041-233x
a. athanassiou: https://orcid.org/0000-0002-9140-7011
v. tourloukis: https://orcid.org/0000-0002-9527-2708
K. Harvati: https://orcid.org/0000-0001-5998-4794

or atmospheric CO_2 diffusion (van der Merwe and Medina, 1991; Heaton, 1999; Hofman-Kamińska et al., 2018). The interplay of these factors enables further habitat distinctions within the wide range of $\delta^{13}C$ values documented in C_3-dominated ecosystems, since carbon isotopic ratios of herbivores feeding under closed canopy conditions, i.e., dense forests, tend to be lower than for herbivores foraging in open woodlands, open parklands and grasslands, or at the top of the canopy (Drucker et al., 2008; Bocherens and Drucker, 2013).

Oxygen stable isotopic ratios in the skeletal tissues of large mammals essentially reflect those of ingested water. Variation in the isotopic composition of the latter occurs as a result of several geospatial, climatic, and environmental parameters, for instance degree of continentality, altitudinal differences, amount of precipitation, temperature, as well as differences in the hydrological processes of water bodies (for a detailed overview see Pederzani and Britton (2019). In organisms that acquire water predominantly from drinking, i.e., obligate drinkers, oxygen stable isotopes track primarily the isotopic composition of the local meteoric water (Kohn and Cerling, 2002). In middle and high latitudes, the $\delta^{18}O$— provided by the equation $[(^{18}O/^{16}O)sample/(^{18}O/^{16}O)standard - 1] \times 1000$ —of meteoric water is considered to be mainly associated with surface temperature and local precipitation (Fricke and O'Neil, 1996), where higher $\delta^{18}O$ values are observed in warmer and drier environments but lower values indicate colder or more humid periods (Bocherens and Drucker, 2013; Pederzani and Britton, 2019).

Systematic excavations at the Middle Pleistocene open-air site Marathousa 1 (MAR-1) in the Megalopolis Basin (Peloponnese, Greece) revealed the partial skeleton of a straight-tusked elephant (*Palaeoloxodon antiquus*). The elephant was found at the base of the find-bearing sedimentary Unit 3

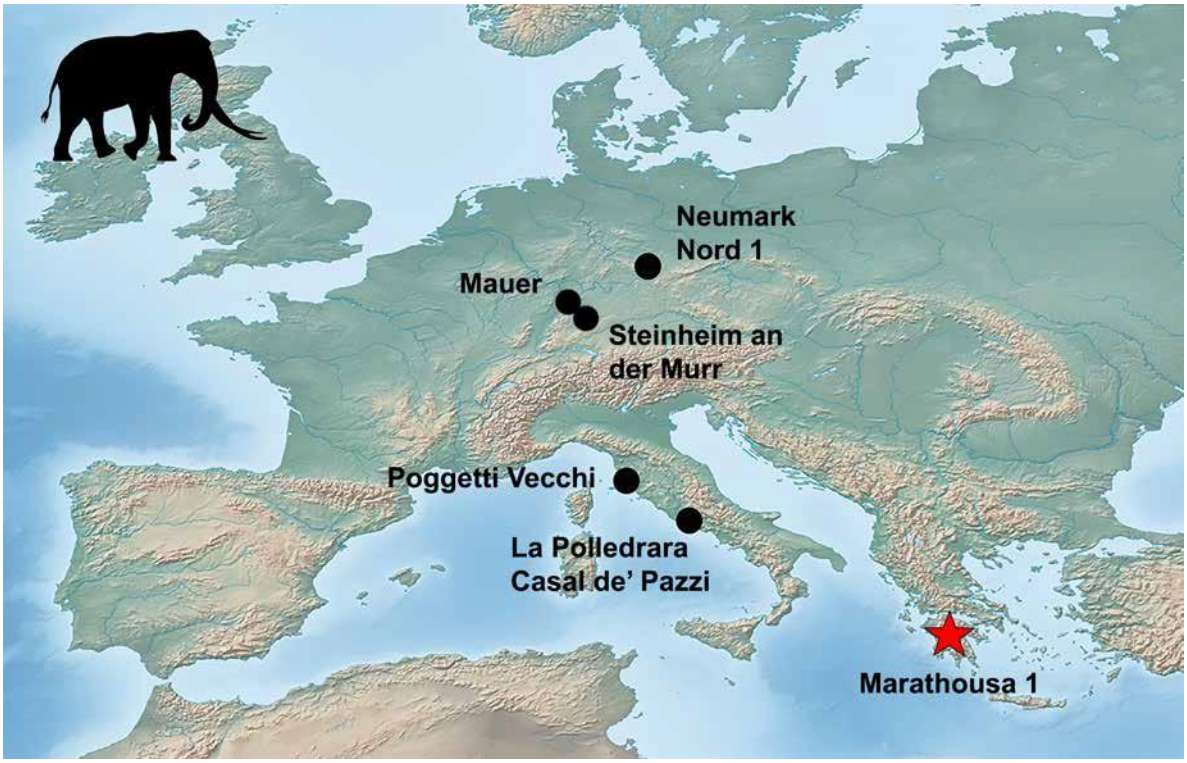

Figure 1: map showing the location of european sites with available stable isotope data for *Palaeoloxodon antiquus* (made with natural earth, naturalearthdata.com).

in Area A and is stratigraphically and spatially associated with lithic artefacts, and faunal (ostracods, molluscs, fishes, amphibians, reptiles, birds, mammals) and floral remains (see Harvati et al., 2018; Panagopoulou et al., 2018). The archaeological deposits are dated to ca. 450 ka and are correlated to the glacial Marine Isotope Stage 12 (Doukas et al., 2018; Jacobs et al., 2018; Karkanas et al., 2018; Tourloukis et al., 2018). The elephant skeleton belongs to a male individual with an estimated upper limit of its ontogenetic age between 64−71 years based on the tooth wear of the preserved upper third molars, which is also consistent with the extent of epiphyseal fusion of the skeletal elements (Konidaris et al., 2018). Additionally, the taphonomic study of the elephant's remains revealed cutmarks on some of the skeletal elements, indicating hominin exploitation of the carcass (Konidaris et al., 2018), while the traceological analysis of stone-tools further confirms that they were used in butchering activities (Guibert-Cardin et al., 2022).

In this study, we employ stable isotope analysis on enamel carbonates in order to reconstruct the average diet, and, subsequently, the preferred foraging habitat of the MAR-1 elephant. Since evidence of butchering directly associates the specimen with hominin activity, the resulting paleoenvironmental data can be used to infer the conditions surrounding hominin presence in the Megalopolis Basin. Because only one individual was available for analysis, we compared our results with published isotopic data for *Palaeoloxodon antiquus* from other European Middle Pleistocene localities, namely La Polledrara di Cecanibbio, Casal de' Pazzi (Palombo et al., 2005), and Poggetti Vecchi (Capalbo, 2018) in Italy; Neumark-Nord 1 (Grube et al., 2010), Steinheim an der Murr, and Mauer (Pushkina et al., 2014) in Germany (Fig. 1).

12.2 MATERIALS AND METHODS

We sampled the second distalmost lamella of the right upper third molar. The sample's surface was mechanically cleaned with a diamond-tipped handheld rotary tool to remove cementum and expose the enamel. Subsequently, the first few millimeters of the enamel layer were also removed to avoid contamination (Koch et al., 1997). Multiple samples were drilled perpendicularly across the tooth-growth axis, each yielding approximately 15 mg of enamel powder. Here, we present the average value obtained by analyzing the individual samples, to simulate a bulk-sampling strategy for the sake of comparison with other published records.

Following the pretreatment protocol described by Bocherens et al. (1994) and Koch et al. (1997), 1.35 ml of 2.5% sodium hypochlorite (NaOCl) was added to the sample vials, homogenized with high-speed vibration, and left to react for 24 hours to remove organic matter. Subsequently, the samples were centrifuged at 35000 rounds/minute for 3 minutes, the solution was removed, and the contents were rinsed repeatedly with MilliQ water. Next, a 1M Acetic Acid Buffer solution was added and left to react with the samples for 24 hours, to remove nonstructural carbonates. After the acetic acid buffer was extracted, the samples were rinsed three times with MilliQ H_2O and dried at 35°C for 72 hours. This process produced approximately 3 mg of purified biogenic apatite, which was reacted with concentrated orthophosphoric acid (H_3PO_4) to release CO_2. Stable isotope ratios were then obtained by analyzing the gaseous CO_2 with continuous multi-flow isotope ratio mass spectrometry (IRMS) at the University of Tübingen. Two international standards, IAEA-603 (International Atomic Energy Agency) and NBS-18 (National Bureau of Standards, now National Institute of Standards and Technology or NIST), as well as three in-house standards were used for calibration.

Results are expressed using the standard δ notation:

$$\delta^{j}X = \frac{(^{j}X/^{i}X)_{sample}}{(^{j}X/^{i}X)_{standard}} - 1$$

where ^{j}X is the heavier isotope and ^{i}X is the lighter isotope (Bond and Hobson, 2012). Measured ratios refer to $^{13}C/^{12}C_{VPDB}$ or $^{18}O/^{16}O_{VSMOW}$, wherein VPDB is Vienna Peedee Belemnite and VSMOW is Vienna Standard Mean Ocean Water.

12.3 RESULTS AND DISCUSSION

The mean $\delta^{13}C$ of the structural carbonate from the enamel of the straight-tusked elephant from MAR-1 is –11.2 ‰ (VPDB). The value falls within the expected range for a diet consisting purely of C_3 vegetation (–19.5 ‰ – –8.0 ‰ VPDB) after applying an enrichment factor of 1.5‰ (Koch et al., 2004; Tipple et al., 2010) to account for the difference in Pleistocene atmospheric CO_2 values relative to present day, due to the effects of fossil fuel burning. Furthermore, a mesic habitat consisting of open woodland can be deduced, considering that, in temperate environments, $\delta^{13}C$ values of Pleistocene herbivores lower than ~–14‰ indicate foraging under closed canopy forests, whereas values between –14‰ and –8‰ suggest more open landscapes (Farquhar et al., 1989; Ehleringer and Monson, 1993; Bocherens, 2003; Domingo et al., 2017; Metcalfe, 2021).

Similar results were obtained from the carbon stable isotope analysis of a *Palaeoloxodon antiquus* individual from the Middle Pleistocene site of Poggetti Vecchi (Italy, MIS 7), which yielded an average $\delta^{13}C$ value of –11.05 ‰ VPDB (Capalbo, 2018). Additionally, the $\delta^{13}C$ value of the MAR-1 specimen falls within the range of $\delta^{13}C$ values (from –13.7 ‰ to –9.9 ‰ VPDB) obtained for the straight-tusked elephant population of Casal de' Pazzi (Italy, MIS 7; Palombo et al., 2005). In contrast, results from La Polledrara di Cecanibbio (Italy, MIS 9) demonstrated higher $\delta^{13}C$ values (from –9 ‰ to –10.9 ‰ VPDB) (Palombo et al., 2005), suggesting that this population was feeding in a drier environment with more open C_3 vegetation compared to the MAR-1 elephant, and the majority of the specimens from Italy correlated with MIS 7. The $\delta^{13}C$ values of *P. antiquus* specimens from three sites in Germany, namely Neumark Nord 1 (MIS 5; Grube et al., 2010), Steinheim an der Murr (MIS 11; Pushkina et al., 2014), and Mauer (MIS 15; Pushkina et al., 2014), appear to be lower than those of the MAR-1 specimen (Fig. 2), suggesting more forested and humid environments for the German localities.

With respect to oxygen isotope ratios, the average $\delta^{18}O$ value of the enamel bioapatite for the MAR-1 elephant (+23.5 ‰ VSMOW) plots lower than those of the Italian *P. antiquus* specimens correlated with MIS 7 and MIS 9, with values ranging between +24.8 ‰ and +27.6 ‰ VSMOW (Fig. 2). Higher oxygen isotopic values (+25.5 ‰ – +28.0 ‰ VSMOW) were also obtained for the specimens of Neumark-Nord 1 in Germany during MIS 5. However, in juxtaposition with the results obtained for the elephants of Steinheim an der Murr, and Mauer, the MAR-1 elephant demonstrates a higher $\delta^{18}O$ value. This likely indicates that the interglacial specimens from La Polledrara, Casal de' Pazzi, and Poggetti Vecchi in Italy, as well as those of Neumark-Nord-1, experienced warmer or more arid climatic conditions compared to the MAR-1 elephant, whereas cooler or more humid conditions characterize the environment of the interglacial populations from Steinheim an der Murr and Mauer in Germany. The influence of continentality may have also contributed in part to this pattern, specifically concerning the comparison of the Mediterranean sites with data from Germany, wherein values are expected to become more ^{18}O-depleted as distance from the coast increases.

Overall, the results are compatible with the

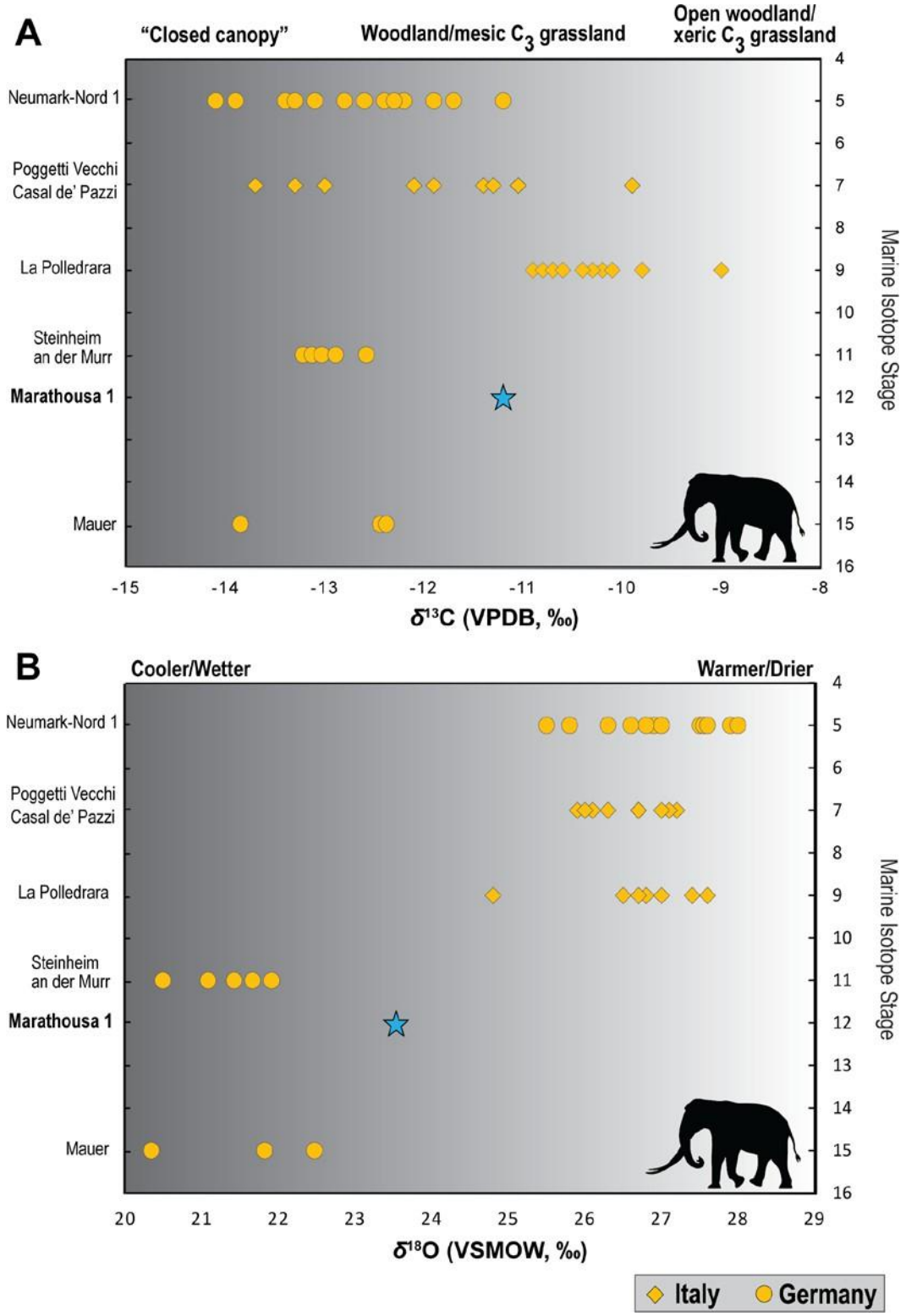

Figure 2: a, mean δ^{13}c values and B, mean δ^{18}o values for the straight-tusked elephant (*Palaeoloxodon antiquus*) of marathousa 1 (mar-1) compared to published *Palaeoloxodon* isotopic data from other european middle pleistocene localities. warm colours have been chosen to indicate interglacial conditions and cool tones to signify glacial stages.

correlation of the archaeological sequence from MAR-1 with a glacial stage (MIS 12; see also Boni et al., this volume; Butiseaca et al., this volume; Kyrikou et al., this volume), reflecting colder conditions in the eastern European peri-Mediterranean region during glacial stages. Nevertheless, the carbon and oxygen isotopic composition of the studied elephant individual suggests that moderately humid conditions likely persisted in the Megalopolis Basin, which, in turn, supported abundant C_3 vegetation cover. This indicates that the effects of the glaciation in the area were less severe, creating conditions that provided essential subsistence resources to both fauna and hominins, therefore aiding their survival.

CONCLUSIONS

The preliminary results of the stable isotope study on the *Palaeoloxodon antiquus* from the Middle Pleistocene of Marathousa 1 highlight the significance of the method in obtaining important palaeoecological insights from an individual organism with the prospect of addressing broader paleoenvironmental concepts. The present study provides additional support to the hypothesis that the region acted as a refugium for fauna and hominins through the palaeoecological characterization of the individual. Future research will focus on the investigation of intra-tooth isotopic profiles with the aim to obtain temporally high-resolution palaeoecological data and investigate in greater detail potential sources of variation in the isotopic composition of the individual, such as possible seasonal fluctuations in resource availability.

ACKNOWLEDGMENTS

Excavation at Marathousa 1 was conducted under a permit granted to the Ephorate of Palaeoanthropology–Speleology, Hellenic Ministry of Culture. It was supported by the ERC Consolidator Grant ERC-CoG-724703 ("CROSSROADS") and the ERC Starting Grant ERC-StG-283503 ("PaGE"), both awarded to K.H. G.E.K., V.T. and K.H. are also supported by the Deutsche Forschungsgemeinschaft (DFG Project no. 463225251, "MEGALOPOLIS"). E.R. and K.H. are also supported by the ERC Advanced Grant ERC-AdG-101019659 ("FIRSTSTEPS"). The authors are grateful to the two reviewers, A. Junginger and D. Pushkina, for their insightful comments and suggestions.

REFERENCES

Bender, M.M., 1971. Variations in the $^{13}C/^{12}C$ ratios of plants in relation to the pathway of photosynthetic carbon dioxide fixation. Phytochemistry, 10(6), pp. 1239−1244.

Bocherens, H., 2003. Isotopic biogeochemistry and the palaeoecology of the mammoth steppe fauna. Deinsea, 9(1), pp. 57−76.

Bocherens, H., Fizet, M. and Mariotti, A., 1994. Diet, physiology and ecology of fossil mammals as inferred from stable carbon and nitrogen isotope biogeochemistry: implications for Pleistocene bears. Palaeogeography, Palaeoclimatology, Palaeoecology, 107(3-4), pp. 213−225.

Bocherens, H., Drucker, D.G., 2013. Carbonate stable isotopes | Terrestrial teeth and bones, in: Elias, S. A. and Mock, C. J.(Eds.), Encyclopedia of Quaternary Science (Second Edition). Amsterdam: Elsevier.

Bond, A. L., Hobson, K. A., 2012. Reporting stable-isotope ratios in ecology: Recommended terminology, guidelines and best practices. Waterbirds, 35(2), pp. 324−331.

Boni, G., Syrides, G., Konidaris, G.E., Athanassiou, A., Tourloukis, V., Koukousioura, O., Panagopoulou, E., Karkanas, P. and Harvati,

K., this volume. Preliminary results on the taxonomy and paleoenvironmental analysis of the mollusc fauna from Marathousa 1, Marathousa 2 and Kyparissia 4 (Middle Pleistocene, Megalopolis Basin, Greece).

Butiseacă, G.A., Vaseliev, I., Tourloukis, V., Junginger, A., Mulch, A., Karkanas, P., Panagopoulou, E. And Harvati, K., this volume. Preliminary biomarker/paleoclimate reconstruction results from the Marathousa 1 Lower Paleolithic site (Megalopolis Basin, Greece).

Capalbo, C., 2018. Multiproxy-based reconstruction of the feeding habits from the late Middle Pleistocene straight-tusked elephant population of Poggetti Vecchi (Southern Tuscany, Italy). Alpine and Mediterranean Quaternary, 31, pp. 113−119.

Cerling, T.E., Harris, J. M., 1999. Carbon isotope fractionation between diet and bioapatite in ungulate mammals and implications for ecological and paleoecological studies. Oecologia, 120, pp. 347−363.

DeNiro, M.J., Epstein, S., 1978. Influence of diet on the distribution of carbon isotopes in animals. Geochimica et cosmochimica acta, 42(5), pp. 495−506.

Domingo, L., Rodríguez-Gómez, G., Libano, I. and Gómez-Olivencia, A., 2017. New insights into the Middle Pleistocene paleoecology and paleoenvironment of the Northern Iberian Peninsula (Punta Lucero Quarry site, Biscay): A combined approach using mammalian stable isotope analysis and trophic resource availability modeling. Quaternary Science Reviews, 169, pp. 243−262.

Doukas, C., Van Kolfschoten, T., Papayianni, K., Panagopoulou, E. and Harvati, K., 2018. The small mammal fauna from the Palaeolithic site Marathousa 1 (Greece). Quaternary International, 497, pp. 95–107.

Drucker, D. G., Bridault, A., Hobson, K. A., Szuma, E. and Bocherens, H., 2008. Can carbon-13 in large herbivores reflect the canopy effect in temperate and boreal ecosystems? Evidence from modern and ancient ungulates. Palaeogeography, Palaeoclimatology, Palaeoecology, 266(1-2), pp. 69-82.

Ehleringer, J.R., Monson, R.K., 1993. Evolutionary and ecological aspects of photosynthetic pathway variation. Annual Review of Ecology and Systematics, 24, pp. 411−439.

Farquhar, G.D., Ehleringer, J. R. and Hubick, K. T., 1989. Carbon isotope discrimination and photosynthesis. Annual review of plant biology, 40, pp. 503−537.

Fricke, H.C., O'Neil, J. R., 1996. Inter- and intra-tooth variation in the oxygen isotope composition of mammalian tooth enamel phosphate: implications for palaeoclimatological and palaeobiological research. Palaeogeography, Palaeoclimatology, Palaeoecology, 126(1-2), pp. 91−99.

Grube, R., Palombo, M., Iacumin, P. and Di Matteo, A., 2010. What did the fossil elephants from Neumark-Nord eat?, in: Meller H. (Ed.), Elefantenreich. Eine Fossilwelt in Europa. Halle: Landesamt für Denkmalpflege und Archäologie Sachsen-Anhalt, pp. 253−272.

Guibert-Cardin, J., Tourloukis, V., Thompson, N., Panagopoulou, E., Harvati, K., Nicoud, E. and Beyries, S., 2022. The function of small tools in Europe during the Middle Pleistocene: The case of Marathousa 1 (Megalopolis, Greece). Journal of lithic studies, 9.

Harvati K., Konidaris G. and Tourloukis V., 2018. Human Evolution at the Gates of Europe, Quaternary International Special Issue, 497, part A, pp. 1−240

Heaton, T. H., 1999. Spatial, species, and temporal variations in the $^{13}C/^{12}C$ ratios of C_3 plants: implications for palaeodiet studies. Journal of Archaeological Science, 26(6), pp. 637−649.

Hofman-Kamińska, E., Bocherens, H., Borowik, T., Drucker, D. G. and Kowalczyk, R., 2018.

Stable isotope signatures of large herbivore foraging habitats across Europe. PLoS ONE, 13, p. e0190723.

Jacobs, Z., Li, B., Karkanas, P., Tourloukis, V., Thompson, N., Panagopoulou, E. and Harvati, K., 2018. Optical dating of K-feldspar grains from Middle Pleistocene lacustrine sediment at Marathousa 1 (Greece). Quaternary International, 497, pp. 170–177.

Karkanas, P., Tourloukis, V., Thompson, N., Giusti, D., Panagopoulou, E. and Harvati, K., 2018. Sedimentology and micromorphology of the Lower Palaeolithic lakeshore site Marathousa 1, Megalopolis Basin, Greece. Quaternary International, 497, pp. 123–136.

Koch, P. L., Tuross, N. and Fogel, M.L., 1997. The effects of sample treatment and diagenesis on the isotopic integrity of carbonate in biogenic hydroxylapatite. Journal of Archaeological Science, 24(5), pp. 417–429.

Koch, P.L., Diffenbaugh, N. S. and Hoppe, K. A., 2004. The effects of late Quaternary climate and pCO_2 change on C_4 plant abundance in the south-central United States. Palaeogeography, Palaeoclimatology, Palaeoecology, 207(3-4), pp. 331–357.

Kohn, M.J., 2010. Carbon isotope compositions of terrestrial C_3 plants as indicators of (paleo) ecology and (paleo)climate. Proceedings of the National Academy of Sciences, 107(46), pp. 19691–19695.

Kohn, M.J., Cerling, T. E., 2002. Stable isotope compositions of biological apatite. Reviews in Mineralogy and Geochemistry, 48(1), pp. 455–488.

Konidaris, G.E., Athanassiou, A., Tourloukis, V., Thompson, N., Giusti, D., Panagopoulou, E. and Harvati, K., 2018. The skeleton of a straight-tusked elephant (*Palaeoloxodon antiquus*) and other large mammals from the Middle Pleistocene butchering locality Marathousa 1 (Megalopolis Basin, Greece): preliminary results. Quaternary International, 497, pp. 65–84.

Kyrikou, S., Marinova, E., Bludau, I. J. E., Karkanas, P., Panagopoulou, E., Tourloukis, V., Junginger, A. and Harvati, K., this volume. The Middle Pleistocene MIS 12 palynological record from Marathousa palaeolake in Southern Greece: Highlighting favourable conditions in Marathousa 1 (MAR-1) refugial region during the severe glacial period.

Metcalfe, J.Z., 2021. C_3 plant isotopic variability in a boreal mixed woodland: implications for bison and other herbivores. PeerJ, 9, p. e12167.

Palombo, M.R., Filippi, M.L., Iacumin, P., Longinelli, A., Barbieri, M. and Maras, A., 2005. Coupling tooth microwear and stable isotope analyses for palaeodiet reconstruction: the case study of late Middle Pleistocene *Elephas* (*Palaeoloxodon*) *antiquus* teeth from Central Italy (Rome area). Quaternary International, 126, pp. 153–170.

Panagopoulou, E., Tourloukis, V., Thompson, N., Konidaris, G., Athanassiou, A., Giusti, D., Tsartsidou, G., Karkanas, P. and Harvati, K., 2018. The Lower Palaeolithic site of Marathousa 1, Megalopolis, Greece: overview of the evidence. Quaternary International, 497, pp. 33–46.

Passey, B.H., Robinson, T.F., Ayliffe, L.K., Cerling, T.E., Sponheimer, M., Dearing, M.D., Roeder, B.L. and Ehleringer, J. R., 2005. Carbon isotope fractionation between diet, breath CO_2, and bioapatite in different mammals. Journal of Archaeological Science, 32(10), pp. 1459–1470.

Pederzani, S., Britton, K., 2019. Oxygen isotopes in bioarchaeology: Principles and applications, challenges and opportunities. Earth-Science Reviews, 188, pp. 77–107.

Pushkina, D., Bocherens, H. and Ziegler, R., 2014. Unexpected palaeoecological features of

the Middle and Late Pleistocene large herbivores in southwestern Germany revealed by stable isotopic abundances in tooth enamel. Quaternary International, 339–340, pp. 164–178.

Tipple, B.J., Meyers, S.R. and Pagani, M., 2010. Carbon isotope ratio of Cenozoic CO_2: A comparative evaluation of available geochemical proxies. Paleoceanography, 25(3), pp. PA3202.

Tourloukis, V., Muttoni, G., Karkanas, P., Monesi, E., Scardia, G., Panagopoulou, E. and Harvati, K., 2018. Magnetostratigraphic and chronostratigraphic constraints on the Marathousa 1 Lower Palaeolithic site and the Middle Pleistocene deposits of the Megalopolis Basin, Greece. Quaternary International, 497, pp. 154–169.

van der Merwe, N.J., Medina, E., 1991. The canopy effect, carbon isotope ratios and foodwebs in Amazonia. Journal of Archaeological Science, 18(3), pp. 249–259.

Appendix B

Study II

Life-history of *Palaeoloxodon antiquus* reveals Middle Pleistocene glacial refugium in the Megalopolis basin, Greece

Authors: Effrosyni Roditi, Hervé Bocherens, George E. Konidaris, Athanassios Athanassiou, Vangelis Tourloukis, Panagiotis Karkanas, Eleni Panagopoulou, Katerina Harvati

Journal: Scientific Reports

Initial submission: 26.10.2023

Accepted: 07.01.2024

DOI: https://doi.org/10.1038/s41598-024-51592-9

scientific reports

Check for updates

OPEN

Life-history of *Palaeoloxodon antiquus* reveals Middle Pleistocene glacial refugium in the Megalopolis basin, Greece

Effrosyni Roditi[1], Hervé Bocherens[2,3], George E. Konidaris[1,3], Athanassios Athanassiou[4], Vangelis Tourloukis[1,5], Panagiotis Karkanas[7], Eleni Panagopoulou[4] & Katerina Harvati[1,3,6]✉

The Balkans are considered a major glacial refugium where flora and fauna survived glacial periods and repopulated the rest of Europe during interglacials. While it is also thought to have harboured Pleistocene human populations, evidence linking human activity, paleoenvironmental indicators and a secure temporal placement to glacial periods is scant. Here, we present the first intra-tooth multi-isotope analysis for the European straight-tusked elephant *Palaeoloxodon antiquus*, on an adult male individual excavated in association with lithic artefacts at the MIS 12 site Marathousa 1 (Megalopolis basin, Greece). The studied find also exhibits anthropogenic modifications, providing direct evidence of hominin presence. We employed strontium, carbon and oxygen isotope analysis on enamel bioapatite to investigate its foraging and mobility behaviour, using a sequential sampling strategy along the tooth growth axis of the third upper molar, to assess ecological changes during the last decade of life. We found a geographically restricted range, in a C_3-dominated open woodland environment, and relatively stable conditions over the examined timeframe. Our results show that, despite the severity of the MIS 12 glacial, the Megalopolis basin sustained a mesic habitat, sufficient plant cover and limited seasonal fluctuations in resource availability, pointing to its role as a glacial refugium for both fauna and hominins.

The Balkan peninsula is considered to have played a major biogeographic role in Pleistocene Europe, broadly acting as a glacial refugium for both plant and animal species, as well as a source for the repopulation of higher latitude regions during interglacial periods (e.g.,[1–6]). In recent years, the Megalopolis basin, southern Greece, has emerged as a potential refugium-within-a-refugium area[7] (or micro-refugium[6]), harbouring favourable environmental conditions, freshwater resources, rich faunal and floral communities, as well as human populations in the Middle Pleistocene[8–15]. Here, we investigate the life history of a straight-tusked elephant (*Palaeoloxodon antiquus*) from Marathousa 1 (hereafter MAR-1; Fig. 1; Supplementary Notes 2), a Lower Paleolithic elephant butchering site dating to the MIS 12 (~478–424 ka BP) glacial[8,11,12,16–18], one of the most impactful glacial intervals, which featured the largest ice volume throughout the Quaternary[19–21]. The MIS 12 cold and arid conditions resulted in vegetational shifts, such as the retraction of temperate forests and expansion of steppe vegetation[21–24] and marked a turning point for hominin adaptations reflected in their subsequent (MIS 11) demographic expansion and the dissemination of diverse locally-developed technological innovations (e.g. refs.[25–29]). In addition to rich cultural remains, comprising more than 2000 stone and bone artifacts[13], MAR-1 has yielded a diverse faunal assemblage, including an elephant partial skeleton (hereafter MAR-1A-5). The MAR-1A-5 preserves anthropogenic cutmarks and was found associated with lithic artefacts, thus providing a direct link to hominin activity at the site[10,13]. We combine carbon ($^{13}C/^{12}C$), oxygen ($^{18}O/^{16}O$), and strontium ($^{87}Sr/^{86}Sr$) isotope analyses to investigate the

[1]Paleoanthropology, Institute for Archaeological Sciences, Department of Geosciences, Eberhard Karls University of Tübingen, Tübingen, Germany. [2]Biogeology, Department of Geosciences, Eberhard Karls University of Tübingen, Tübingen, Germany. [3]Senckenberg Centre for Human Evolution and Paleoenvironment, University of Tübingen, Tübingen, Germany. [4]Hellenic Ministry of Culture, Ephorate of Paleoanthropology–Speleology, Athens, Greece. [5]Department of History and Archaeology, School of Philosophy, University of Ioannina, Ioannina, Greece. [6]DFG Centre for Advanced Studies 'Words, Bones, Genes, Tools', Eberhard Karls University of Tübingen, Tübingen, Germany. [7]M.H. Wiener Laboratory for Archaeological Science, American School of Classical Studies, Athens, Greece. ✉email: katerina.harvati@ifu.uni-tuebingen.de

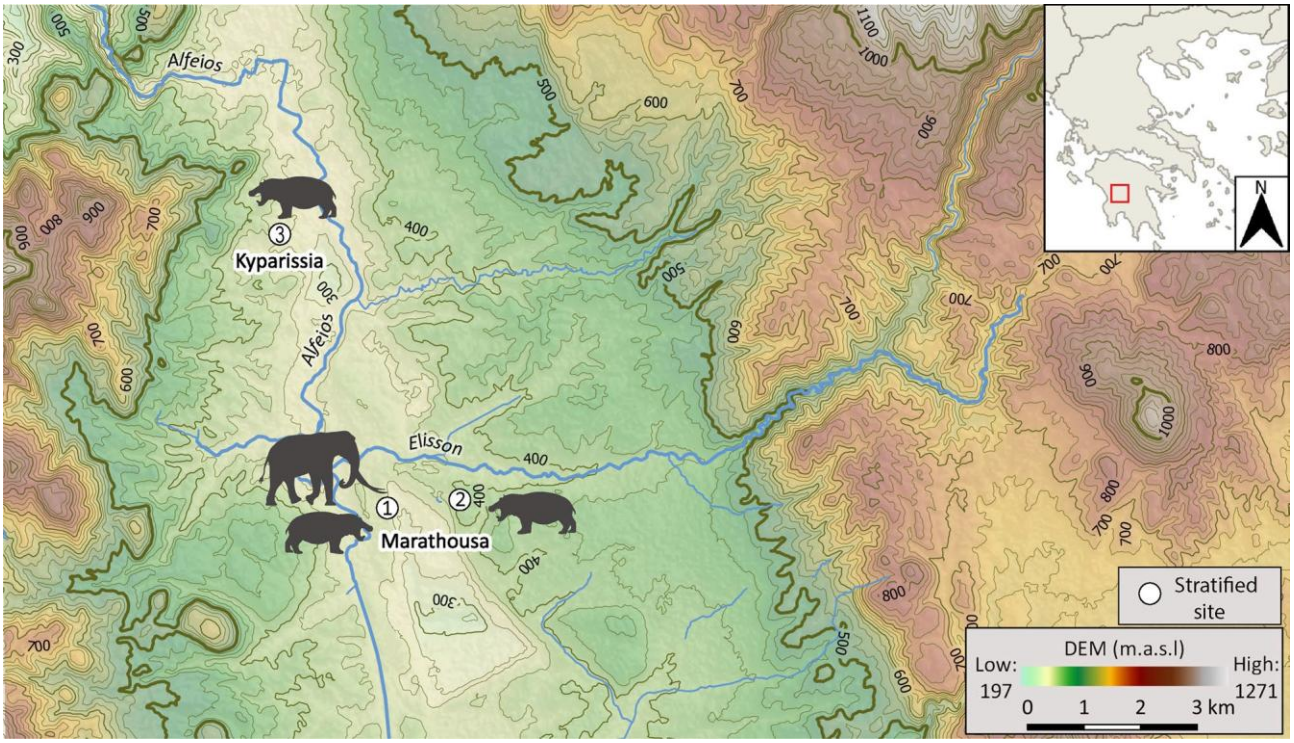

Figure 1. Topographic map of the Megalopolis basin showing the location of the sites: (1) Marathousa 1; (2) Marathousa 2; (3) Kyparissia 4. Contour interval: 25 m. Digital Elevation Model (DEM) from the Shuttle Radar Topography Mission (SRTM) version 3[126]. The map was created using QGIS version 3.16 (https://www.qgis.org).

foraging and mobility patterns of this individual, and to help reconstruct paleoenvironmental conditions in the basin during its lifetime.

Straight-tusked elephants (genus *Palaeoloxodon*) originated in Africa and dispersed to Eurasia towards the end of the Early Pleistocene[30], becoming common in Eurasian Middle–Late Pleistocene assemblages. The European species, *P. antiquus*, occupied a broad spectrum of habitats[31,32], demonstrating high dietary flexibility and foraging behaviour, ranging from exclusive browsing to grazing, depending on the available resources[33,34]. Despite its ecological adaptability, it is generally associated with temperate climatic conditions[32]. In central Europe, it was widely distributed during interglacial or interstadial phases, while during glacial stages, its range was mostly restricted to southern Europe[35–38]. Its occurrence is widely documented in Greece, including the Megalopolis basin[37,39]. In MAR-1 at least two individuals have been discovered during excavation, both preserving evidence of anthropogenic modifications[10].

Proboscideans played an important role in the adaptations and subsistence of Paleolithic hominins[10,40–42]. The geographic distribution and ecological signal of *P. antiquus* largely overlapped with the ecological preferences of Middle Pleistocene hominins[42]. Due to its high fat and meat quantity it likely constituted a crucial component in their diet[43,44]. Remains of *P. antiquus* associated with hominin activity either directly (e.g., cut marks, bone breakages, artefacts made from proboscidean bone) or indirectly (contextual linkage of carcasses with cultural finds), are common in the Middle Pleistocene record of western Eurasia[42]. Such associations allow paleoecological investigations of proboscidean diets and habitats to shed light also on hominin environments and subsistence (e.g.,[45,46]). Here we show that the MIS 12 individual MAR-1A-5, and, by extension, the hominins that processed its carcass, lived in relatively stable conditions with sufficient plant cover and limited seasonality.

Results

We sampled sequentially the second distalmost lamella of the MAR-1A-5 upper right M3, representing approximately the last ten years of the individual's lifespan, to obtain intra-tooth strontium, carbon and oxygen isotopic profiles. This multi-proxy strategy targeted the reconstruction of MAR-1A-5's mobility, diet and habitat, and paleoclimate, respectively. For the strontium analysis, the baseline relied on published data covering the Peloponnese[47], as well as on fossil *Hippopotamus* samples from three Middle Pleistocene localities of the Megalopolis basin. No significant correlation was observed between Sr–C or between Sr–O isotopes in the sequential profile.

Strontium isotopes

$^{87}Sr/^{86}Sr$ ratios were relatively homogenous for the majority of the profile (0.70868–0.70887; variability of 0.00019), with the exception of sample 28, taken closest to the cervix (Fig. 2A & SU Table 1; 0.70844 ± 0.00003). This result was likely related to differences in enamel maturation and/or diagenesis. We therefore considered it as

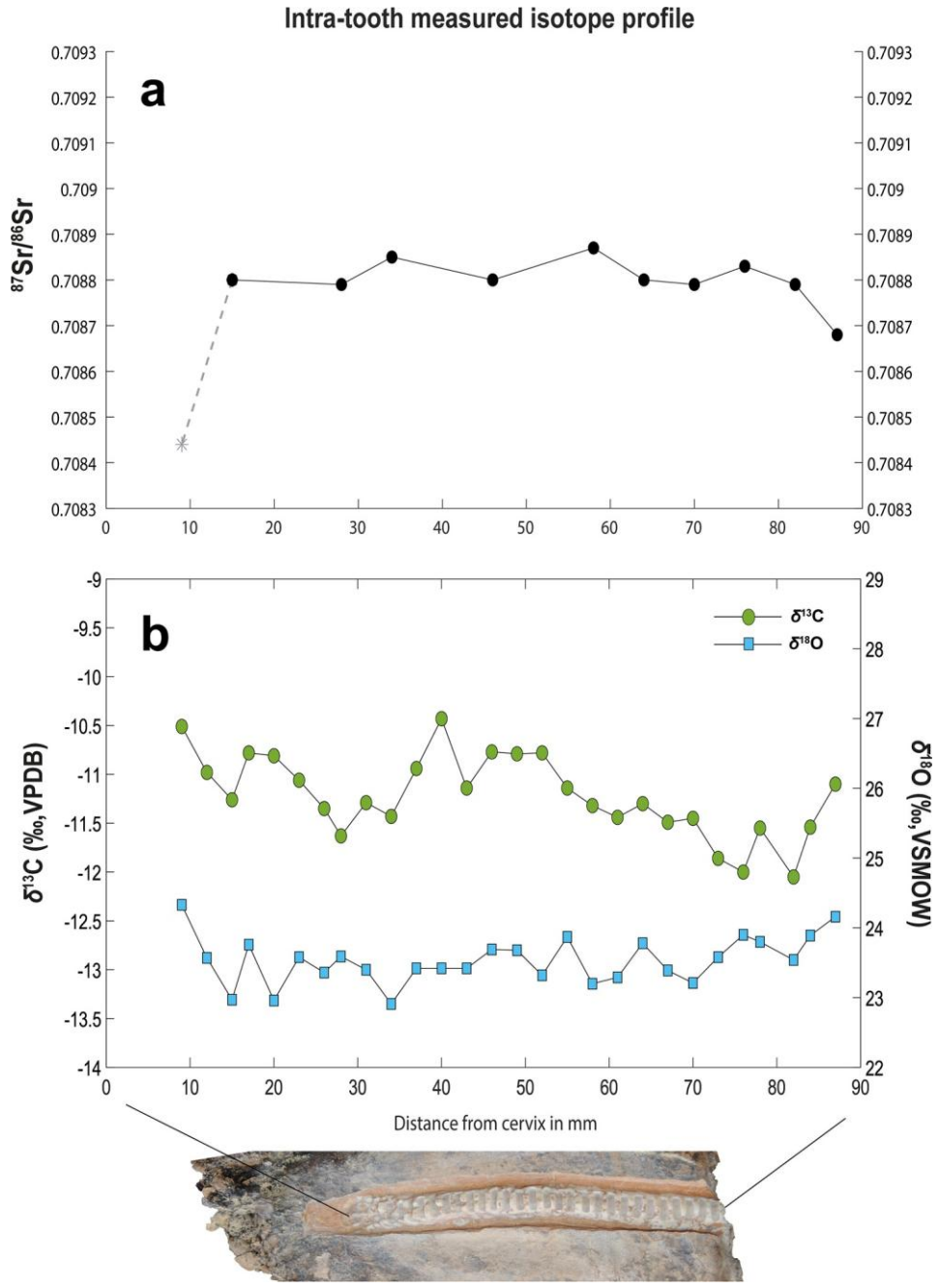

Figure 2. Enamel intra-tooth strontium isotope ratios (**a**) and intra-tooth carbon and oxygen stable isotope results (**b**) for the *Palaeoloxodon antiquus* of Marathousa 1. In (**a**), the gray dashed line represents an outlier.

an outlier and excluded it from further analysis. The remaining ratios approximated the value obtained from the fossil *Hippopotamus antiquus* excavated at the same site (MAR-1B-8; 0.70870 ± 0.00002). The $^{87}Sr/^{86}Sr$ ratio from the *H. antiquus* specimen MAR-2B-2 from the broadly contemporaneous nearby locality Marathousa 2[14] was notably higher (0.70906 ± 0.00003), as expected for an individual feeding near the outcrops of the Tripolis geotectonic unit[47]; whereas the value obtained from the Kyparissia 4 *H. antiquus*[48] (KYP4A-1004) (0.70838 ± 0.00001) was consistent with the strontium range of the Pindos geotectonic unit[47]. These results were in agreement with the localities' respective geographic locations (See Supplementary Fig. 1).

Measured carbon and oxygen isotopic values

Measured $\delta^{13}C$ values ranged between –10.4 and –12.1‰ VPDB (mean –11.2‰ VPDB) (Full data in Supplementary Table 1). The amplitude of variation (1.62‰) indicated relatively low intra-tooth variability. Nevertheless, a quasi-sinusoidal trend was observed both in the intra-tooth profile and in the moving average of $\delta^{13}C$ values.

This trend was expressed by at least two downward and one upward periods occurring on an inter-annual scale (Fig. 2B).

Measured $\delta^{18}O$ values ranged between + 22.9‰ and + 24.3‰ VSMOW (mean + 23.5‰ VSMOW) (Supplementary Table 1). A sinusoidal pattern was also observed in the oxygen isotope time series, with fluctuations occurring at relatively regular intervals (Fig. 2B). However, their low amplitude of variation (1.42‰), suggested an attenuated seasonal signal or, alternatively, a lack of seasonal effects in the isotopic composition of the local meteoric water and, subsequently, in the animal's body fluids for the measured enamel $\delta^{18}O$ series.

Modelled carbon and oxygen isotopic values

Sampling geometry and differential enamel formation processes can dampen the amplitude of the primary dietary and body water signal. We employed inverse modelling to reduce such effects[49,50]. This increased the range of carbon intra-tooth variability to 4‰. The magnitude of variation between two successive wave heights ranged from 1.4‰ to 2.1‰, suggesting moderate intensity of sub-annual isotopic change. The moving average of the modelled carbon profile (28–87 mm from the cervix) showed 5 peaks and 5 troughs. Additionally, a trend towards more positive $\delta^{13}C$ values was observed in the earlier forming section of the lamella (from the apex until approximately 56 mm in the profile), with carbon values progressively declining thereafter (Fig. 3A). Hence, the multi-seasonal pattern was prominent in both measured and modelled carbon enamel data. All carbon values fell within the expected range for a diet consisting of C_3 vegetation (see Methods).

The modelled $\delta^{18}O$ data showed a larger range of values (+ 21.6‰ – + 25.5‰) and more pronounced fluctuations, which appeared relatively regularly at a distance from 28 to 87 mm from the cervix (Fig. 3B). The estimated amplitude in adjacent wave heights ranged between 1.9 and 3.9‰.

Discussion

The *P. antiquus* foraging ecology remains relatively poorly understood. Most studies as yet have focused on dental micro- and mesowear, thus providing information for a specific temporal frame that captures the diet of the last days/weeks before the death of the individual or the average annual diet, respectively[33,34,51–55]. Stable isotope analyses for the species, which offer more long-term foraging inferences, are scarce. Published isotopic data from six Pleistocene European localities provided a comparative framework for our analysis (see Online methods and SU Table 2). Compared to *P. antiquus* from Italy, the MAR-1A-5 average $\delta^{13}C$ value approximates carbon values from MIS 7 interglacial individuals[53,56,57], indicating a similar mesic/open woodland habitat with glacial MIS 12 Megalopolis basin. In contrast, the MAR-1A-5 carbon values are lower than those recorded from MIS 9 interglacial individuals[53], suggesting a more densely forested, humid habitat in Megalopolis. Furthermore, when compared to MIS 5, 11 and 15 interglacial specimens from Germany[54,58], the MAR-1A-5 carbon values point to more open / drier conditions. In terms of climate, the MAR-1A-5 mean $\delta^{18}O$ value indicates a cooler and / or more humid setting than either MIS 7 or MIS 9 at the Italian sites[53,56,57], but warmer and / or drier conditions than two Middle Pleistocene interglacial German localities[58] (Fig. 4; see also SU 4). The inter-site comparison of the currently available *P. antiquus* stable isotope data agrees with the correlation of the MAR-1 archaeological sequence with a glacial stage (MIS 12), reflecting colder conditions in the eastern European peri-Mediterranean region. Nevertheless, the MAR-1A-5 isotopic composition also indicates the persistence of a moderately humid setting in the Megalopolis basin, supporting sufficient amounts of C_3 vegetation cover.

Carbon isotope variability can be used to infer vegetation shifts and possible seasonality. Our measured carbon isotope intra-tooth series indicates periodic variability, which is stronger on a multi-annual rather than a sub-annual temporal scale. The trend persists also in the modelled carbon isotopic composition albeit with an increase from a low to a moderate magnitude of variation. These fluctuations can be related to environmental or dietary patterns, as inherent seasonal fluctuations in the isotopic composition of C_3 plants, but also variation between plant parts (i.e., leaves relative to seeds and flowers) can result in differences of 1–3‰ in plant $\delta^{13}C$[59]. The temporal interval of change in the isotopic profile of MAR-1A-5 suggests that, although low to moderate seasonal effects may have conditioned the isotopic composition of its diet and body water, multi-season habitat or dietary shifts were equally, if not more, pronounced. Climate variability, for example prolonged changes in water availability and precipitation lasting several years, is unlikely to underlie the carbon isotope trend, as such shifts would also manifest in the $\delta^{18}O$ series but are lacking in our data. The long-term fluctuations in the $\delta^{13}C$ series may therefore be ascribed to multi-annual ranging mobility between different microhabitats or plant communities with varying canopy cover within the basin, while still using local water-sources with similar oxygen isotopic composition. In this scenario, the consistency of $^{87}Sr/^{86}Sr$ ratios may reflect the geological homogeneity of the area or, alternatively, the slow enamel maturation processes, resulting in strontium averaging and thus hindering the identification of short-scale nomadic events.

The measured enamel $\delta^{18}O$ profile yielded an attenuated signal, which could be interpreted as low seasonality in precipitation and temperature. However, such a pattern may also be produced by dampening related to hydrological processes (i.e., drinking from long-lived resident water bodies, such as lakes[60]). A recent multi-proxy study on the water-level history of MAR-1 showed that, at the time of deposition of the MAR-1A-5 elephant skeleton, seasonal ponds had developed under a mostly dry and cold climate, conditions which persisted over ~10 ka[8]. We therefore consider signal dampening due to such hydrological processes unlikely. Rather, the observed low amplitude of variation is in part influenced by the geometry of sampling and differential enamel formation processes along the tooth growth axis[50,61,62]. When inverse modelling was undertaken to minimise these effects, stronger fluctuations in the oxygen isotope time series were revealed (~ 4‰). Nevertheless, even the modelled oxygen data are inconsistent with strong seasonal fluctuations in rainfall and temperature in the MIS 12 Megalopolis basin. Even taking the difference between modelled and measured enamel data into account, the amplitude of seasonal oxygen variation for MAR-1A-5 is still much lower compared to seasonal data obtained

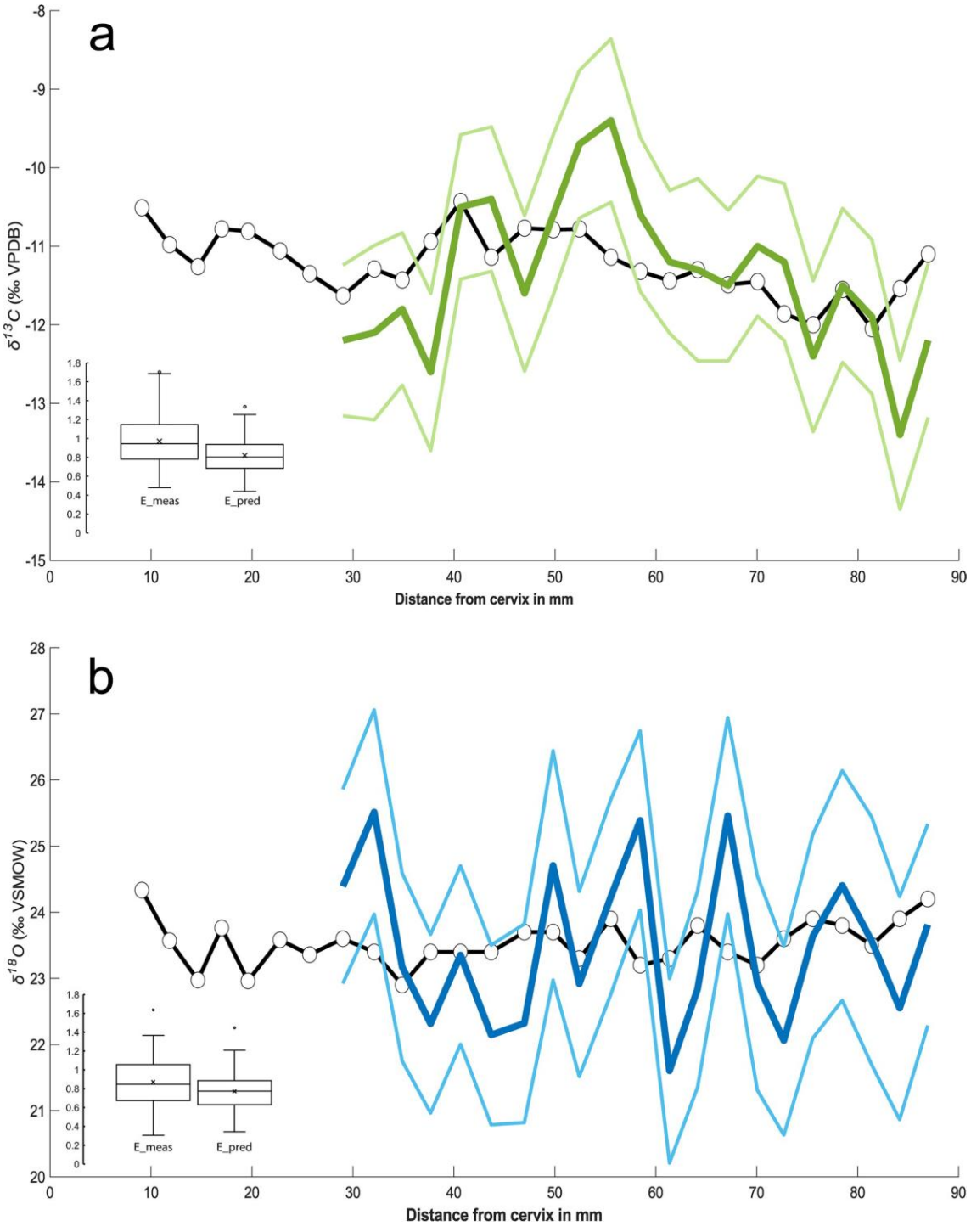

Figure 3. Inverse model results for $\delta^{13}C$ (**a**) and $\delta^{18}O$ (**b**). Bold coloured lines represent the average estimated input signal from 100 solutions (± 1σ) and circles represent measured stable isotope data. In both models l_a=30 mm, l_m=70 mm, openindx=1, r2($\sigma_{\Delta x}$)=0.3 mm, and r3($\sigma_{\Delta z}$)=0.5 mm. For (A), r1=0.1‰, ε^2=0.007, and the reference vector (RV)=−12.1 to−10.4‰. For (B) r1=0.2‰, ε^2=0.003, and RV=+22.9 to+24.2‰. Data from within 25 mm of the cervix are excluded from the inversion. Boxplots show the comparison between measured error (E_meas) and predicted error (E_pred) (see ref.[49]). The climaxes identified in the $\delta^{18}O$ series, which coincide with climaxes in $\delta^{13}C$ values, likely reflect summer conditions, whereas estimated minima in $\delta^{18}O$ and the corresponding $\delta^{13}C$ troughs express winter-time conditions over a period of ~5 years (from 28 to 87 mm along the profile).

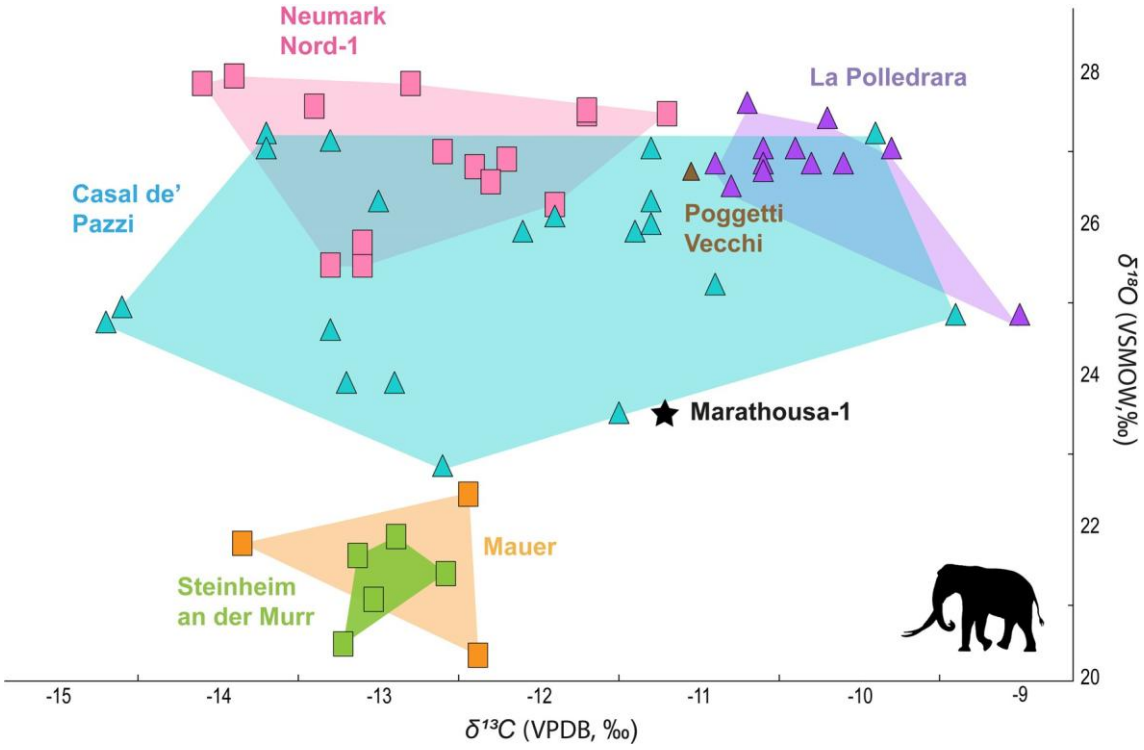

Figure 4. Bivariate plot showing $\delta^{13}C_{sc}$ (VPDB) and $\delta^{18}O_{sc}$ (VSMOW) values for *Palaeoloxodon antiquus* in European Middle Pleistocene localities. For details of the studied localities and the data used for the inter-site comparison see Methods and Supplementary Table 2. Convex hulls are used as visual representations of the range of isotopic values between different sites and have no statistical meaning.

from North American mammoths and mastodons (intra-tooth variation of 6–11‰)[63–65], further supporting moderate seasonality for MIS 12 Marathousa 1.

Strontium isotopes are used to infer animal mobility patterns. Both the MAR-1A-5 strontium ratios and those of the three Middle Pleistocene *Hippopotamus* specimens analysed fall within the range of published environmental strontium values of the Tripolis and Pindos geotectonic units[47], the local predominant geological outcrops. The relative consistency of the MAR-1A-5 strontium ratios indicates that the Marathousa elephant likely maintained strong site fidelity (i.e., a tendency to occupy the same area over a larger time frame[66]) during the decade represented by our samples, staying within the Megalopolis catchment.

In summary, our multi-isotope incremental approach indicates that MAR-1A-5 maintained a limited home range and did not exhibit large-distance mobility. It likely responded to differential seasonal food availability by consuming relatively more grasses during the wet season and relatively more woody, fruity, or leafy vegetation during drier months. Similar behavioural patterns are observed in African savannah and forest elephants (*Loxodonta africana, Loxodonta cyclotis*)[67–70] and Asian elephants (*Elephas maximus*)[71,72]. The isotopic data also show that seasonal effects, both in climatic variables and in plant productivity, were moderate, therefore ensuring essential forage within the Megalopolis catchment throughout the year over the examined time frame. Therefore, a scenario of nomadic mobility, *i.e.*, irregular inter- or intra-annual movement patterns within the Megalopolis basin, is most likely for MAR-1A-5. Such a hypothesised pattern of long-term recursion —the return to a previously utilised foraging patch after a long time— has been observed in Asian[73] and African elephants[74]. This behavior is attributed to vegetation regeneration and resource replenishing of previously overutilized patches, highlighting the strong influence of spatial memory of available resources in the movement decisions of elephants[73–78].

Although extant proboscideans have also been reported to travel over long distances (> 500 km), such long ranging behaviour is associated with severe environmental stress and habitat degradation[79,80]. The lack of long-distance ranging in our data, therefore, further points to environmental stability over the time period sampled.

The locality MAR-1 is correlated to MIS 12, considered the coldest Pleistocene glacial episode and coinciding with the largest expansion of ice cover in northern and eastern Europe. In Greece, it resulted in the formation of large ice fields on Mount Tymphi and the northern slopes of Mount Smolikas, as well as on Mount Chelmos in the Peloponnese[81,82]. Pollen records from Tenaghi Philippon (north-east Greece)[24] and Lake Ohrid (North Macedonia-Albania)[21] show that arboreal pollen reached its absolute minimum during the MIS 12 glacial maximum. This indicates extreme contraction of tree populations even in southern areas of the Balkans, considered a principal glacial refugium of Europe. Nevertheless, the prevalent climatic and environmental conditions of the Megalopolis basin remained suitable for the habitation of *P. antiquus*, a species commonly associated with temperate climates, forests, and warmer conditions. The continuous presence of *P. antiquus* through multiple periods in the Megalopolis basin ([10,83–85], ongoing studies) highlights the resilience and adaptability of the species,

which survived under diverse climatic conditions and occupied a broad range of habitats, including woodland and open grassland.

Multiple proxies have been employed to reconstruct the paleoenvironmental conditions of the archaeological layers at MAR-1. Phytoliths, diatoms and plant macrofossils demonstrated that the surrounding vegetation was diverse, suggesting still water conditions and a depositional context near a marginal reed swamp. The occurrence of plant taxa such as Palmae, *Acer, Quercus, Ulmus, Salvinia natans,* stratigraphically associated with MAR-1A-5, indicates a temperate climate at the time of the elephant's death, with mixed habitat components of dry and damp woodland, reed swamp, open damp ground, and open water[9]. The vertebrates recorded at the site comprise terrestrial (e.g., *Macaca, Bison, Cervus, Dama, Canis*) and semi-aquatic mammals (e.g., *Castor, Hippopotamus, Lutra*)[10,15] and freshwater birds (e.g., *Anas*)[86]. It is indicative of a landscape with substantial woodland components as well as more open areas and the existence of a permanent freshwater body with mean summer temperatures reaching 10–15 °C (approximately 11 °C colder than present-day summer temperatures) in the Megalopolis basin[8,10]. These paleoenvironmental interpretations are consistent with a C_3-dominated ecosystem consisting of C_3 woodland/open grassland under mesic conditions and low to moderate seasonality indicated by our isotopic analysis.

The effects of the MIS 12 glaciation in the Megalopolis area therefore appear relatively mild, maintaining conditions that allowed the persistence of a diverse temperate fauna and flora, including elephants, monkeys, hippopotami and deer, some of them exploited by Middle Pleistocene hominins[10,14]. Additionally, habitat heterogeneity and moderate seasonality, as indicated by the composition of the floral and faunal indices and the present isotope analysis, provided diverse foraging options to mammalian species, including hominins, facilitating the persistence of organisms with different ecological and dietary requirements.

Conclusions

Our study of the MAR-1A-5 *Palaeoloxodon antiquus* from the MAR-1 Lower Paleolithic elephant butchering site (Megalopolis basin, southern Greece) provides the first intra-tooth multi-isotope analysis of the European straight-tusked elephant. It is also the first stable isotope study of this species from a peri-Mediterranean glacial context, shedding new light on the foraging ecology and habitat of both this emblematic megaherbivore and the hominins exploiting it. The decadal and sub-annual scale inferences provided by our detailed life history reconstruction of MAR-1A-5 add new high-resolution detail to the paleoenvironmental reconstruction of the Megalopolis basin during MIS 12, one of the most impactful glacial periods in Europe. Our results strongly support the hypothesised role of the Megalopolis basin as a 'refugium-within-a-refugium'[7], a distinct refugial area within the major Balkan glacial refugium, where not only a diverse temperate fauna and flora, but also hominins, persisted even during the harshest glacial periods of the Middle Pleistocene.

Methods

Sampling and proboscidean enamel formation

Enamel samples were obtained from the second distalmost lamella of the fragmented upper right third molar (M3). The molars of adult elephants are formed over a timespan of approximately 10–12 years. Plate formation is sequential and proceeds on a mesial–distal direction[87], wherein the resulting effect is the development of more pronounced dental wear in the mesial part of the tooth compared to the distal one. Hence, sequential sampling of the distal lamellae is intended to provide a longer isotopic record.

Stable isotope ratios for chemical elements incorporated in tooth enamel matrix during enamel formation do not remodel once mineralization is completed. Therefore, the isotopic composition of incremental samples in hypsodont teeth, such as elephantid molars, is considered to record annual or sub-annual climatic and dietary shifts, whose temporal resolution depends on the species-specific enamel secretion and mineralization times, as well as on the implemented sampling design[88–90]. The vertical extension rate of elephantid molar plates, i.e., in the occlusal–basal direction, has been estimated to approximately 15–22 mm/year[61,91–93]. At the same time, amelogenesis, the process with which enamel forms, occurs at two stages. The secretory stage involves the incremental deposition of enamel matrix by ameloblasts, which transpires at a low angle from the enamel-dentine junction (EDJ) to the outermost surface[61]. The second stage involves the prolonged maturation of enamel, during which enamel crystals become progressively denser. This latter process results in signal attenuation and lower temporal resolution pertaining to both the timing of enamel maturation, as well as sampling geometry[88,94], although the extent of dampening is lately considered smaller than originally predicted[95].

Here, we followed an incremental sampling strategy to generate intra-tooth isotopic profiles, wherein several samples were obtained along the tooth growth axis in 2–3 mm intervals and ~ 20 mg of powdered enamel was extracted for each sample across the full enamel thickness. Prior to sampling, a section of tooth cementum over the area of interest was mechanically removed using a handheld rotary tool equipped with a diamond burr to expose the enamel. In addition, approximately 1 mm of the outer enamel surface was drilled away, to remove impurities and minimize the risk of sample contamination.

Inverse modelling

In order to minimize signal attenuation and obtain a more reliable representation of the primary isotopic input signal through the application of conventional sampling, we applied the inverse modelling procedure developed by Passey et al.[49] using the code provided by the authors. The model accounts for the contribution of isotopic signals from adjacent enamel increments that formed during different seasons and, through mathematical inversion, produces an estimated input signal that better reflects the amplitude of variation in the isotopic composition of diet and drinking water. Model input parameters include measured isotope ratios, sample geometry (length and depth), and their respective measurement uncertainties (1σ), as well as parameters related to enamel

formation, namely the length of apposition (l_a), length of maturation (l_m) and initial mineral content during enamel deposition (f_i). To measure sampling geometry with maximized accuracy, a silicon mould of the entire sampled profile was sectioned and scanned with a flatbed-scanner. Measurements were obtained using the software ImageJ[96]. With respect to enamel formation parameters, we used values established for the extant African savannah elephant *Loxodonta africana* and the extinct Columbian mammoth *Mammuthus columbi* as proxies for *P. antiquus*, where l_m = 70 mm, f_i = 65% FD, and l_a = 30 mm[50]. Samples obtained within 25 mm from the cervix were excluded from the modelling procedure, as suggested by Uno et al.[50], due to changes in enamel growth rate and geometry close to the root apex[50,93]. Conventional sampling at intervals of 2–3 mm on molars of the Elephantinae subfamily followed by the application of inverse modelling is considered sufficient for the recovery of sub-annual trends[50].

Chemical pretreatment and analysis

The acquired samples were chemically treated at the Biogeology laboratory of the University of Tübingen (Germany). Following the protocol described by Bocherens et al.[97]; Koch et al.[98], the sampled enamel powder was reacted with 2.5% sodium hypochlorite (NaOCl) for 24 h to remove organic components. After the reaction time, the vial contents were centrifuged at 3.500 rounds/minute for 3 min, the supernatant was removed, and the contents were rinsed repeatedly with distilled water. Next, samples were soaked to 1 M acetic acid buffer and left to react for 24 h, to remove non-structural, diagenetic carbonates. Once the supernatant was removed, the powder was rinsed repeatedly with Milli-Q H_2O and dried at 35° C for 72 h. Around 3 mg of purified biogenic apatite obtained through this process was reacted with concentrated (99%) orthophosphoric acid (H_3PO_4) for 4 h at 70 °C. Carbon and oxygen stable isotope ratios were obtained by analysing the gaseous CO_2 reaction products using a Multi-Flow-Geo interfaced with the Elementar Iso Prime 100 IRMS. Two international standards, IAEA-603 (International Atomic Energy Agency; $\delta^{13}C$ = + 2.46‰, $\delta^{18}O$ = –2.37‰, relative to VPDB) and NBS-18 (National Bureau of Standards, now National Institute of Standards and Technology or NIST; $\delta^{13}C$ = –5.00‰ and $\delta^{18}O$ = –22.96‰, relative to VPDB), as well as three in-house standards (Elephant CRM, Hippo CRM, Laaser Marmor CRM), were used for calibration. The analytical precision of the measurements is higher than 0.1‰ and 0.2‰ for carbon and oxygen respectively, based on multiple isotopic analysis of modern tooth enamel of elephant and hippopotamus prepared and analysed at the same time as the fossil samples. Carbon and oxygen stable isotope results are expressed using the standard δ notation:

$$\delta^{j}X = \frac{{}^{j}X/{}^{i}X_{\text{sample}}}{{}^{j}X/{}^{i}X_{\text{standard}}} - 1$$

where jX is the heavier isotope and iX is the lighter isotope[99]. Measured ratios refer to $^{13}C/^{12}C$ VPDB or $^{18}O/^{16}O$ VSMOW, wherein VPDB is Vienna Peedee Belemnite and VSMOW is Vienna Standard Mean Ocean Water. Information on the isotopic integrity of the samples can be found in Supplementary Notes 3.

We performed strontium isotope analysis on samples already analysed for carbon and oxygen isotope ratios, allowing for a direct correlation of potential dietary or environmental shifts to changes in $^{87}Sr/^{86}Sr$ ratios. We selected 11 enamel sub-samples based on the adequacy of sample-size and the presence of corresponding peaks in carbon and oxygen values. Strontium isotope analysis of sampled enamel aliquots was conducted at the Curt-Engelhorn-Center for Archaeometry gGmbH, Mannheim (Germany). Further processing of 5 mg of pretreated powdered enamel, including strontium separation in Teflon columns with Eichrome Sr-spec ion exchange resin, was carried out under clean-lab conditions following the analytical procedures described in Knipper et al.[100]; Blank et al.[101]. $^{87}Sr/^{86}Sr$ ratios by High-Resolution Multi Collector-ICP-MS (Neptune). The raw data were corrected according to the exponential mass fractionation law to $^{88}Sr/^{86}Sr$ = 8.375209. $^{87}Sr/^{86}Sr$ data are reported relative to the NBS 987 standard, which was run along with the samples and yielded $^{87}Sr/^{86}Sr$ ratios of 0.71030 ± 0.00001 (n = 7). Blank values during the whole clean lab procedure were less than 50 pg Sr (< 0.1% of the total Sr sample).

Recent studies have shown that enamel formation-related signal dampening can also influence strontium incremental samples, which, upon the application of time-resolute sampling or analytical techniques, have the potential to identify seasonal or even monthly animal mobility patterns[102,103]. However, our analytical strategy prevented the application of inverse modelling to strontium isotopic values.

Our data are correlated to the multi-proxy environmental strontium baseline provided by Frank et al.[47], which is specifically developed for the Peloponnese. The authors report that bioavailable strontium values from soil leachates and plants correspond well with the values of the underlying geological outcrops, whereas the effects of exogenous mixing inputs, such as precipitation, Saharan dust particles, and sea-spray, play a minimal role in the strontium isotopic composition of the region. The Pindos zone, which can be found predominantly in the west and northwest parts of the Megalopolis Basin (Supplementary Notes 1), is characterized by lower average $^{87}Sr/^{86}Sr$ values (between 0.70805 and 0.70855), while higher strontium values are reported for the Tripolis and Arna units, encountered mostly in the north, northeast and east parts of the basin (~ 0.7095)[47] (Supplementary Notes 1). A single entry from the Megalopolis Basin, collected from Pleistocene clastic sediments of the Pindos geotectonic unit, reports average values of 0.70847 and 0.70835 for plants and soil leachates respectively, (Frank et al.[47], Supplementary). As a control analysis, we also measured $^{87}Sr/^{86}Sr$ ratios in three *Hippopotamus antiquus* individuals from fossiliferous localities within the Megalopolis Basin (Roditi et al. in prep.), to complement the published baseline and define a range of local values for the area. The extant common hippopotamus (*Hippopotamus amphibius*) has small home ranges, estimated to between 3 and 23 km^2 for both resident and migrant[104]. Assuming similar ecological characteristics for its extinct relative (*Hippopotamus antiquus*), the samples from the hippopotami are likely to track the strontium signature of the local geology. The first specimen

originates from the same site (Marathousa 1, Area B; UB2); the second comes from the site of Marathousa 2 (MAR-2)[14], situated 1.5 km east of MAR-1; the third sampled specimen, an upper third molar, was discovered at Kyparissia 4 (KYP-4)[48,85], located at the NW part of the basin on top of a Late Cretaceous limestone outcrop of the Pindos geotectonic unit (Fig. 1). The strontium values for the hippopotamus (MAR-1B-8) from MAR-1 corresponded closely to the average $^{87}Sr/^{86}Sr$ ratios of plants and soil leachates sampled over the limestone of the Tripolis formation outcrops (Frank et al.[45], Supplementary), which can be found to the east, north-east, and south of the Megalopolis Basin (Supplementary Notes 1 and Fig. 1). More radiogenic values were observed for the hippopotamus from MAR-2 (MAR-2B-2), corresponding to the Tripolis geotectonic unit. The $^{87}Sr/^{86}Sr$ ratio of the latter specimen could have been further influenced by the surrounding lithology, specifically the more radiogenic schist outcrops found east of the Megalopolis basin[47,105] (Supplementary Fig. 1). Metamorphic clasts (schist, quartzite etc.) mixed with lacustrine sediments have also been observed in the eastern part of the basin. Finally, the $^{87}Sr/^{86}Sr$ ratio of the Kyparissia 4 individual (KYP4A-1004) was lower and consistent with the strontium range of the Pindos geotectonic unit.

Principles of stable isotope analysis

Carbon isotopes ($\delta^{13}C$)

The source of carbon atoms in mammals is their dietary intake. In this regard, the ratios of stable carbon isotopes in the tissues of primary consumers reflect the isotopic composition of the ingested vegetation[106]. In terrestrial ecosystems, the isotopic signature of plant carbon varies between plants that utilize the two main photosynthetic pathways, i.e., C_4 and C_3[107]. Plant communities following the C photosynthetic pathway, consist of warm growth season grasses and demonstrate $\delta_{13}C$ values that range in modern environments between −17‰ and −9‰ (average −13‰). On the other hand, modern C_3 plants (trees, shrubs, and cool growth season grasses and sedges) yield $\delta^{13}C$ values ranging from −36‰ to −22‰ (average −27‰)[108,109]. Within plant communities utilizing the C_3 photosynthetic pathway, the carbon isotopic composition of vegetation is subjected to additional environmentally controlled fractionation, which is influenced by multiple factors, such as the degree of canopy closure, water availability, temperature, light intensity, or atmospheric CO_2 diffusion[110–112]. The interplay of these factors enables further habitat distinctions within C_3-dominated ecosystems, wherein negative carbon isotope values (modern $\delta^{13}C$ lower than −30‰) are characteristic of a closed canopy forest and higher values (modern $\delta^{13}C$ between −25‰ and −22‰) characterize C_3 vegetation under conditions with high irradiance, increased aridity and/or water scarcity[59,112,113].

The carbon isotopic signature of bioapatite in large herbivores will record the $\delta^{13}C$ of plants with an enrichment in ^{13}C of ~ 14.1 ± 0.5‰ due to biomineralization and metabolic processes[114,115]. Additionally, the effects of fossil fuel burning have resulted in the isotopic depletion of modern atmospheric CO_2 values (−8‰) relative to the Pleistocene (−6.5‰)[116,117], necessitating the application of a correction factor (+ 1.5‰) in fossil herbivore and plant $\delta^{13}C$ to account for this difference. Upon consideration of the atmospheric CO_2 correction and the fractionation of diet-enamel bioapatite, the habitats of primary consumers can be categorized into closed canopy forests (<−14.5‰), woodlands-mesic C_3 grasslands (−14.5‰ to −9.5‰), open woodlands-xeric C_3 grasslands (−9.5‰ to −6.5‰), mixed C_3-C_4 grasslands (−6.5‰ to −1.5‰), and pure C4 grassland (> −1.5‰)[118,119]. Overall, herbivore carbon isotope values become more negative with increasing canopy closure.

Oxygen isotopes ($\delta^{18}O$)

Oxygen stable isotopic ratios in the skeletal tissues of medium and large mammals are in equilibrium with the isotopic composition of body-water. In turn, the $\delta^{18}O$ of body water is influenced by species physiology and drinking behaviour. The main fluxes of oxygen compounds into mammals occur either through diet-water (e.g., leaf water) or by drinking from open water source. Water-dependent taxa (obligate drinkers), such as elephants, track primarily the isotopic composition of the local meteoric water[120]. Variation in the isotopic composition of the latter is governed by several geospatial, climatic, and environmental parameters, for instance the degree of continentality, altitudinal differences of water sources, the amount of local precipitation, surface temperature, as well as differences in the hydrological processes of water bodies (for a detailed overview see Pederzani and Britton[60]). In mid- and high-latitudes, the dominant controls of the $\delta^{18}O$ of meteoric water are surface temperature and local precipitation[121]. In this context, higher $\delta^{18}O$ values are observed in herbivores inhabiting warmer and drier environments and lower values characterize the isotopic composition of animals occupying colder or more humid habitats[60,122].

Seasonal variability in temperature and rainfall, as well as animal migration patterns, can further influence the $\delta^{18}O$ of mammalian organisms. Sub-annual climate-related fluctuations are expressed in the $\delta^{18}O$ sequential series as a sinusoidally-shaped profile, wherein peaks record the higher temperatures and aridity of summer months, whereas troughs represent the low temperatures and increased rainfall amount in winter[60]. Regarding the influence of animal mobility, non-migrant individuals are expected to display higher intra-tooth $\delta^{18}O$ because the isotopic composition of body water tracks primarily the seasonal effects of temperature and precipitation in the utilized water source. In contrast, homogenous oxygen intra-individual profiles are expected in seasonally migrant large herbivores that consume water from different sources along their migration route[45–48].

Strontium isotopes ($^{87}Sr/^{86}Sr$)

Strontium assimilates into the body of mammals primarily from ingested food sources and to a lesser extent from drinking sources and consumed atmospheric or soil particles. Weathering processes of bedrock materials result in the release of strontium in soils, groundwater, or surface water sources, which is, subsequently, absorbed by plants. Within the geosphere, the strontium isotopic composition of the parent material is a factor of bedrock composition and age. Following the principle of radioactive decay, ^{87}Rb (Rubidium) decays to ^{87}Sr, with a half-life

of 4.96 × 1010[123]. Hence, in general, younger geological units are expected to have lower $^{87}Sr/^{86}Sr$ compared to older ones. Within biological tissues, strontium substitutes calcium (Ca) and, in contrast to carbon and oxygen isotopes, strontium isotope ratios are not influenced significantly by physical or chemical alterations between the source and the target tissue (i.e., fractionation)[124]. Thus, the primary factor determining strontium composition within the food chain is the local geological substrate. Strontium in the mineral components of enamel will reflect the average dietary strontium intake during the time of enamel formation[125].

Published comparative data

Comparative data for the stable isotope analysis for *P. antiquus* were taken from published works for the following Middle Pleistocene localities of Europe: Mauer (MIS 15, Germany)[58], Steinheim an der Murr (MIS 11, Germany)[58], La Polledrara di Cecanibbio (MIS 9, Italy)[53], Casal de' Pazzi (MIS 7, Italy)[53,56], Poggetti Vecchi (MIS 7, Italy)[57], and Neumark-Nord 1 (MIS 5, Germany)[54]. All of the localities document hominin presence, while La Polledrara, Casal de' Pazzi, Poggetti Vecchi, and Neumark-Nord 1 additionally preserve direct evidence of *Palaeoloxodon* exploitation in the form of cut marks, human-made bone fractures and/or proboscidean bone artefacts (Konidaris and Tourloukis[42] and references cited therein; and Gaudzinski-Windheuser et al.[40] for Neumark-Nord 1).

Data availability

The isotope dataset generated during this study, as well as additional associated information and figures, are provided in this published article and the Supplementary Information files.

Received: 26 October 2023; Accepted: 7 January 2024
Published online: 16 January 2024

References

1. Nieto Feliner, G. Southern European glacial refugia: A tale of tales. *TAXON* **60**, 365–372. https://doi.org/10.1002/tax.602007 (2011).
2. Hewitt, G. M. Post-glacial re-colonization of European biota. *Biol. J. Linn. Soc. Lond* **68**, 87–112 (1999).
3. Hewitt, G. M. The genetic legacy of the quaternary ice ages. *Nature* **405**, 907–913 (2000).
4. Hewitt, G. M. Speciation, hybrid zones and phylogeography—Or seeing genes in space and time. *Mol. Ecol.* **10**, 537–549. https://doi.org/10.1046/j.1365-294x.2001.01202.x (2001).
5. Tzedakis, P. C. *et al.* Ecological thresholds and patterns of millennial-scale climate variability: The response of vegetation in Greece during the last glacial period. *Geology* **32**, 109–112. https://doi.org/10.1130/G20118.1 (2004).
6. Jones, E. L. What is a refugium? Questions for the Middle-Upper Palaeolithic transition in peninsular southern Europe. *J. Quat. Sci.* **37**, 136–141. https://doi.org/10.1002/jqs.3274 (2022).
7. Gómez, A. & Lunt, D. H. Refugia within refugia: Patterns of phylogeographic concordance in the Iberian Peninsula. In *Phylogeography of Southern European Refugia: Evolutionary Perspectives on the Origins and Conservation of European Biodiversity* (eds Weiss, S. & Ferrand, N.) 155–188 (Springer Netherlands, 2007).
8. Bludau, I. J. *et al.* Lake-level changes and their paleo-climatic implications at the MIS12 lower paleolithic (Middle Pleistocene) site Marathousa 1, Greece. *Front. Earth Sci.* **9**, 441 (2021).
9. Field, M. H. *et al.* A palaeoenvironmental reconstruction (based on palaeobotanical data and diatoms) of the Middle Pleistocene elephant (*Palaeoloxodon antiquus*) butchery site at Marathousa, Megalopolis, Greece. *Quat. Int.* **497**, 108–122 (2018).
10. Konidaris, G. E. *et al.* The skeleton of a straight-tusked elephant (*Palaeoloxodon antiquus*) and other large mammals from the Middle Pleistocene butchering locality Marathousa 1 (Megalopolis Basin, Greece): Preliminary results. *Quat. Int.* **497**, 65–84 (2018).
11. Panagopoulou, E. *et al.* Marathousa 1: A new Middle Pleistocene archaeological site from Greece. *Antiquity* **343**, 1–8 (2015).
12. Panagopoulou, E. *et al.* The Lower Palaeolithic site of Marathousa 1, Megalopolis, Greece: Overview of the evidence. *Quat. Int.* **497**, 33–46 (2018).
13. Tourloukis, V. *et al.* Lithic artifacts and bone tools from the Lower Palaeolithic site Marathousa 1, Megalopolis, Greece: Preliminary results. *Quat. Int.* **497**, 47–64. https://doi.org/10.1016/j.quaint.2018.05.043 (2018).
14. Konidaris, G. *et al.* Marathousa 2: A New Middle Pleistocene Locality in the Megalopolis Basin (Greece) with evidence of hominin exploitation of megafauna (*Hippopotamus*). *PaleoAnthropology* **2023**, 34–55 (2023).
15. Konidaris, G. E., Athanassiou, A., Panagopoulou, E. & Harvati, K. First record of *Macaca* (Cercopithecidae, Primates) in the Middle Pleistocene of Greece. *J. Hum. Evol.* **162**, 103104. https://doi.org/10.1016/j.jhevol.2021.103104 (2022).
16. Blackwell, B. A. *et al.* ESR dating ungulate teeth and molluscs from the Paleolithic site Marathousa 1, Megalopolis Basin, Greece. *Quaternary* **1**, 22 (2018).
17. Jacobs, Z. *et al.* Optical dating of K-feldspar grains from Middle Pleistocene lacustrine sediment at Marathousa 1 (Greece). *Quat. Int.* **497**, 170–177 (2018).
18. Tourloukis, V. *et al.* Magnetostratigraphic and chronostratigraphic constraints on the Marathousa 1 Lower Palaeolithic site and the Middle Pleistocene deposits of the Megalopolis basin, Greece. *Quat. Int.* **497**, 154–169. https://doi.org/10.1016/j.quaint.2018.03.043 (2018).
19. Lang, N. & Wolff, E. W. Interglacial and glacial variability from the last 800 ka in marine, ice and terrestrial archives. *Clim. Past* **7**, 361–380 (2011).
20. Lauer, T. & Weiss, M. Timing of the Saalian- and Elsterian glacial cycles and the implications for Middle: Pleistocene hominin presence in central Europe. *Sci. Rep.* **8**, 5111. https://doi.org/10.1038/s41598-018-23541-w (2018).
21. Koutsodendris, A., Kousis, I., Peyron, O., Wagner, B. & Pross, J. The Marine Isotope Stage 12 pollen record from Lake Ohrid (SE Europe): Investigating short-term climate change under extreme glacial conditions. *Quat. Sci. Rev.* **221**, 105873. https://doi.org/10.1016/j.quascirev.2019.105873 (2019).
22. Kafetzidou, A., Fatourou, E., Panagiotopoulos, K., Marret, F. & Kouli, K. Vegetation composition in a typical Mediterranean setting (Gulf of Corinth, Greece) during successive Quaternary climatic cycles. *Quaternary* **6**, 30 (2023).
23. Sassoon, D., Lebreton, V., Combourieu-Nebout, N., Peyron, O. & Moncel, M.-H. Palaeoenvironmental changes in the southwestern Mediterranean (ODP site 976, Alboran sea) during the MIS 12/11 transition and the MIS 11 interglacial and implications for hominin populations. *Quat. Sci. Rev.* **304**, 108010. https://doi.org/10.1016/j.quascirev.2023.108010 (2023).
24. Tzedakis, P. C., Hooghiemstra, H. & Pälike, H. The last 1.35 million years at Tenaghi Philippon: Revised chronostratigraphy and long-term vegetation trends. *Quat. Sci. Rev.* **25**, 3416–3430. https://doi.org/10.1016/j.quascirev.2006.09.002 (2006).

25. Biddittu, I. *et al.* Stratigraphy, sedimentology, and archaeology of Middle Pleistocene localities near Ceprano, Campogrande area, Italy. *Quat. Res.* **93**, 155–171. https://doi.org/10.1017/qua.2019.52 (2020).
26. Moncel, M.-H. *et al.* Early Levallois core technology between marine isotope stage 12 and 9 in Western Europe. *J. Hum. Evol.* **139**, 102735 (2020).
27. Moncel, M.-H. *et al.* Tracking behavioral persistence and innovations during the Middle Pleistocene in Western Europe. Shift in occupations between 700 and 450 ka at la Noira site (Centre, France). *J. Hum. Evol.* **156**, 103009. https://doi.org/10.1016/j.jhevol.2021.103009 (2021).
28. Ravon, A.-L., García-Medrano, P., Moncel, M.-H. & Ashton, N. Acheulean variability in Western Europe: The case of Menez-Dregan I (Plouhinec, Finistère, France). *J. Hum. Evol.* **162**, 103103. https://doi.org/10.1016/j.jhevol.2021.103103 (2022).
29. Davis, R. & Ashton, N. Landscapes, environments and societies: The development of culture in Lower Palaeolithic Europe. *J. Anthropol. Archaeol.* **56**, 101107. https://doi.org/10.1016/j.jaa.2019.101107 (2019).
30. Saegusa, H. & Gilbert, H. W. Elephantidae in *Homo erectus* (eds W. Henry Gilbert & Asfaw Berhane) Ch. 9, 193–226 (University of California Press, 2009).
31. Davies, P. *The straight-tusked elephant (Palaeoloxodon antiquus) in Pleistocene Europe* (University of London, 2002).
32. Palombo, M., Albayrak, E. & Marano, F. The straight-tusked elephants from Neumark Nord, a glance to a lost world. *Elefantenreich-Eine Fossilwelt in Europa, Begleitband zur Sonderausstellung im Landesmuseum für Vorgeschichte Halle. Halle (Saale)*, 219–247 (2010).
33. Rivals, F., Semprebon, G. M. & Lister, A. M. Feeding traits and dietary variation in Pleistocene proboscideans: A tooth microwear review. *Quat. Sci. Rev.* **219**, 145–153. https://doi.org/10.1016/j.quascirev.2019.06.027 (2019).
34. Saarinen, J. & Lister, A. M. Dental mesowear reflects local vegetation and niche separation in Pleistocene proboscideans from Britain. *J. Quat. Sci.* **31**, 799–808 (2016).
35. Tsoukala, E. & Lister, A. Remains of straight-tusked elephant, *Elephas (Palaeoloxodon) antiquus* Falc. & Caut. (1847) ESR-dated to oxygen isotope Stage 6 from Grevena (W. Macedonia, Greece). *Boll. Soc. Paleontol. Ital.* **37**, 117–140 (1998).
36. Lister, A. M. Ecological interactions of elephantids in Pleistocene Eurasia: *Palaeoloxodon* and *Mammuthus* in *Human paleoecology in the Levantine Corridor* (eds. Goren-Inbar N., Speth J.D.), 53–60 (2004).
37. Athanassiou, A. The fossil record of continental elephants and mammoths (Mammalia: Proboscidea: Elephantidae). In *Fossil Vertebrates of Greece Vol. 1: Basal vertebrates, Amphibians, Reptiles, Afrotherians, Glires, and Primates*. Vol. 1 (ed. Vlachos, E.) 345–391 (Springer, 2022).
38. Stuart, A. J. The extinction of woolly mammoth (*Mammuthus primigenius*) and straight-tusked elephant (*Palaeoloxodon antiquus*) in Europe. *Quat. Int.* **126–128**, 171–177. https://doi.org/10.1016/j.quaint.2004.04.021 (2005).
39. Tsoukala, E. *et al. Elephas antiquus* in Greece: New finds and a reappraisal of older material (Mammalia, Proboscidea, Elephantidae). *Quat. Int.* **245**, 339–349 (2011).
40. Gaudzinski-Windheuser, S., Kindler, L., MacDonald, K. & Roebroeks, W. Hunting and processing of straight-tusked elephants 125000 years ago: Implications for Neanderthal behavior. *Sci. Adv.* **9**, eadd8186. https://doi.org/10.1126/sciadv.add8186 (2023).
41. Starkovich, B. M. Perception versus reality: Implications of elephant hunting by Neanderthals. *Sci. Adv.* **9**, eadg6072. https://doi.org/10.1126/sciadv.adg6072 (2023).
42. Konidaris, G. E. & Tourloukis, V. Proboscidea-*Homo* interactions in open-air localities during the Early and Middle Pleistocene of western Eurasia: A palaeontological and archaeolocigal perspective perspective in *Human-elephant interactions: From past to present* (eds. Konidaris G.E., Barkai R., Tourloukis V., Harvati K.) (2021).
43. Ben-Dor, M., Gopher, A., Hershkovitz, I. & Barkai, R. Man the Fat Hunter: The demise of *Homo erectus* and the emergence of a new Hominin lineage in the Middle Pleistocene (ca. 400 kyr) Levant. *PLOS ONE* **6**, e28689. https://doi.org/10.1371/journal.pone.0028689 (2011).
44. Reshef, H. & Barkai, R. A taste of an elephant: The probable role of elephant meat in Paleolithic diet preferences. *Quat. Int.* **379**, 28–34 (2015).
45. Metcalfe, J. Z. Proboscidean isotopic compositions provide insight into ancient humans and their environments. *Quat. Int.* **443**, 147–159. https://doi.org/10.1016/j.quaint.2016.12.003 (2017).
46. Bocherens, H. & Drucker, D. G. Isotopic insights on ecological interactions between humans and woolly mammoths during the Middle and Upper Palaeolithic in Europe in *Human-elephant interactions: From past to present* (eds. Konidaris G.E., Barkai R., Tourloukis V., Harvati K.) (2021).
47. Frank, A. B. *et al.* Isotopic range of bioavailable strontium on the Peloponnese peninsula, Greece: A multi-proxy approach. *Sci. Total Environ.* **774**, 145181 (2021).
48. Athanassiou, A. *et al.* Pleistocene vertebrates from the Kyparíssia lignite mine, Megalopolis Basin, S. Greece: Testudines, Aves, Suiformes. *Quat. Int.* **497**, 178–197. https://doi.org/10.1016/j.quaint.2018.06.030 (2018).
49. Passey, B. H. *et al.* Inverse methods for estimating primary input signals from time-averaged isotope profiles. *Geochim. Cosmochim. Acta* **69**, 4101–4116 (2005).
50. Uno, K. T. *et al.* Forward and inverse methods for extracting climate and diet information from stable isotope profiles in proboscidean molars. *Quat. Int.* **557**, 92–109 (2020).
51. Filippi, M. *et al.* Isotope and microwear analyses on teeth of late Middle Pleistocene *Elephas antiquus* from the Rome area (La Polledrara, Casal de'Pazzi). *World Elephants-Int. Congress Rome* **2001**, 534–539 (2001).
52. Rivals, F., Semprebon, G. & Lister, A. An examination of dietary diversity patterns in Pleistocene proboscideans (*Mammuthus, Palaeoloxodon, and Mammut*) from Europe and North America as revealed by dental microwear. *Quat. Int.* **255**, 188–195 (2012).
53. Palombo, M. R. *et al.* Coupling tooth microwear and stable isotope analyses for palaeodiet reconstruction: The case study of Late Middle Pleistocene *Elephas* (*Palaeoloxodon*) *antiquus* teeth from Central Italy (Rome area). *Quat. Int.* **126**, 153–170 (2005).
54. Grube, R., Palombo, M., Iacumin, P. & Di Matteo, A. What did the fossil elephants from Neumark–Nord eat? In *Elefantenreich – Eine Fossilwelt in Europa.* (ed. Meller, H.) 253–272 (Landesamt für Denkmalpflege und Archäologie Sachsen-Anhalt, 2010).
55. Rivals, F. & Lister, A. M. Dietary flexibility and niche partitioning of large herbivores through the Pleistocene of Britain. *Quat. Sci. Rev.* **146**, 116–133. https://doi.org/10.1016/j.quascirev.2016.06.007 (2016).
56. Briatico, G. & Bocherens, H. Middle Pleistocene ecology in central Italy. New isotopic insights from fauna tooth enamel of Casal de' Pazzi (Rome, Italy). *J. Mediterr. Earth Sci.* **15** (2023).
57. Capalbo, C. Multiproxy-Based reconstruction of the feeding habits from the late Middle Pleistocene straight-tusked elephant population of Poggetti Vecchi (Southern Tuscany, Italy). *Alp. Mediter. Quat.* **31**, 113–119 (2018).
58. Pushkina, D., Bocherens, H. & Ziegler, R. Unexpected palaeoecological features of the Middle and Late Pleistocene large herbivores in southwestern Germany revealed by stable isotopic abundances in tooth enamel. *Quat. Int.* **339–340**, 164–178. https://doi.org/10.1016/j.quaint.2013.12.033 (2014).
59. Metcalfe, J. Z. C_3 plant isotopic variability in a boreal mixed woodland: Implications for bison and other herbivores. *PeerJ* **9**, e12167–e12167. https://doi.org/10.7717/peerj.12167 (2021).
60. Pederzani, S. & Britton, K. Oxygen isotopes in bioarchaeology: Principles and applications, challenges and opportunities. *Earth Sci. Rev.* **188**, 77–107 (2019).
61. Metcalfe, J. Z. & Longstaffe, F. J. Mammoth tooth enamel growth rates inferred from stable isotope analysis and histology. *Quat. Res.* **77**, 424–432 (2012).

62. Zazzo, A., Balasse, M. & Patterson, W. P. High-resolution $\delta^{13}C$ intratooth profiles in bovine enamel: Implications for mineralization pattern and isotopic attenuation. *Geochim. Cosmochim. Acta* **69**, 3631–3642. https://doi.org/10.1016/j.gca.2005.02.031 (2005).
63. Metcalfe, J. Z. & Longstaffe, F. J. Environmental change and seasonal behavior of mastodons in the Great Lakes region inferred from stable isotope analysis. *Quat. Res.* **82**, 366–377 (2014).
64. Metcalfe, J. Z., Longstaffe, F. J., Ballenger, J. A. & Haynes, C. V. Jr. Isotopic paleoecology of Clovis mammoths from Arizona. *Proc. Natl. Acad. Sci.* **108**, 17916–17920 (2011).
65. Widga, C. *et al.* Life histories and niche dynamics in late Quaternary proboscideans from Midwestern North America: Evidence from stable isotope analyses. *bioRxiv* https://doi.org/10.1101/2020.01.08.896647 (2020).
66. Switzer, P. V. Site fidelity in predictable and unpredictable habitats. *Evol. Ecol.* **7**, 533–555 (1993).
67. Clegg, B. W. & O'Connor, T. G. Determinants of seasonal changes in availability of food patches for elephants (*Loxodonta africana*) in a semi-arid African savanna. *PeerJ* **5**, e3453 (2017).
68. Codron, J. *et al.* Elephant (*Loxodonta africana*) diets in Kruger National Park, South Africa: Spatial and landscape differences. *J. Mammal.* **87**, 27–34. https://doi.org/10.1644/05-MAMM-A-017R1.1 (2006).
69. Short, J. C. Density and seasonal movements of forest elephant (*Loxodonta africana cyclotis*, Matschie) in Bia National Park, Ghana. *Afr. J. Ecol.* **21**, 175–184. https://doi.org/10.1111/j.1365-2028.1983.tb01179.x (1983).
70. Tchamba, M. N. & Seme, P. M. Diet and feeding behaviour of the forest elephant in the Santchou Reserve. *Cameroon. Afr. J. Ecol.* **31**, 165–171. https://doi.org/10.1111/j.1365-2028.1993.tb00529.x (1993).
71. Baskaran, N., Balasubramanian, M., Swaminathan, S. & Desai, A. A. Feeding ecology of the Asian elephant *Elephas maximus* Linnaeus in the Nilgiri Biosphere Reserve, southern India. *J. Bombay Nat. Hist. Soc.* **107**, 3 (2010).
72. Koirala, R. K., Ji, W., Aryal, A., Rothman, J. & Raubenheimer, D. Dispersal and ranging patterns of the Asian elephant (*Elephas maximus*) in relation to their interactions with humans in Nepal. *Ethol. Ecol. Evol.* **28**, 221–231. https://doi.org/10.1080/03949370.2015.1066872 (2016).
73. English, M. *et al.* Foraging site recursion by forest elephants *Elephas maximus borneensis*. *Curr. Zool.* **60**, 551–559. https://doi.org/10.1093/czoolo/60.4.551 (2014).
74. Polansky, L., Kilian, W. & Wittemyer, G. Elucidating the significance of spatial memory on movement decisions by African savannah elephants using state–space models. *Proc. R. Soc. B* **282**, 20143042 (2015).
75. MacArthur, R. H. & Pianka, E. R. On optimal use of a patchy environment. *Am. Natural.* **100**, 603–609 (1966).
76. Senft, R. L. *et al.* Large herbivore foraging and ecological hierarchies. *Bioscience* **37**, 789–799. https://doi.org/10.2307/1310545 (1987).
77. Charnov, E. L. Optimal foraging, the marginal value theorem. *Theor Popul Biol* **9**, 129–136 (1976).
78. Bailey, D. W. *et al.* Mechanisms that result in large herbivore grazing distribution patterns. *J. Range Manag.* **49**, 386–400 (1996).
79. Bai, D. *et al.* The recent Asian elephant range expansion in Yunnan, China, is associated with climate change and enforced protection efforts in human-dominated landscapes. *Front. Ecol. Evol.* https://doi.org/10.3389/fevo.2022.889077 (2022).
80. Wang, H. *et al.* What triggered the Asian elephant's northward migration across southwestern Yunnan?. *Innovation* **2**, 100142. https://doi.org/10.1016/j.xinn.2021.100142 (2021).
81. Hughes, P. D., Woodward, J. C. & Gibbard, P. L. Middle Pleistocene cold stage climates in the Mediterranean: New evidence from the glacial record. *Earth Planet. Sci. Lett.* **253**, 50–56. https://doi.org/10.1016/j.epsl.2006.10.019 (2007).
82. Leontaritis, A. D., Kouli, K. & Pavlopoulos, K. The glacial history of Greece: A comprehensive review. *Mediterr. Geosci. Rev.* **2**, 65–90. https://doi.org/10.1007/s42990-020-00021-w (2020).
83. Melentis, J. K. Die Dentition der pleistozänen Proboscidier des Beckens von Megalopolis im Peloponnes (Griechenland). *Ann. Geol. Pays Helléniques* **12**, 153–262 (1961).
84. Melentis, J. K. Die Osteologie der pleistozänen Proboscidier des Beckens von Megalopolis im Peloponnes (Griechenland). *Ann. Geol. Pays Helléniques* **14**, 1–107 (1963).
85. Athanassiou, A. Pleistocene vertebrates from the Kyparíssia lignite mine, Megalopolis Basin, S. Greece: Rodentia, Carnivora, Proboscidea, Perissodactyla, Ruminantia. *Quat. Int.* **497**, 198–221. https://doi.org/10.1016/j.quaint.2018.06.042 (2018).
86. Michailidis, D., Konidaris, G. E., Athanassiou, A., Panagopoulou, E. & Harvati, K. The ornithological remains from Marathousa 1 (Middle Pleistocene; Megalopolis basin, Greece). *Quat. Int.* **497**, 85–94 (2018).
87. Maschenko, E. N. Individual development, biology and evolution of the woolly mammoth. *Cranium* **19**, 4–120 (2002).
88. Balasse, M. Potential biases in sampling design and interpretation of intra-tooth isotope analysis. *Int. J. Osteoarch.* **13**, 3–10. https://doi.org/10.1002/oa.656 (2003).
89. Balasse, M. Reconstructing dietary and environmental history from enamel isotopic analysis: Time resolution of intra-tooth sequential sampling. *Int. J. Osteoarch.* **12**, 155–165. https://doi.org/10.1002/oa.601 (2002).
90. Trayler, R. B. & Kohn, M. J. Tooth enamel maturation reequilibrates oxygen isotope compositions and supports simple sampling methods. *Geochim. Cosmochim. Acta* **198**, 32–47 (2017).
91. Dirks, W., Bromage, T. G. & Agenbroad, L. D. The duration and rate of molar plate formation in *Palaeoloxodon cypriotes* and *Mammuthus columbi* from dental histology. *Quat. Int.* **255**, 79–85. https://doi.org/10.1016/j.quaint.2011.11.002 (2012).
92. Uno, K. T. *et al.* Bomb-curve radiocarbon measurement of recent biologic tissues and applications to wildlife forensics and stable isotope (paleo)ecology. *Proc. Natl. Acad. Sci.* **110**, 11736–11741. https://doi.org/10.1073/pnas.1302226110 (2013).
93. Kowalik, N. *et al.* Revealing seasonal woolly mammoth migration with spatially-resolved trace element, Sr and O isotopic records of molar enamel. *Quat. Sci. Rev.* **306**, 108036. https://doi.org/10.1016/j.quascirev.2023.108036 (2023).
94. Passey, B. H. & Cerling, T. E. Tooth enamel mineralization in ungulates: Implications for recovering a primary isotopic time-series. *Geochim. Cosmochim. Acta* **66**, 3225–3234 (2002).
95. Trayler, R. & Kohn, M. Tooth enamel maturation reequilibrates oxygen isotope compositions and supports simple sampling methods. *Geochim. Cosmochim. Acta* https://doi.org/10.1016/j.gca.2016.10.023 (2017).
96. Abràmoff, M. D., Magalhães, P. J. & Ram, S. J. Image processing with ImageJ. *Biophotonics Int.* **11**(36), 42 (2004).
97. Bocherens, H., Fizet, M. & Mariotti, A. Diet, physiology and ecology of fossil mammals as inferred from stable carbon and nitrogen isotope biogeochemistry: Implications for Pleistocene bears. *Palaeogeogr. Palaeoclimatol. Palaeoecol.* **107**, 213–225 (1994).
98. Koch, P. L., Tuross, N. & Fogel, M. L. The effects of sample treatment and diagenesis on the isotopic integrity of carbonate in biogenic hydroxylapatite. *J. Archaeol. Sci.* **24**, 417–429 (1997).
99. Bond, A. L. & Hobson, K. A. Reporting Stable isotope ratios in ecology: Recommended terminology, guidelines and best practices. *Waterbirds* **35**, 324–331 (2012).
100. Knipper, C. *et al.* Mobility in Thuringia or mobile Thuringians: A strontium isotope study from early Medieval central Germany. In *Population Dynamics in Prehistory and Early History* (eds Kaiser, E. *et al.*) 287–310 (De Gruyter, 2012).
101. Blank, M., Sjögren, K.-G., Knipper, C., Frei, K. M. & Storå, J. Isotope values of the bioavailable strontium in inland southwestern Sweden—A baseline for mobility studies. *PloS one* **13**, e0204649 (2018).
102. Lazzerini, N. *et al.* Monthly mobility inferred from isoscapes and laser ablation strontium isotope ratios in caprine tooth enamel. *Sci. Rep.* **11**, 2277. https://doi.org/10.1038/s41598-021-81923-z (2021).

103. Le Corre, M., Grimes, V., Lam, R. & Britton, K. Comparison between strip sampling and laser ablation methods to infer seasonal movements from intra-tooth strontium isotopes profiles in migratory caribou. *Sci. Rep.* **13**, 3621. https://doi.org/10.1038/s41598-023-30222-w (2023).
104. Stears, K., Nuñez, T. A., Muse, E. A., Mutayoba, B. M. & McCauley, D. J. Spatial ecology of male hippopotamus in a changing watershed. *Sci. Rep.* **9**, 15392. https://doi.org/10.1038/s41598-019-51845-y (2019).
105. EGDI. *Map Viewer*, <https://www.europe-geology.eu/data-and-services/map-viewer/> (2023).
106. DeNiro, M. J. & Epstein, S. Influence of diet on the distribution of carbon isotopes in animals. *Geochim. Cosmochim. Acta* **42**, 495–506 (1978).
107. Ehleringer, J. R., Sage, R. F., Flanagan, L. B. & Pearcy, R. W. Climate change and the evolution of C_4 photosynthesis. *Trends Ecol. Evol.* **6**, 95–99. https://doi.org/10.1016/0169-5347(91)90183-X (1991).
108. Bender, M. M. Variations in the $^{13}C/^{12}C$ ratios of plants in relation to the pathway of photosynthetic carbon dioxide fixation. *Phytochemistry* **10**, 1239–1244. https://doi.org/10.1016/S0031-9422(00)84324-1 (1971).
109. Kohn, M. J. Carbon isotope compositions of terrestrial C_3 plants as indicators of (paleo)ecology and (paleo)climate. *Proc. Natl. Acad. Sci.* **107**, 19691–19695. https://doi.org/10.1073/pnas.1004933107 (2010).
110. Heaton, T. H. Spatial, species, and temporal variations in the $^{13}C/^{12}C$ ratios of C_3 plants: Implications for palaeodiet studies. *J. Archaeol. Sci.* **26**, 637–649 (1999).
111. Hofman-Kamińska, E., Bocherens, H., Borowik, T., Drucker, D. G. & Kowalczyk, R. Stable isotope signatures of large herbivore foraging habitats across Europe. *PLOS ONE* **13**, e0190723. https://doi.org/10.1371/journal.pone.0190723 (2018).
112. van der Merwe, N. J. & Medina, E. The canopy effect, carbon isotope ratios and foodwebs in Amazonia. *J. Archaeol. Sci.* **18**, 249–259 (1991).
113. Drucker, D. G., Bridault, A., Hobson, K. A., Szuma, E. & Bocherens, H. Can carbon-13 in large herbivores reflect the canopy effect in temperate and boreal ecosystems? Evidence from modern and ancient ungulates. *Palaeogeogr. Palaeoclimatol. Palaeoecol.* **266**, 69–82. https://doi.org/10.1016/j.palaeo.2008.03.020 (2008).
114. Cerling, T. E. & Harris, J. M. Carbon isotope fractionation between diet and bioapatite in ungulate mammals and implications for ecological and paleoecological studies. *Oecologia* **120**, 347–363. https://doi.org/10.1007/s004420050868 (1999).
115. Passey, B. H. *et al.* Carbon isotope fractionation between diet, breath CO_2, and bioapatite in different mammals. *J. Archaeol. Sci.* **32**, 1459–1470 (2005).
116. Koch, P. L., Diffenbaugh, N. S. & Hoppe, K. A. The effects of late Quaternary climate and pCO_2 change on C_4 plant abundance in the south-central United States. *Palaeogeogr. Palaeoclimatol. Palaeoecol.* **207**, 331–357. https://doi.org/10.1016/j.palaeo.2003.09.034 (2004).
117. Tipple, B. J., Meyers, S. R. & Pagani, M. Carbon isotope ratio of Cenozoic CO_2: A comparative evaluation of available geochemical proxies. *Paleoceanography* https://doi.org/10.1029/2009PA001851 (2010).
118. Domingo, L. *et al.* Late Neogene and Early Quaternary paleoenvironmental and paleoclimatic conditions in Southwestern Europe: Isotopic analyses on mammalian taxa. *PLOS ONE* **8**, e63739. https://doi.org/10.1371/journal.pone.0063739 (2013).
119. Domingo, L., Rodríguez-Gómez, G., Libano, I. & Gómez-Olivencia, A. New insights into the Middle Pleistocene paleoecology and paleoenvironment of the Northern Iberian Peninsula (Punta Lucero Quarry site, Biscay): A combined approach using mammalian stable isotope analysis and trophic resource availability modeling. *Quat. Sci. Rev.* **169**, 243–262 (2017).
120. Kohn, M. J. & Cerling, T. E. Stable isotope compositions of biological apatite. *Rev. Mineral. Geochem.* **48**, 455–488. https://doi.org/10.2138/rmg.2002.48.12 (2002).
121. Fricke, H. C. & O'Neil, J. R. Inter- and intra-tooth variation in the oxygen isotope composition of mammalian tooth enamel phosphate: Implications for palaeoclimatological and palaeobiological research. *Palaeogeogr. Palaeoclimatol. Palaeoecol.* **126**, 91–99. https://doi.org/10.1016/S0031-0182(96)00072-7 (1996).
122. Bocherens, H. & Drucker, D. G. Carbonate stable isotopes: Terrestrial teeth and bones. In *Encyclopedia of Quaternary Science* (eds Elias, Scott A. & Mock, Cary J.) 304–314 (Elsevier, 2013).
123. Rotenberg, E., Davis, D. W., Amelin, Y., Ghosh, S. & Bergquist, B. A. Determination of the decay-constant of ^{87}Rb by laboratory accumulation of ^{87}Sr. *Geochim. Cosmochim. Acta* **85**, 41–57. https://doi.org/10.1016/j.gca.2012.01.016 (2012).
124. Slovak, N. M. & Paytan, A. Applications of sr isotopes in archaeology. In *Handbook of Environmental Isotope Geochemistry* Vol. I (ed. Baskaran, M.) 743–768 (Springer, 2012).
125. Bentley, A. R. Strontium isotopes from the earth to the archaeological skeleton: A review. *J. Archaeol. Method Theory* **13**, 135–187 (2006).
126. JPL, N. (ASA EOSDIS Land Processes Distributed Active Archive Center, 2013).

Acknowledgements

This research was supported by the European Research Council (ERC-CoG-724703 "CROSSROADS"). Excavation at Marathousa 1 was conducted under a permit granted to the Ephorate of Palaeoanthropology–Speleology, Hellenic Ministry of Culture and was supported by the ERC-CoG-724703 ("CROSSROADS") and the ERC-StG-283503 ("PaGE"), both awarded to K. Harvati. K.H. and E.R. are supported by the ERC-AdG-101019659 ("FIRSTSTEPS"). G.E.K., V.T. and K.H. are also supported by the Deutsche Forschungsgemeinschaft (DFG Project no. 463225251; DFG FOR 2237). We thank the Ephorate of Palaeoanthropology-Speleology and the Hellenic Ministry of Culture for granting us permission to perform the analyses (ΥΠΠΟΑ/ΓΔΑΠΚ/ΔΣΑΝΜ/ΤΕΕ/Φ77/ 529453/374527/6110/323). We are extremely grateful to Aristeidis Varis for the topographic map used in Fig. 1 and to Nicholas Thompson for his help during sampling, as well as two anonymous reviewers for their helpful comments and suggestions.

Author contributions

Conceptualization and supervision: K.H., H.B. and G.E.K.; Writing—original draft: E.R. and K.H.; Writing—review and editing: E.R., H.B., G.E.K., A.A., V.T., P.K., E.P., K.H.; Sampling & laboratory preparations: E.R.; Methodology: E.R. & H.B.; Data analysis: E.R.; Project administration: E.P. and K.H.

Funding

Open Access funding enabled and organized by Projekt DEAL.

Competing interests

The authors declare no competing interests.

Additional information

Supplementary Information The online version contains supplementary material available at https://doi.org/10.1038/s41598-024-51592-9.

Correspondence and requests for materials should be addressed to K.H.

Reprints and permissions information is available at www.nature.com/reprints.

Publisher's note Springer Nature remains neutral with regard to jurisdictional claims in published maps and institutional affiliations.

1.Supplementary Notes: Geography, geology and climate of the Megalopolis Basin

The Megalopolis Basin is an intramontane, post-orogenic graben located in the central part of the Peloponnese, southern Greece. The area has an altitude of 330–450 meters above sea level (m.a.s.l) and covers a total of 250 km^2, with its longer axis extending approximately 20 km in a NW–SE direction. The Mainalo, Lykaion, and Taygetos mountain ranges border the basin on the east, west, and south respectively. As regards its geology, the basin formed during the Late Miocene–Pliocene on the Mesozoic–Paleogene basement of the Peloponnese, while during the Pleistocene it periodically hosted a large lake[1,2]. In the north-eastern part of the basin, the Plattenkalk series (Mani geotectonic unit) crops out, consisting of Permian to Eocene/Lower Oligocene crystalline carbonates, marbles, and flysch[3]. Outcrops of Carboniferous–Lower Triassic metamorphic rocks, phyllites, schists, and quartzites comprise the Phyllite/Quartzite series (Arna geotectonic unit) and can be found on the south-east and southern extents of the basin[3]. The Tripolis geotectonic zone is present in the eastern, north-eastern, and northern catchment of the graben and consists of the volcano-sedimentary Tyros beds at its base, followed by Upper Triassic–Upper Eocene limestones and dolomites and Upper Eocene–Upper Oligocene flysch[3,4]. Upper Cretaceous to Palaeocene flysch of the Pindos geotectonic zone encompasses the basin in the west and north-west, whereas Upper Cretaceous limestones of the Pindos zone can be found in the east, south-east, west, and north-west (Supplementary Figure 1). The Plio-Pleistocene sedimentary sequence consists of lacustrine, fluvio-lacustrine, and alluvial fan

deposits[1,2,5]. Within this sequence, silts, clays, and sands which intercalate cyclically with lignite seams characterize the Pleistocene lacustrine Marathousa Member (Choremi Formation)[2,5]. Marathousa 1 is stratigraphically placed in this member.

At present, the Megalopolis region is characterized by a Mediterranean climate with humid, cool winters and hot, dry summers. Higher temperatures and lower precipitation are recorded between May and September, whereas the lowest temperatures are observed in January and the highest amount of rainfall occurs in December.

2. Supplementary Notes: Marathousa 1

Marathousa 1 (MAR-1) is a Middle Pleistocene open-air site located at the central-western part of the Megalopolis Basin. The site was discovered in 2013, when stratified faunal remains and lithic artifacts were identified at an exposed section in the Marathousa mine, during a targeted field survey conducted by a joint team of the Ephorate of Palaeoanthropology-Speleology of the Hellenic Ministry of Culture, and the University of Tübingen[6-9]. Subsequent systematic excavations between 2013 and 2019 in two areas —Area A and Area B, located approximately 60 meters apart— revealed a sequence containing micro- and macro-faunal remains[10-13], micro- and macro-floral remains[14], as well as lithic and bone artifacts[15]. The main find-bearing layers (stratigraphic units UA3c/4 and UB4c/5) are situated between Lignite seams IIb and IIIa at an elevation of 350 m.a.s.l. and consist mainly of organic and interclast-rich silty sands[5]. They belong to the same depositional event as evidenced by lithostratigraphic and geochemical data[5], spatial taphonomy[16], as well as archaeological and

palaeontological evidence [11,15]. Electron Spin Resonance (ESR)[17], post-infrared Infrared Stimulated Luminescence[18], magnetostratigraphy[19], and mammal biochronology[13] date the archaeological sequence to ca. 500–400 ka and correlate it to the glacial Marine Isotope Stage (MIS) 12.

The partial skeleton of the straight-tusked elephant was discovered in Area A, at the contact between units UA3c and UA4. Several skeletal elements (vertebrae, ribs, humerus, ulna, femur, tibia, pelvis, carpals, tarsals, metapodials, phalanges) have been excavated in approximate anatomical association, including the cranium bearing both upper third molars[11]. The skeleton belonged to a male individual at its late adulthood, with an upper ontogenetic age-limit between 64–71 years, live skeletal height around 3.7 m at the shoulder, and body mass around 9.0 tonnes[11]. Traces of anthropogenic modifications in the form of cut marks were identified on the astragalus and the tibia, providing direct evidence for the exploitation of the carcass by hominins[11]. This is further confirmed by the spatial and stratigraphic association of the skeleton with lithic artifacts, some of which preserve use-wear traces indicative of butchering activities[16,20]. Further evidence of elephant butchering (e.g., cut marks, breakages in the form of peeling) is present also on bones belonging to another elephant individual from Area B[11], while a thick diaphyseal fragment that may also belong to an elephant is interpreted as a percussor[15].

3. Supplementary Notes: Isotopic signal preservation & integrity

A diaphyseal bone fragment of the MAR-1 (Area A) elephant was initially subjected

to elemental composition analysis (%N and %C yields) and indicated poor collagen preservation; therefore, the present study focused on carbon, oxygen, and strontium isotope analyses on tooth enamel, which, unlike bone and dentine, is considered diagenetically resistant on account of its physical properties, namely its low organic content (<1%) and high crystallinity and, thus, more likely to preserve unaltered the primary isotopic signal[21-24]. Carbon and oxygen stable isotope values for 28 enamel sequential samples from the M^3 of the *P. antiquus* individual from MAR-1 are listed in Supplementary Table 1. To evaluate the fidelity of the isotopic results, we assessed the carbonate content (%$CaCO_3$) of dentine, cementum, and enamel from the same molar[21,22,25,26]. The range of %CO_3 (from 4.32 to 5.20 wt%) in the enamel structural carbonates of the straight-tusked elephant falls within the span of $CaCO_3$ contents of modern enamel (~3.0–5.5 wt%)[27] and close to the range observed in ungulate enamel bioapatite (4.5–5.1 wt%)[28]. Unlike the case of enamel carbonates, the %CO_3 of dentine and cementum are significantly higher (6.99 wt% and 8.74 wt%, respectively), demonstrating that the biogenic signal of these two tissues has been diagenetically altered. Additionally, the presence of intra-tooth, periodic variation in δ-values — likely the result of environmentally induced changes— suggests that the primary isotopic signal is, at least partially, preserved. Such patterns are expected to become homogenized if isotopic re-equilibration has occurred[29,30]. Based on this evidence, we consider the effects of diagenesis in the stable isotope record of the MAR-1 elephant to be negligible and did not obscure the biogenic patterns.

4. Supplementary Discussion: Detailed inter-site comparison of *P. antiquus* isotopic data

In Italy, a C_3-dominated foraging habitat composed of woodland and mesic grassland has been inferred for a *P. antiquus* individual found at the Middle Pleistocene site of Poggetti Vecchi (MIS 7), which yielded a mean $\delta^{13}C$ value, close to the one obtained from the MAR-1 specimen (–11.05 ‰ VPDB)[31]. Carbon isotope analysis demonstrated a wide range of $\delta^{13}C$ values (from –14.7‰ to –9.4‰ VPDB) for the straight-tusked elephant population of Casal de' Pazzi during MIS 7[32,33], whereas sampled specimens from La Polledrara di Cecanibbio (Italy, MIS 9) yielded higher and more constrained $\delta^{13}C$ values (–9‰ to –10.9‰ VPDB)[32]. These data suggest that the latter population was feeding in more open C_3 habitats with water-stress conditions in comparison to the elephant from MAR-1, as well as to the majority of the specimens from Italy correlated with MIS 7[32,33]. At Neumark-Nord 1, $\delta^{13}C$ values for the site's straight-tusked elephant population are depleted when compared to the individual from MAR-1, indicating significant canopy cover during MIS 5[34]. Similarly, analysed specimens from Steinheim an der Murr (MIS 11) and Mauer (MIS 15)[35], yielded lower carbon isotope values compared to those of the MAR-1 specimen, suggesting foraging under increased canopy closure and/or humid environments for the German localities.

The inter-site comparison of oxygen isotopic values shows that the elephant from MAR-1 displays lower average $\delta^{18}O$ compared to most of the Italian *P. antiquus* specimens correlated to MIS 7 and MIS 9, whose values range between +22.8 ‰ and +27.6 ‰ (VSMOW). Higher oxygen isotopic values (+25.5 – +28.0‰) were also obtained for the specimens of Neumark-Nord 1 in Germany during MIS 5. Contrariwise,

the MAR-1 elephant demonstrates a higher $\delta^{18}O$ value compared to the range obtained for the elephants of Steinheim an der Murr and Mauer in Germany. Overall, the comparison of the oxygen isotope data suggests that the interglacial specimens from La Polledrara and Poggetti Vecchi in Italy, as well as the majority of the individuals from Casal de' Pazzi likely experienced warmer or more arid climatic conditions compared to the elephant from MAR-1, whereas cooler or more humid conditions characterize the environment of the interglacial populations from Steinheim an der Murr and Mauer in Germany. The unusually higher oxygen isotopic values of the Neumark Nord-1 population in comparison to both MAR-1 and the other German localities are likely the result of a drier and warmer climate during the Eemian, combined with the effects of evaporative enrichment in the large lake from which the individuals drank water[34,36]. We should note that the effects of continentality could influence the interpretation of the inter-site $\delta^{18}O$ record between Germany and the peri-Mediterranean sites; however, comparisons between Italian and Greek sites should not be significantly subjected to this control.

References

1 Vinken, R. Stratigraphie und Tektonik des Beckens von Megalopolis (Peloponnes, Griechenland). *Geol. Jahrb* **83**, 97–148 (1965).

2 Van Vugt, N., De Bruijn, H., Van Kolfschoten, T., Langereis, C. & Okuda, M. Magneto- and cyclostratigraphy and mammal-fauna's of the Pleistocene lacustrine Megalopolis Basin, Peloponnesos, Greece. *Geologica Ultrajectina* **189**, 69-92 (2000).

3 Tsiftsis, E. V. *Geology and Hydrogeology of the Megalopolis Basin, Peloponnese, Greece*, University of Bristol, (1987).

4 Papanikolaou, D. & Vassilakis, E. Thrust faults and extensional detachment faults in Cretan tectono-stratigraphy: Implications for Middle Miocene extension. *Tectonophysics* **488**, 233–247 (2010).

5 Karkanas, P. *et al.* Sedimentology and micromorphology of the Lower Palaeolithic lakeshore site Marathousa 1, Megalopolis basin, Greece. *Quat. Int.* **497**, 123–136 (2018).
6 Panagopoulou, E. *et al.* Marathousa 1: a new Middle Pleistocene archaeological site from Greece. *Antiquity* **343**, 1–8 (2015).
7 Panagopoulou, E. *et al.* The Lower Palaeolithic site of Marathousa 1, Megalopolis, Greece: overview of the evidence. *Quat. Int.* **497**, 33–46 (2018).
8 Harvati, K., Konidaris, G. & Tourloukis, V. Paleoanthropology at the Gates of Europe: Recent research in Greece in the frame of the PaGE ERC Starting Grant project. *Quat. Int.* **497**, 1–3, doi:10.1016/j.quaint.2018.11.024 (2018).
9 Thompson, N., Tourloukis, V., Panagopoulou, E. & Harvati, K. In search of Pleistocene remains at the gates of Europe: Directed surface survey of the Megalopolis Basin (Greece). *Quat. Int.* **497**, 22–32 (2018).
10 Konidaris, G. E., Athanassiou, A., Panagopoulou, E. & Harvati, K. First record of *Macaca* (Cercopithecidae, Primates) in the Middle Pleistocene of Greece. *J. Hum. Evol.* **162**, 103104, doi:https://doi.org/10.1016/j.jhevol.2021.103104 (2022).
11 Konidaris, G. E. *et al.* The skeleton of a straight-tusked elephant (*Palaeoloxodon antiquus*) and other large mammals from the Middle Pleistocene butchering locality Marathousa 1 (Megalopolis Basin, Greece): preliminary results. *Quat. Int.* **497**, 65–84 (2018).
12 Michailidis, D., Konidaris, G. E., Athanassiou, A., Panagopoulou, E. & Harvati, K. The ornithological remains from Marathousa 1 (Middle Pleistocene; Megalopolis basin, Greece). *Quat. Int.* **497**, 85–94 (2018).
13 Doukas, C., van Kolfschoten, T., Papayianni, K., Panagopoulou, E. & Harvati, K. The small mammal fauna from the Palaeolithic site Marathousa 1 (Greece). *Quat. Int.* **497**, 95–107 (2018).
14 Field, M. H. *et al.* A palaeoenvironmental reconstruction (based on palaeobotanical data and diatoms) of the Middle Pleistocene elephant (*Palaeoloxodon antiquus*) butchery site at Marathousa, Megalopolis, Greece. *Quat. Int.* **497**, 108–122 (2018).
15 Tourloukis, V. *et al.* Lithic artifacts and bone tools from the Lower Palaeolithic site Marathousa 1, Megalopolis, Greece: Preliminary results. *Quat. Int.* **497**, 47–64, doi:https://doi.org/10.1016/j.quaint.2018.05.043 (2018).
16 Giusti, D. *et al.* Beyond maps: patterns of formation processes at the Middle Pleistocene open-air site of Marathousa 1, Megalopolis Basin, Greece. *Quat. Int.* **497**, 137–153 (2018).
17 Blackwell, B. A. *et al.* ESR dating ungulate teeth and molluscs from the Paleolithic site Marathousa 1, Megalopolis Basin, Greece. *Quaternary* **1**, 22 (2018).
18 Jacobs, Z. *et al.* Optical dating of K-feldspar grains from Middle Pleistocene lacustrine sediment at Marathousa 1 (Greece). *Quat. Int.* **497**, 170–177, doi:https://doi.org/10.1016/j.quaint.2018.06.029 (2018).
19 Tourloukis, V. *et al.* Magnetostratigraphic and chronostratigraphic constraints on the Marathousa 1 Lower Palaeolithic site and the Middle Pleistocene deposits of the Megalopolis basin, Greece. *Quat. Int.* **497**, 154–169, doi:https://doi.org/10.1016/j.quaint.2018.03.043 (2018).
20 Guibert-Cardin, J. *et al.* The function of small tools in Europe during the Middle Pleistocene: The case of Marathousa 1 (Megalopolis, Greece). *Journal of lithic studies* **9** (2022).

21 Lee-Thorp, J. A. & Van der Merwe, N. J. Aspects of the chemistry of modern and fossil biological apatites. *J. Archaeol. Sci.* **18**, 343–354 (1991).
22 van der Merwe, N. J. & Medina, E. The canopy effect, carbon isotope ratios and foodwebs in Amazonia. *J. Archaeol. Sci.* **18**, 249–259 (1991).
23 Zazzo, A., Lécuyer, C. & Mariotti, A. Experimentally-controlled carbon and oxygen isotope exchange between bioapatites and water under inorganic and microbially-mediated conditions. *Geochim. Cosmochim. Acta* **68**, 1–12, doi:https://doi.org/10.1016/S0016-7037(03)00278-3 (2004).
24 Bocherens, H., Sandrock, O., Kullmer, O. & Schrenk, F. Hominin palaeoecology in Late Pliocene Malawi: First insights from isotopes (^{13}C, ^{18}O) in mammal teeth. *S. Afr. J. Sci.* **107**, 1-6 (2011).
25 Ayliffe, L., Chivas, A. R. & Leakey, M. The retention of primary oxygen isotope compositions of fossil elephant skeletal phosphate. *Geochim. Cosmochim. Acta* **58**, 5291–5298 (1994).
26 Wang, Y. & Cerling, T. E. A model of fossil tooth and bone diagenesis: implications for paleodiet reconstruction from stable isotopes. *Palaeogeogr. Palaeoclimatol. Palaeoecol.* **107**, 281–289 (1994).
27 Sydney-Zax, M., Mayer, I. & Deutsch, D. Carbonate content in developing human and bovine enamel. *J. Dent. Res.* **70**, 913–916, doi:10.1177/00220345910700051001 (1991).
28 Rink, W. J. & Schwarcz, H. P. Tests for diagenesis in tooth enamel: ESR dating signals and carbonate contents. *J. Archaeol. Sci.* **22**, 251–255, doi:https://doi.org/10.1006/jasc.1995.0026 (1995).
29 Goedert, J. *et al.* Preliminary investigation of seasonal patterns recorded in the oxygen isotope compositions of theropod dinosaur tooth enamel *Palaios* **31**, 10–19 (2016).
30 Owocki, K., Kremer, B., Cotte, M. & Bocherens, H. Diet preferences and climate inferred from oxygen and carbon isotopes of tooth enamel of *Tarbosaurus bataar* (Nemegt Formation, Upper Cretaceous, Mongolia). *Palaeogeogr. Palaeoclimatol. Palaeoecol.* **537**, 109190, doi:https://doi.org/10.1016/j.palaeo.2019.05.012 (2020).
31 Capalbo, C. Multiproxy-Based reconstruction of the feeding habits from the late Middle Pleistocene straight-tusked elephant population of Poggetti Vecchi (Southern Tuscany, Italy). *Alp. Mediterr. Quat.* **31**, 113–119 (2018).
32 Palombo, M. R. *et al.* Coupling tooth microwear and stable isotope analyses for palaeodiet reconstruction: the case study of Late Middle Pleistocene *Elephas (Palaeoloxodon) antiquus* teeth from Central Italy (Rome area). *Quat. Int.* **126**, 153–170 (2005).
33 Briatico, G. & Bocherens, H. Middle Pleistocene ecology in central Italy. New isotopic insights from fauna tooth enamel of Casal de'Pazzi (Rome, Italy). *J. Mediterr. Earth Sci.* **15** (2023).
34 Grube, R., Palombo, M., Iacumin, P. & Di Matteo, A. What did the fossil elephants from Neumark-Nord eat in *Elefantenreich. Eine Fossilwelt in Europa* (ed. H. Meller) 253–272 (Landesamt für Denkmalpflege und Archäologie Sachsen-Anhalt, 2010).
35 Pushkina, D., Bocherens, H. & Ziegler, R. Unexpected palaeoecological features of the Middle and Late Pleistocene large herbivores in southwestern Germany revealed by stable isotopic abundances in tooth enamel. *Quat. Int.* **339-340**, 164–178, doi:https://doi.org/10.1016/j.quaint.2013.12.033 (2014).

36 Pop, E. & Bakels, C. Semi-open environmental conditions during phases of hominin occupation at the Eemian Interglacial basin site Neumark-Nord 2 and its wider environment. *Quaternary Science Reviews* **117**, 72-81, doi:https://doi.org/10.1016/j.quascirev.2015.03.020 (2015).

Supplementary Figures & Tables

Supplementary Figure 1: Simplified geological map of south-western Peloponnese showing the location of Marathousa 1. The figure was generated using Adobe Illustrator CC 2017 (https://www.adobe.com/).

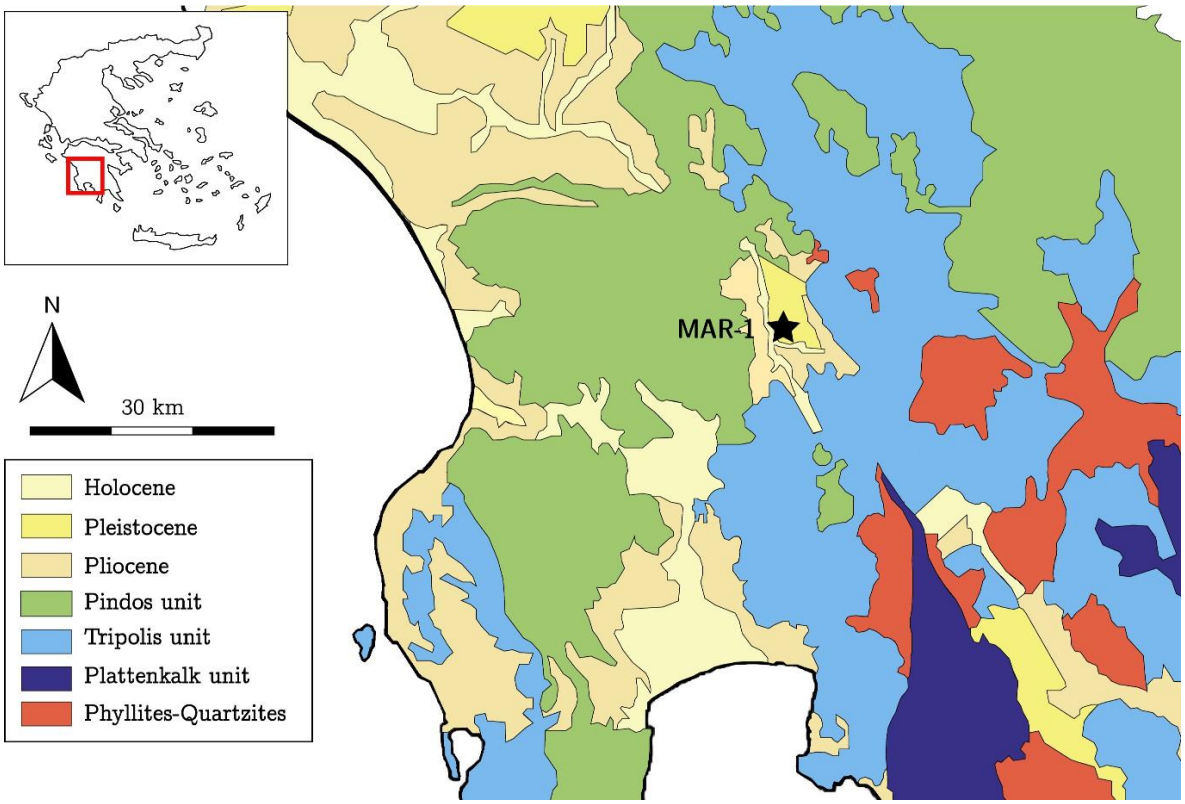

Supplementary Table 1. Main results of the incremental C, O, and Sr isotopic measurements from the right upper third molar of *Palaeoloxodon antiquus,* and Sr results from the teeth of *Hippopotamus antiquus.*

Taxon	Specimen	Sample	$\delta^{13}C$ (VPDB)	$\delta^{18}O$ (VSMOW)	$^{87}Sr/^{86}Sr$	CO_3 (%$CaCO_3$)	Distance from cervix (mm)
Palaeoloxodon antiquus	MAR-1A-5	MAR-1-942-676.1	-11.1	24.2	0.7087	4.3	87
		MAR-1-942-676.2	-11.5	23.9		4.5	84
		MAR-1-942-676.3	-12.1	23.5	0.7088	4.4	82
		MAR-1-942-676.4	-11.5	23.8		4.8	78
		MAR-1-942-676.5	-12.0	23.9	0.7088	4.5	76
		MAR-1-942-676.6	-11.9	23.6		4.3	73
		MAR-1-942-676.7	-11.5	23.2	0.7088	4.4	70
		MAR-1-942-676.8	-11.5	23.4		4.5	67
		MAR-1-942-676.9	-11.3	23.8	0.7088	4.6	64
		MAR-1-942-676.10	-11.4	23.3		4.5	61
		MAR-1-942-676.11	-11.3	23.2	0.7089	4.6	58
		MAR-1-942-676.12	-11.1	23.9		4.7	55
		MAR-1-942-676.13	-10.8	23.3		4.9	52
		MAR-1-942-676.14	-10.8	23.7		4.8	49
		MAR-1-942-676.15	-10.8	23.7	0.7088	4.7	46
		MAR-1-942-676.16	-11.1	23.4		4.7	43
		MAR-1-942-676.17	-10.4	23.4		5.2	40
		MAR-1-942-676.18	-10.9	23.4		5.1	37
		MAR-1-942-676.19	-11.4	22.9	0.7089	4.8	34
		MAR-1-942-676.20	-11.3	23.4		4.8	31
		MAR-1-942-676.21	-11.6	23.6	0.7088	4.6	28
		MAR-1-942-676.22	-11.4	23.4		4.5	26
		MAR-1-942-676.23	-11.1	23.6		4.8	23
		MAR-1-942-676.24	-10.8	23.0		5.2	20
		MAR-1-942-676.25	-10.8	23.8		5.2	17
		MAR-1-942-676.26	-11.3	23.0	0.7088	4.9	15
		MAR-1-942-676.27	-11.0	23.6		4.8	12
		MAR-1-942-676.28	-10.5	24.3	0.7084	5.1	9
		MAR-1-942-676.dent	1.9	24.9		7.0	
		MAR-1-942-676.cem	-3.9	24.0		8.7	
Hippopotamus antiquus	MAR-1B-8	-			0.7087		
	MAR-2B-2	-			0.7091		
	KYP4A-1004	-			0.7084		

Supplementary table 2: Published SI data on *Palaeoloxodon antiquus* used for inter-site comparison.

Region	Site	MIS	$\delta^{13}C$ (VPDB)	$\delta^{18}O$ (VSMOW)	Sampling	Reference
Italy	Casal de' Pazzi	7	-11.9	26.1	Bulk sample	Palombo et al. 2005[4]
			-9.9	27.2		
			-11.3	27.0		
			-12.1	25.9		
			-11.4	25.9		
			-11.3	26.3		
			-11.3	26.0		
			-13.0	26.3		
			-13.7	27.2		
			-13.3	27.1		
			-13.7	27.0		
			-13.2	23.9		Briatico & Bocherens 2023[1]
			-13.3	24.6		
			-11.5	23.5		
			-14.6	24.9		
			-14.7	24.7		
			-12.9	23.9		
			-10.9	25.2		
			-12.6	22.8		
			-9.4	24.8		
	La Polledrara di Ceccanibio	9	-9.0	24.8	Bulk sample	Palombo et al. 2005[4]
			-10.2	27.4		
			-10.9	26.8		
			-10.8	26.5		
			-10.3	26.8		
			-10.6	27.0		
			-10.7	27.6		
			-10.4	27.0		
			-10.1	26.8		
			-9.8	27.0		
			-10.6	26.8		
			-10.6	26.7		
	Poggetti Vecchi	7	-11.1	26.7	Bulk sample	Capalbo et al. 2018[2]
Germany	Neumark Nord-1	5e	-12.2	26.9	Bulk sample	Grube et al. 2010[3]
			-11.2	27.5		
			-13.1	25.5		
			-11.7	27.5		
			-11.7	27.6		
			-12.6	27.0		
			-14.1	27.9		
			-13.4	27.6		
			-12.8	27.9		
			-13.9	28.0		
			-12.4	26.8		
			-12.3	26.6		
			-11.9	26.3		
			-13.3	25.5		
			-13.1	25.8		
	Mauer	15	-13.9	21.8	Bulk sample	Pushkina et al. 2014[5]
			-12.4	22.5		
			-12.4	20.3		
	Steinheim an der Murr	11	-13.2	20.5	Bulk sample	Pushkina et al. 2014[5]
			-13.1	21.7		
			-13.0	21.1		
			-12.9	21.9		
			-12.6	21.4		

References

1. Briatico, G. and Bocherens, H. 2023. Middle Pleistocene ecology in central Italy. New isotopic insights from fauna tooth enamel of Casal de'Pazzi (Rome, Italy). Journal of Mediterranean Earth Sciences, 15.

2. Capalbo, C. 2018. Multiproxy-Based reconstruction of the feeding habits from the late Middle Pleistocene straight-tusked elephant population of Poggetti Vecchi (Southern Tuscany, Italy). Alpine and Mediterranean Quaternary, 31, pp. 113–119.

3. Grube, R., Palombo, M., Iacumin, P. and Di Matteo, A. 2010. What did the fossil elephants from Neumark-Nord eat, in: Meller, H.(ed.) Elefantenreich. Eine Fossilwelt in Europa. Landesamt für Denkmalpflege und Archäologie Sachsen-Anhalt, Halle. Halle: Landesamt für Denkmalpflege und Archäologie Sachsen-Anhalt.

4. Palombo, M. R., Filippi, M. L., Iacumin, P., Longinelli, A., Barbieri, M. and Maras, A. 2005. Coupling tooth microwear and stable isotope analyses for palaeodiet reconstruction: the case study of Late Middle Pleistocene *Elephas (Palaeoloxodon) antiquus* teeth from Central Italy (Rome area). Quaternary International, 126, pp. 153–170.

5. Pushkina, D., Bocherens, H. and Ziegler, R. 2014. Unexpected palaeoecological features of the Middle and Late Pleistocene large herbivores in southwestern Germany revealed by stable isotopic abundances in tooth enamel. Quaternary International, 339-340, pp. 164–178.

Appendix C

Study III

Ecological variability of Hippopotamus antiquus from the Middle Pleistocene of Megalopolis Basin (Greece): Evidence for dynamic habitats in a glacial microrefugium

Authors: Effrosyni Roditi, Hervé Bocherens, George E. Konidaris, Athanassios Athanassiou, Vangelis Tourloukis, Eleni Panagopoulou, Panagiotis Karkanas, Katerina Harvati

Manuscript ready for submission[†]

[†] The following version is based on the authors formatting of the manuscript and figures. General layout and position of Tables and Figures may differ in the final published manuscript

ECOLOGICAL VARIABILITY OF HIPPOPOTAMUS ANTIQUUS FROM THE MIDDLE PLEISTOCENE OF MEGALOPOLIS BASIN (GREECE): EVIDENCE FOR DYNAMIC HABITATS IN A GLACIAL MICROREFUGIUM

Effrosyni Roditi[1], Hervé Bocherens[2], George E. Konidaris[1], Athanassios Athanassiou[3], Vangelis Tourloukis[1,4], Eleni Panagopoulou[3], Panagiotis Karkanas[5], Katerina Harvati[1]

[1] Paleoanthropology, Institute for Archaeological Sciences and Senckenberg Centre for Human Evolution and Paleoenvironment, Department of Geosciences, Eberhard Karls University of Tübingen, Tübingen, Germany

[2] Biogeology, Department of Geosciences and Senckenberg Centre for Human Evolution and Paleoenvironment, Eberhard Karls University of Tübingen, Tübingen, Germany

[3] Hellenic Ministry of Culture, Ephorate of Paleoanthropology–Speleology, Athens, Greece

[4] Department of History and Archaeology, School of Philosophy, University of Ioannina, Greece

[5] M.H. Wiener Laboratory for Archaeological Science, American School of Classical Studies at Athens, Greece

Abstract

This study investigates the ecology of the extinct species *Hippopotamus antiquus* from the Middle Pleistocene (ca. 700 to 430 ka) sequence of the Megalopolis Basin, a glacial micro-refugium for temperate taxa in southern Greece. Using intra-tooth stable carbon ($\delta^{13}C$) and oxygen ($\delta^{18}O$) isotope analyses of enamel bioapatite from five *Hippopotamus* individuals, we reconstruct past habitat conditions, dietary variability, and hydrological or climatic changes on an infra-annual, multi-annual, and millennial scale. The isotopic data suggest a broader aridification trend from MIS 16 to MIS 12. The studied individuals demonstrate seasonally variable dietary habits and record potential short-term climatic or hydrological shifts, which likely further impacted habitat or resource availability in the area. The incidence of enamel hypoplasia on two specimens from the early Middle Pleistocene, which was tentatively correlated to cooler conditions, shows that the taxon survived in the region even during stressful, less optimal periods. These findings provide a crucial framework to better understand

the ecological niche of the species, as well as the impact of dynamic ecosystems on large mammal and hominin adaptations in the European Middle Pleistocene.

1.Introduction

The fossil record of the extinct European hippopotamus, *Hippopotamus antiquus*, attests to its wide paleogeographical distribution over western Eurasia during the Early and Middle Pleistocene, with frequent occurrences in the northern peri-Mediterranean regions of Europe (Athanassiou, 2022; Fidalgo, Rosas, Madurell-Malapeira, et al., 2023) and occasional expansions to more northern latitudes (e.g. United Kingdom, Germany) (e.g., Kahlke, 2001; Adams et al., 2022; Athanassiou, 2022). Having an African origin, the species is thought to have entered Europe in the first part of the Early Pleistocene (~2.1 Ma) (Fidalgo et al., 2021; Fidalgo, Rosas, Madurell-Malapeira, et al., 2023; Iannucci et al., 2023; Martino & Pandolfi, 2022), but a wider geographical extension is only noted from 1.5 my (e.g., Adams et al., 2022; Konidaris and Kostopoulos, 2024; Madurell-Malapeira et al., 2014; Martínez-Navarro et al., 2015). Much of the species' presence in Europe, before its extinction at ca. 450 ka (Martino et al., 2023; Konidaris et al., 2023), captures the Early/Middle Pleistocene transition (EMPT), a climatic event that is generally called the "Mid-Pleistocene Revolution" and spanned approximately between ~1.4 and 0.4 Ma (e.g., Head et al., 2015; Palombo, 2014). The EMPT was characterized by intense climatic oscillations, an increase in the global ice volume, and a shift from ~40 ky to 100 ky periodicity between glacial and interglacial periods (Berends et al., 2021; Clark et al., 2006; Head & Gibbard, 2015), which resulted in the progressive expansion of open landscapes. These conditions facilitated a biotic reorganization in the second half of the Early Pleistocene (during the late Villafranchian–Epivillafranchian European Land Mammal Ages) and the dispersal of hominins in Southwest Europe (e.g., Kahlke et al., 2011; Madurell-Malapeira et al., 2014; Palombo, 2010, 2014; Zanazzi et al., 2022).

The severity of glacial events and the contrast between glacial and interglacial periods intensified after 900 ka and persisted until ~0.42 my, around the MIS (Marine Isotope Stage) 12/11 transition. These severe glacial periods characterized by progressively increased seasonality and aridity (Fidalgo, Rosas, Bartolini-Lucenti, et al., 2023; Joannin et al., 2007; Palombo, 2014; Strani et al., 2019) are considered to have restricted *H. antiquus* in South European peninsular refugia (Fidalgo, Rosas, Madurell-Malapeira, et al., 2023; Konidaris et al., 2023) with dispersals into northern latitudes occurring during interglacial periods.

Hippopotamus antiquus is a common faunal element in the Megalopolis Basin, central Peloponnese (Greece), present in multiple stratigraphic layers (including both interglacial and glacial stages) of the basin that cover the late Early to Middle Pleistocene (Athanassiou, 2022; Athanassiou et al., 2018; Konidaris et al., 2023; Konidaris et al., 2024; Melentis, 1965). Growing evidence testifies to the significance of the area as a glacial micro-refugium for

temperate faunal taxa, such as the straight-tusked elephant *Palaeoloxodon antiquus*, the Barbary macaque *Macaca sylvanus*, the European pond turtle *Emys orbicularis* and several temperate-adapted birds (e.g., Konidaris et al., 2022; Konidaris et al., 2024; Konidaris et al., 2018; Roditi et al., 2024; Vlachos and Delfino, 2016; Michailidis et al., 2018); however, apart from broader inferences regarding milder and temperate climatic conditions persisting in these areas, there is a general lack of research in local environmental dynamics and the ecological adaptations or tolerances of temperate taxa, including *H. antiquus*, within Middle Pleistocene microrefugia. Stable isotope investigations of individual mammalian ecologies can be used to reconstruct mobility, diet, landscapes and infer local past climatic conditions at high-resolution temporal scales, ranging from a couple of years to several decades (e.g., Balasse, 2002; Heddell-Stevens et al., 2024; Julien et al., 2012; Kowalik et al., 2018; Roditi et al., 2024; Souron et al., 2012; Uno et al., 2020; Yang et al., 2024; Zanazzi et al., 2022). A direct contextual connection between anthropogenic activity and sampled faunal specimens can extend paleoclimatic and habitat inferences to the reconstruction of the hominin niche and paleoenvironment.

In this study, we sought to reconstruct long-term environmental and hydrological conditions in the Megalopolis Basin (Greece), through the ecology of the extinct *Hippopotamus antiquus*. We present carbon ($^{13}C/^{12}C$) and oxygen ($^{18}O/^{16}O$) stable isotope data from five Middle Pleistocene *H. antiquus* individuals recovered from different fossiliferous localities within the basin. Our approach provides ecological and environmental inferences, such as habitat reconstruction and hydrology, on a multi-annual, decadal, and millennial-scale to reveal the conditions that facilitated hippopotamus presence and survival in the basin. The contemporaneity of hominin activity with these individuals, as evidenced by the presence of cutmarks on hippopotamus remains or their contextual association with lithic artefacts, further supplements our current knowledge of hominin environments.

2.Materials and geo-chronological background

The Megalopolis Basin is an intramontane, post-orogenic graben located in the central part of the Peloponnese, southern Greece. The area has an altitude of 330–450 meters above sea level (m a.s.l) and covers a total of 250 km^2, with its longer axis extending approximately 20 km in an NW–SE direction. The Mainalo, Lykaion, and Taygetos mountain ranges surround the basin on the east, west, and south, respectively. The basin formed during the Late Miocene–Pliocene on the Mesozoic–Paleogene basement of the Peloponnese, while during the Early and Middle Pleistocene, it periodically hosted a large lake. Over the years, numerous faunal remains have been collected from the area, including hippopotamids (Melentis, 1965), but few of them have well-constrained stratigraphic provenance. The latest targeted field surveys conducted by a joint team of the Ephorate of Palaeoanthropology-Speleology of the

Hellenic Ministry of Culture and the University of Tübingen (Germany), have led to the discovery of several new fossil-bearing sites/findspots and the recovery of fossil hippopotamids from well-defined stratigraphic contexts (Athanassiou et al., 2018; Konidaris et al., 2023; Konidaris et al., 2024) within the Marathousa Member (Mb) of the Choremi formation. The lacustrine deposits of the Marathousa Mb are characterized by alternating Lignite seams (limnic conditions) and detrital beds (limno-telmatic conditions), representing oscillations between glacials/interglacials in the period between ca. 900–350 ky (Tourloukis, Muttoni et al. 2018; van Vugt et al. 2000). The sampled dental material (Figure 1) originates from five archaeo-paleontological localities, found within the Megalopolis lignite mines during the latest excavation and survey campaigns, and is stored in the facilities of the Ephorate of Paleoanthropology-Speleology.

An upper third molar (M3, MAR-1B-8; Figure 1D) was recovered at the Lower Palaeolithic open-air site Marathousa 1 (MAR-1) that was systematically excavated between 2013 – 2019. The site is located at an elevation of ca. 350 meters above sea level (m a.s.l) and consists of two excavation areas (Areas A and B) located approximately 60 meters apart (Panagopoulou et al., 2015; Panagopoulou et al., 2018; Thompson et al., 2018). The excavation revealed a sequence containing rich micro-and macro-faunal remains (Bludau et al., 2021; Boni et al., in press, Doukas et al., 2018; Konidaris et al., 2024; Konidaris et al., 2018; Michailidis et al., 2018; Vlachos et al., in press), micro- and macro-flora (Field et al., 2018), as well as lithic and bone artifacts (Tourloukis, Thompson, et al., 2018). Evidence of anthropogenic exploitation is further documented in several bones of large mammals, including elephants, as well as identified from the use wear study of the lithic artefacts (Konidaris et al., 2018; Guibert-Cardin et al., 2022). The find-bearing layers are situated between Lignite seams IIb and IIIa and belong to the same depositional event as evidenced by lithostratigraphic, geochemical, spatial, and archaeo-palaeontological observations (Giusti et al., 2018; Karkanas et al., 2018; Konidaris et al., 2018; Tourloukis, Thompson, et al., 2018). Radiometric, magnetostratigraphic, and bio-chronological dating place the archaeological sequence to ca. 430 ka and correlate it to the glacial MIS 12 (Butiseacă et al. 2024, Blackwell et al., 2018; Doukas et al., 2018; Jacobs et al., 2018; Tourloukis, Muttoni, et al., 2018). The herein studied *Hippopotamus* upper third molar was collected together with other dental and postcranial hippopotamus remains during the initial opening of the site (in Area B) in 2013. During the 2019 field campaign, additional postcranial elements were excavated in situ within stratigraphic unit UB2b (Karkanas et al., 2018; Konidaris et al., 2024). The remains of 2019 were found in close spatial and anatomical proximity, and together with those of 2013, likely belong to a single, skeletally immature individual (Konidaris et al., 2024).

In 2018, a second open-air locality was discovered in the Marathousa mine. The new site, named Marathousa 2 (MAR-2), is located ~1.5 km east of MAR-1 and is also stratigraphically

placed between Lignite seams IIb and IIIa. Therefore, it is broadly considered as contemporaneous to the latter and associated with the MIS 12 glacial period, though it is positioned closer to the glacial termination than Marathousa 1 (Karkanas et al., in press; Konidaris et al., 2023). *Hippopotamus* remains were collected from two areas (Area A and Area B) within the same depositional event —reflected in stratigraphic units UA6 and UB6—, which represent the margins of a small and permanent water body. The site yielded several *Hippopotamus antiquus* elements, among which an upper canine (hereafter MAR-2B-2, Figure 1A) from Area B, which was sampled for the purposes of this study. Noteworthy is also the presence of cutmarks on a hippopotamus thoracic vertebra in Area A, as well as the spatial and stratigraphic association of the remains with a lithic artefact, which establishes the presence of hominins at the site and the exploitation of a *Hippopotamus* carcass (Konidaris et al., 2023).

Specimen KYP3-46, a lower right canine (Figure 1C), was collected from the fossiliferous locality Kyparissia 3 (KYP-3) within the Kyparissia lignite mine (Athanassiou, 2018; Athanassiou et al., 2018). KYP-3 is part of the upper clastic unit underlying Lignite Seam II and is located at an elevation of 346 m.a.s.l. (Athanassiou et al., 2018; Karkanas et al., in press). The stratigraphic model by Tourloukis, Muttoni, et al. (2018), in combination with bio-chronological evidence from the recent study of micromammals (Konidaris et al., 2024), suggests a tentative attribution to MIS 16. During the recent re-investigation of the site within the framework of the MegaPal project (2018–2022) lithic artefacts were discovered in direct association with cervid, suid, elephant and hippopotamus remains indicating the presence of hominins at the site (Karkanas et al., in press; Konidaris et al., 2024).

A cranial fragment with the left maxilla preserving the P4–M3 row (KYP4A-1004, Figure 1E) (Athanassiou et al., in press) was found recently at Kyparissia 4 (KYP-4). The site is placed close to the top of Lignite Seam I (~ 330 masl) and is, therefore, located stratigraphically lower than KYP-3 (Athanassiou et al., in press; Athanassiou et al., 2018; Karkanas et al., in press). In addition to its stratigraphic position, recent bio-chronological data further suggest an early Middle Pleistocene age, post-dating 780 ka and pre-dating MIS 16 (van Kolfschoten et al., in press; Konidaris et al., 2024). The large mammal fauna is rich including beaver (*Castor fiber*), macaque (*Macaca sylvanus*), elephant (*Palaeoloxodon antiquus*), hippopotamus (*H. antiquus*), giant deer (*Praemegaceros verticornis),* red deer *(Cervus elaphus),* fallow deer *(Dama sp.*), bison (*Bison sp.*), wild boar (*Sus scrofa*), horse (*Equus* spp.), rhinoceros (*Stephanorhinus* cf. *hemitoechus*), found together with a small assemblage of stone tools, mainly small-sized debitage products and few retouched pieces, making KYP-4 the oldest stratified archaeological site in Greece (Athanassiou et al., in press; Karkanas et al., in press; Konidaris et al., 2024).

The KYPT-842 upper incisor (I1, Figure 1B) was discovered in 2012 at the KYP-T site, which is located within the Kyparissia lignite mine close to the western margin of Megalopolis Basin (Athanassiou et al., 2018). The site was originally placed on the top of Lignite Seam II, based on the thin limestone layer overlying the lignite (Athanassiou et al., 2018); however, recent stratigraphic investigations of the Kyparissia sequence revealed that KYP-T lies at the same altitude as KYP-4 and is more likely to be positioned close to the top of Lignite seam I, thus, stratigraphically lower than previously considered (Karkanas et al., in press; Konidaris et al., 2024)

3.Methods

3.1 Sampling, pre-treatment and analysis

All specimens were sampled at the facilities of the Ephorate of Paleoanthropology-Speleology. The obtained enamel samples were chemically prepared at the Biogeology Laboratory of the University of Tübingen. The surface of each tooth was superficially abraded with a handheld rotary tool to remove cementum or adhering matrix, as well as the outermost few millimeters of enamel. All teeth were sequentially sampled by conventional drilling using a handheld rotary drill with a diamond-coated tip, to examine intra-tooth variations in carbon and oxygen isotopic profiles. Samples were obtained in 2-3 mm intervals to achieve the highest possible resolution. Canines were sampled near the enamel-dentine arch following Souron et al. (2012). Sample distance for hippopotamus tusks was measured along the inner curve following the enamel-dentine arch, from the open pulp cavity to the distal end. Molars were sampled perpendicularly to the growth axis of the tooth, from the enamel root junction to the occlusal surface. Special attention was given to avoid cracks or impurities in the enamel that could introduce diagenesis/contamination. A total of 215 enamel samples (Supplementary Tables 1–5), each weighing approximately 10 mg, were obtained for analysis.

Treatment of enamel powder follows the protocol described by Bocherens et al. (1994) and Koch et al. (1997a). Briefly, the sampled enamel powder was reacted in 1.35 ml of 2.5% sodium hypochlorite (NaOCl) for 24 hours to remove organic content. The vial contents were then centrifuged at 5000 rounds/minute for 5 minutes, the supernatant was extracted, and the remaining powder was rinsed repeatedly with MilliQ water. Next, samples were reacted with 1M Acetic Acid Buffer solution for 24 hours to remove non-structural, diagenetic carbonates, then repeatedly rinsed with MilliQ H_2O and dried at 35° C for 72 hours. This process produced approximately 3 mg of purified biogenic apatite, which was reacted with concentrated orthophosphoric acid (H_3PO_4) to release CO_2. Stable isotope ratios were obtained by analyzing the gaseous CO_2 with continuous multi-flow isotope ratio mass spectrometry (IRMS) at the University of Tübingen. Two international standards, IAEA-603 (International Atomic Energy Agency) and NBS-18 (National Bureau of Standards, now National Institute of Standards and

Technology or NIST), as well as three in-house standards were used for calibration. Results are expressed using the standard δ notation in per mil (‰):

$$\delta^{j}X = \frac{(\,{}^{j}X/\,{}^{i}X)_{sample}}{(\,{}^{j}X/\,{}^{i}X)_{standard}} - 1$$

where ^{j}X is the heavier isotope and ^{i}X is the lighter isotope (Bond & Hobson, 2012). Measured ratios refer to $^{13}C/^{12}C_{VPDB}$ or $^{18}O/^{16}O_{VSMOW}$, wherein VPDB is Vienna Peedee Belemnite and VSMOW is Vienna Standard Mean Ocean Water.

3.2 Carbon ($\delta^{13}C$) and oxygen ($\delta^{18}O$) stable isotope analysis of enamel bioapatite

Carbon isotopes ($\delta^{13}C_{apatite}$) in herbivore enamel reflect the values of consumed vegetation and are, thus, used to infer the animal's diet and reconstruct their habitat. However, physiological and metabolic processes result in isotopic fractionation between diet and enamel carbon values (Cerling et al., 2021; Cerling & Harris, 1999; Passey, Robinson, et al., 2005). The isotopic enrichment ($\varepsilon^{*}_{diet\text{-}bioapatite}$) in medium- and large-sized mammalian tissues has been estimated between 12‰ and 14‰ (Lee-Thorp & Van der Merwe, 1991; Passey, Robinson, et al., 2005), with a standard factor of 14.1±0.5 (Cerling & Harris, 1999) commonly employed in most isotopic studies. Recently, Tejada-Lara et al. (2018) proposed a dependence of $\varepsilon^{*}_{diet\text{-}bioapatite}$ to mammalian body mass within hindgut and foregut fermenters. A critical appraisal by Cerling et al. (2021) demonstrated that digestive function and methane production may, nonetheless, have a stronger influence on bioapatite-diet ^{13}C enrichment, especially when distinct digestive strategies —ruminant and non-ruminant foregut fermenters, coprophagus and non-coprophagus hindgut fermenters— are considered separately. Since hippopotamus is a non-ruminant foregut fermenter, we opted for a ^{13}C enrichment factor of 12.5 per mil (‰) following Cerling et al. (2021), to reconstruct $\delta^{13}C_{diet}$ from $\delta^{13}C_{bioapatite}$. However, species-specific body-mass corrected $\delta^{13}C$ values using the formula $\varepsilon^{*} = e^{[2.34+0.05(BM)]}$ suggested by Tejada-Lara et al. (2018) for foregut fermenters and an average body mass (BM) of 2027 kg estimated for Middle Pleistocene *Hippopotamus antiquus* in the Megalopolis basin (Konidaris et al., under review) are provided in the Supplementary Tables.

Differences related to carbon fixation in terrestrial vegetation influence the isotopic composition of plants and enable a distinction between flora with different photosynthetic pathways (C_3 and C_4). The C_3 photosynthetic pathway is utilized by most trees, shrubs, and cool-season grasses, whereas the C_4 photosynthetic pathway is more common in warm-season grasses and sedges. Carbon isotope values of modern C_3 vegetation range from −36‰ to −22‰ (average −27‰), whereas C_4 vegetation values vary between −17‰ and −9‰ (average −13‰) (Bender, 1971; Kohn, 2010). Within terrestrial C_3-dominated environments, plants exhibit large $\delta^{13}C$ variations,

which are influenced by a combination of environmental factors including light intensity, water stress, CO_2 availability, and temperature (Basu et al., 2021; Farquhar et al., 1989; Hartman & Danin, 2010; van der Merwe & Medina, 1991). These variations can be used to infer habitat openness and relative humidity. Modern C_3 vegetation growing in the understory layer of dense canopy cover is expected to have $\delta^{13}C$ values lower than −30‰ (Drucker et al., 2008), whereas $\delta^{13}C_{C3}$ values in the upper limits of the range indicate water stress conditions in open, xeric environments (>~−25‰).

In aquatic ecosystems, freshwater primary producers have large $\delta^{13}C$ ranges (−47‰ to −8‰) (Chappuis et al., 2017; Clementz et al., 2008; Finlay & Kendall, 2007; Osmond et al., 1981). Carbon isotope variability of aquatic vegetation is strongly related to the source of carbon (CO_2 or HCO_3–) for photosynthesis, seasonal variations in hydrology, temperature or irradiance, as well as dissolved inorganic carbon (DIC) concentrations and water pH (Chappuis et al., 2017; Finlay & Kendall, 2007; Liu et al., 2020). Overall, C_3 emergent aquatic macrophytes and algae, that use CO_2 for photosynthesis, have lower $\delta^{13}C$ values (~−27‰), largely overlapping with those of C_3 terrestrial communities, whereas submerged C_3 plants, which utilize inorganic carbon and HCO_3, often demonstrate higher carbon isotope ratios (Chappuis et al., 2017; Cloern et al., 2002; Liu et al., 2020). Nonetheless, due to the large overlap of values, an isotopic distinction between aquatic and terrestrial vegetation remains difficult.

The environmentally driven isotopic variation in plant $\delta^{13}C$ can be used to examine animal "ecological partitioning". By extension, herbivore foraging habitats can be divided into closed canopy forest, woodland-mesic C_3 grassland, open woodland/xeric C_3 grassland, C_3-C_4 grassland, and pure C_4 grassland (Domingo et al., 2013). To define end-member carbon isotope values of Pleistocene C_3 and C_4 vegetation ($\delta^{13}C_{1750}$) modern plant $\delta^{13}C$ values were adjusted to account for the ~1.5‰ ^{13}C depletion in pCO_2 due to the effects of fossil fuel burning (Tipple et al., 2010). Upon accounting for the diet-enamel fractionation, hippopotamus habitat endmembers are defined as follows: closed canopy forest (<−15.4‰), woodland-mesic C_3 grassland (−15.4 to −10.1‰), open woodland-xeric grassland (−10.1‰ to −7.3‰), C_3-C_4 grassland (−7.3‰ to −2.2‰), and pure C4 grassland (-2.2‰ to +5.9‰).

Stable oxygen isotope analysis of enamel bioapatite is widely employed as a paleoclimatic proxy. The oxygen isotopic composition of enamel carbonates is in equilibrium with the $\delta^{18}O$ of body water, offset by a constant temperature-dependent fractionation in homeothermic mammals. The $\delta^{18}O_{body\ water}$ is, in turn, controlled by the animal's physiology, drinking behavior, diet, as well as climate (Bocherens et al., 1996; Bryant & Froelich, 1995; Longinelli, 1984; Pederzani & Britton, 2019). The $\delta^{18}O_{enamel}$ composition of water-dependent, semi-aquatic hippopotamids is considered to closely reflect the hydrological chemistry of local water bodies

($\delta^{18}O_{surface\ water}$) in which they live in (Clementz et al., 2008; Clementz & Koch, 2001; Levin et al., 2006), largely owning to their physiological adaptation for rapid body water turnover through increased urine and fecal water loss.

The $\delta^{18}O$ of meteoric water is conditioned by external influences, such as the degree of continentality, altitudinal differences of water sources, the amount of local precipitation, surface temperature, as well as differences in the hydrological processes of water bodies (Pederzani and Britton 2019). At middle and high latitudes, the oxygen isotopic composition of surface water is primarily influenced by precipitation and the atmospheric temperature. Seasonal isotopic variations recorded in local $\delta^{18}O$ of meteoric water in these contexts are ascribed mostly to the temperature effect (Pederzani & Britton, 2019). In this context, higher $\delta^{18}O$ values in herbivore enamel are found in individuals inhabiting warmer and/or drier environments, whereas lower $\delta^{18}O$ values characterize the isotopic composition of animals occupying colder and/or more humid habitats (Bocherens & Drucker, 2013; Pederzani & Britton, 2019).

Seasonality can be identified in the enamel isotopic composition of herbivores, when an incremental sampling strategy is employed at the appropriate resolution. Following the aforementioned principles, temperature- and precipitation-driven sub-annual variation in the oxygen isotopic values of water bodies and, by extension, herbivore bioapatite, would result in a sinusoidal pattern with lower $\delta^{18}O$ representing winter (cool/humid season) and higher $\delta^{18}O$ reflecting summer (warm/arid season) in a Mediterranean context (Wagner et al., 2019). The amplitude of isotopic variation between peaks and valleys in incremental isotopic profiles is often used to estimate relative intensity of climatic seasonality. Yet the expression of environmental seasonality in the isotopic signal of mammalian enamel can be further influenced by extrinsic factors, such as local hydrology, wherein water mixing in sources with long residence times or the influx of non-local, isotopically distinct water results in dampening of seasonal variations in the water reservoir, (Britton, 2020; Pederzani & Britton, 2019), as well as intrinsic processes, for instance the rate of enamel apposition and the duration of mineralization (see section 3.4).

3.4 Inter- and intra-tooth isotopic data

Sequential sampling of tooth enamel and the investigation of isotopic shifts in intra-tooth profiles are used to explore short-term ecological and environmental changes during the time of tooth formation. However, adequate knowledge of enamel formation and mineralization patterns is essential for the interpretation of intra-tooth isotopic profiles (Balasse, 2003; Passey & Cerling, 2002; Passey, Cerling, et al., 2005; Souron et al., 2024; Uno et al., 2020; Zazzo et al., 2005). Few studies have addressed enamel formation for *Hippopotamus amphibius* in the past with a special focus on canines (Passey, Cerling, et al., 2005; Souron et al., 2012; Uno et al., 2013), while research expanding on molar formation and revision of previously established

parameters (Green et al., 2023; Souron et al., 2024) is anticipated to supplement the current consensus. Molar formation and growth patterns in hippopotamids differ from those of canines and incisors, the latter having much thinner enamel than molars and longer formation times, as they are continuously growing. Green et al. (2023) suggest a maximum formation time of approximately 2.5 years for fossil hippopotamid third molars. Souron et al. (2024) estimate a molar enamel extension rate (EER) of 70-130μm/increment but larger angles of enamel apposition in comparison to canines, which may result in stronger isotopic averaging when conventional sampling is employed. For upper canines, Uno et al. provided an average growth rate of 19.4±3.1 mm/year. Growth rates for lower canines show large variations— from a minimum estimate of 13-14 mm per year (Passey, Cerling, et al., 2005) to a maximum of 74.7mm/year (Uno et al., 2013)—, possibly due to sexual dimorphism and age-related differences. Nevertheless, most of the available data point to estimates between 30 and 40 mm/year (Harris et al., 2008; Passey, Cerling, et al., 2005; Souron et al., 2012; Uno et al., 2013). In addition, an isotopic offset may apply between molars and tusks, similarly to what has been observed in other taxa (Yang et al., 2020). With these limitations in mind, intra-tooth isotopic profiles are discussed for each individual tooth separately, within the context of their respective tooth formation and growth parameters. Potential correlation between $\delta^{13}C$ and $\delta^{18}O$ intra-tooth series was evaluated using Pearson's correlation coefficient. Analyses and graphical representations were performed using SPSS and MATLAB.

4.Results

Enamel stable isotope results are summarized in Table 1. Bioapatite carbon isotope values ($\delta^{13}C_{enamel}$) of all five individuals range from −14.2‰ to −10.0‰ and indicate a pure C_3 diet for *Hippopotamus antiquus* in the Megalopolis basin. On average, the lowest carbon isotope values were obtained from KYP3-46 and ranged from −14.2‰ to −11.2‰ (median −13.6‰). On the other hand, the highest $\delta^{13}C$ were observed in MAR-1B-8 (−12.8‰ to −10.0‰, median −11.3‰). Overall, specimens from the Kyparissia mine attributed to the early Middle Pleistocene, displayed lower carbon isotope values compared to samples from Marathousa. Oxygen isotope values ranged between +21.0‰ and +24.2‰ for all individuals combined. The lowest $\delta^{18}O$ values were obtained from KYP4A-1004 (+21.1‰ to +23.1‰, median +21.8‰). Specimen KYP-T-842 yielded the highest $\delta^{18}O$ values, ranging from +23.1‰ to +24.2‰ (median +23.8‰) (Figure 2).

Two specimens (MAR-2B-2 and KYPT-842) demonstrate regular and continuous sinusoidal patterns in both carbon and oxygen intra-tooth series (Figure 3B and 3C, respectively). The MAR-2B-2 intra-tooth isotopic profile provides a long isotopic record with consistent periodicity and a minimum of 12 peaks and valleys. Intriguingly, the pattern is easier discernible in the carbon rather than the oxygen intra-tooth profile. The Pearson's correlation coefficient

demonstrates an inverse correlation between $\delta^{13}C$ and $\delta^{18}O$ for this individual ($r(77)=-.39$, $p=0.001$). Additionally, the amplitude of variation in the $\delta^{18}O$ series of MAR-2B-2 (2.9‰) is the highest observed in our sample. On the other hand, KYPT-842 shows a weak cyclicity in $\delta^{18}O$ (range 1.1‰) with at least 8 cycles clearly visible in the oxygen isotopic record. Fluctuations are also visible in the carbon isotope profile (range 2.4‰); however, carbon and oxygen isotope values are not significantly correlated ($r(24)=.11$, $p=0.63$). In contrast to the latter two specimens, both carbon and oxygen intra-tooth isotopic profiles of the KYP3-46 lower canine appear more noisy, with less regular fluctuations, making it difficult to distinguish annual cycles. A 3-point moving average was calculated to aid visualization, and tentatively shows a quasi-sinusoidal pattern with 6 peaks and at least 5 troughs, which, given the sampling gaps, likely reflects a minimum record of the cycles represented in this specimen (Figure 3A). The carbon and oxygen isotopic series were positively correlated ($r(77) = .67$, $p=.01$). A sharp apparent reduction in $\delta^{13}C$ values is observed at the earlier stages of tooth formation, near the distal end of the canine, and is most likely the main cause for the large $\delta^{13}C$ range (amplitude 3.0‰), the highest recorded among our samples. Fluctuations are also visible in the intra-tooth isotopic profiles of the two M3s, namely MAR-1B-8 and KYP4A-1004 (Figure 4A and 4B, respectively). The carbon isotope intra-tooth profile of MAR-1B-8 demonstrates a relatively sharp increase in δ-values at the earlier stages of tooth formation, from −12.8‰ to −10.2‰, with an apparent decrease in $\delta^{18}O$ values within the same timeframe. However, carbon and oxygen isotope series from this individual were not significantly correlated (r (16) =−.32, $p=0.22$). On the contrary, a significant positive correlation between $\delta^{13}C$ and $\delta^{18}O$ was obtained for KYP4A-1004 (r (17) = .50, $p=0.04$).

5.Discussion

5.1 Isotopic signal preservation

Tooth enamel is particularly resistant to diagenetic alterations. Its low organic content (less than 1%) and high crystallinity enhance the ability of the tissue to preserve unaltered biogenic isotopic signal, in contrast to the more porous and less crystalline cementum and dentine (Wang & Cerling, 1994; Zazzo et al., 2004). To monitor diagenesis or sample contamination, dentine and, wherever available, cementum were also sampled, pretreated and analyzed together with enamel powder and the carbonate content (%$CaCO_3$) of the different tissues was compared. The carbonate content of enamel bioapatite (n=215) in our dataset ranged from 3.3 to 5.4 wt%, falling within the normal range of modern, non-diagenetically altered enamel (2.3–5.5 wt%) (Koch et al., 1997b; Rink & Schwarcz, 1995; Sydney-Zax et al., 1991). Diagenetically altered dentine and cementum are expected to yield higher %CO_3. The carbonate content of dentine (n=5) in our samples varied between 5.8 and 8.0 wt%, whereas cementum (n=2) had carbonate contents between 6.15 and 8.0wt%. Three samples from the KYP3-46 dataset were

deemed unreliable for interpretation and were excluded from the study. One sample (KYP-3-46-27) yielded unusually low carbonate content and also demonstrated abnormal stable isotopic values deviating from the expected sinusoidal pattern, whereas two samples near the distal end (KYP-46b & KYP-3-46c) had slightly higher carbonate contents and stable isotopic values approximating those of dentine, indicating they may have been contaminated during sampling (See supplementary materials). Finally, all five specimens demonstrate intra-tooth periodicity in *δ*-values, reflecting environmentally induced variation, which, in case of diagenesis and isotopic re-equilibration, is expected to become homogenized. Considering the aforementioned, reliable biological origin of the measured isotopic signal can be inferred.

Sequential sampling of individual specimens can yield several months to years of isotopic data, that reflect ecological and environmental shifts during the time of enamel formation and mineralization. On a local scale, the amplitude of short-term variations in isotopic data series is usually interpreted as a reflection of the degree of seasonality and environmental instability. However, we note that the data discussed here are unlikely to accurately represent the amplitude of seasonal environmental variation. Attenuation occurs due to enamel maturation, mineralization, and physiological processes (Kohn, 1996; Passey & Cerling, 2002; Uno et al., 2020; Zazzo et al., 2005). In general, conventional sampling of tooth enamel in ever-growing and hypsodont teeth incorporates enamel increments formed during different seasons within one sample, resulting in isotopic averaging. A mathematical correction of isotopic attenuation using inverse modelling has been previously employed to obtain estimates of the primary isotopic signal from *Hippopotamus* canines (Harris et al., 2008; Passey, Cerling, et al., 2005). However, recent evidence suggests higher complexity in canine growth and enamel extension rates for *H. amphibius* (Souron et al., 2024), leading to difficulties in obtaining a reliable estimation of the primary input signal through this technique. Therefore, in this study, we refrained from the application of such techniques to correct for isotopic averaging, until the parameters of hippopotamid enamel formation and mineralization are further refined. Despite that, studies have shown that sequential enamel sampling of hippopotamus teeth can be a reliable proxy for ecological and climatic changes, albeit qualitatively rather than quantitatively.

5.2 Marathousa 1

Median carbon isotope values closer to the cut-off $\delta^{13}C_{1750}$ between woodland/mesic grassland and open woodland/xeric grassland conditions suggest that the MAR-1B-8 individual partly foraged in a drier and more open habitat in comparison to the other sampled *Hippopotamus* individuals. Warmer and drier, more sparsely vegetated conditions at Marathousa 1 during the deposition of stratigraphic unit UB2 have also been inferred by the abundance of Chloridoids, short grasses growing in open and warm grasslands (Field et al., 2018), as well as from the stable isotopic study of leaf waxes(Butiseacă et al., 2024) and the study of pollen (Kyrikou et

al., in press). Despite yielding the highest $\delta^{13}C$ values in our sample, the MAR-1B-8 molar exhibited intermediate oxygen isotopic values, close to those of the broadly contemporaneous MAR-2B-2. A multi-proxy shoreline level reconstruction suggested that hydrological conditions in Unit UB2b, where the MAR-1 hippopotamus molar was deposited, were shifting from the presence of seasonal ponds to a "*swamp-like environment reflecting permanent stagnatic anoxic water body*" and overall drier climatic conditions (Bludau et al., 2021). This would be consistent with the more positive carbon isotope values observed in this individual, reflecting a drier landscape with more open vegetation. The absence of particularly high $\delta^{18}O$ values from this tooth, that would suggest significantly warmer or drier climatic conditions compared to the other sites, especially Marathousa 2, could be explained by meltwater influx from surrounding melting glaciers, as hypothesized by Bludau et al. (2021). Meltwater influx would result in the transport of isotopically depleted water, leading to a depletion in the $\delta^{18}O$ of the source water. Additional support to these conditions stems from the sedimentological study revealing a very shallow lake environment with the contribution of high energy fluviatile flows, possibly associated with the gradual transition from glacial to interglacial conditions (Karkanas et al., 2018). The comparatively low magnitude of variation in $\delta^{18}O$ (1.8‰) could also be related to isotopic mixing of non-local water or meltwater within the water pool, or to significant isotopic averaging due to enamel formation and maturation in comparison to the two sampled canines and the incisor. Either way, the carbon isotope profile exhibits considerably greater variability, which could indicate that this individual foraged on different plant resources or different microhabitats during the time of tooth formation. These observations favor a scenario of masked hydrological variability in conjunction with environmental heterogeneity.

5.3 Marathousa 2

The significant correlation of the $\delta^{13}C$ and $\delta^{18}O$ data from the MAR-2B-2 upper canine, as well as the relatively regular fluctuation in the carbon isotope profile could indicate a seasonally adaptive diet, if we consider an average growth rate of ~15–20 mm/year (Fidalgo, Rosas, Bartolini-Lucenti, et al., 2023; Uno et al., 2013). Three scenarios could explain the inverse correlation between $\delta^{13}C$ and $\delta^{18}O$ in this individual's intra-tooth profiles:

a) A seasonal feeding strategy with the incorporation of different plant tissues between seasons. New plant growth in C_3 vascular plants has higher $\delta^{13}C$ values than mature plant parts (Vogado et al., 2020; Wang et al., 2017; Werth et al., 2015). The possible incorporation of C_3 grasses with a winter/spring growth season would result in the consumption of new plant growth with higher $\delta^{13}C$ during the cooler months. On the other hand, if new growth was limited during the summer, the MAR-2B-2 hippopotamus would continue to feed on mature and dried-out plant matter available in its surroundings, thus resulting in lower $\delta^{13}C$.

b) A seasonal contribution of high-altitude water or snow meltwater runoff into the basin's water reservoirs, which could result in lower $\delta^{18}O_{water}$ during spring/summer and higher water $\delta^{18}O$ values in fall/winter (Rank et al., 2018; Rodhe, 1998). Such effects are more likely to be observed in smaller water bodies, as inferred for MAR-2 (Konidaris et al., 2023; Papadopoulou et al., in press; Boni et al., in press), which are not significantly impacted by isotopic mixing of seasonal signals.

c) The inverse correlation is not driven by sub-annual trends but by a supra-annual pattern with increased $\delta^{18}O$ corresponding to decreased $\delta^{13}C$ during the earlier tooth forming phase and a shift to the opposite trend from the middle of the profile (at ~160 mm) to the proximal end. An abrupt increase in $\delta^{18}O$ coinciding with a sharp decrease in $\delta^{13}C$ is seen at the proximal end of the canine.

Seasonal fluctuations are certainly visible in the carbon isotope profile, especially during the earlier phase of tooth formation; however, a visual examination of the correspondence between peaks and troughs in the isotopic series suggests that the third scenario, supporting a supra-annual ecological change as the main reason behind the inverse correlation, is more likely. A possible explanation for the shifts observed in both $\delta^{13}C$ and $\delta^{18}O$ values is the relocation of the MAR-2 hippopotamus to a different micro-habitat and the utilization of an isotopically different water body. Fluctuations in $\delta^{18}O$ appear more prominent in the proximal half of the canine (amplitude 2.5‰) compared to the distal half (amplitude 1.2‰) and could be consistent with a transition from a deeper, stagnant water body, which was isotopically averaged due to longer water residence time, to a shallower one that better reflected seasonal variations. Alternatively, a climate-induced change in the flooding/hydrological regime or changes in water flow could be responsible for the pattern and could have further influenced the composition of the plant community and the $\delta^{13}C$ values of plants (e.g., Liljedahl et al., 2020). In addition, long-resident water bodies are subjected to evaporative enrichment (Pederzani & Britton, 2019), which would further explain the higher $\delta^{18}O$ in the distal half of the profile. In this interpretive scheme, an alternative explanation for the rising trend in $\delta^{13}C$ could be the onset of a drought, as plant $\delta^{13}C$ values in temperate and Mediterranean systems seem to correlate positively with rainfall (Hartman & Danin, 2010). Whether this shift is indicative of a relocation or a gradual climatic transition leading to changes in hydrological conditions, *i.e.,* a possible drought-related reduction of water volume, remains to be further investigated. Preliminary analysis of the malacofauna from the stratigraphic context of MAR-2B-2 (unit UB6), shows stressful conditions for the freshwater mollusks, further indicating the presence of a relatively small water body at Marathousa 2 and, possibly, dry conditions (Konidaris et al., 2023).

5.4 Kyparissia 3

More densely forested conditions are suggested for the *H. antiquus* from KYP-3 in comparison to all other sites based on the lower median $\delta^{13}C_{enamel}$. The $\delta^{13}C$ isotopic profile suggests two significant changes in the specimen's diet —one at the beginning and one at the end of the profile —, both associated with climatic or hydrological shifts (Figure 3A). The KY3-46 lower canine also shows enamel defects, attributed to linear enamel hypoplasia (LEH) (Figure 5). The hypoplastic defects are not particularly severe. The pathology is observed at ~269, 187 and 173 mm from the proximal end, corresponding to samples KYP-3-46r, KYP-3-46O, and KYP-3-46T respectively. At least two more linear defects are visible between 40 and 80 mm from the proximal end, but no enamel samples were obtained from that area due to fragmentation near the enamel-dentine arch (Figure 1C). Increased incidence of dental enamel hypoplasia has been recently identified in several European Early Pleistocene *Hippopotamus antiquus* specimens and was correlated to nutritional or environmental stress due to increased seasonality (Fidalgo, Rosas, Bartolini-Lucenti, et al., 2023). The concurrence of LEH with the onset of depleting $\delta^{18}O$ values, which also correspond to lower $\delta^{13}C$, suggests that climatic cooling might have been the dominant factor for physiological stress. Considering a growth rate between 30–40 mm per year for the lower canine, it seems plausible that the isotopic fluctuations represent annual cycles, with the LEH corresponding to the onset of winter. Nonetheless, cooler and more humid conditions likely persisted for a significant part of the KYP-3 hippopotamus' life, based on both carbon and oxygen isotopic profiles of the lower canine.

5.5 Kyparissia 4

The low median $\delta^{18}O$ of the KYP4A-1004 molar indicates a colder and/or more humid climate or cooler hydrological conditions at KYP-4 in comparison to both MAR-1 and MAR-2, which have been associated with the glacial MIS 12, as well as compared to KYP-3 and KYP-T (Figure 2). Interpretations of the intra-tooth series from this sample to infer differences in the degree of seasonality are perhaps more meaningful in comparison to the MAR-1 molar, considering differential enamel growth patterns between molars and tusks. Variability in $\delta^{18}O$ was also relatively low for the majority of this profile, suggesting a similar degree of seasonality to MAR-1. These results are in agreement with the study of ostracods, pointing to the presence of cold (<15°C) carbonate springs at the site and a humid climate with stable temperatures throughout the year (Papadopoulou et al., in press). However, a sharp increase in oxygen isotope values is noted towards the EDJ and could be indicative of a short-term change in environmental conditions or habitat use. The large mammal fauna from KYP-4, although largely similar in composition to MAR-1, includes some taxa with a preference for more open habitats, such as the extinct giant deer *Praemegaceros verticornis*, rhinoceroses, and horses (Athanassiou, 2018; Athanassiou et al., in press; Konidaris et al., under review), which has led

to hypothesize that slightly more open conditions could have prevailed at KYP-4 in comparison to MAR-1 (Konidaris et al., under review); however, the *H. antiquus* enamel isotopic composition from the two sites indicates the opposite, at least in comparison to the MAR-1 hippopotamus-bearing stratigraphic unit (UB2b). The presence of woodland and forested habitats around the KYP-4 water source is also inferred by the presence of mostly forest-dwelling faunal taxa, such as *Vulpes, Ursus*, and *Macaca* (Athanassiou et al. in press; Konidaris et al., under review). A larger isotopic sample with the inclusion of additional species from both localities may provide further clarification, as the possibility of niche partitioning between *H. antiquus* and the aforementioned taxa cannot be excluded.

5.6 Kyparissia T

Specimen KYPT-842 yielded the highest oxygen isotope values in our sample. The oxygen isotopic composition of this individual could be consistent with a warmer or drier phase. The stratigraphic proximity of the KYP-T *Hippopotamus* skeletal accumulation to a lignite layer (Athanassiou et al. 2018; Fig. 2), which is considered to represent warmer (interglacial/interstadial) conditions (Okuda et al., 2002; Siavalas et al., 2009) further corroborates this observation. The KYPT-842 incisor demonstrated low-amplitude (1.1‰) but consistent cyclical variations in $\delta^{18}O$, possibly suggesting weaker seasonality in comparison to the rest of the specimens. Despite a lack of significant correlations between the oxygen and carbon isotope records of KYPT-842, variability in the $\delta^{13}C$ values is pronounced and partly suggests dietary changes in a tentatively stable climatic or hydrological environment. Mild dental enamel hypoplasia is also present on this specimen, occurring every ~9 mm. In this case, the enamel defects —in the form of grooves— are more difficult to associate with specific samples. However, a tentative visual correlation to samples corresponding to $\delta^{18}O$ troughs implies sensitivity to lower temperatures, similarly to what was observed for KYP3-46. A temporal lag in the expression of dietary shifts in enamel bioapatite is possible and could explain the lack of a significant correlations between $\delta^{18}O$ and $\delta^{13}C$ fluctuations, a phenomenon which has also been observed in other taxa, including suids (Yang et al., 2024) and horses (de Winter et al., 2016).

5.7 Hippopotamus antiquus ecology in the Megalopolis basin: a case study in early/mid- Middle Pleistocene resilience

The range of $\delta^{13}C$ values in all five hippopotami demonstrates the dominance of a C_3 woodland/mesic grassland foraging habitat throughout the Middle Pleistocene in the Megalopolis Basin and a diet consisting of terrestrial C_3 vegetation or freshwater macrophytes. Overall, the three individuals from the early Middle Pleistocene sites (KYP-3, 4, KYPT) within the Kyparissia mine likely foraged in more closed or humid habitats compared to those of the mid-Middle Pleistocene *Hippopotamus* (MAR-1, 2) found in the Marathousa mine. Recent

studies on the broader climatic conditions in the Mediterranean during the early Middle Pleistocene, and particularly between MIS 19–17, show increased moisture and precipitation, even during the glacial MIS 18, which supported the maintenance of forested habitats after 800ka (Sánchez Goñi et al., 2023; Strani et al., 2019); These conditions are likely reflected in the isotopic record of the KYP-4 *Hippopotamus*. In contrast, drier and more open landscapes are inferred from ~600ka onwards (Strani, 2021; Strani et al., 2019; Zanazzi et al., 2022), as well as more extreme glacial maxima (Blain et al., 2018) accompanied by a turnover in vegetation communities (Tzedakis et al., 2006). The MIS 12 glacial, represented in our sample by the MAR-1 and MAR-2 individuals, although similar to MIS 16 —the latter possibly reflected in the KYP3-46 record— in ice volume and expansion, was more severe and long-lasting than both MIS 16 and MIS 18 (Martínez-Dios et al., 2021) and recorded the most extreme tree population contraction (Tzedakis et al., 2006). Until now, no other enamel isotopic data beyond our study exists for *Hippopotamus antiquus* to allow for inter-regional and wider inter-temporal comparisons beyond the Megalopolis Basin. However, a recent stable isotope study of *H. amphibius* from the interglacial layers (MIS 7) of Casal de' Pazzi in Italy presented bulk oxygen isotope values largely overlapping with those observed in our dataset (+21.3–+23.2‰ VSMOW) but overall lower carbon isotope values (−13.7–−15.8‰ VPDB) (Briatico et al., 2023) than most of the specimens analyzed in this study, with the exception of KYP3-46, suggesting more open and arid habitats for the Middle Pleistocene *H. antiquus* in the Megalopolis basin.

The co-varying fluctuations in carbon and oxygen intra-tooth isotope series of the MAR-2-2B and KYP3-46 tusks, as well as the KYP4A-1004 molar, suggest a correlation between diet and climate. Seasonal variations in the diet of the extant *H. amphibius,* with the inclusion of more C_4 vegetation during the dry season and more C_3 plants during the wet season have been observed (Scotcher & Breen, 1978; Souron et al., 2012) and attributed to the nutritional value and palatability of the plants (Scotcher & Breen, 1978). In the Megalopolis Basin, C_4 vegetation is absent (or rare, see Butiseaca et al. in press) during the Middle Pleistocene, which is consistent with the values obtained by the specimens analyzed in this study and those reported in Roditi et al. (2024) for the European straight-tusked elephant (*Palaeoloxodon antiquus*) from MAR-1. Within this C_3-dominated ecosystem, the regular fluctuations in the $\delta^{13}C$ diet of hippopotamus could partly reflect intrinsic seasonal variations in terrestrial plant carbon values, whose magnitude can reach up to 1–2‰, seasonal contributions of browse, stems, roots or fruits, which are expected to differ in $\delta^{13}C$ from C_3 grasses and herbaceous vegetation (Metcalfe, 2021), or a combination of both. Alternatively, this pattern could be attributed to the consumption of freshwater aquatic macrophytes, which are characterized by increased sensitivity to a combination of parameters, including water pH, dissolved inorganic carbon (DIC) in the water column, and temperature. Shifting dietary contributions between terrestrial and aquatic vegetation in extant hippopotamus have been observed during shortages of

terrestrial forage (Field, 1970; Inman, 2020; Mugangu & Hunter, 1992) but also in relation to changing flooding regimes and precipitation, wherein during the dry season the aquatic feeding increased (Inman, 2020). While this hypothesis is difficult to address with the approach employed in this study due to the overlapping $\delta^{13}C$ values of terrestrial and freshwater vegetation, increased aquatic foraging compared to the extant hippopotamus has already been proposed for *H. antiquus* (Palmqvist et al., 2003; Palmqvist et al., 2022). Nonetheless, the persistence of the examined individuals demonstrating increased dietary variability through the years in the Megalopolis Basin indicates that significant resource diversity accommodated their survival.

Oxygen isotopes from hippopotamus teeth seem to consistently under-represent environmental isotopic variation (Chritz, 2015; Green et al., 2023; Lüdecke et al., 2022; Souron et al., 2012; Uno & Bibi, 2022). The dampening of environmentally driven variation in $\delta^{18}O_{body\ water}$ may be partly related to the physiology of the taxon, its thermoregulatory strategies (Fernandez et al., 2020; Noirard et al., 2008), as well as differential tooth enamel formation (Passey, Cerling, et al., 2005; Souron et al., 2024). A previous study by Souron et al. (2012) estimated the magnitude of seasonal signal attenuation between extant hippopotamus canines and river water to be over 60%. Hence, we caution that the values presented here should be considered as minimum solutions. Nonetheless, seasonal cyclicity in hippopotamus $\delta^{18}O_{enamel}$ has been previously reported (Chritz, 2015; Chritz et al., 2016; Souron et al., 2012; Souron et al., 2024) and is also recognized in this study.

An increasing body of research reports both physiological and ecological responses of the extant *Hippopotamus amphibious* to seasonal cyclicity of climate and resources, as well as increased sensitivity to larger scale climatic events (Chritz, 2015; Chritz et al., 2016; Souron et al., 2012; Souron et al., 2024; Uno et al., 2013). Environmental vulnerability likely also characterized the extinct *Hippopotamus antiquus*, as revealed by this and other (e.g., Fidalgo, Rosas, Bartolini-Lucenti, et al., 2023) studies. Temporal changes —sub-annual, annual, or multi-annual— in water availability and hydrological conditions, such as those manifested in our dataset, may have had substantial effects in hippopotamus distribution and mortality. The amphibious lifestyle and its dependency on nearby water-sources restricts the species' range for feeding trips, making it more susceptible to nutritional and physiological stress, in comparison to other taxa that can adapt behaviorally to fluctuating resource availability by moving to more favorable and productive habitats (e.g., Britton et al., 2009; Heddell-Stevens et al., 2024; Kowalik et al., 2018; Marín-Leyva et al., 2021). The presence of enamel hypoplasia on two of the specimens, associated with the onset of lower $\delta^{18}O$ values, as well as with dietary changes, is an indication that colder conditions had a profound effect on the species'

subsistence strategies. In addition to the apparent behavioral influence, physiological responses to colder and harsher climatic conditions could also explain the smaller dimensions of *H. antiquus* from the Megalopolis Basin (Konidaris et al., under review, Mazza & Bertini, 2013). Behavioral changes have been observed in response to lower temperatures also in the extant *H. amphibius* (Fernandez et al., 2020; Noirard et al., 2008). In addition, the higher incidence of LEH in two of the three early Middle Pleistocene individuals, implying physiological or nutritional stress during the adverse season, conforms to observations from other Mediterranean regions pointing to dietary diversification of grazing taxa after 900ka, as a response to increased seasonality (Strani et al., 2019).

This evidence highlights that even within a putative microrefugium such as the Megalopolis Basin, in which the effects of climate on resource availability are considered to be minimized, a high degree of adaptability was still necessary to survive in these dynamic habitats, that frequently underwent changes in plant communities and hydrological regimes. The case of *H. antiquus* adaptability in the face of environmental fluctuations in Middle Pleistocene Greece provides a valuable basis for unraveling hominin adaptations as well. The continuous presence and persistence of hominin populations in a spatially and temporally heterogenous and fluctuating environment points to a significant degree of adaptability, which also manifested in behavioral adaptations and technological innovations (Hardy et al., 2018; Moncel et al., 2018; Moncel et al., 2020; Ollé et al., 2023; Sánchez-Bandera et al., 2023). The examination of hominin subsistence and technological aspects from the long stratigraphic sequence of the Megalopolis Basin within the growing paleoenvironmental record of the region will further our knowledge of local adaptations.

6.Conclusions

In this study, we employed stable carbon and oxygen isotope analysis on enamel bioapatite of five *H. antiquus* specimens from the Megalopolis Basin in Greece and presented the first intra-tooth isotopic reconstruction for the extinct *Hipppotamus antiquus*. This technique provided new ecological insights for this taxon, through the investigation of individual ecologies. Our results suggest increased dietary variability for *H. antiquus*, mainly driven by climatic oscillations. The inter-site comparison of the isotopic data allowed the evaluation of past environments in the basin from ~700 to 430 ka and revealed fluctuating hydrological conditions and possible changes in vegetation, especially between the early- and mid-Middle Pleistocene, including periods during which conditions were likely less favorable for the subsistence of *H. antiquus*. Seasonality was observed in continuously growing canines and incisors, which represent the infra-annual scale more reliably. Additionally, we demonstrated that environmental sensitivity also characterized the extinct *H. antiquus*, similarly to what has been observed in its extant counterpart. Overall, our results promote the existence of dynamic

environments in the Megalopolis Basin during glacial periods, which nevertheless offered a diversity of resources to allow for the survival of both resilient (e.g., *Palaeoloxodon antiquus*, Roditi et al., 2024; Konidaris et al., 2024) and more vulnerable taxa, like the *Hippopotamus.*

Nonetheless, the palaeoecological reconstruction of *H. antiquus* will greatly benefit from the application of complementary analyses, such as dental microwear (currently underway), and the construction of an isotopic baseline to aid interpretations of enamel stable isotopes. Multidisciplinary research, including approaches such as those employed for MAR-1 (e.g., shoreline reconstruction, palynological analysis, and plant biomarkers) can prove particularly useful to set the hydrological and vegetative basis for comparison with mammalian isotopic data. Methodological progress in the field of stable isotope ecology has been immense and the possibilities to accurately reconstruct past environmental conditions and extinct species ecologies have increased. With upcoming studies expected to further decipher enamel formation and isotopic fractionation of *Hippopotamus* teeth (Green et al., 2023; Souron et al., 2024), and the in-progress application of additional techniques, including the preparation of a baseline for both vegetation and hydrology at the studied sites, the data presented here may be further refined in the future to reconstruct more precisely the ecological niche of the extinct *H. antiquus* in the Megalopolis Basin.

Acknowledgements

We are grateful to Ruth Rey (Department of Geosciences, University of Tübingen) and Peter Tung (Senckenberg HEP, University of Tübingen) for their technical and scientific support in sample preparation and isotopic analyses. Excavation at Marathousa 1 was conducted under a permit granted to the Ephoreia of Palaeoanthropology-Speleology, Hellenic Ministry of Culture. This research was funded by the European Research Council (ERC-StG-283503 and ERC-CoG-724703, awarded to K. Harvati). Megalopolis Palaeoenvironmental Project (MEGAPAL) is a collaboration between the Ephoreia of Palaeoanthropology-Speleology and the American School of Classical Studies at Athens, under the direction of Dr. Panagopoulou, Dr. Karkanas and Prof. Dr. Harvati and funded by the European Research Council (CoG 724703). K.H., G.E.K., V.T., and E.R. were also supported by the DFG Project no. 463225251 ("MEGALOPOLIS"). E.R. and K.H. are also supported by ERC-AdG-101019659.

References

Adams, N. F., Candy, I., & Schreve, D. C. (2022). An Early Pleistocene hippopotamus from Westbury Cave, Somerset, England: support for a previously unrecognized temperate interval in the British Quaternary record. *Journal of Quaternary Science*, *37*(1), 28-41.

Athanassiou, A. (2018). Pleistocene vertebrates from the Kyparíssia lignite mine, Megalopolis Basin, S. Greece: Rodentia, Carnivora, Proboscidea, Perissodactyla, Ruminantia. *Quaternary International*, *497*, 198-221. https://doi.org/https://doi.org/10.1016/j.quaint.2018.06.042

Athanassiou, A. (2022). The fossil record of continental hippopotamids (Mammalia: Artiodactyla: Hippopotamidae) in Greece. *Fossil Vertebrates of Greece Vol. 2: Laurasiatherians, Artiodactyles, Perissodactyles, Carnivorans, and Island Endemics*, 281-299.

Athanassiou, A., Konidaris, G. E., Tourloukis, V., Thompson, N., Giusti, D., Panagopoulou, E., Karkanas, P., & Harvati, K. (in press). The Middle Pleistocene large mammal fauna from Kyparissia (Peloponnese, S. Greece): New collected material. In K., Harvati, M., Ioannidou, Eds.; *Human Evolution at the CROSSROADS: Research in Greece and beyond,* Tübingen University Press: Tübingen.

Athanassiou, A., Michailidis, D., Vlachos, E., Tourloukis, V., Thompson, N., & Harvati, K. (2018). Pleistocene vertebrates from the Kyparíssia lignite mine, Megalopolis Basin, S. Greece: Testudines, Aves, Suiformes. *Quaternary International*, *497*, 178–197. https://doi.org/https://doi.org/10.1016/j.quaint.2018.06.030

Balasse, M. (2002). Reconstructing dietary and environmental history from enamel isotopic analysis: time resolution of intra-tooth sequential sampling. *International Journal of Osteoarchaeology*, *12*(3), 155–165. https://doi.org/https://doi.org/10.1002/oa.601

Balasse, M. (2003). Potential biases in sampling design and interpretation of intra-tooth isotope analysis. *International Journal of Osteoarchaeology*, *13*(1-2), 3–10. https://doi.org/https://doi.org/10.1002/oa.656

Basu, S., Ghosh, S., & Chattopadhyay, D. (2021). Disentangling the abiotic versus biotic controls on C_3 plant leaf carbon isotopes: Inferences from a global review. *Earth-Science Reviews*, *222*, 103839. https://doi.org/https://doi.org/10.1016/j.earscirev.2021.103839

Bender, M. M. (1971). Variations in the $^{13}C/^{12}C$ ratios of plants in relation to the pathway of photosynthetic carbon dioxide fixation. *Phytochemistry*, *10*(6), 1239–1244. https://doi.org/https://doi.org/10.1016/S0031-9422(00)84324-1

Berends, C., Köhler, P., Lourens, L., & Van de Wal, R. (2021). On the cause of the Mid-Pleistocene transition. In: Wiley Online Library.

Blackwell, B. A., Sakhrani, N., Singh, I. K., Gopalkrishna, K. K., Tourloukis, V., Panagopoulou, E., Karkanas, P., Blickstein, J. I., Skinner, A. R., & Florentin, J. A. (2018). ESR dating ungulate teeth and molluscs from the Paleolithic site Marathousa 1, Megalopolis Basin, Greece. *Quaternary*, *1*(3), 22.

Blain, H.-A., Cruz Silva, J. A., Jiménez Arenas, J. M., Margari, V., & Roucoux, K. (2018). Towards a Middle Pleistocene terrestrial climate reconstruction based on herpetofaunal assemblages from the Iberian Peninsula: State of the art and perspectives. *Quaternary Science Reviews*, *191*, 167-188. https://doi.org/https://doi.org/10.1016/j.quascirev.2018.04.019

Bludau, I. J., Papadopoulou, P., Iliopoulos, G., Weiss, M., Schnabel, E., Thompson, N., Tourloukis, V., Zachow, C., Kyrikou, S., Konidaris, G. E., Karkanas, P., Panagopoulou, E., Harvati, K., & Junginger, A. (2021). Lake-Level Changes and Their Paleo-Climatic Implications at the MIS12 Lower Paleolithic (Middle Pleistocene) Site Marathousa 1, Greece. *Frontiers in Earth Science*, *9*, 441.

Bocherens, H., & Drucker, D. G. (2013). CARBONATE STABLE ISOTOPES | Terrestrial Teeth and Bones. In S. A. Elias & C. J. Mock (Eds.), *Encyclopedia of Quaternary Science (Second Edition)* (pp. 304–314). Elsevier. https://doi.org/https://doi.org/10.1016/B978-0-444-53643-3.00341-1

Bocherens, H., Fizet, M., & Mariotti, A. (1994). Diet, physiology and ecology of fossil mammals as inferred from stable carbon and nitrogen isotope biogeochemistry: implications for Pleistocene bears. *Palaeogeography, Palaeoclimatology, Palaeoecology*, *107*(3-4), 213–225.

Bocherens, H., Koch, P. L., Mariotti, A., Geraads, D., & Jaeger, J.-J. (1996). Isotopic biogeochemistry (^{13}C, ^{18}O) of mammalian enamel from African Pleistocene hominid sites. *Palaios*, 306–318.

Bond, A. L., & Hobson, K. A. (2012). Reporting Stable-Isotope Ratios in Ecology: Recommended Terminology, Guidelines and Best Practices. *Waterbirds*, *35*(2), 324–331. https://doi.org/10.1675/063.035.0213

Boni, G., Syrides, G., Konidaris, G.E., Athanassiou, A., Tourloukis, V., Koukousioura, O., Panagopoulou, E., Karkanas, P., Harvati, K., Preliminary results on the taxonomy and palaeoenvironmental analysis of the mollusc fauna from Marathousa 1, Marathousa 2 and Kyparissia 4 (Middle Pleistocene, Megalopolis Basin, Greece). In K., Harvati, M., Ioannidou, Eds.; *Human Evolution at the CROSSROADS: Research in Greece and beyond,* Tübingen University Press: Tübingen.

Briatico, G., Gioia, P., & Bocherens, H. (2023). Diet and habitat of the late Middle Pleistocene mammals from the Casal de' Pazzi site (Rome, Italy) using stable carbon and oxygen isotope ratios. *Quaternary International*, *676*, 53-62. https://doi.org/https://doi.org/10.1016/j.quaint.2023.11.002

Britton, K. (2020). Isotope Analysis for Mobility and Climate Studies. In K. Britton & M. P. Richards (Eds.), *Archaeological Science: An Introduction* (pp. 99–124). Cambridge University Press. https://doi.org/DOI: 10.1017/9781139013826.005

Britton, K., Grimes, V., Dau, J., & Richards, M. P. (2009). Reconstructing faunal migrations using intra-tooth sampling and strontium and oxygen isotope analyses: a case study of modern caribou (*Rangifer tarandus granti*). *Journal of Archaeological Science*, *36*(5), 1163–1172.

Bryant, J. D., & Froelich, P. N. (1995). A model of oxygen isotope fractionation in body water of large mammals. *Geochimica et Cosmochimica Acta*, *59*(21), 4523–4537.

Butiseacă, G. A., Vasiliev, I., van der Meer, M. T. J., Bludau, I. J. E., Karkanas, P., Tourloukis, V., Junginger, A., Mulch, A., Panagopoulou, E., & Harvati, K. (2024). The expression of the MIS 12 glacial stage in Southeastern Europe and its impact over the Middle Pleistocene hominins in Megalopolis Basin (Greece). *Global and Planetary Change*, *242*, 104585. https://doi.org/https://doi.org/10.1016/j.gloplacha.2024.104585

Cerling, T. E., Bernasconi, S. M., Hofstetter, L. S., Jaggi, M., Wyss, F., Rudolf von Rohr, C., & Clauss, M. (2021). CH_4/CO_2 ratios and carbon isotope enrichment between diet and breath in herbivorous mammals. *Frontiers in Ecology and Evolution*, *9*, 638568.

Cerling, T. E., & Harris, J. M. (1999). Carbon isotope fractionation between diet and bioapatite in ungulate mammals and implications for ecological and paleoecological studies. *Oecologia*, *120*(3), 347–363. https://doi.org/10.1007/s004420050868

Chappuis, E., Seriñá, V., Martí, E., Ballesteros, E., & Gacia, E. (2017). Decrypting stable-isotope ($\delta^{13}C$ and $\delta^{15}N$) variability in aquatic plants. *Freshwater Biology*, *62*(11), 1807-1818.

Chritz, K. L. (2015). *Isotopic records of ecological variability in modern and ancient environments in Kenya*. The University of Utah.

Chritz, K. L., Blumenthal, S. A., Cerling, T. E., & Klingel, H. (2016). Hippopotamus (*H. amphibius*) diet change indicates herbaceous plant encroachment following megaherbivore population collapse. *Scientific Reports*, *6*(1), 32807.

Clark, P. U., Archer, D., Pollard, D., Blum, J. D., Rial, J. A., Brovkin, V., Mix, A. C., Pisias, N. G., & Roy, M. (2006). The middle Pleistocene transition: characteristics, mechanisms, and implications for long-term changes in atmospheric pCO2. *Quaternary Science Reviews*, *25*(23-24), 3150-3184.

Clementz, M. T., Holroyd, P. A., & Koch, P. L. (2008). Identifying aquatic habits of herbivorous mammals through stable isotope analysis. *Palaios*, *23*(9), 574-585.

Clementz, M. T., & Koch, P. L. (2001). Differentiating aquatic mammal habitat and foraging ecology with stable isotopes in tooth enamel. *Oecologia*, *129*(3), 461–472.

Cloern, J. E., Canuel, E. A., & Harris, D. (2002). Stable carbon and nitrogen isotope composition of aquatic and terrestrial plants of the San Francisco Bay estuarine system. *Limnology and Oceanography*, *47*(3), 713–729.

de Winter, N. J., Snoeck, C., & Claeys, P. (2016). Seasonal Cyclicity in Trace Elements and Stable Isotopes of Modern Horse Enamel. *PLOS ONE*, *11*(11), e0166678. https://doi.org/10.1371/journal.pone.0166678

Domingo, L., Koch, P. L., Hernández Fernández, M., Fox, D. L., Domingo, M. S., & Alberdi, M. T. (2013). Late Neogene and Early Quaternary Paleoenvironmental and Paleoclimatic Conditions in Southwestern Europe: Isotopic Analyses on Mammalian Taxa. *PLOS ONE*, *8*(5), e63739. https://doi.org/10.1371/journal.pone.0063739

Doukas, C., van Kolfschoten, T., Papayianni, K., Panagopoulou, E., & Harvati, K. (2018). The small mammal fauna from the Palaeolithic site Marathousa 1 (Greece). *Quaternary International*, *497*, 95–107.

Drucker, D. G., Bridault, A., Hobson, K. A., Szuma, E., & Bocherens, H. (2008). Can carbon-13 in large herbivores reflect the canopy effect in temperate and boreal ecosystems? Evidence from modern and ancient ungulates. *Palaeogeography, Palaeoclimatology, Palaeoecology*, *266*(1), 69–82. https://doi.org/https://doi.org/10.1016/j.palaeo.2008.03.020

Farquhar, G. D., Ehleringer, J. R., & Hubick, K. T. (1989). Carbon isotope discrimination and photosynthesis. *Annual review of plant biology*, *40*(1), 503–537.

Fernandez, E. J., Ramirez, M., & Hawkes, N. C. (2020). Activity and pool use in relation to temperature and water changes in zoo hippopotamuses (*Hippopotamus amphibious*). *Animals*, *10*(6), 1022. https://www.mdpi.com/2076-2615/10/6/1022

Fidalgo, D., Galli, E., Madurell-Malapeira, J., & Rosas, A. (2021). Earliest Pleistocene European hippos: a review. *Comunicações Geológicas*, *108*, 69–73.

Fidalgo, D., Rosas, A., Bartolini-Lucenti, S., Boisserie, J.-R., Pandolfi, L., Martínez-Navarro, B., Palmqvist, P., Rook, L., & Madurell-Malapeira, J. (2023). Increase on environmental seasonality through the European Early Pleistocene inferred from dental enamel hypoplasia. *Scientific Reports*, *13*(1), 16941.

Fidalgo, D., Rosas, A., Madurell-Malapeira, J., Pineda, A., Huguet, R., García-Tabernero, A., Cáceres, I., Ollé, A., Vallverdú, J., & Saladie, P. (2023). A review on the Pleistocene occurrences and palaeobiology of *Hippopotamus antiquus* based on the record from the Barranc de la Boella Section (Francolí Basin, NE Iberia). *Quaternary Science Reviews*, *307*, 108034.

Field, C. R. (1970). A study of the feeding habits of the hippopotamus (*Hippopotamus amphibius* Linn.) in the Queen Elizabeth National Park, Uganda, With Some Management Implications. *Zoologica Africana*, *5*(1), 71-86. https://doi.org/10.1080/00445096.1970.11447382

Field, M. H., Ntinou, M., Tsartsidou, G., van Berge Henegouwen, D., Risberg, J., Tourloukis, V., Thompson, N., Karkanas, P., Panagopoulou, E., & Harvati, K. (2018). A palaeoenvironmental reconstruction (based on palaeobotanical data and diatoms) of the Middle Pleistocene elephant (*Palaeoloxodon antiquus*) butchery site at Marathousa, Megalopolis, Greece. *Quaternary International*, *497*, 108–122.

Finlay, J. C., & Kendall, C. (2007). Stable isotope tracing of temporal and spatial variability in organic matter sources to freshwater ecosystems. *Stable isotopes in ecology and environmental science*, 283-333.

Giusti, D., Tourloukis, V., Konidaris, G., Thompson, N., Karkanas, P., Panagopoulou, E., & Harvati, K. (2018). Beyond maps: patterns of formation processes at the Middle Pleistocene open-air site of Marathousa 1, Megalopolis Basin, Greece. *Quaternary International*, *497*, 137–153.

Green, D. R., Witzel, C., Colman, A., Kierdorf, H., Smith, T. M., Williams, I. S., Lewis, J. E., Boës, X., Uno, K. T., & Harmand, S. (2023). Hydrological seasonality bracketing the 3.3 Ma LOM3 archaeological site of Lomekwi, Kenya, via fossil hippopotamid oxygen isotope compositions and Bayesian inverse methods. *AGU23*.

Guibert-Cardin, J., Tourloukis, V., Thompson, N., Panagopoulou, E., Harvati, K., Nicoud, E., & Beyries, S. (2022). The function of small tools in Europe during the Middle Pleistocene: The case of Marathousa 1 (Megalopolis, Greece*). Journal of Lithic studies*, 9(1).

Hardy, B. L., Moncel, M.-H., Despriée, J., Courcimault, G., & Voinchet, P. (2018). Middle Pleistocene hominin behavior at the 700ka Acheulean site of la Noira (France). *Quaternary Science Reviews*, *199*, 60-82. https://doi.org/https://doi.org/10.1016/j.quascirev.2018.09.013

Harris, J., Cerling, T., Leakey, M., & Passey, B. (2008). Stable isotope ecology of fossil hippopotamids from the Lake Turkana Basin of East Africa. *Journal of Zoology*, *275*(3), 323-331.

Hartman, G., & Danin, A. (2010). Isotopic values of plants in relation to water availability in the Eastern Mediterranean region. *Oecologia*, *162*, 837–852.

Head, M. J., & Gibbard, P. L. (2015). Early–Middle Pleistocene transitions: linking terrestrial and marine realms. *Quaternary International*, *389*, 7–46.

Heddell-Stevens, P., Jöris, O., Britton, K., Matthies, T., Lucas, M., Scott, E., Le Roux, P., Meller, H., & Roberts, P. (2024). Multi-isotope reconstruction of Late Pleistocene large-herbivore biogeography and mobility patterns in Central Europe. *Communications Biology*, *7*(1), 568.

Iannucci, A., Mecozzi, B., & Sardella, R. (2023). Beware of the "Wolf event"–Remarks on large mammal dispersals in Europe and the late Villafranchian faunal turnover. *Alpine and Mediterranean Quaternary*, *36*(1), 75-90.

Inman, V. (2020). *Population size, distribution, and small-scale seasonal variations in pod dynamics, habitat selection, and behaviour of hippopotamus (Hippopotamus amphibius) in the Okavango Delta, northern Botswana* UNSW Sydney].

Jacobs, Z., Li, B., Karkanas, P., Tourloukis, V., Thompson, N., Panagopoulou, E., & Harvati, K. (2018). Optical dating of K-feldspar grains from Middle Pleistocene lacustrine sediment at Marathousa 1 (Greece). *Quaternary International*, *497*, 170–177. https://doi.org/https://doi.org/10.1016/j.quaint.2018.06.029

Joannin, S. b., Cornée, J.-J., Moissette, P., Suc, J.-P., Koskeridou, E., Lécuyer, C., Buisine, C. d., Kouli, K., & Ferry, S. (2007). Changes in vegetation and marine environments in the eastern Mediterranean (Rhodes, Greece) during the Early and Middle Pleistocene. *Journal of the Geological Society*, *164*(6), 1119–1131.

Julien, M.-A., Bocherens, H., Burke, A., Drucker, D. G., Patou-Mathis, M., Krotova, O., & Péan, S. (2012). Were European steppe bison migratory? ^{18}O, ^{13}C and Sr intra-tooth isotopic variations applied to a palaeoethological reconstruction. *Quaternary International*, *271*, 106–119.

Kahlke, R.D., 2001. Schädelreste von *Hippopotamus* aus dem Unterpleistozän von Untermaßfeld, in: Kahlke, R.D. (Ed.), Das Pleistozän von Untermaßfeld bei Meiningen (Thüringen), Teil 2. Monographien des Römisch-Germanischen Zentralmuseums Mainz, Dr. Rudolf Habelt, Bonn, pp. 483-500.

Kahlke, R.-D., García, N., Kostopoulos, D. S., Lacombat, F., Lister, A. M., Mazza, P. P., Spassov, N., & Titov, V. V. (2011). Western Palaearctic palaeoenvironmental conditions during the Early and

early Middle Pleistocene inferred from large mammal communities, and implications for hominin dispersal in Europe. *Quaternary Science Reviews*, *30*(11-12), 1368–1395.

Karkanas, P., Tourloukis, V., Thompson, N., Giusti, D., Panagopoulou, E., & Harvati, K. (2018). Sedimentology and micromorphology of the Lower Palaeolithic lakeshore site Marathousa 1, Megalopolis basin, Greece. *Quaternary International*, *497*, 123–136.

Karkanas, P., Tourloukis, V., Thompson, N., Giusti, D., Tsartsidou, G., Athanassiou, A., Konidaris, G., Roditi, E., Panagopoulou, E., & Harvati, K. (in press). The Megalopolis Paleoenvironmental Project (MEGAPAL). In K., Harvati, M., Ioannidou, Eds.; *Human Evolution at the CROSSROADS: Research in Greece and beyond,* Tübingen University Press: Tübingen.

Koch, P. L., Tuross, N., & Fogel, M. L. (1997a). The effects of sample treatment and diagenesis on the isotopic integrity of carbonate in biogenic hydroxylapatite. *Journal of Archaeological Science*, *24*(5), 417–429.

Koch, P. L., Tuross, N., & Fogel, M. L. (1997b). The Effects of Sample Treatment and Diagenesis on the Isotopic Integrity of Carbonate in Biogenic Hydroxylapatite. *Journal of Archaeological Science*, *24*(5), 417-429. https://doi.org/https://doi.org/10.1006/jasc.1996.0126

Kohn, M. J. (1996). Predicting animal $\delta^{18}O$: Accounting for diet and physiological adaptation. *Geochimica et Cosmochimica Acta*, *60*(23), 4811–4829. https://doi.org/https://doi.org/10.1016/S0016-7037(96)00240-2

Kohn, M. J. (2010). Carbon isotope compositions of terrestrial C_3 plants as indicators of (paleo)ecology and (paleo)climate. *Proceedings of the National Academy of Sciences*, *107*(46), 19691–19695. https://doi.org/doi:10.1073/pnas.1004933107

Konidaris, G., Tourloukis, V., Boni, G., Athanassiou, A., Giusti, D., Thompson, N., Syrides, G., Panagopoulou, E., Karkanas, P., & Harvati, K. (2023). Marathousa 2: A new Middle Pleistocene locality in the Megalopolis Basin (Greece) with evidence of hominin exploitation of megafauna (*Hippopotamus*). *PaleoAnthropology*, *2023*(1), 34–55.

Konidaris, G. E., Athanassiou, A., Panagopoulou, E., & Harvati, K. (2022). First record of *Macaca* (Cercopithecidae, Primates) in the Middle Pleistocene of Greece. *Journal of Human Evolution*, *162*, 103104. https://doi.org/https://doi.org/10.1016/j.jhevol.2021.103104

Konidaris, G. E., Athanassiou, A., Tourloukis, V., Chitoglou, K., van Kolfschoten, T., Giusti, D., Thompson, N., Tsartsidou, G., Roditi, E., Panagopoulou, E., Karkanas, P., & Harvati, K. (2024). The late Early-Middle Pleistocene mammal fauna from the Megalopolis Basin (Peloponnese, Greece) and its importance for biostratigraphy and palaeoenvironment. *Quaternary*.

Konidaris, G. E., Athanassiou, A., Tourloukis, V., Thompson, N., Giusti, D., Panagopoulou, E., & Harvati, K. (2018). The skeleton of a straight-tusked elephant (*Palaeoloxodon antiquus*) and other large mammals from the Middle Pleistocene butchering locality Marathousa 1 (Megalopolis Basin, Greece): preliminary results. *Quaternary international*, *497*, 65–84.

Konidaris, G. E., & Kostopoulos, D. S. (2024). The Late Pliocene–Middle Pleistocene large mammal Faunal Units of Greece. *Quaternary*, *7*(2), 27.

Kowalik, N., Anczkiewicz, R., Müller, W., Wojtal, P., Wilczyński, J., Bondioli, L., & Spötl, C. (2018, April 01, 2018). *Sr isotope, trace elements and oxygen isotope record in molar enamel as indicator of seasonal wooly mammoth migration in Central Europe* https://ui.adsabs.harvard.edu/abs/2018EGUGA..2016058K

Kyrikou, S., Marinova, E., Bludau, I., Karkanas, P., Panagopoulou, E., Tourloukis, V., Junginger, A., & Harvati, K. (in press). The Middle Pleistocene MIS 12 palynological record from Marathousa palaeolake in Southern Greece: Highlighting favourable conditions in Marathousa 1 refugial region during the severe glacial period. In K. Harvati & M. Ioannidou (Eds.), Human Evolution at the CROSSROADS: Research in Greece and beyond. Tübingen University Press.

Lüdecke, T., Leichliter, J. N., Aldeias, V., Bamford, M. K., Biro, D., Braun, D. R., Capelli, C., Cybulski, J. D., Duprey, N. N., & Ferreira da Silva, M. J. (2022). Carbon, nitrogen, and oxygen stable isotopes in modern tooth enamel: A case study from Gorongosa National Park, central Mozambique. *Frontiers in Ecology and Evolution*, *10*, 958032.

Lee-Thorp, J. A., & Van der Merwe, N. J. (1991). Aspects of the chemistry of modern and fossil biological apatites. *Journal of Archaeological Science*, *18*(3), 343–354.

Levin, N. E., Cerling, T. E., Passey, B. H., Harris, J. M., & Ehleringer, J. R. (2006). A stable isotope aridity index for terrestrial environments. *Proceedings of the National Academy of Sciences*, *103*(30), 11201–11205.

Liljedahl, A. K., Timling, I., Frost, G. V., & Daanen, R. P. (2020). Arctic riparian shrub expansion indicates a shift from streams gaining water to those that lose flow. *Communications Earth & Environment*, 1(1), 50.

Liu, J., Cheng, L., Yao, S., & Xue, B. (2020). Variations in stable carbon isotopes in different components of aquatic macrophytes from Taihu Lake, China. *Ecological Indicators*, *118*, 106721. https://doi.org/https://doi.org/10.1016/j.ecolind.2020.106721

Longinelli, A. (1984). Oxygen isotopes in mammal bone phosphate: a new tool for paleohydrological and paleoclimatological research? *Geochimica et cosmochimica Acta*, *48*(2), 385–390.

Madurell-Malapeira, J., Ros-Montoya, S., Espigares, M., Alba, D. M., & Aurell-Garrido, J. (2014). Villafranchian large mammals from the Iberian Peninsula: paleobiogeography, paleoecology and dispersal events. *Journal of Iberian Geology*, *40*(1), 167–178.

Marín-Leyva, A. H., Schaaf, P., Solís-Pichardo, G., Hernández-Treviño, T., García-Zepeda, M. L., Ponce-Saavedra, J., Arroyo-Cabrales, J., & Alberdi, M. T. (2021). Tracking origin, home range, and mobility of Late Pleistocene fossil horses from west-central Mexico. *Journal of South American Earth Sciences*, *105*, 102926. https://doi.org/https://doi.org/10.1016/j.jsames.2020.102926

Martínez-Dios, A., Pelejero, C., Cobacho, S., Movilla, J., Dinarès-Turell, J., & Calvo, E. (2021). A 1-Million-Year Record of Environmental Change in the Central Mediterranean Sea from Organic Molecular Proxies. *Paleoceanography and Paleoclimatology*, *36*(10), e2021PA004289. https://doi.org/https://doi.org/10.1029/2021PA004289

Martínez-Navarro, B., Madurell-Malapeira, J., Ros-Montoya, S., Espigares, M.-P., Medin, T., Hortola, P., & Palmqvist, P. (2015). The Epivillafranchian and the arrival of pigs into Europe. *Quaternary International*, *389*, 131–138.

Martino, R., & Pandolfi, L. (2022). The Quaternary *Hippopotamus* records from Italy. *Historical Biology*, *34*(7), 1146-1156.

Martino, R., Ríos, M. I., Mateus, O., & Pandolfi, L. (2023). Taxonomy, chronology, and dispersal patterns of Western European Quaternary hippopotamuses: New insight from Portuguese fossil material. *Quaternary International*, *674*, 121–137.

Mazza, P.P. & Bertini, A. (2013). Were Pleistocene hippopotamuses exposed to climate-driven body size changes?. *Boreas*, *42*(1), 194–209.

Melentis, J. (1965). Über *Hippopotamus antiquus* DESMAREST aus dem Mittelpleistozän des Beckens von Megalopolis in Peloponnes (Griechenland). *Ann. Géol. Pays Hellén*, *16*, 403–435.

Metcalfe, J. Z. (2021). C_3 plant isotopic variability in a boreal mixed woodland: implications for bison and other herbivores. *PeerJ*, *9*, e12167–e12167. https://doi.org/10.7717/peerj.12167

Moncel, M.-H., Landais, A., Lebreton, V., Combourieu-Nebout, N., Nomade, S., & Bazin, L. (2018). Linking environmental changes with human occupations between 900 and 400 ka in Western Europe. *Quaternary International*, *480*, 78–94. https://doi.org/10.1016/j.quaint.2016.09.065

Moncel, M.-H., Santagata, C., Pereira, A., Nomade, S., Voinchet, P., Bahain, J.-J., Daujeard, C., Curci, A., Lemorini, C., Hardy, B., Eramo, G., Berto, C., Raynal, J.-P., Arzarello, M., Mecozzi, B., Iannucci, A., Sardella, R., Allegretta, I., Delluniversità, E., . . . Piperno, M. (2020). The origin of early Acheulean expansion in Europe 700 ka ago: new findings at Notarchirico (Italy). *Scientific Reports*, *10*(1), 13802. https://doi.org/10.1038/s41598-020-68617-8

Mugangu, T. & Hunter, Jr, M. (1992). Aquatic foraging by *Hippopotamus* in Zaïre: Response to a food shortage?. Mammalia, 56(3), 345–350. https://doi.org/10.1515/mamm.1992.56.3.345

Noirard, C., Le Berre, M., Ramousse, R., & Lena, J. P. (2008). Seasonal variation of thermoregulatory behaviour in the *Hippopotamus (Hippopotamus amphibius*). *Journal of Ethology*, *26*(1), 191–193. https://doi.org/10.1007/s10164-007-0052-1

Okuda, M., van Vugt, N., Nakagawa, T., Ikeya, M., Hayashida, A., Yasuda, Y., & Setoguchi, T. (2002). Palynological evidence for the astronomical origin of lignite–detritus sequence in the Middle Pleistocene Marathousa Member, Megalopolis, SW Greece. *Earth and Planetary Science Letters*, *201*(1), 143–157. https://doi.org/https://doi.org/10.1016/S0012-821X(02)00706-9

Ollé, A., Lombao, D., Asryan, L., García-Medrano, P., Arroyo, A., Fernández-Marchena, J. L., Yeşilova, G. C., Cáceres, I., Huguet, R., López-Polín, L., Pineda, A., García-Tabernero, A., Fidalgo, D., Rosas, A., Saladié, P., & Vallverdú, J. (2023). The earliest European Acheulean: new insights into the large shaped tools from the late Early Pleistocene site of Barranc de la Boella (Tarragona, Spain) [Original Research]. *Frontiers in Earth Science*, *11*. https://doi.org/10.3389/feart.2023.1188663

Osmond, C., Valaane, N., Haslam, S., Uotila, P., & Roksandic, Z. (1981). Comparisons of δ^{13} C values in leaves of aquatic macrophytes from different habitats in Britain and Finland; some implications for photosynthetic processes in aquatic plants. *Oecologia*, *50*, 117–124.

Palmqvist, P., Gröcke, D. R., Arribas, A., & Farina, R. A. (2003). Paleoecological reconstruction of a lower Pleistocene large mammal community using biogeochemical (δ^{13}C, δ^{15}N, δ^{18}O, Sr, Zn) and ecomorphological approaches. *Paleobiology*, *29*(2), 205–229.

Palmqvist, P., Rodriguez-Gomez, G., Figueirido, B., García-Aguilar, J. M., & Pérez-Claros, J. A. (2022). On the ecological scenario of the first hominin dispersal out of Africa. *L'Anthropologie*, *126*(1), 102998.

Palombo, M. R. (2010). A scenario of human dispersal in the northwestern Mediterranean throughout the Early to Middle Pleistocene. *Quaternary International*, *223-224*, 179–194. https://doi.org/10.1016/j.quaint.2009.11.016

Palombo, M. R. (2014). Deconstructing mammal dispersals and faunal dynamics in SW Europe during the Quaternary. *Quaternary Science Reviews*, *96*, 50–71. https://doi.org/10.1016/j.quascirev.2014.05.013

Panagopoulou, E., Tourloukis, V., Thompson, N., Athanassiou, A., Tsartsidou, G., Konidaris, G. E., Giusti, D., Karkanas, P., & Harvati, K. (2015). Marathousa 1: a new Middle Pleistocene archaeological site from Greece. *Antiquity*, *343*, 1–8.

Panagopoulou, E., Tourloukis, V., Thompson, N., Konidaris, G., Athanassiou, A., Giusti, D., Tsartsidou, G., Karkanas, P., & Harvati, K. (2018). The lower palaeolithic site of Marathousa 1, Megalopolis, Greece: overview of the evidence. *Quaternary International*, *497*, 33–46.

Papadopoulou, P., Tsoni, M., Konidaris, G. E., Tourloukis, V., Panagopoulou, E., Karkanas, P., Harvati, K., & Iliopoulos, G. (in press). Ostracod contribution to the palaeoenvironmental study of Kyparissia 4 (Megalopolis Basin, Greece). In K., Harvati, M., Ioannidou, Eds.; *Human Evolution at the CROSSROADS: Research in Greece and beyond,* Tübingen University Press: Tübingen.

Passey, B. H., & Cerling, T. E. (2002). Tooth enamel mineralization in ungulates: implications for recovering a primary isotopic time-series. Geochimica et Cosmochimica Acta, 66(18), 3225–3234.

Passey, B. H., Cerling, T. E., Schuster, G. T., Robinson, T. F., Roeder, B. L., & Krueger, S. K. (2005). Inverse methods for estimating primary input signals from time-averaged isotope profiles. *Geochimica et Cosmochimica Acta*, *69*(16), 4101–4116.

Passey, B. H., Robinson, T. F., Ayliffe, L. K., Cerling, T. E., Sponheimer, M., Dearing, M. D., Roeder, B. L., & Ehleringer, J. R. (2005). Carbon isotope fractionation between diet, breath CO_2, and bioapatite in different mammals. *Journal of Archaeological Science*, *32*(10), 1459–1470.

Pederzani, S., & Britton, K. (2019). Oxygen isotopes in bioarchaeology: Principles and applications, challenges and opportunities. Earth-Science Reviews, 188, 77–107.

Rank, D., Wyhlidal, S., Schott, K., Weigand, S., & Oblin, A. (2018). Temporal and spatial distribution of isotopes in river water in Central Europe: 50 years experience with the Austrian network of isotopes in rivers. Isotopes in Environmental and Health Studies, 54(2), 115–136.

Rink, W. J., & Schwarcz, H. P. (1995). Tests for Diagenesis in Tooth Enamel: ESR Dating Signals and Carbonate Contents. *Journal of Archaeological Science*, *22*(2), 251–255. https://doi.org/https://doi.org/10.1006/jasc.1995.0026

Rodhe, A. (1998). Snowmelt-dominated systems. In Isotope tracers in catchment hydrology (pp. 391-433). Elsevier.

Roditi, E., Bocherens, H., Konidaris, G. E., Athanassiou, A., Tourloukis, V., Karkanas, P., Panagopoulou, E., & Harvati, K. (2024). Life-history of *Palaeoloxodon antiquus* reveals Middle Pleistocene glacial refugium in the Megalopolis basin, Greece. *Scientific Reports*, *14*(1), 1390.

Sánchez-Bandera, C., Fagoaga, A., Serrano-Ramos, A., Solano-García, J., Barsky, D., DeMiguel, D., Ochando, J., Saarinen, J., Piñero, P., Lozano-Fernández, I., Courtenay, L. A., Titton, S., Luzón, C., Bocherens, H., Yravedra, J., Fortelius, M., Agustí, J., Carrión, J. S., Oms, O., . . . Jiménez-Arenas, J. M. (2023). Glacial/interglacial climate variability in southern Spain during the late Early Pleistocene and climate backdrop for early Homo in Europe. *Palaeogeography, Palaeoclimatology, Palaeoecology*, *625*, 111688. https://doi.org/https://doi.org/10.1016/j.palaeo.2023.111688

Sánchez Goñi, M. F., Extier, T., Polanco-Martínez, J. M., Zorzi, C., Rodrigues, T., & Bahr, A. (2023). Moist and warm conditions in Eurasia during the last glacial of the Middle Pleistocene Transition. *Nature Communications*, *14*(1), 2700. https://doi.org/10.1038/s41467-023-38337-4

Scotcher, J., Stewart, DRM**, & Breen, C. (1978). The diet of the hippopotamus in Ndumu Game Reserve Natal, as determined by faecal analysis. *South African Journal of Wildlife Research-24-month delayed open access*, *8*(1), 1–11.

Siavalas, G., Linou, M., Chatziapostolou, A., Kalaitzidis, S., Papaefthymiou, H., & Christanis, K. (2009). Palaeoenvironment of Seam I in the Marathousa Lignite Mine, Megalopolis Basin (Southern Greece). *International Journal of Coal Geology*, *78*(4), 233-248. https://doi.org/https://doi.org/10.1016/j.coal.2009.03.003

Snyder, K. A., Robinson, S. A., Schmidt, S., & Hultine, K. R. (2022). Stable isotope approaches and opportunities for improving plant conservation. *Conservation Physiology*, *10*(1). https://doi.org/10.1093/conphys/coac056

Souron, A., Balasse, M., & Boisserie, J.-R. (2012). Intra-tooth isotopic profiles of canines from extant *Hippopotamus amphibius* and late Pliocene hippopotamids (Shungura Formation, Ethiopia): insights into the seasonality of diet and climate. *Palaeogeography, Palaeoclimatology, Palaeoecology*, *342*, 97–110.

Souron, A., Couvrat, M., Pubert, É., Santos, F., Yang, D., Frémondeau, D., Nékoulnang, C., & Otero, O. (2024). *Variable enamel growth rates in hippopotamid canines: Implications for seasonality reconstructions using inverse modeling of intra-tooth isotope data*. Copernicus GmbH. https://dx.doi.org/10.5194/egusphere-egu24-22198

Strani, F. (2021). Impact of Early and Middle Pleistocene major climatic events on the palaeoecology of Southern European ungulates. *Historical Biology*, *33*(10), 2260–2275. https://doi.org/10.1080/08912963.2020.1782898

Strani, F., DeMiguel, D., Alba, D. M., Moyà-Solà, S., Bellucci, L., Sardella, R., & Madurell-Malapeira, J. (2019). The effects of the “0.9 Ma event” on the Mediterranean ecosystems during the Early-Middle Pleistocene transition as revealed by dental wear patterns of fossil ungulates. *Quaternary Science Reviews*, *210*, 80–89. https://doi.org/10.1016/j.quascirev.2019.02.027

Sydney-Zax, M., Mayer, I., & Deutsch, D. (1991). Carbonate Content in Developing Human and Bovine Enamel. *Journal of Dental Research*, *70*(5), 913–916. https://doi.org/10.1177/00220345910700051001

Tejada-Lara, J. V., MacFadden, B. J., Bermudez, L., Rojas, G., Salas-Gismondi, R., & Flynn, J. J. (2018). Body mass predicts isotope enrichment in herbivorous mammals. *Proceedings of the Royal Society B: Biological Sciences*, *285*(1881), 20181020. https://doi.org/doi:10.1098/rspb.2018.1020

Thompson, N., Tourloukis, V., Panagopoulou, E., & Harvati, K. (2018). In search of Pleistocene remains at the Gates of Europe: Directed surface survey of the Megalopolis Basin (Greece). *Quaternary International*, *497*, 22–32. https://doi.org/10.1016/j.quaint.2018.03.036

Tipple, B. J., Meyers, S. R., & Pagani, M. (2010). Carbon isotope ratio of Cenozoic CO_2: A comparative evaluation of available geochemical proxies. *Paleoceanography*, *25*(3). https://doi.org/https://doi.org/10.1029/2009PA001851

Tourloukis, V., Muttoni, G., Karkanas, P., Monesi, E., Scardia, G., Panagopoulou, E., & Harvati, K. (2018). Magnetostratigraphic and chronostratigraphic constraints on the Marathousa 1 Lower Palaeolithic site and the Middle Pleistocene deposits of the Megalopolis basin, Greece. *Quaternary International*, *497*, 154–169. https://doi.org/10.1016/j.quaint.2018.03.043

Tourloukis, V., Thompson, N., Panagopoulou, E., Giusti, D., Konidaris, G. E., Karkanas, P., & Harvati, K. (2018). Lithic artifacts and bone tools from the Lower Palaeolithic site Marathousa 1, Megalopolis, Greece: Preliminary results. *Quaternary International*, *497*, 47–64. https://doi.org/10.1016/j.quaint.2018.05.043

Tzedakis, P. C., Hooghiemstra, H., & Pälike, H. (2006). The last 1.35 million years at Tenaghi Philippon: revised chronostratigraphy and long-term vegetation trends. *Quaternary Science Reviews*, *25*(23), 3416–3430. https://doi.org/https://doi.org/10.1016/j.quascirev.2006.09.002

Uno, K. T., & Bibi, F. (2022). Stable isotope paleoecology of the Baynunah Formation. In *Sands of Time: Ancient life in the late Miocene of Abu Dhabi, United Arab Emirates* (pp. 299-331). Springer International Publishing Cham.

Uno, K. T., Fisher, D. C., Wittemyer, G., Douglas-Hamilton, I., Carpenter, N., Omondi, P., & Cerling, T. E. (2020). Forward and inverse methods for extracting climate and diet information from stable isotope profiles in proboscidean molars. *Quaternary International*, *557*, 92–109.

Uno, K. T., Quade, J., Fisher, D. C., Wittemyer, G., Douglas-Hamilton, I., Andanje, S., Omondi, P., Litoroh, M., & Cerling, T. E. (2013). Bomb-curve radiocarbon measurement of recent biologic tissues and applications to wildlife forensics and stable isotope (paleo)ecology. *Proceedings of the National Academy of Sciences*, *110*(29), 11736–11741. https://doi.org/doi:10.1073/pnas.1302226110

van der Merwe, N. J., & Medina, E. (1991). The canopy effect, carbon isotope ratios and foodwebs in Amazonia. *Journal of archaeological science*, *18*(3), 249–259.

van Kolfschoten, T., Konidaris, G.E., Doukas, C., Athanassiou, A., Tourloukis, V., Panagopoulou, E., Karkanas, P., Harvati, K., Voles (Rodentia, Mammalia) as a proxy to date the site Kyparissia 4 (Megalopolis Basin, Greece). In Human Evolution at the CROSSROADS: Research in Greece and beyond, Harvati, K., Ioannidou, M., Eds.; Tübingen University Press: Tübingen, in press

van Vugt, N., De Bruijn, H., Van Kolfschoten, T., Langereis, C. G., & Okuda, M. (2000). Magneto-and cyclostratigraphy and mammal-fauna’s of the Pleistocene lacustrine Megalopolis Basin, Peloponnesos, Greece. *Geologica Ultrajectina*, 189, 69–92.

Vlachos, E., & Delfino, M. (2016). Food for thought: Sub-fossil and fossil chelonian remains from Franchthi Cave and Megalopolis confirm a glacial refuge for *Emys orbicularis* in Peloponnesus

(S. Greece). *Quaternary Science Reviews*, *150*, 158–171. https://doi.org/https://doi.org/10.1016/j.quascirev.2016.08.027

Vlachos, E., Georgalis, G.L., Konidaris, G.E., Athanassiou, A., Tourloukis, V., Thompson, N., Panagopoulou, E., Harvati, K. 1079 Preliminary results on the reptiles from the Middle Pleistocene of Marathousa 1, Megalopolis Basin (Greece). In K., Harvati, M., Ioannidou, Eds.; *Human Evolution at the CROSSROADS: Research in Greece and beyond,* Tübingen University Press: Tübingen.

Vogado, N. O., Winter, K., Ubierna, N., Farquhar, G. D., & Cernusak, L. A. (2020). Directional change in leaf dry matter $\delta^{13}C$ during leaf development is widespread in C_3 plants. *Annals of Botany*, *126*(6), 981–990. https://doi.org/10.1093/aob/mcaa114

Wagner, B., Vogel, H., Francke, A., Friedrich, T., Donders, T., Lacey, J. H., Leng, M. J., Regattieri, E., Sadori, L., & Wilke, T. (2019). Mediterranean winter rainfall in phase with African monsoons during the past 1.36 million years. *Nature*, *573*(7773), 256–260.

Wang, M., Liu, G.-h., Jin, T.-t., Li, Z.-s., Gong, L., Wang, H., & Ye, X. (2017). Age-related changes of leaf traits and stoichiometry in an alpine shrub (*Rhododendron agglutinatum*) along altitudinal gradient. *Journal of Mountain Science*, *14*(1), 106–118. https://doi.org/10.1007/s11629-016-4096-y

Wang, Y., & Cerling, T. E. (1994). A model of fossil tooth and bone diagenesis: implications for paleodiet reconstruction from stable isotopes. *Palaeogeography, Palaeoclimatology, Palaeoecology*, *107*(3-4), 281–289.

Werth, M., Mehltreter, K., Briones, O., & Kazda, M. (2015). Stable carbon and nitrogen isotope compositions change with leaf age in two mangrove ferns. *Flora - Morphology, Distribution, Functional Ecology of Plants*, *210*, 80–86. https://doi.org/https://doi.org/10.1016/j.flora.2014.11.001

Yang, D., Uno, K. T., Cerling, T. E., Mwebi, O., Leakey, L. N., Grine, F. E., & Souron, A. (2024). Intra-tooth stable isotope analysis reveals seasonal dietary variability and niche partitioning among bushpigs/red river hogs and warthogs. *Current Zoology*, zoae007.

Yang, D., Uno, K. T., Souron, A., McGrath, K., Pubert, É., & Cerling, T. E. (2020). Intra-tooth stable isotope profiles in warthog canines and third molars: Implications for paleoenvironmental reconstructions. *Chemical Geology*, *554*, 119799.

Zanazzi, A., Fletcher, A., Peretto, C., & Hohenstein, U. T. (2022). Middle Pleistocene paleoclimate and paleoenvironment of Central Italy and their relationship with hominin migrations and evolution. *Quaternary International*, *619*, 12–29.

Zazzo, A., Balasse, M., & Patterson, W. P. (2005). High-resolution $\delta^{13}C$ intratooth profiles in bovine enamel: Implications for mineralization pattern and isotopic attenuation. *Geochimica et Cosmochimica Acta*, *69*(14), 3631–3642. https://doi.org/https://doi.org/10.1016/j.gca.2005.02.031

Zazzo, A., Lécuyer, C., & Mariotti, A. (2004). Experimentally-controlled carbon and oxygen isotope exchange between bioapatites and water under inorganic and microbially-mediated conditions. *Geochimica et Cosmochimica Acta*, *68*(1), 1–12. https://doi.org/https://doi.org/10.1016/S0016-7037(03)00278-3

Figures

Figure 1. *Hippopotamus antiquus* specimens from the Middle Pleistocene sequence of the Megalopolis Basin (Greece) sampled sequentially for stable carbon and oxygen isotope analysis: A) Upper canine (MAR-2B-2); B) upper first incisor (KYPT-842); C) lower canine (KYP3-46); D) upper third molar (MAR-1B-8); E) upper third molar (KYP4A-1004).

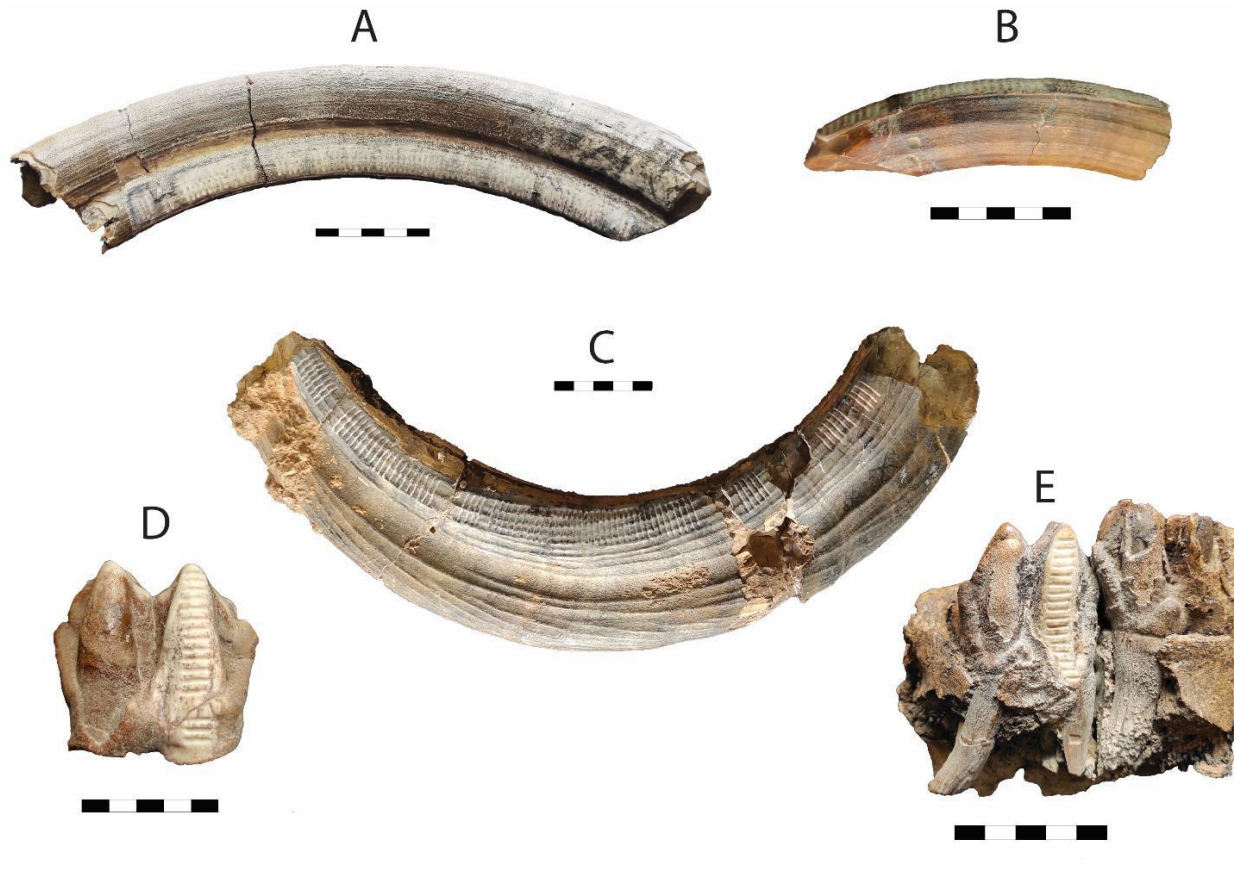

Figure 2. Bivariate plots showing A) median $\delta^{13}C_{enamel}$ (VPDB) and $\delta^{18}O_{enamel}$ (VSMOW) values and standard deviation and B) datapoint distribution of $\delta^{13}C_{enamel}$ (VPDB) and $\delta^{18}O_{enamel}$ (VSMOW) values for each sampled *Hippopotamus antiquus* specimen from the Megalopolis Basin. Dashed grey line represents the cut-off between $C_{3\ woodland\text{-}mesic\ grassland}$ and $C_{3\ open\ woodland\text{-}xeric\ grassland}$.

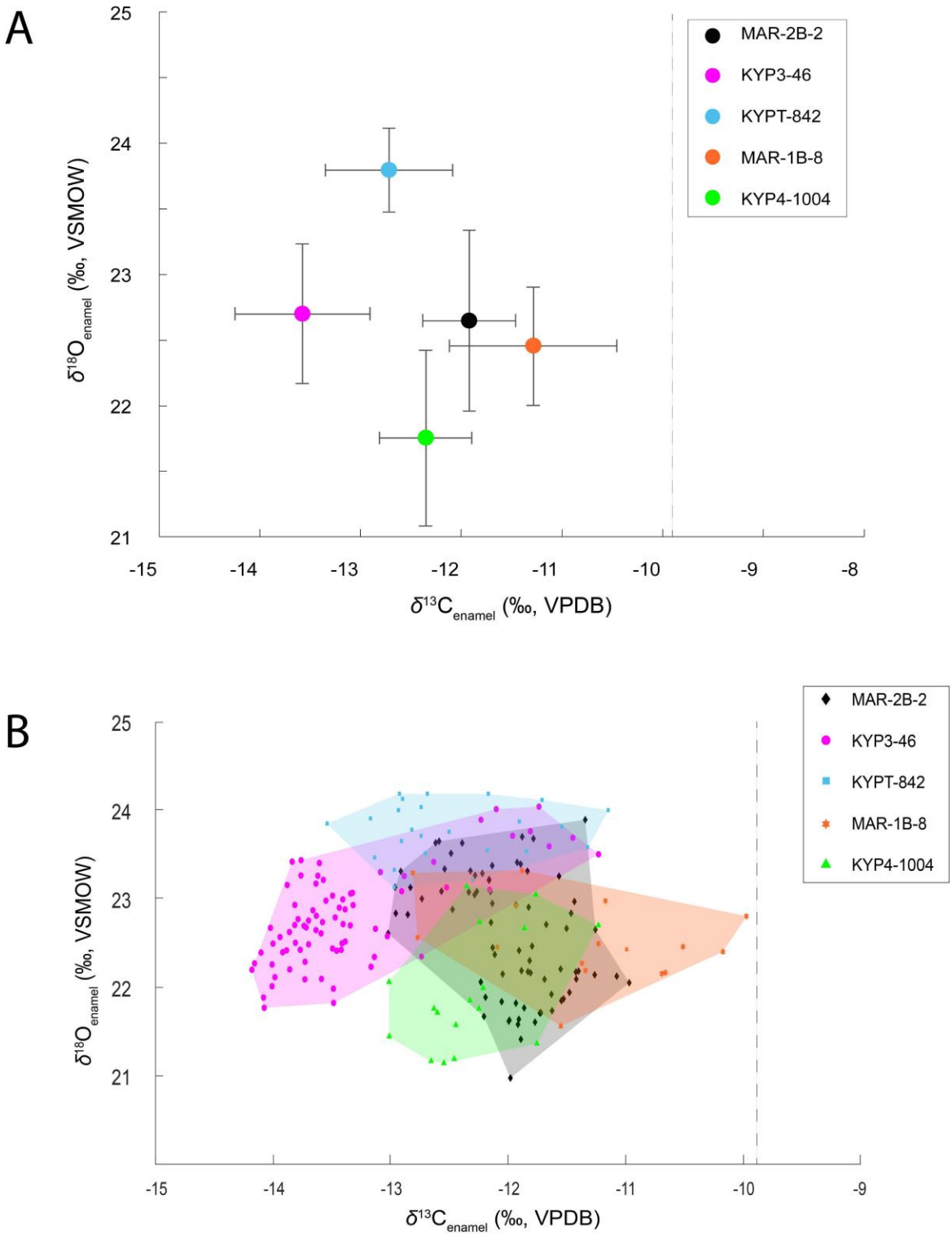

Figure 3. Intra-tooth isotopic profiles of continuously growing *H. antiquus* teeth: A) KYP3-46, B) MAR-2B-2, and C) KYPT-842. Blue circles (top series) correspond to $\delta^{18}O$, magenta circles (bottom series) correspond to $\delta^{13}C$. The black dashed line represents the calculated 3-point moving average. The vertical gray dashed line denotes the occurrence of enamel hypoplasia.

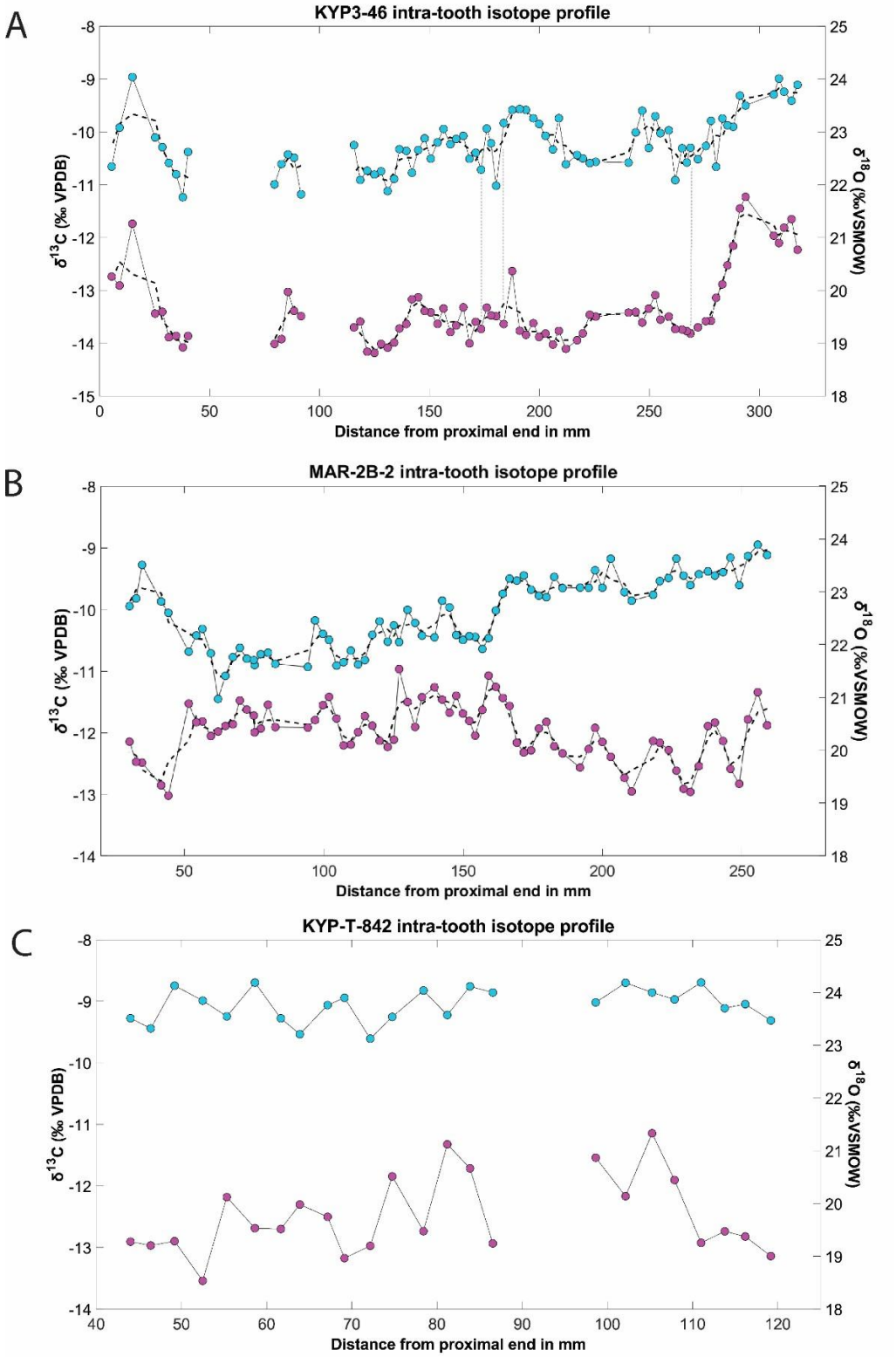

Figure 4. Intra-tooth isotopic profiles of *H. antiquus* molars: A) MAR-1B-8 and B) KYP4-1004. Blue circles (top series) correspond to $\delta^{18}O$, magenta circles (bottom series) correspond to $\delta^{13}C$.

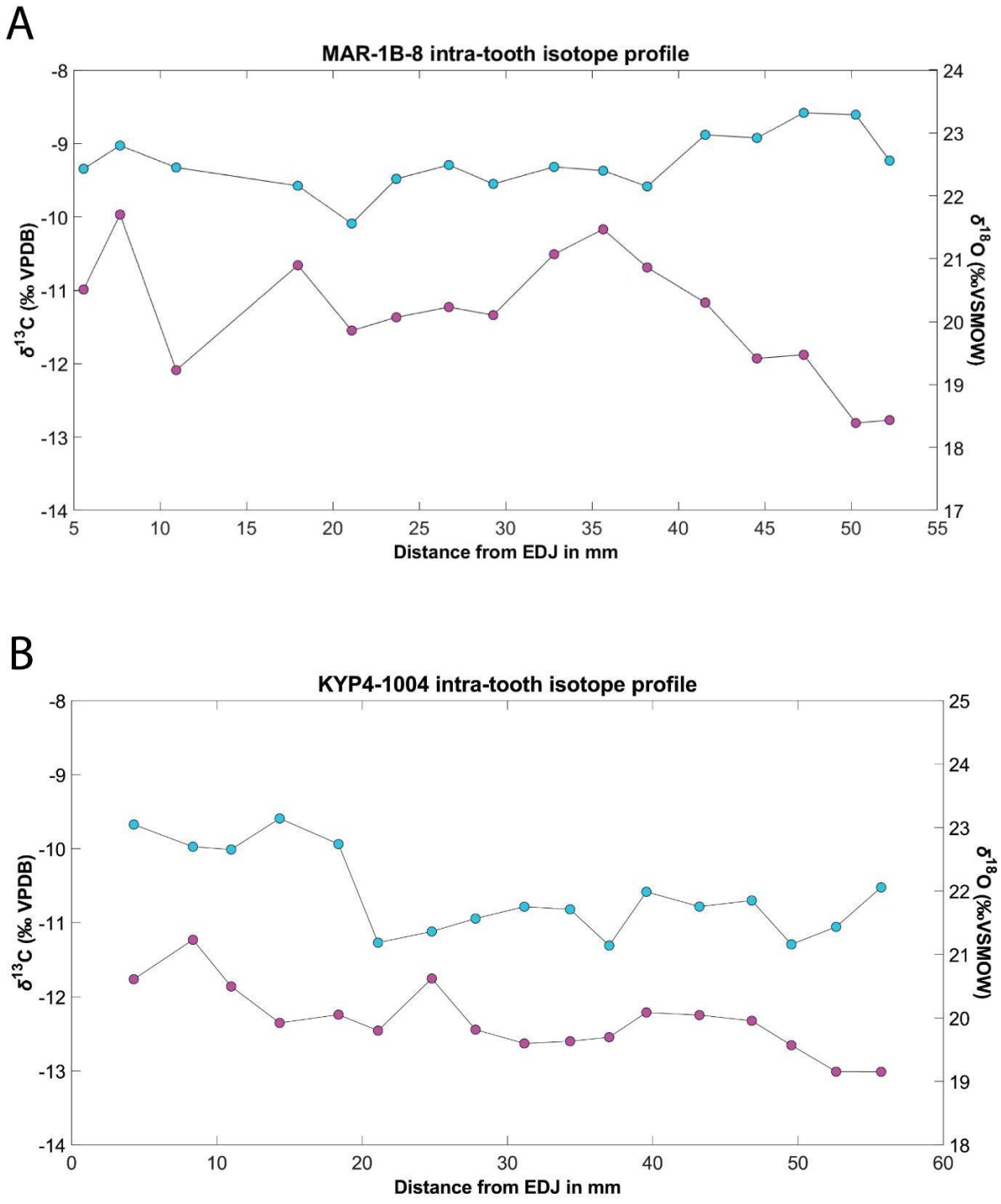

Figure 5. Detail of the KYP3-46 canine. Black arrows indicate the occurrence of mild Linear Enamel Hypoplasia (LEH).

TABLES

Table 1. Summary of stable carbon and oxygen isotopic results of *Hippopotamus antiquus* from the Megalopolis Basin (Greece).

Specimen	δ^{13}C (VPDB, ‰)					δ^{18}O (VSMOW, ‰)				
	Min	Max	Average	Median	Amplitude	Min	Max	Average	Median	Amplitude
KYP-3-46	-14.2	-11.2	-13.4	-13.6	3.0	19.5	24.0	22.7	22.7	4.6
KYP-T-842	-13.5	-11.1	-12.5	-12.7	2.4	23.1	24.2	23.8	23.8	1.1
KYP4-1004	-13.0	-11.2	-12.3	-12.4	1.8	21.1	23.1	22.0	21.8	2.0
MAR-2B-2	-13.0	-11.0	-12.0	-11.9	2.1	21.0	23.9	22.6	22.6	2.9
MAR-1B-8	-12.8	-10.0	-11.3	-11.3	2.8	21.6	23.3	22.5	22.5	1.8

Ecological variability of *Hippopotamus antiquus* from the Middle Pleistocene of Megalopolis Basin (Greece): Evidence for dynamic habitats in a glacial microrefugium

Effrosyni Roditi, Hervé Bocherens, George E. Konidaris, Athanassios Athanassiou, Vangelis Tourloukis, Eleni Panagopoulou, Panagiotis Karkanas, Katerina Harvati

Supplementary Tables

Supplementary Table 1. Main results of the incremental C and O isotopic measurements from the KYP3-46 *H. antiquus* lower canine. *Samples in red colour have been excluded from the analysis due to possible diagenetic influence.

Sample code	$\delta^{13}C$ (VPDB)	$\varepsilon^*_{\text{diet-bioapatite}}$ (Tejada Lara et al. 2018)	$\delta^{18}O$ (VPDB)	SMOW	CO3 (%)	Distance from proximal to distal end along the arch in mm
KYP-3-46a*	-11.9	-27.1	-6.9	23.8	5.2	325
KYP-3-46b*	-11.2	-26.4	-6.5	24.2	5.5	323
KYP-3-46c*	-10.2	-25.4	-6.0	24.7	5.5	319
KYP-3-46d	-12.2	-27.4	-6.8	23.9	5.0	317
KYP-3-46e	-11.7	-26.9	-7.1	23.6	4.6	315
KYP-3-46f	-11.8	-27.0	-6.9	23.8	4.8	311
KYP-3-46g	-12.1	-27.3	-6.6	24.0	4.9	309
KYP-3-46h	-12.0	-27.2	-6.9	23.7	5.0	307
KYP-3-46i	-11.2	-26.4	-7.1	23.5	4.8	294
KYP-3-46j	-11.4	-26.6	-7.0	23.7	5.1	291
KYP-3-46k	-12.2	-27.4	-7.5	23.1	4.6	288
KYP-3-46l	-12.5	-27.7	-7.5	23.1	4.5	285
KYP-3-46m	-12.9	-28.1	-7.4	23.3	4.4	283
KYP-3-46n	-13.1	-28.3	-8.3	22.3	4.5	280
KYP-3-46o	-13.6	-28.8	-7.4	23.2	4.4	278
KYP-3-46p	-13.6	-28.8	-7.9	22.7	4.4	276
KYP-3-46q	-13.7	-28.9	-8.1	22.5	4.5	272
KYP-3-46r	-13.8	-29.0	-7.9	22.7	4.4	269
KYP-3-46s	-13.8	-29.0	-8.2	22.4	4.4	267
KYP-3-46t	-13.7	-28.9	-7.9	22.7	4.4	265
KYP-3-46u	-13.7	-28.9	-8.5	22.1	4.5	262
KYP-3-46v	-13.5	-28.7	-7.6	23.0	4.7	259
KYP-3-46w	-13.5	-28.7	-7.6	23.0	4.6	255
KYP-3-46x	-13.1	-28.3	-7.3	23.3	4.8	253
KYP-3-46y	-13.3	-28.5	-7.9	22.7	4.9	250
KYP-3-46z	-13.6	-28.8	-7.2	23.4	4.6	247
KYP-3-46A-	-13.4	-28.6	-7.6	23.0	4.2	244
KYP-3-46B-	-13.4	-28.6	-8.2	22.4	4.0	240
KYP-3-46C-	-13.5	-28.7	-8.2	22.4	4.0	226
KYP-3-46D-	-13.5	-28.7	-8.2	22.4	4.3	223
KYP-3-46E-	-13.8	-29.0	-8.1	22.5	4.3	220
KYP-3-46F-	-13.9	-29.1	-8.0	22.6	4.5	217
KYP-3-46G-	-14.1	-29.3	-8.2	22.4	4.6	212
KYP-3-46H-	-13.8	-29.0	-7.4	23.3	4.8	209
KYP-3-46I-	-14.0	-29.2	-7.9	22.7	4.8	206
KYP-3-46J-	-13.8	-29.0	-7.7	22.9	4.6	203
KYP-3-46K-	-13.9	-29.1	-7.5	23.2	4.5	200
KYP-3-46L-	-13.6	-28.8	-7.4	23.3	4.5	197
KYP-3-46M-	-13.8	-29.0	-7.2	23.4	4.4	194

Supplementary Table 1 (cont.). Main results of the incremental C and O isotopic measurements from the KYP3-46 *H. antiquus* lower canine. *Samples in red colour have been excluded from the analysis due to possible diagenetic influence.

KYP-3-46N-	-13.8	-29.0	-7.2	23.4	4.9	191
KYP-3-46O-	-12.6	-27.8	-7.2	23.4	5.3	188
KYP-3-46P-	-13.6	-28.8	-7.5	23.2	4.8	184
KYP-3-46Q-	-13.5	-28.7	-8.6	22.0	4.6	180
KYP-3-46R-	-13.5	-28.7	-7.8	22.8	4.3	178
KYP-3-46S-	-13.3	-28.5	-7.6	23.1	4.5	176
KYP-3-46T-	-13.7	-28.9	-8.3	22.3	4.4	173
KYP-3-46U-	-13.6	-28.8	-8.0	22.6	4.3	171
KYP-3-46V-	-14.0	-29.2	-8.1	22.5	4.3	168
KYP-3-46W-	-13.3	-28.5	-7.7	22.9	4.6	165
KYP-3-46X-	-13.7	-28.9	-7.8	22.9	4.3	162
KYP-3-46Y-	-13.8	-29.0	-7.9	22.8	4.2	159
KYP-3-46Z	-13.3	-28.5	-7.6	23.1	4.4	156
KYP-3-46_1	-13.6	-28.8	-7.8	22.8	4.4	154
KYP-3-46_2	-13.4	-28.6	-8.1	22.5	4.5	151
KYP-3-46_3	-13.4	-28.6	-7.7	22.9	4.2	148
KYP-3-46_4	-13.1	-28.3	-8.0	22.7	4.8	145
KYP-3-46_5	-13.2	-28.4	-8.4	22.2	4.9	142
KYP-3-46_6	-13.6	-28.8	-8.0	22.6	5.0	139
KYP-3-46_7	-13.7	-28.9	-7.9	22.7	5.4	136
KYP-3-46_8	-14.0	-29.2	-8.5	22.1	4.7	134
KYP-3-46_9	-14.1	-29.3	-8.7	21.9	4.5	131
KYP-3-46_10	-14.0	-29.2	-8.3	22.3	4.3	128
KYP-3-46_11	-14.2	-29.4	-8.4	22.2	4.4	125
KYP-3-46_12	-14.2	-29.4	-8.3	22.3	4.5	122
KYP-3-46_13	-13.6	-28.8	-8.5	22.1	4.5	118
KYP-3-46_14	-13.7	-28.9	-7.9	22.8	4.4	116
KYP-3-46_15	-13.5	-28.7	-8.8	21.8	4.2	92
KYP-3-46_16	-13.4	-28.6	-8.1	22.5	4.7	88
KYP-3-46_17	-13.0	-28.2	-8.0	22.6	4.6	86
KYP-3-46_18	-13.9	-29.1	-8.2	22.4	4.3	83
KYP-3-46_19	-14.0	-29.2	-8.6	22.0	4.7	80
KYP-3-46_20	-13.9	-29.1	-8.0	22.6	4.5	40
KYP-3-46_21	-14.1	-29.3	-8.8	21.8	4.5	38
KYP-3-46_22	-13.9	-29.1	-8.4	22.2	4.4	35
KYP-3-46_23	-13.9	-29.1	-8.2	22.4	4.3	31
KYP-3-46_24	-13.4	-28.6	-7.9	22.7	4.4	29
KYP-3-46_25	-13.4	-28.6	-7.7	22.9	4.5	25
KYP-3-46_26	-11.7	-26.9	-6.6	24.0	4.7	15
KYP-3-46_27*	-12.9	-28.1	-11.0	19.5	3.6	12
KYP-3-46_28	-12.9	-28.1	-7.5	23.1	4.3	9
KYP-3-46_29	-12.7	-27.9	-8.3	22.3	4.4	5
KYP-3-46_dent	-4.2		-5.9	25	6	

Supplementary Table 2. Main results of the incremental C and O isotopic measurements from the MAR-2B-2 *H. antiquus* upper canine.

Sample code	$\delta^{13}C$ (VPDB)	$\varepsilon^*_{diet\text{-}bioapatite}$ (Tejada Lara et al. 2018)	$\delta^{18}O$ (VPDB)	SMOW	CO3 (%)	Distance from root to apex along the arc (mm)
GMAR-2-2Ba	-11.9	-27.1	-6.9	23.7	4.4	259
GMAR-2-2Bb	-11.3	-26.5	-6.8	23.9	4.9	256
GMAR-2-2Bc	-11.8	-27.0	-7.0	23.7	4.6	252
GMAR-2-2Bd	-12.8	-28.0	-7.5	23.1	4.5	249
GMAR-2-2Be	-12.6	-27.8	-7.0	23.6	4.8	246
GMAR-2-2Bf	-12.1	-27.3	-7.3	23.4	4.2	243
GMAR-2-2Bg	-11.8	-27.0	-7.3	23.3	4.4	240
GMAR-2-2Bh	-11.9	-27.1	-7.2	23.4	4.6	238
GMAR-2-2Bi	-12.5	-27.7	-7.3	23.3	4.4	235
GMAR-2-2Bj	-13.0	-28.2	-7.5	23.1	4.1	231
GMAR-2-2Bk	-12.9	-28.1	-7.3	23.3	4.3	229
GMAR-2-2Bl	-12.6	-27.8	-7.0	23.6	4.5	226
GMAR-2-2Bm	-12.3	-27.5	-7.4	23.3	4.4	224
GMAR-2-2Bn	-12.2	-27.4	-7.4	23.2	4.3	221
GMAR-2-2Bo	-12.1	-27.3	-7.7	22.9	4.3	218
GMAR-2-2Bp	-13.0	-28.2	-7.8	22.8	4.3	210
GMAR-2-2Bq	-12.7	-27.9	-7.6	23.0	4.0	208
GMAR-2-2Br	-12.4	-27.6	-7.0	23.6	4.3	203
GMAR-2-2Bs	-12.1	-27.3	-7.5	23.1	4.0	200
GMAR-2-2Bt	-11.9	-27.1	-7.2	23.4	4.4	197
GMAR-2-2Bu	-12.3	-27.5	-7.5	23.1	4.1	195
GMAR-2-2Bv	-12.6	-27.8	-7.5	23.1	4.2	192
GMAR-2-2Bw	-12.3	-27.5	-7.6	23.1	4.0	186
GMAR-2-2Bx	-12.2	-27.4	-7.3	23.3	4.2	183
GMAR-2-2By	-11.8	-27.0	-7.7	22.9	4.1	180
GMAR-2-2Bz	-11.9	-27.1	-7.7	22.9	4.0	177
GMAR-2-2B-1	-12.3	-27.5	-7.6	23.0	4.2	174
GMAR-2-2B-2	-12.3	-27.5	-7.3	23.3	4.2	172
GMAR-2-2B-3	-12.2	-27.4	-7.4	23.2	4.3	169
GMAR-2-2B-4	-11.6	-26.8	-7.4	23.3	4.5	167
GMAR-2-2B_5	-11.4	-26.6	-7.7	23.0	4.1	164
GMAR-2-2B_6	-11.3	-26.5	-8.0	22.6	4.3	162
GMAR-2-2B_7	-11.1	-26.3	-8.5	22.1	4.2	159
GMAR-2-2B_8	-11.6	-26.8	-8.7	21.9	4.3	157
GMAR-2-2B_9	-12.0	-27.2	-8.5	22.1	4.1	154
GMAR-2-2B_10	-11.8	-27.0	-8.4	22.2	4.4	152
GMAR-2-2B_11	-11.7	-26.9	-8.5	22.1	4.1	150
GMAR-2-2B_12	-11.4	-26.6	-8.4	22.2	4.2	148
GMAR-2-2B_13	-11.7	-26.9	-7.9	22.7	4.3	145
GMAR-2-2B_14	-11.5	-26.7	-7.8	22.8	4.2	143

Supplementary Table 2 (cont.). Main results of the incremental C and O isotopic measurements from the MAR-2B-2 *H. antiquus* upper canine.

GMAR-2-2B_15	-11.3	-26.5	-8.5	22.1	4.1	140
GMAR-2-2B_16	-11.4	-26.6	-8.4	22.2	4.2	135
GMAR-2-2B_17	-11.9	-27.1	-8.2	22.4	4.3	133
GMAR-2-2B_18	-11.5	-26.7	-8.0	22.7	4.4	130
GMAR-2-2B_19	-11.0	-26.2	-8.5	22.0	4.5	127
GMAR-2-2B_20	-12.1	-27.3	-8.2	22.4	4.3	125
GMAR-2-2B_21	-12.2	-27.4	-8.5	22.1	4.3	123
GMAR-2-2B_22	-12.1	-27.3	-8.2	22.4	4.1	120
GMAR-2-2B_23	-11.9	-27.1	-8.4	22.2	4.2	117
GMAR-2-2B_24	-11.7	-26.9	-8.9	21.7	4.2	115
GMAR-2-2B_25	-12.0	-27.2	-9.0	21.6	4.1	112
GMAR-2-2B_26	-12.2	-27.4	-8.7	21.9	4.1	110
GMAR-2-2B_27	-12.2	-27.4	-8.9	21.7	4.3	107
GMAR-2-2B_28	-11.8	-27.0	-9.0	21.6	4.3	105
GMAR-2-2B_29	-11.4	-26.6	-8.5	22.1	4.3	102
GMAR-2-2B_30	-11.6	-26.8	-8.4	22.2	4.1	100
GMAR-2-2B_31	-11.8	-27.0	-8.1	22.5	4.1	97
GMAR-2-2B_32	-11.9	-27.1	-9.0	21.6	4.2	94
GMAR-2-2B_33	-11.9	-27.1	-8.9	21.6	4.3	83
GMAR-2-2B_34	-11.5	-26.7	-8.7	21.8	4.2	80
GMAR-2-2B_35	-11.9	-27.1	-8.8	21.8	4.5	77
GMAR-2-2B_36	-12.0	-27.2	-9.0	21.6	4.3	75
GMAR-2-2B_37	-11.7	-26.9	-8.9	21.7	4.4	75
GMAR-2-2B_38	-11.6	-26.8	-8.9	21.7	4.5	72
GMAR-2-2B_39	-11.5	-26.7	-8.7	21.9	4.6	70
GMAR-2-2B_40	-11.9	-27.1	-8.8	21.8	4.6	67
GMAR-2-2B_41	-11.9	-27.1	-9.2	21.4	4.5	65
GMAR-2-2B_42	-12.0	-27.2	-9.6	21.0	4.5	62
GMAR-2-2B_43	-12.1	-27.3	-8.8	21.8	4.6	60
GMAR-2-2B_44	-11.8	-27.0	-8.3	22.3	4.3	57
GMAR-2-2B_45	-11.8	-27.0	-8.4	22.2	4.3	54
GMAR-2-2B_46	-11.5	-26.7	-8.7	21.9	4.5	52
GMAR-2-2B_47	-13.0	-28.2	-8.0	22.6	4.8	44
GMAR-2-2B_48	-12.9	-28.1	-7.8	22.8	4.9	42
GMAR-2-2B_49	-12.5	-27.7	-7.1	23.5	5.3	35
GMAR-2-2B_50	-12.5	-27.7	-7.7	22.9	5.0	33
GMAR-2-2B_51	-12.1	-27.3	-7.9	22.7	5.0	30
GMAR-2-2B_cem	-9.0		-5.9	24.8	6.2	
GMAR-2-2B_dent	3.1		5.5	25.2	7.2	

Supplementary Table 3. Main results of the incremental C and O isotopic measurements from the KYPT-842 *H. antiquus* upper incisor.

Sample Code	$\delta^{13}C$ (VPDB)	$\varepsilon^*_{\text{diet-bioapatite}}$ (Tejada Lara et al. 2018)	$\delta^{18}O$ (VPDB)	SMOW	CO3 (%)	Distance from root to apex (mm)
KYP-T-842a	-13.1	-28.3	-7.2	23.5	5.0	119.2
KYP-T-842b	-12.8	-28.0	-6.9	23.8	4.8	116.2
KYP-T-842c	-12.7	-27.9	-6.9	23.7	5.0	113.8
KYP-T-842d	-12.9	-28.1	-6.5	24.2	4.6	111.0
KYP-T-842e	-11.9	-27.1	-6.8	23.9	4.8	107.9
KYP-T-842f	-11.1	-26.3	-6.7	24.0	4.5	105.2
KYP-T-842g	-12.2	-27.4	-6.5	24.2	4.9	102.1
KYP-T-842h	-11.5	-26.7	-6.8	23.8	4.4	98.6
KYP-T-842i	-12.9	-28.1	-6.7	24.0	4.8	86.5
KYP-T-842j	-11.7	-26.9	-6.5	24.1	4.8	83.9
KYP-T-842k	-11.3	-26.5	-7.1	23.6	4.6	81.2
KYP-T-842l	-12.7	-27.9	-6.6	24.0	4.8	78.4
KYP-T-842m	-11.8	-27.0	-7.1	23.5	4.8	74.7
KYP-T-842n	-13.0	-28.2	-7.5	23.1	4.4	72.2
KYP-T-842o	-13.2	-28.4	-6.8	23.9	4.9	69.1
KYP-T-842p	-12.5	-27.7	-6.9	23.8	4.7	67.2
KYP-T-842q	-12.3	-27.5	-7.4	23.2	4.8	63.9
KYP-T-842r	-12.7	-27.9	-7.1	23.5	4.7	61.7
KYP-T-842s	-12.7	-27.9	-6.5	24.2	4.7	58.6
KYP-T-842t	-12.2	-27.4	-7.1	23.5	4.4	55.3
KYP-T-842u	-13.5	-28.7	-6.8	23.8	4.7	52.5
KYP-T-842v	-12.9	-28.1	-6.5	24.1	5.0	49.2
KYP-T-842w	-13.0	-28.2	-7.3	23.3	4.8	46.4
KYP-T-842x	-12.9	-28.1	-7.1	23.5	4.4	44.0
KYP-T-842dent	3.0			25.4	7.6	

Supplementary Table 3. Main results of the incremental C and O isotopic measurements from the MAR-1B-8 *H. antiquus* third molar.

Sample code	δ^{13}C (VPDB)	$\varepsilon^*_{\text{diet-bioapatite}}$ (Tejada Lara et al. 2018)	δ^{18}O (VPDB)	SMOW	CO3 (%)	Distance from EDJ
GMAR-1-8Ba	-12.8	-28.0	-8.05	22.56	4.69	52.2
GMAR-1-8Bb	-12.8	-28.0	-7.3	23.3	4.41	50.3
GMAR-1-8Bc	-11.9	-27.1	-7.3	23.3	4.28	47.3
GMAR-1-8Bd	-11.9	-27.1	-7.7	22.9	4.32	44.6
GMAR-1-8Be	-11.2	-26.4	-7.7	23.0	4.31	41.6
GMAR-1-8Bf	-10.7	-25.9	-8.5	22.2	4.27	38.2
GMAR-1-8Bg	-10.2	-25.4	-8.2	22.4	4.64	35.7
GMAR-1-8Bh	-10.5	-25.7	-8.2	22.5	4.13	32.8
GMAR-1-8Bi	-11.3	-26.5	-8.4	22.2	4.13	29.3
GMAR-1-8Bj	-11.2	-26.4	-8.1	22.5	4.16	26.7
GMAR-1-8Bk	-11.4	-26.6	-8.3	22.3	4.4	23.7
GMAR-1-8Bl	-11.6	-26.8	-9.0	21.6	4.35	21.1
GMAR-1-8Bm	-10.7	-25.9	-8.4	22.2	4.32	18.0
GMAR-1-8Bn	-12.1	-27.3	-8.2	22.5	4.24	10.9
GMAR-1-8Bo	-10.0	-25.2	-7.8	22.8	4.57	7.7
GMAR-1-8Bp	-11.0	-26.2	-8.2	22.4	4.64	5.6
GMAR-1-8Bdent	-4.1	-19.3	-6.6	24.1	8.04	
GMAR-1-8Bcem	-0.8	-16.0	-6.7	24.0	8.01	

Supplementary Table 5. Main results of the incremental C and O isotopic measurements from the KYP4A-1004 *H. antiquus* third molar.

Sample code	$\delta^{13}C$ (VPDB)	$\varepsilon^*_{\text{diet-bioapatite}}$ (Tejada Lara et al. 2018)	$\delta^{18}O$ (VPDB)	$\delta^{18}O$ (SMOW)	CO3 (%)	Distance from EDJ
KYP-4-F6a	-13.0	-28.2	-8.5	22.1	3.51	55.7
KYP-4-F6b	-13.0	-28.2	-9.1	21.4	3.45	52.6
KYP-4-F6c	-12.7	-27.9	-9.4	21.2	3.29	49.5
KYP-4-F6d	-12.3	-27.5	-8.7	21.9	3.49	46.8
KYP-4-F6e	-12.2	-27.4	-8.8	21.8	3.99	43.2
KYP-4-F6f	-12.2	-27.4	-8.6	22.0	4.30	39.6
KYP-4-F6g	-12.5	-27.7	-9.4	21.1	3.57	37.0
KYP-4-F6h	-12.6	-27.8	-8.9	21.7	3.31	34.3
KYP-4-F6i	-12.6	-27.8	-8.8	21.8	3.34	31.2
KYP-4-F6j	-12.4	-27.6	-9.0	21.6	3.80	27.8
KYP-4-F6k	-11.8	-27.0	-9.2	21.4	4.18	24.8
KYP-4-F6l	-12.5	-27.7	-9.4	21.2	3.35	21.1
KYP-4-F6m	-12.2	-27.4	-7.9	22.7	3.64	18.4
KYP-4-F6n	-12.4	-27.6	-7.5	23.1	3.88	14.3
KYP-4-F6o	-11.9	-27.1	-8.0	22.7	3.86	11.0
KYP-4-F6p	-11.2	-26.4	-7.9	22.7	4.25	8.4
KYP-4-F6q	-11.8	-27.0	-7.6	23.0	4.32	4.3
KYP-4-F6dent	-2.1	-17.3	-6.2	24.5	6.26	